AD_____

Award Number: DAMD17-01-1-0776

TITLE: Biochemical Markers for Exposure to Low Doses of Organophosphorus Insecticides

PRINCIPAL INVESTIGATOR: Oksana Lockridge, Ph.D.

CONTRACTING ORGANIZATION: University of Nebraska Medical Center
Omaha, NE 68198-6810

REPORT DATE: August 2005

TYPE OF REPORT: Final

PREPARED FOR: U.S. Army Medical Research and Materiel Command
Fort Detrick, Maryland 21702-5012

DISTRIBUTION STATEMENT: Approved for Public Release;
Distribution Unlimited

The views, opinions and/or findings contained in this report are those of the author(s) and should not be construed as an official Department of the Army position, policy or decision unless so designated by other documentation.

20051101 050

Best Available Copy

REPORT DOCUMENTATION PAGE

1. REPORT DATE (DD-MM-YYYY)	2. REPORT TYPE	3. DATES COVERED (From - To)
01-08-2005	Final	1 Aug 01 – 31 Jul 05

4. TITLE AND SUBTITLE

Biochemical Markers for Exposure to Low Doses of Organophosphorus Insecticides

5a. CONTRACT NUMBER

5b. GRANT NUMBER
DAMD17-01-1-0776

5c. PROGRAM ELEMENT NUMBER

6. AUTHOR(S)
Oksana Lockridge, Ph.D.

E-Mail: olockrid@unmc.edu

5d. PROJECT NUMBER

5e. TASK NUMBER

5f. WORK UNIT NUMBER

7. PERFORMING ORGANIZATION NAME(S) AND ADDRESS(ES)

University of Nebraska Medical Center
Omaha, NE 68198-6810

8. PERFORMING ORGANIZATION REPORT NUMBER

9. SPONSORING / MONITORING AGENCY NAME(S) AND ADDRESS(ES)
U.S. Army Medical Research and Materiel Command
Fort Detrick, Maryland 21702-5012

10. SPONSOR/MONITOR'S ACRONYM(S)

11. SPONSOR/MONITOR'S REPORT NUMBER(S)

12. DISTRIBUTION / AVAILABILITY STATEMENT
Approved for Public Release; Distribution Unlimited

13. SUPPLEMENTARY NOTES

14. ABSTRACT:

See attached.

15. SUBJECT TERMS
Gulf War Illness, Insecticide, Nerve Agent, Low Dose, Biochemical Markers, Organophosphate, Acetylcholinesterase

16. SECURITY CLASSIFICATION OF:

a. REPORT	b. ABSTRACT	c. THIS PAGE	17. LIMITATION OF ABSTRACT	18. NUMBER OF PAGES	19a. NAME OF RESPONSIBLE PERSON USAMRMC
U	U	U	UU	119	19b. TELEPHONE NUMBER (include area code)

ABSTRACT

.The acute toxicity of organophosphorus agents (OP) is explained by inhibition of acetylcholinesterase (AChE). However, toxicity from low dose exposure is not understood. Using mass spectroscopy, we developed the hypothesis that multiple targets for each OP exist, and that target identity varies with the OP. Thus, dichlorvos covalently binds to acetylcholinesterase, butyrylcholinesterase, platelet-activating factor acetylhydrolase alpha 2, and acylpeptide hydrolase. FP-biotin binds not only to these proteins, but also to albumin, platelet-activating factor acetylhydrolase alpha 1, esterase 10, and fatty acid amide hydrolase. Covalent binding to a set of proteins is hypothesized to explain low dose toxicity. Each OP is hypothesized to bind to a slightly different set, and therefore to have a unique mechanism of toxicity. In vivo studies in mice with a biotinylated OP showed 12 OP labeled proteins in mouse blood. The most intensely labeled protein was albumin, thus identifying albumin as a new biomarker of OP exposure. People partially deficient in AChE are expected to be healthy and fertile, but to be unusually sensitive to OP. Our studies with AChE deficient mice predict that some cases of low dose toxicity will be explained by partial AChE deficiency in humans.

Table of Contents

Abbreviations

AChE	acetylcholinesterase enzyme
amu	atomic mass units
BChE	butyrylcholinesterase enzyme
BSA	bovine serum albumin
CAD	collision activated dissociation
CPO	chlorpyrifos oxon
DFP	diisopropylfluorophosphate
DTNB	dithiobisnitrobenzoic acid; color reagent for activity assay
+EMS	positive ion enhanced mass spectrum
+EPI	positive ion enhanced product ion
+ER	positive ion enhanced resolution
FP-biotin	biotinylated organophosphate where the leaving group is the fluoride ion and the marker is biotin; 10-(fluoroethoxyphos phinyl)-N-(biotinamidopentyl) decanamide
HABA	4-hydroxy azobenzene-2-carboxylic acid
iso-OMPA	tetraisopropyl pyrophosphoramide; inhibitor for BChE
LC-MS/MS	liquid chromatography-tandem mass spectrometry
MALDI	matrix assisted laser desorption ionization
MS	mass spectrometry
MS/MS	tandem mass spectrometry
OP	organophosphorus toxicant
PVDF	polyvinylidene difluoride; membrane for binding proteins
SDS	sodium dodecyl sulfate
SDS PAGE	sodium dodecyl sulfate, polyacrylamide gel electrophoresis
TIC	total ion chromatogram
TPCK	N-p-tosyl-L-phenylalanine chloromethyl ketone
VX	O-ethyl S-[2-(diisopropylamino)ethyl] methylphosphonothioate; nerve agent
XIC	extracted ion chromatogram

Introduction

The purpose of this work is to identify proteins that react with low doses of organophosphorus agents (OP). There is overwhelming evidence that acute toxicity of OP is due to inhibition of acetylcholinesterase (AChE). However, we have found that the AChE knockout mouse, which has zero AChE, is supersensitive to low doses of OP. The AChE-/- mouse dies at doses of OP that are not lethal to wild-type mice (Duysen et al., 2001). This demonstrates that non-AChE targets are involved in OP toxicity. Our goal is to identify new biological markers of exposure to organophosphorus agents.

Our strategy uses biotinylated OP to label proteins, which are then visualized with streptavidin conjugated to a fluorophore. Labeled proteins are identified by mass spectrometry.

Since some cases of Gulf War Illness may have been caused by exposure to low doses of OP, our studies may lead to an explanation for the neurologic symptoms in some of our Gulf War veterans.

List of tasks
Task 1
Biotinylated OP will be synthesized in the laboratory of Dr. Charles Thompson at the University of Montana. 1-20 mg of biotinylated OP will be provided to Dr. Lockridge.

Task 1 was completed in Annual report 2002.

Task 2
The toxicity of various doses of chlorpyrifos oxon, dichlorvos, diazinon-O-analog, and malathion-O-analog will be tested in mice deficient in acetylcholinesterase. The goal is to find a dose that is toxic only to AChE deficient mice (AChE +/- and AChE -/-), and is not toxic to wild-type (AChE +/+) mice.

Task 2 was completed in Annual report 2004.

Task 3
Human and mouse brains will be extracted and treated with biotinylated OP. The biotinylated proteins will be purified with avidin-Sepharose, and separated by gel electrophoresis. The number and size of proteins that reacted with biotinylated OP will be visualized on blots by treating with avidin conjugated to an indicator.

Task 3 was completed for mouse brain in Annual reports 2002 and 2003, and for human brain in the Final report.

Task 4
The protein bands isolated in task 3 will be partially sequenced. The partial sequences will be used to search the Human and Mouse Genome

Databases, for the purpose of obtaining the complete amino acid sequences and identifying the proteins.

Task 4 was completed for mouse brain in Annual Report 2003, and for Human brain in the Final report.

Task 5

The reactivity with insecticides of the new biochemical markers will be compared to the reactivity of AChE and BChE with the same insecticides. The set of proteins identified in task 3, as well as AChE and BChE, will be ranked for reactivity with chlorpyrifos oxon, dichlorvos, diazinon-O-analog, and malathion-O-analog. This will be accomplished by measuring second order rate constants for individual proteins in brain extracts.

Task 5 was completed in Annual reports 2002 and 2003.

Task 6

The toxicological relevance of the biochemical markers identified in task 3 will be determined. Mice will be treated with the dose of insecticide determined in Task 2, that is, a dose that is not toxic to wild-type mice, but is toxic to AChE deficient mice.

Progress on Task 6 is reported in the Final report.

Task 1

Biotinylated OP will be synthesized in the laboratory of Dr. Charles
Thompson at the University of Montana. 1-20 mg of biotinylated OP
will be provided to Dr. Lockridge.

Relation to statement of work. Task 1 has been completed.

Synthesis of FP-biotin

Abstract

A biotinylated OP, called FP-biotin, was synthesized in the laboratory of Dr. Charles
Thompson at the University of Montana. The FP-biotin was delivered to Dr. Lockridge.

Introduction

We decided to use biotinylated OP to fish out proteins that react with OP because the biotin
label not only marks the protein but also allows one-step purification of biotinylated proteins
on avidin conjugated to Sepharose. After we made this decision we found a method for
synthesizing the compound we wanted in the literature (Liu et al., 1999). Therefore, we
adapted their synthesis scheme to make FP-biotin. We are using the FP-biotin to test our
hypothesis. Our hypothesis is that proteins other than AChE react with low doses of
insecticide OP, and that these reactions cause toxicity.

Methods and Results

Synthesis of FP-biotin. Troy Voelker, in Dr. Thompson's laboratory, synthesized, purified,
and sent to us 15.5 mg of 10-(fluoroethoxyphos phinyl)-N-(biotinamidopentyl) decanamide
(FP-biotin). See Figure 1.1.
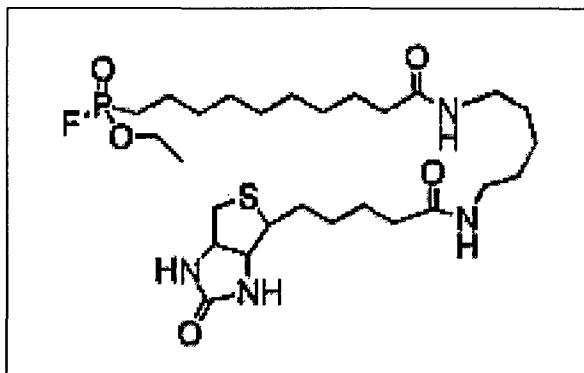
Figure 1.1. FP-biotin structure. The OP has a reactive phosphonofluoridate group
tethered to biotin via a spacer arm.

The steps in the synthesis of FP-biotin are shown in Figure 1.2. They follow the procedure of (Liu et al., 1999). 1-Hydroxy-10-undecene (2) was reacted with toluenesulfonyl chloride in pyridine to form the corresponding tosylate (3). Displacement of the tosylate with iodide formed 1-iodo-10-undecene (4), which was reacted with triethylphosphite to form 1-(diethyoxyphosphonyl)-10-undecene (5). Monodealkylation of one of the ethyl esters with TMS-Br formed the phosphorus monoacid (6). Ruthenium chloride-promoted oxidative cleavage resulted in formation of the decanoic acid (7). The acid 7 was converted to the phosphonofluoridate 8 using DAST and then coupled to 5-(biotinamido)-pentylamine (BAPA; 8; Lee, 1988) to form FP-biotin. Yield for each step was noted except for the final two transformations, which are combined. The overall yield for the multistep synthesis was estimated to be about 6%.
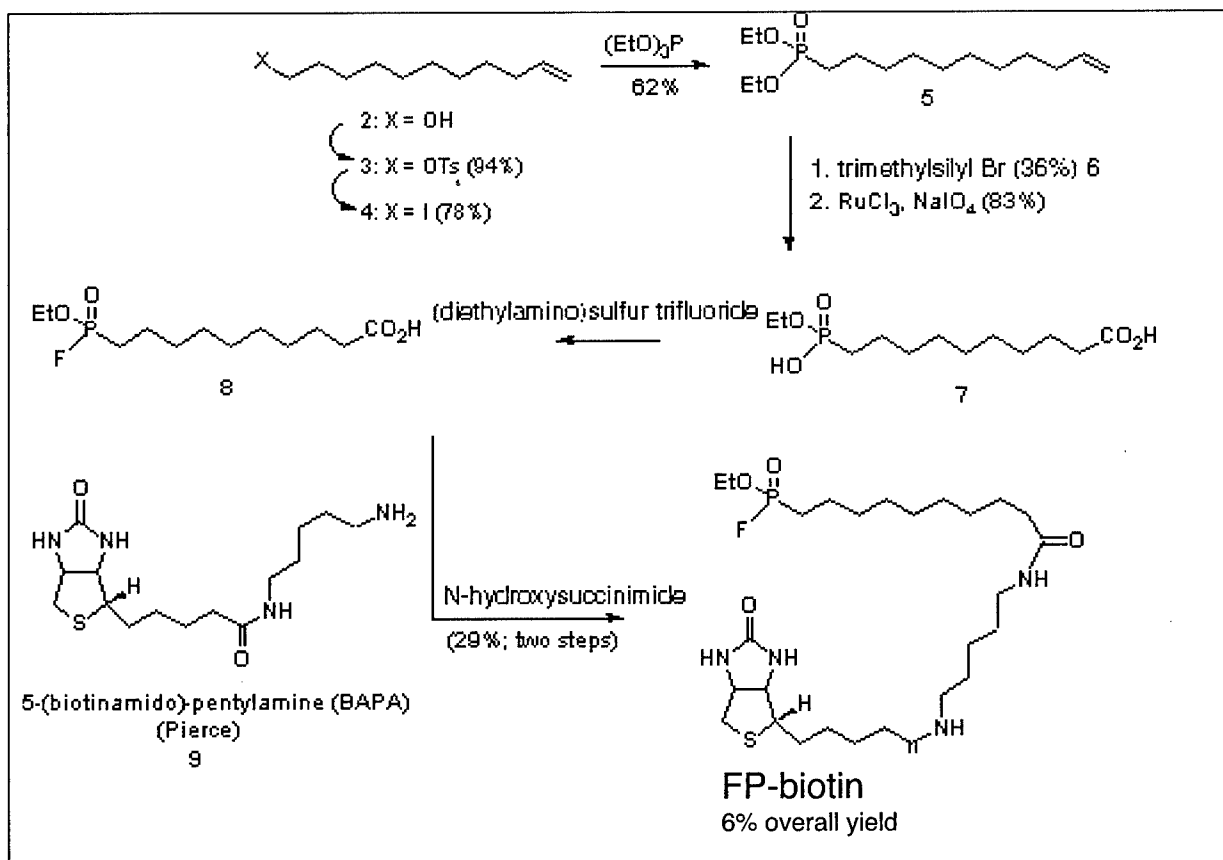
Figure 1.2. Synthesis of FP-biotin.

Purification and characterization of FP-biotin. FP-biotin was purified by washing the crystals sequentially with diethyl ether and ethyl acetate.

The identity of the biotinylated OP and of the intermediates was confirmed by H-1, C-13 and P-31 NMR, absorbance spectra in the UV-Vis wavelength range, and combustion analysis. Phosphorous NMR showed a doublet (36.0 and 29.3 ppm from H_3PO_4) as expected. Mass spectrometry (TOF MS ES+) showed that FP-biotin had a mass to charge ratio of 593.5 (*m/z*). The expected *m/z* for FP-biotin, $C_{27}FH_{50}N_4O_5PS$

+H$^+$, is 593.3. There was a peak at 297.3 (m/z), i.e. 1/2 of the major peak, and at 615.6 (m/z), i.e. the major peak plus one sodium. No evidence for contamination was detected.

Storage of FP-biotin. The FP-biotin arrived dry, in two sealed glass ampoules (7.1 mg and 8.4 mg), and was stored at -70°C. The 7.1 mg portion was dissolved in 0.7 ml of methanol (HPLC grade, from EM Science), divided into 7 aliquots (100 µl each), which were placed into Pyrex tubes cleaned in a muffle oven. The aliquots were dried under vacuum in a Speedvac, at room temperature. Six of the seven dried aliquots were returned to storage at -70°C. One ml of methanol was added to one aliquot to give a 1 mg/ml, or 1.7 mM, stock solution of FP-biotin. This methanol stock solution was stored at -70°C.

Concentration of FP-biotin. The concentration of biotin in the FP-biotin stock solution was checked by titration against a complex of avidin (Sigma) and HABA (4-hydroxy azobenzene-2-carboxylic acid, from Sigma) as described (Green, 1965). The titration yielded a concentration for biotin in the methanol stock solution of 1.78 mM or 105% of the expected concentration obtained by weight.

Discussion
The FP-biotin synthesized by the laboratory of Dr. Charles Thompson is a high quality reagent. It is pure by mass spectrometry and by titration with avidin. FP-biotin has good reactivity with human AChE and BChE despite its large biotin group, as demonstrated in Task 6.1.

Task 2

The toxicity of various doses of chlorpyrifos oxon,
dichlorvos, diazinon-O-analog, and malathion-O-analog will
be tested in mice deficient in acetylcholinesterase. The
goal is to find a dose that is toxic only to AChE deficient
mice (AChE +/- and AChE -/-), and is not toxic to wild-type
(AChE +/+) mice.

Relation to statement of work. Task 2 has been completed.

Toxicity of chorpyrifos oxon, dichlorvos, and malaoxon in AChE deficient mice

Abstract
The goal was to find a dose of OP that was toxic only to AChE deficient mice (AChE +/- and AChE -/-) and was not toxic to wild-type mice. The minimal toxic doses found were 0.75 mg/kg ip chlorpyrifos oxon, and 15 mg/kg ip malaoxon. No single dose of dichlorvos was found that produced some toxicity in AChE +/- mice and was not lethal to AChE-/- mice. Therefore dichlorvos doses were 7 mg/kg ip for AChE+/+ and +/- mice, and 1 mg/kg ip for AChE-/- mice. The best discrimination between the three AChE genotypes was obtained by malaoxon at a dose of 15 mg/kg ip. This dose of malaoxon had almost no toxic effects on AChE +/+ mice, had moderate effects on AChE+/- mice, and was severely toxic to AChE-/- mice.

Introduction
In Task 2 we have determined doses of OP that can be considered low. We have defined a low dose as a dose that has no acute effects in wild-type mice but is toxic to AChE-/- mice.

Materials and Methods
Materials. Chlorpyrifos Oxon was from Dow Elanco AGR203674; O-analog recertification date April 15, 1998. MW 335 g/mole. The dry compound was dissolved in 200 proof ethyl alcohol to make a 10 mg/ml stock solution, which was stored at –80°C. Just before injection into animals, the stock solution was diluted to 1 mg/ml in 10 % ethanol (2.9 mM).

Dichlorvos was from Chem Service Inc., West Chester, PA.. (PS-89) Lot 209-130B Purity: 98% Exp 06/00, MW 221, SG 1.42 g/ml. A 1 mg/ml stock solution was prepared in 0.9% NaCl (Sigma S8776 lot 33K2413). Aliquots were stored at –80°C.

Malathion-O-analog (also called malaoxon) was from Chem Service, Inc., West Chester, PA. MET-86C, lot 299-68A Purity 97.8%, Exp. 09/03. MW= 330.36.

Malathion-O-analog is only slightly soluble in water. Therefore corn oil (Mazola, Best Food, Englewood Cliffs, NJ) was used as the diluent. A stock solution of 5.0 mg/ml was prepared in corn oil and stored at –20°C.

Mice. The Institutional Animal Care and Use Committee of the University of Nebraska Medical Center approved all procedures involving mice. Animal care was provided in accordance with the principles and procedures outlined in the National Research Council Guide for the Care and Use of Laboratory Animals. AChE -/- mice were made by gene targeting at the University of Nebraska Medical Center (Xie et al., 2000). The animals are in strain 129Sv genetic background. The colony is maintained by breeding heterozygotes because AChE -/- mice do not breed (Duysen et al., 2002). Wild-type mice are littermates of AChE-/- mice.

The chlorpyrifos oxon treatment group used 5 adult males of each genotype AChE -/-, +/-, and +/+. Each animal received 0.75 mg/kg i.p. The average age of each group of animals was 66 days (AChE -/-), 60 days (AChE +/-), and 71 days (AChE +/+) with a 10% variation. The average weight of each group was 19.9 g (AChE -/-), 29.0 g (AChE +/-), and 30.0 g (AChE +/+) with a standard deviation of 1-10%.

The dichlorvos treatment group used 5 adult female mice of each AChE genotype. AChE+/+ and +/- mice received 7 mg/kg ip, while AChE-/- mice received 1 mg/kg ip. The average age of each group of animals was 60 days (AChE-/-), 60 days (AChE+/-), and 55 days (AChE+/+) with a 10% variation. The average weight of each group was 16.8 g (AChE-/-), 22.1 g (AChE+/-), and 20.4 g (AChE+/+) with a standard deviation of 10%.

The malaoxon treatment group used 5 adult males of each AChE genotype. Each animal received 15 mg/kg ip. The average age of each group of animals was 75 days (AChE-/-), 78 days (AChE+/-), and 81 days (AChE+/+) with up to 17% variation. The average weight of each group was 17 g (AChE-/-), 29 g (AChE+/-), and 29 g (AChE+/+) with a standard deviation of 3-18%.

Determination of Minimum Toxic Dose. Each animal was weighed, its surface body temperature measured, and a functional observational battery of tests performed prior to treatment. OP was injected intraperitoneally with a Hamilton syringe. After the toxin was administered the animals were observed for toxic signs for a period of two hours. Temperature was measured every 5 min for the first 20 minutes, and every 10 minutes thereafter up to 2 hours.

Functional Observational Battery. The tests for toxicity (McDaniel and Moser, 1993; Moser, 1995) included observation of lacrimation, salivation, posture, gait, defecation, urination, piloerection, myoclonic jerks, tremor, arousal, body temperature, changes in body weight, vocalization, palpebral closure, reaction to being handled, hydration, mobility, stereotypic behavior including retropulsion, Straub tail, and writhing.

Results

Chlorpyrifos oxon

The minimum toxic dose of chlorpyrifos oxon was 0.75 mg/kg ip for AChE +/- mice (n=

5). This dose produced very few symptoms in the wild type (n=5) and relatively severe symptoms in AChE -/- mice (n=5). The results from the functional observational battery of tests are in Table 2.1.

Table 2.1 Toxic signs in mice treated with 0.75 mg/kg chlorpyrifos oxon ip. N=5 adult male mice in each group.

ID	Age days	Wt (g)	Temp maxΔ	hunched	twitch	tremor	myoc jerks	less alert	saliva tion	lacrim ation	piloer ection
heterozygote											
M2+/-	69	28.9	+1.0	yes	no	no	no	yes	no	no	yes
M3+/-	59	28.7	+0.1	yes	yes	no	no	yes	no	no	yes
M8+/-	54	26.0	+0.9	yes	yes	no	no	yes	no	no	no
M5+/-	59	32.3	+0.3	yes	yes	no	no	yes	no	no	no
M4+/-	59	28.9	+0.9	yes	no	no	no	yes	no	no	yes
Avg	60	29.0	+0.6	5/5	3/5	0/0	0/0	5/5	0/0	0/0	3/5
SD	5.5	2.2	0.4								
Wild type											
M4+/+	78	35.5	+0.9	no	no	no	no	yes	no	no	no
M3+/+	76	28.3	+0.5	no	no	no	no	no	no	no	no
M2+/+	83	29.4	+0.3	no	no	no	no	yes	no	no	no
M3+/+	58	28.6	+0.3	yes	no	no	no	yes	no	no	yes
M6+/+	59	27.3	+0.1	no	no	no	no	yes	no	no	no
Avg	71	30.0	+0.4	1/0	0/0	0/0	0/0	4/5	0/0	0/0	1/5
SD	11.5	3.3	0.3								
nullizygote											
M6-/-	67	20.8	-1.2	yes	yes	yes	yes	yes	yes	no	yes
M8-/-	63	19.8	-1.4	yes	no	yes	yes	yes	yes	no	yes
M2-/-	64	21.4	-1.6	yes	yes	yes	yes	yes	yes	no	yes
M3-/-	64	18.6	-1.6	yes	no	yes	yes	yes	yes	no	yes
M5-/-	73	18.9	-1.0	yes	yes	yes	yes	yes	yes	no	yes
Avg	66	19.9	-1.4	5/5	3/5	5/5	5/5	5/5	5/5	0/0	5/5
SD	5.5	2.2	0.4								

The maximum change in temperature (°C) over a period of 120 minutes post-dosing is reported.

Both AChE +/- and +/+ animals had slight increases in body temperature at the 0.75 mg/kg dose of chlorpyrifos oxon, while the AChE -/- animals had a significant decrease (1.4°C ± 0.4). All AChE -/- and +/- animals displayed hunched posture at some point during the treatment, while only one AChE +/+ animal had a hunched posture. Six of ten AChE -/- and +/- animals had a twitch either in their ears or on their skin at some point in the two hours following treatment. No AChE +/+ animals exhibited a twitch or lacrimation. All five AChE -/- animals developed a clonic tremor and myoclonic jerks above their innate mild tremor. No AChE +/- or +/+ animals developed tremors or myoclonic jerks. All of the animals tested with the exception of one AChE +/+ animal became less alert, that is, they had fewer exploratory movements and they had periods of immobility.

All five AChE -/- animals had an increase in salivation ranging from mild to severe. No AChE +/- or +/+ animals had increased salivation. Lacrimation was not observed in any animal of any genotype. All the AChE -/- animals, three of five AChE +/- animals, and one AChE +/+ animal displayed piloerection. The same wild type

12

animal that was hunched had piloerection. Two AChE +/- animals had red paws and snout. Other cholinergic symptoms noted in the AChE -/- group included retropulsion, frantic activity for a brief period immediately after dosing, partially closed eyes, mucus in the eyes, ataxic gait, splayed legs, flattened posture, severe tremor, and Straub tail.

Dichlorvos

During dose finding experiments it was noticed that AChE+/+ and +/- mice had severe symptoms after receiving 10 mg/kg dichlorvos ip, but slight to no symptoms after 5 mg/kg. A dose of 7.0 mg/kg dichlorvos was chosen as a dose that produced mild symptoms in the +/+ and +/- animals, while eliciting a temperature difference between the genotypes. Five +/+ and five +/- animals were tested. The +/- animals had a significantly larger decrease in body temperature compared to the +/+ animals (see Figure 2.1). Treatment with 7.0 and 5.0 mg/kg dichlorvos was fatal to nullizygotes, therefore five nullizygotes were tested with 1.0 mg/kg to determine cholinergic symptoms at this lower non-lethal dose.
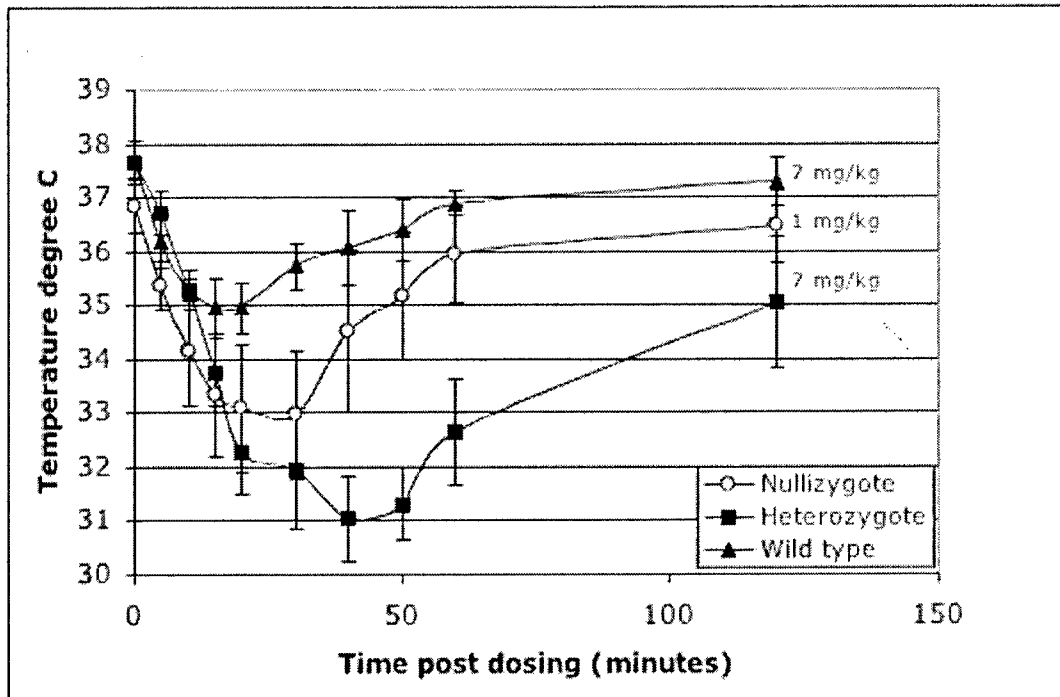
Figure 2.1. Effect of dichlorvos on body temperature. Surface body temperature was measured after ip injection of 7 mg/kg dichlorvos to AChE +/+ and +/- mice, and 1 mg/kg to AChE-/- mice (n=5 adult females per group).

Figure 2.1 shows that a dose of 7.0 mg/kg dichlorvos discriminates AChE+/+ from AChE+/- animals. Surface body temperature of AChE+/+ mice decreased 2.8°C (SD±0.5) at 15 minutes and then slowly returned to normal. In contrast the body temperature of AChE+/- animals decreased an average of 6.9°C (SD±0.8), reaching a minimum temperature 40 minutes after dosing. The temperature was still well below normal 2 hours after dosing. The body temperature of AChE-/- mice treated with 1.0

mg/kg dichlorvos decreased 4.5°C at 30 min post dosing. At two hours, the temperature was still low.

Table 2.2. Toxic signs in mice treated with dichlorvos. AChE+/- and +/+ received 7 mg/kg ip. AChE-/- received 1 mg/kg ip. N=5 adult females in each group.

ID	Age days	Wt (g)	Temp maxΔ (°)	hunched	twitch	tremor	myoc jerks	less alert	saliva tion	lacrim ation	piloer ection
Heterozygote											
F2+/-	57	18.98	-7.9	yes	yes	yes	no	yes	no	yes-mucus	yes
F2+/-	51	21.22	-5.8	yes	no	no	no	yes	no	no	yes
F3+/-	57	18.63	-7.1	yes	no	yes	no	yes	no	no	yes
F3+/-	56	22.64	-6.5	yes	no	no	no	yes	no	yes mucus	yes
F4+/-	56	20.3	-7.0	yes	no	yes	no	yes	no	no	yes
Avg	55.4	20.4	-6.9	5/5	1/5	3/5	0/5	5/5	0/0	2/5	5/5
SD	2.5	1.6	0.8								
Wild type											
F1+/+	55	22.76	-3.6	yes	no	no	no	yes	no	no	yes
F5+/+	70	23.19	-2.3	yes	no	no	no	yes	no	no	no
F9+/+	51	19.97	-2.9	yes	yes	no	no	yes	no	no	yes
F4+/+	70	24.28	-2.7	yes	yes	yes	no	yes	no	no	yes
F5+/+	56	20.5	-2.6	yes	no	yes	no	yes	no	no	yes
Avg	60.4	22.14	-2.8	5/5	2/5	2/5	0/5	5/5	0/0	0/5	4/5
SD	9.0	1.83	0.5								
Nullizygote											
F2-/-	69	19.06	-4.9	yes	yes	yes	yes	yes	no	yes	yes
F1-/-	55	15.68	-4.8	yes	yes	yes	yes	yes	no	yes	yes
F3-/-	63	16.07	-4.0	yes	yes	yes	no	yes	no	yes	yes
F3-/-	61	14.23	-4.2	yes	yes	yes	yes	yes	no	yes	yes
F5-/-	53	18.9	-4.5	yes	yes	yes	no	yes	no	yes	yes
Avg	60.2	16.8	-4.5	5/5	5/5	5/5	3/5	5/5	0/0	5/5	5/5
SD	6.4	2.1	0.4								

The maximum change in temperature (°C) over a period of 120 minutes post-dosing is reported.

The response of AChE+/+ and +/- mice to 7.0 mg/kg dichlorvos was similar in all parameters tested, with the exception of the body temperature shown in Figure 2.1. Both genotypes had hunched posture, piloerection, and were less alert. A few had twitch and tremor. None had myoclonic jerks. See Table 2.2. The cholinergic signs of toxicity were more severe in AChE-/- mice even though the dose of dichlorvos was only 1.0 mg/kg. The AChE-/- mice had hunched posture, twitch, tremor, lacrimation, piloerection, and they were less alert. A few had myoclonic jerks. In addition their rate of respiration increased, eyes were partly closed, they had splayed feet and ataxic gait, flattened body and they vocalized. No animals salivated in response to dichlorvos.

All doses of dichlorvos that caused even slight toxic symptoms in AChE +/+ and +/- animals were fatal to the -/- animals. Therefore a dose of 1.0 mg/kg dichlorvos was used in the AChE -/- animals to demonstrate cholinergic toxicity, even though this dose elicited no toxic symptoms in AChE +/+ and +/- animals.

Malaoxon

At a dose of 15 mg/kg malaoxon ip, five AChE +/- animals showed moderate cholinergic symptoms (Table 2.3) including an average drop in temperature of -2.7°C (SD±0.6), hunched posture (5/5), twitching or quivers of the ears and skin (4/5), decreased alertness (5/5), piloerection (5/5), splayed hind limbs (2/5), reduced body tone (3/5), rapid respirations (5/5), Straub tail (1/5), flattened posture (1/5), red paws and red snout (3/5). The AChE +/- mice recovered their body temperature and normal activity within 30 minutes post dosing. Wild type animals (n=5) treated with the same dose of 15 mg/kg had virtually no cholinergic symptoms. The only symptom noted was decreased arousal (4/5). The wild type animals had an average increase in temperature of 0.5°C (SD±1.0). The AChE -/- mice treated with 15 mg/kg malaoxon displayed moderately severe to severe cholinergic symptoms. These animals had an average drop in temperature of 2.5°C (SD±0.6), similar to the drop in temperature in AChE +/- animals, although the nullizygotes took longer to regain their normal body temperature. Other symptoms in AChE-/- mice included hunched posture (5/5), twitching or quivers of the ears and skin (5/5), severe whole body tremors (5/5), myoclonic jerks (5/5), decreased arousal (5/5), salivation (slight) (5/5), piloerection (5/5), splayed hind limbs (5/5), rapid respirations (5/5), flattened posture (5/5), red paws and snout (1/5), eyes partially closed (1/5), mucus in eyes (4/5), ataxic gait (5/5), penis protruding (1/5), and loose feces (2/5). Lacrimation was not found in any animal of any genotype.

Table 2.3. Toxic signs in mice treated with 15 mg/kg malaoxon ip. N=5 adult males in each group

ID	Age days	Wt (g)	Temp maxΔ	hunched	twitch	tremor	myoc jerks	less alert	saliv ation	lacrim ation	piloer ection
Heterozygote											
M6+/-	68	26.68	-3.4	yes	yes	no	no	yes	no	no	yes
M5+/-	89	29.15	-1.9	yes	no	no	no	yes	no	no	yes
M3+/-	83	27.87	-2.3	yes	yes	no	no	yes	no	no	yes
M4+/-	83	29.4	-2.7	yes	yes	no	no	yes	no	no	yes
M3+/-	69	30.4	-3.0	yes	yes	no	no	yes	no	no	yes
Avg	78	29	-2.7	5/5	4/5	0/5	0/5	5/5	0/5	0/0	5/5
SD	9.4	1.4	0.6								
Wild type											
M7+/+	88	26.88	+ 1.8	no	no	no	no	yes	no	no	no
M2+/+	92	28.86	+0.6	no	no	no	no	no	no	no	no
M5+/+	92	33.52	-1.0	no	no	no	no	yes	no	no	no
M1+/+	66	28.9	+0.8	no	no	no	no	yes	no	no	no
M3+/+	66	26.4	+0.3	no	no	no	no	yes	no	no	no
Avg	81	29	+0.5	0/5	0/5	0/5	0/5	4/5	0/5	0/0	0/5
SD	13.6	2.8	1.0								
Nullizygote											
M6-/-	71	18.64	-3.0	yes	yes	yes	yes	yes	yes	no	yes
M7-/-	71	12.97	-2.4	yes	yes	yes	yes	yes	yes	no	yes
M1-/-	92	19.05	-1.7	yes	yes	yes	yes	yes	yes	no	yes
M8-/-	71	15.77	-2.1	yes	yes	yes	yes	yes	yes	no	yes
M10-/-	71	18.03	-3.1	yes	yes	yes	yes	yes	yes	no	yes
Avg	75	17	-2.5	5/5	5/5	5/5	5/5	5/5	5/5	0/0	5/5
SD	9.4	2.5	0.6								

The maximum change in temperature (°C) over a period of 120 minutes post-dosing is reported.

15

A single dose of malaoxon caused very different toxicity in AChE+/+, +/-, and -/-mice. AChE+/+ mice had no symptoms, AChE+/- mice had moderate symptoms, and AChE-/- mice had severe symptoms after 15 mg/kg malaoxon ip.

Discussion

Toxic signs. Chlorpyrifos oxon, dichlorvos, and malaoxon had the same acute effects. AChE-/- mice had the most severe symptoms. These cholinesterase inhibitors produced hypothermia, tremors, gait and posture changes, decrease in exploratory behavior, and myoclonic jerks. None of the OP caused both salivation and lacrimation at the doses tested. Chlorpyrifos oxon and malaoxon caused salivation but no lacrimation, while dichlorvos caused no salivation but did cause lacrimation. This is in agreement with Moser, who had previously reported that chlorpyrifos is not as effective in producing lacrimation as other compounds (Moser, 1995). The toxic signs observed in AChE-/- mice are characteristic of cholinergic overstimulation, attributed to inhibition of AChE. However, the AChE-/- mice have no AChE enzyme or AChE protein. They do have normal amounts of butyrylcholinesterase (BChE). It seems reasonable to conclude that the mechanism of OP toxicity in AChE-/- mice involves inhibition of BChE.
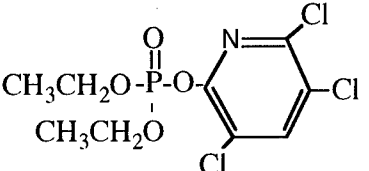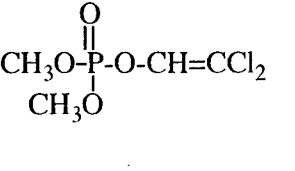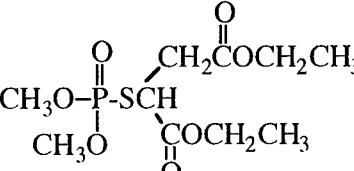
Additional sites of action of OP. Toxicologists have found that OP have other biological actions in addition to their cholinesterase-inhibitory properties (Moser, 1995; Pope, 1999). Some compounds interact directly with muscarinic or nicotinic receptors. Chlorpyrifos alters the activity of the adenylyl cyclase signaling cascade (Song et al., 1997). Acylpeptide hydrolase is more sensitive than AChE to inhibition by chlorpyrifos methyl oxon, dichlorvos, and DFP (Richards et al., 2000). The goal of this work is to identify these additional sites.

Why is the minimal toxic dose different for each OP? Chlorpyrifos oxon is twenty times more potent than malaoxon in mice. If potency were explained entirely by inhibition of AChE and BChE, then potency should correlate with the rate constant for inhibition of AChE and BChE. Table 2.4 shows an 80 fold difference in the rate constants for reaction with AChE, and a 120,000 fold difference in the rate constants for reaction with BChE when comparing chlorpyrifos oxon and malaoxon.

Table 2.4. Comparison of rate constants for reaction of OP with human AChE, human BChE, and the minimal toxic dose in wild-type mice

OP	k, M^{-1} min^{-1} AChE	k, M^{-1} min^{-1} BChE	Reference	Minimal toxic dose, mg/kg ip
Chlorpyrifos oxon	1.0×10^7	1.7×10^9	(Amitai et al., 1998)	0.75
Dichlorvos	1.2×10^5	8.7×10^5	(Skrinjaric-Spoljar et al., 1973)	7 (1 for AChE-/-)
Malaoxon	1.3×10^5	1.5×10^4	(Rodriguez et al., 1997)	15

AChE-/- mice have only BChE but no AChE. Therefore, it could be expected that chlorpyrifos oxon would be 120,000 times more potent than malaoxon. This was not found. Chlorpyrifos oxon was indeed more potent than malaoxon but only 20 fold more potent. Factors other than rate of inhibition of BChE must be important. Fat solubility and ability to cross membranes probably influence toxicity. The structures of chlorpyrifos oxon and malaoxon in Figure 2.2 show both OP to be hydrophobic compounds, more soluble in organic than in aqueous solvents.

chlorpyrifos oxon	dichlorvos	malaoxon

Figure 2.2. OP structures.

Scavengers other than BChE could play a role. In Task 4 we report that albumin is a scavenger of OP. Albumin appears to act as a sink for OP. Since the concentration of albumin is very high, exceeding the BChE concentration by 10,000 fold, a considerable amount of OP could be neutralized by binding to albumin.

Relevance to humans. Malathion is widely used. The cities and suburbs of California as well as New York city are sprayed with malathion to kill mosquitoes that carry the West Nile virus. The active component of malathion is malaoxon. We have shown that AChE deficient mice are more senstitive to the toxicity of malaoxon than wild-type mice. By analogy, we expect that AChE deficient humans will be intoxicated by doses of malaoxon that cause no symptoms in the average person. AChE deficiency in humans has not yet been identified but it must exist. People who are sensitive to pesticides are good candidates for AChE deficiency.

Task 3

Human and mouse brains will be extracted and treated with
biotinylated OP. The biotinylated proteins will be
purified with avidin-Sepharose, and separated by gel
electrophoresis. The number and size of proteins that
reacted with biotinylated OP will be visualized on blots by
treating with avidin conjugated to an indicator.

Task 3.1. Relation to statement of work. Task 3 has been completed.

3.1. OP Reactive Proteins in Mouse Brain

Abstract

Mouse brains were extracted and treated with FP-biotin. The proteins were separated
by gel electrophoresis and transferred to a membrane. Biotinylated proteins were
visualized by hybridization with streptavidin conjugated to a fluorophore. About 55 FP-
biotin labeled proteins were identified in the 100,000xg supernatant of mouse brain. To
prepare proteins for identification by mass spectrometry, we developed techniques to
purify FP-biotin-labeled proteins. Purification was achieved by binding to avidin-
agarose followed by gel electrophoresis.

Introduction

The purpose of this work is to identify proteins that react with organophosphorus
agents (OP). We are especially interested in proteins that react with OP at doses that
do not significantly inhibit acetylcholinesterase (AChE). It is generally agreed that the
acute toxicity of OP is due to inhibition of AChE, however little is known about low dose
effects. Biomarkers for low dose exposure to OP are needed. The techniques
developed in this report are intended to identify new biomarkers.

Methods
Preparation of sub-cellular fractions from mouse brain, and protein quantitation.
Mouse brain was separated into its sub-cellular fractions by centrifugation, essentially
as described (Gray and Whittaker, 1962). Brain tissue was homogenized by two 1-
minute disruptions with a Potter-Elvehjem homogenizer (Teflon pestle with glass vessel)
rotating at 840 rpm (in 10-volumes of ice cold 50 mM TrisCl buffer, pH 8.0, containing
0.32 M sucrose, to prevent disruption of organelles). The suspension was centrifuged
at 1000xg for 10 minutes at 4°C to pellet nuclei, mitochondria, plasma membranes and
unbroken cells. The supernatant was re-centrifuged at 17,000xg for 55 minutes at 4°C
to pellet myelin, synaptosomes and mitochondria. That supernatant was re-centrifuged
at 100,000xg for 60 minutes at 4°C to separate microsomes (pellet) from soluble

proteins (supernatant).

Protein in the supernatant fraction was estimated by absorbance at 280 nm, using A_{280} = 1.0 for 1 mg protein/ ml. The 100,000xg supernatant was divided into 0.4 ml aliquots and stored at -70°C, along with the other sub-cellular fractions.

Labeling proteins with FP-biotin. Mouse brain supernatant (0.1 ml of 1.25 mg protein/ml was reacted with 2-40 μM FP-biotin in 50 mM TrisCl buffer, pH 8.0, containing 5 mM EDTA and 2.4% methanol at 25°C for up to 450 minutes. Reaction was stopped by addition of 1/5 volume of 10% SDS, 30% glycerol, 0.6 M dithiothreitol, and 0.012% bromophenol blue in 0.2 M TrisCl buffer, pH 6.8; followed by heating at 80°C for 5 minutes.

Visualization of FP-biotin labeled proteins. For determination of the number and size of proteins labeled by FP-biotin, proteins were subjected to SDS gel electrophoresis, the proteins transferred to a PVDF membrane, and the protein bands visualized with a fluorescent probe. The details of the procedure follow.

A 10-20% gradient SDS-PAGE with 4% stacking gel was poured in a Hoefer gel apparatus. The dimensions of the sandwich were 16x18x0.075 cm, with 20 wells. Twenty-four to thirty micrograms of protein were loaded per lane. Electrophoresis was for 4000 volt-hours in the cold room (4°C), with stirring. The bottom tank contained 4.5 L of 60 mM TrisCl buffer, pH 8.1, plus 0.1% SDS. The top tank buffer contained 0.6 L of 25 mM Tris, 192 mM glycine buffer, pH 8.2, plus 0.1% SDS.

Proteins were transferred from the gel to PVDF membrane (Immun-Blot from BioRad) electrophoretically in a tank using plate electrodes (TransBlot from BioRad), at 0.5 amps, for 1 hour, in 3 L of 25 mM Tris/192 mM glycine buffer, pH 8.2, in the cold room (4°C), with stirring. The membrane was blocked with 3% gelatin (BioRad) in 20 mM TrisCl buffer, pH 7.5, containing 0.5 M NaCl for 1 hour at room temperature. The 3% gelatin solution had been prepared by heating the gelatin in buffer in a microwave oven for several seconds. The blocked membrane was washed twice with 20 mM TrisCl buffer, pH 7.5, containing 0.5 M NaCl and 0.05% Tween-20, for 20 minutes.

Biotinylated proteins were labeled with 9.5 nM Streptavidin-Alexa 680 fluorophore in 20 mM TrisCl buffer, pH 7.5, containing 0.5 M NaCl and 1% gelatin, for 2 hours, at room temperature, protected from light. Shorter reaction times resulted in less labeling. The membrane was washed twice with 20 mM TrisCl buffer, pH 7.5, containing 0.5 M NaCl and 0.05% Tween-20, and twice with 20 mM TrisCl buffer, pH 7.5, containing 0.5 M NaCl, for 20 minutes each. This is essentially the BioRad protocol (BioRad Lit 171 Rev D).

Membranes were scanned with the Odyssey Infrared Imaging System (LI-COR, Lincoln, NE) at 42 microns per pixel. The Odyssey employs an infrared laser to excite a fluorescent probe which is attached to the target protein, and then collects the emitted light. The emitted light intensity is directly proportional to the amount of probe. Both the laser and the detector are mounted on a moving carriage positioned directly below the membrane. The membrane can be scanned in step sizes as small as 21 microns, providing resolution comparable to x-ray film. Data are collected using a 16-bit dynamic range, and can be transferred directly to the Kodak 1D analysis program. The fluorophore is stable in the laser, making it possible to scan the membrane repeatedly, while using

different intensity settings to optimize data collection for both strong and weak signals. The membrane is kept wet during scanning.

The intensity of the signal from each labeled protein was determined using a Gaussian deconvolution routine from the Kodak 1D Image Analysis program, v 3.5.3 (Kodak).

Isolation of FP-biotin labeled protein. To prepare OP-labeled proteins for mass spectrometry, FP-biotin labeled proteins were purified on avidin-agarose beads and separated by SDS polyacrylamide gel electrophoresis. The following method was modified from (Kidd et al., 2001) . Protein (6.3 mg in 4.5 ml of 50 mM TrisCl, pH 8.0, containing 5 mM EDTA) was reacted with 10 µM FP-biotin for 5 hours at 25°C. The reaction mixture was passed over a 3.5 x 32 cm Sephadex G-25 gel filtration column (Pharmacia) to separate unreacted FP-biotin from protein. The protein eluant was heated in the presence of 0.5% SDS at 85°C for 3 minutes to enhance accessibility of the biotin label. The protein was diluted 2.5-fold with the starting buffer, to yield 0.2% SDS, and incubated with 200 µl of avidin-agarose beads (catalog # A-9207 Sigma-Aldrich.com, 1.9 mg avidin/ml of beads) overnight at room temperature, with continuous mixing. Beads were washed three times with the TrisCl/EDTA buffer, containing 0.2% SDS. Fifty µl of 6x SDS PAGE loading buffer (0.2 M TrisCl, pH 6.8, 10% SDS, 30% glycerol, 0.6 M dithiothreitol and 0.012% bromophenol blue) were added to the 200 µl of beads, and the mixture was heated at 85°C for 3 minutes. This step released the biotinylated proteins from the avidin beads. Equal amounts of the bead mixture were loaded directly into two dry wells of a 10-20% gradient SDS PAGE (10-well format, 1.5 mm thick) and run for 4000 volt-hours in the cold room. The gel was stained with Coomassie blue G250 (Bio-Safe from BioRad), and destained with water. Coomassie G250 is reportedly 2-8 fold more sensitive than Coomassie R250 (BioRad specifications). In order to minimize contamination from keratin, the staining dish had been cleaned with sulfuric acid, and the water was Milli-Q purified. For the same reason, gloves were worn for all operations involving the gel.

Results
Resolution of the screening procedure. When the SDS PAGE electrophoresis was run for 3600-4000 volt-hours the OP-labeled proteins resolved into 55 bands (see Figure 3.1.1).
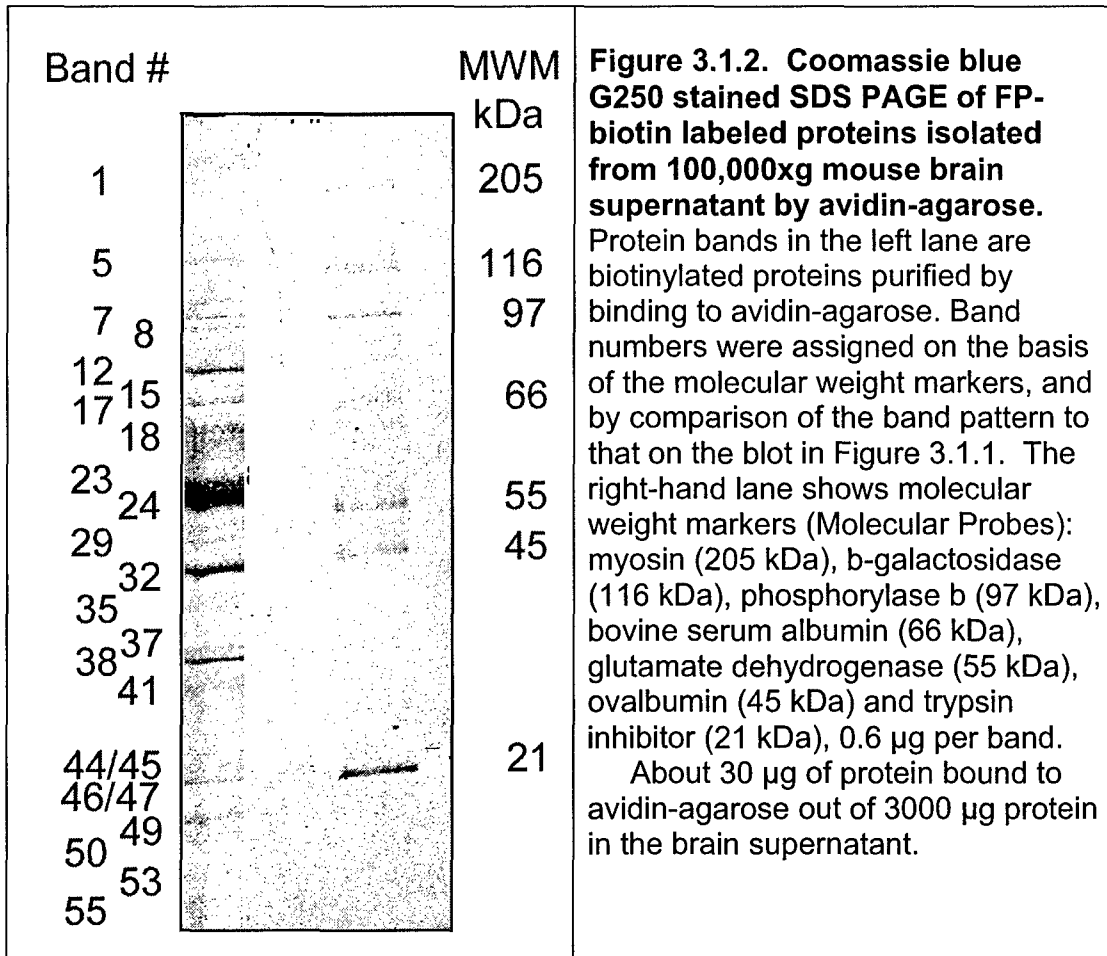
A series of experiments similar to that in Figure 3.1.1, using a range of FP-biotin concentrations, showed that a reaction time of 300 minutes with 10 µM FP-biotin gave maximum labeling. Use of lower concentrations of FP-biotin required longer reaction times to achieve maximum labeling. It was estimated that the proteins capable of reacting with FP-biotin had a concentration of 1 µM, so that 10 µM FP-biotin was a 10-fold excess. Figure 3.1.1 shows that 55 biotinylated bands could be resolved. Three out of 55 bands were endogenous biotinylated proteins. The endogenous biotinylated proteins were bands 1, 14, and 15.
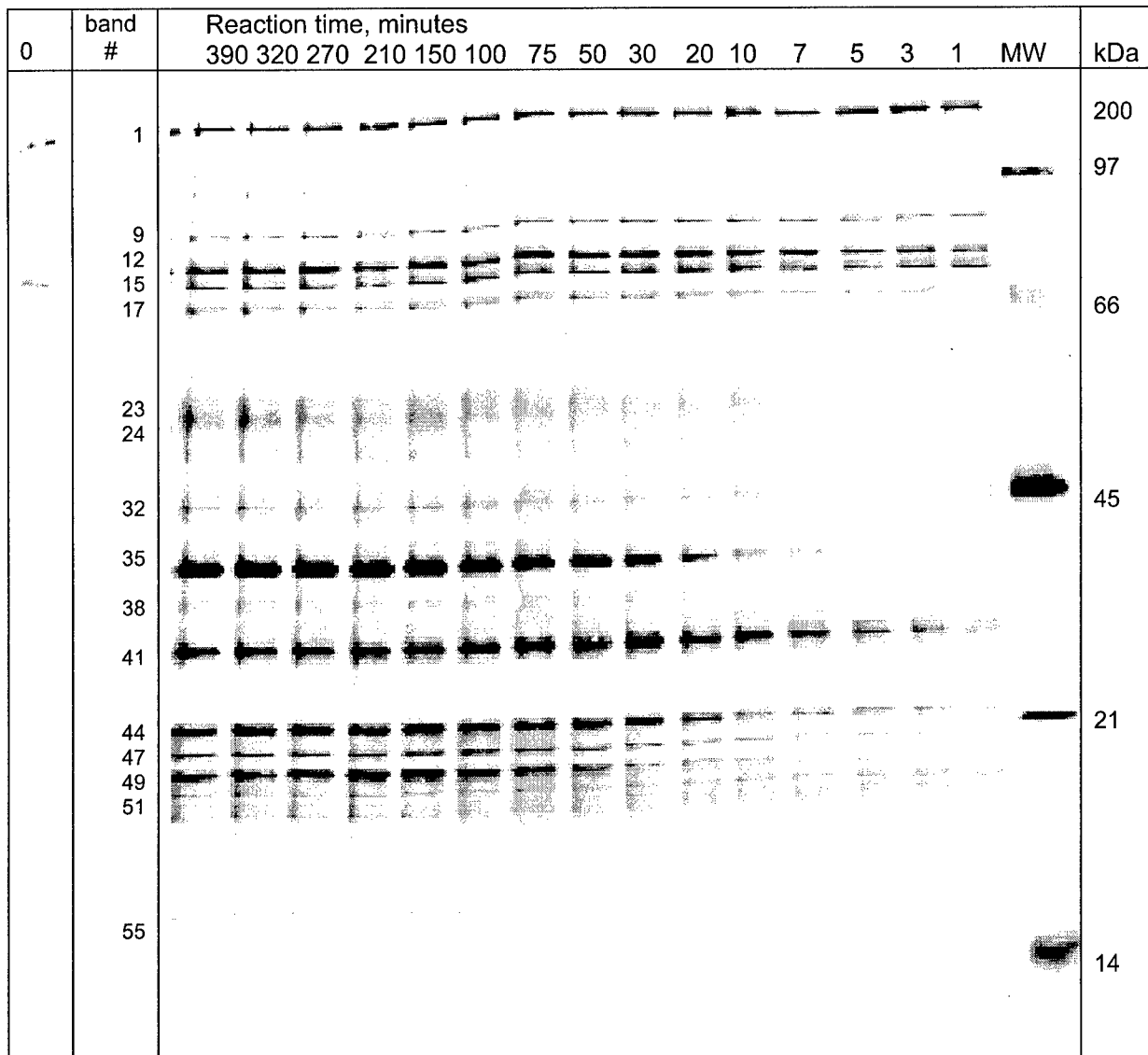
Figure 3.1.1. SDS-PAGE showing the time course for the reaction of FP-biotin with proteins extracted from mouse brain. The 10 µM FP-biotin was reacted with 1.25 mg protein/ml of mouse brain supernatant in 50 mM TrisCl buffer, pH 8.0, containing 5 mM EDTA and 2.4% methanol, at 25°C, for selected times. The numbers above each lane indicate the reaction times in minutes. 30 µg protein was loaded per lane. Biotinylated molecular weight markers were from BioRad. Endogenous biotinylated proteins are in bands 1, 14, and 15. A total of 55 biotinylated protein bands are visible.

Isolation of FP-biotin labeled proteins. To prepare FP-biotin labeled proteins for identification by mass spectrometry, FP-biotin labeled proteins were purified by binding to avidin-agarose and separated by electrophoresis on SDS polyacrylamide gel.

Twenty-two bands could be seen on a Coomassie G250 stained, SDS PAGE gel, of biotin labeled proteins extracted from the 100,000xg mouse brain supernatant and purified on avidin-agarose (Figure 3.1.2). Numbers were assigned to the bands based on the band positions relative to the molecular weight markers, and by comparison of the band pattern to the blot in Figure 3.1.1.

| Band # | | MWM kDa | Figure 3.1.2. Coomassie blue G250 stained SDS PAGE of FP-biotin labeled proteins isolated from 100,000xg mouse brain supernatant by avidin-agarose. |

Figure 3.1.2. Coomassie blue G250 stained SDS PAGE of FP-biotin labeled proteins isolated from 100,000xg mouse brain supernatant by avidin-agarose. Protein bands in the left lane are biotinylated proteins purified by binding to avidin-agarose. Band numbers were assigned on the basis of the molecular weight markers, and by comparison of the band pattern to that on the blot in Figure 3.1.1. The right-hand lane shows molecular weight markers (Molecular Probes): myosin (205 kDa), b-galactosidase (116 kDa), phosphorylase b (97 kDa), bovine serum albumin (66 kDa), glutamate dehydrogenase (55 kDa), ovalbumin (45 kDa) and trypsin inhibitor (21 kDa), 0.6 µg per band.
About 30 µg of protein bound to avidin-agarose out of 3000 µg protein in the brain supernatant.

There were 22 Coomassie stained bands in Figure 3.1.2. The 22 bands in Figure 3.1.2 corresponded to bands 1, 5, 7, 8, 12, 15, 17, 18, 23, 24, 29, 32, 35, 37, 38, 41, 44+45, 46+47, 49, 50, 53, and 55 in Figure 3.1.1.

To determine whether all the Coomassie stained protein bands were biotinylated, the same avidin-agarose purified protein sample was transferred to PVDF membrane and stained with streptavidin Alexafluor. Figure 3.1.3 compares the staining patterns and shows that every Coomassie stained band has a corresponding fluorescent band. The pattern of staining is different in panels A and B of Figure 3.1.3, indicating that the fluorescent signal from binding to streptavidin Alexafluor does not correlate with the quantity of protein revealed by staining with Coomassie blue.

The pattern of fluorescent bands in Figure 3.1.3 for the avidin-agarose purified proteins is similar to the pattern of fluorescent bands in Figure 3.1.1 where proteins had

not been purified on avidin-agarose before gel electrophoresis. This means that all biotinylated proteins bound with similar affinity to the avidin-agarose beads and that no protein was selectively excluded.
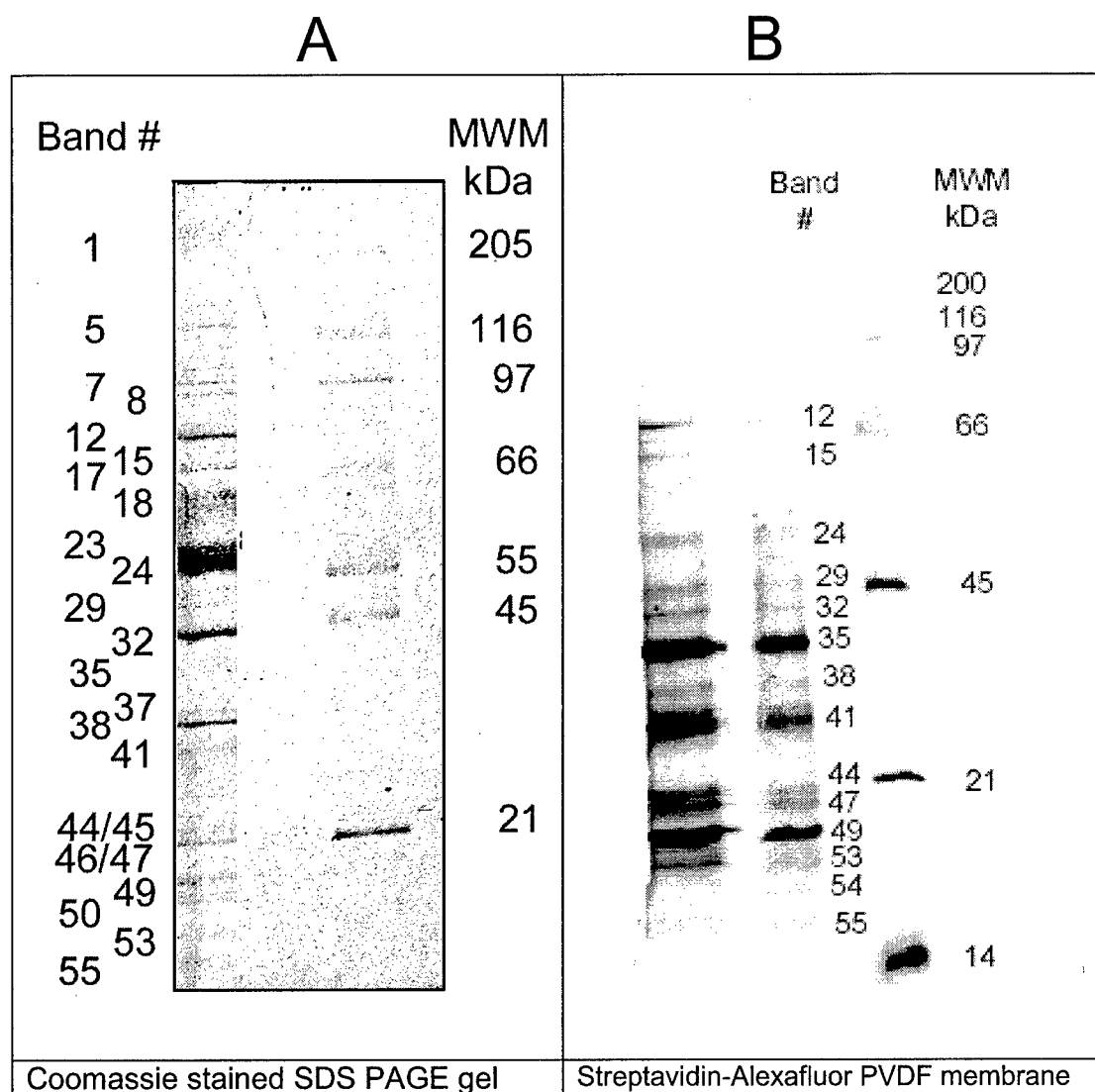

Figure 3.1.3. Comparison of Coomassie blue staining and fluorescent signal intensity. The same sample of avidin-agarose purified FP-biotin labeled protein was loaded into three lanes of an SDS PAGE gel. One lane was stained with Coomassie blue in panel A, while protein in two other lanes was transferred to PVDF membrane and stained with avidin-Alexafluor in panel B.

Discussion
Number of proteins that react with FP-biotin. Soluble mouse brain extract had 55 biotinylated bands after reaction with FP-biotin. Of these, 3 were endogenous

biotinylated proteins and 52 were produced by reaction with FP-biotin. Liu et al (Liu et al., 1999) found 12 protein bands in the soluble fraction of rat brain after labeling with FP-biotin. The lower number of bands found by Liu et al. (Liu et al., 1999) is explained by shorter reaction time (30 min rather than 2 h), lower concentration of FP-biotin (2 µM rather than 10 µM), use of a lower resolution gel, and detection with chemiluminescence rather than with fluorescence.
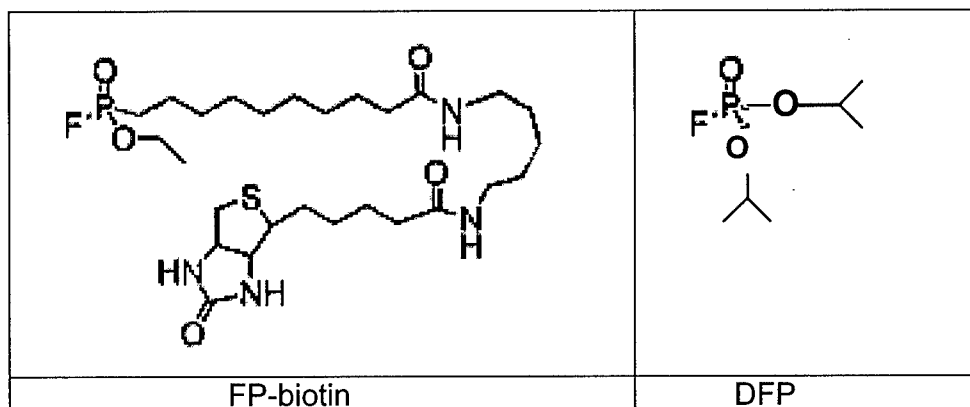
| FP-biotin | DFP |

Figure 3.1.4. Structures of FP-biotin and DFP.

FP-biotin is similar in structure to DFP, with the difference that biotin on a 17 atom spacer is substituted for one of the isopropyl groups of DFP and ethanol is substituted for the other isopropyl group (Figure 3.1.4). FP-biotin reacts with serine hydrolases, for example BChE and AChE, and with serine proteases, for example trypsin (Liu et al., 1999) to make an irreversible covalent bond with the active site serine. Similarly, DFP makes a covalent bond with serine hydrolases and serine proteases by binding to the active site serine. The same mechanism of action of these two compounds allows one to assume that DFP and FP-biotin will label overlapping sets of proteins.

Keshavarz-Shokri et al. (Keshavarz-Shokri et al., 1999) separated 9 bands on gel electrophoresis after labeling chicken brain proteins with 3H-DFP; the sizes were 30 to 155 kDa (Liu et al., 2003). Carrington and Abou-Donia (Carrington and Abou-Donia, 1985) saw 8 DFP-labeled bands in chicken brain ranging in size from 32 to 160 kDa. Richards and Lees (Richards and Lees, 2002) resolved 24 protein spots by 2D-gel electrophoresis of brain proteins labeled with tritiated DFP. Thus, the 52 bands observed in our experiments are a reasonable representation of OP-reactive proteins in the brain. The sizes ranged from 16 to 110 kDa.

Task 3.2. Relation to statement of work. This published paper uses some of the data developed in Task 3.1 to demonstrate the existence of many OP reactive proteins in mouse.

3.2 Life Without Acetylcholinesterase: The Implications of Cholinesterase Inhibitor Toxicity in AChE-Knockout Mice

Oksana Lockridge, Ellen G. Duysen, Troy Voelker, Charles M. Thompson, Lawrence M. Schopfer

Abstract
The acetylcholinesterase (AChE) knockout mouse is a new tool for identifying physiologically relevant targets of organophosphorus toxicants (OP). If AChE were the only important target for OP toxicity, then mice with zero AChE would have been expected to be resistant to OP. The opposite was found. AChE -/- mice were more sensitive to the lethality of DFP, chlorpyrifos oxon, iso-OMPA, and the nerve agent VX. A lethal dose of OP caused the same cholinergic signs of toxicity in mice with zero AChE as in mice with normal amounts of AChE. This implied that the mechanism of toxicity of a lethal dose of OP in AChE -/- mice was the same as in mice that had AChE, namely accumulation of excess acetylcholine followed by overstimulation of receptors. OP lethality in AChE-/- mice could be due to inhibition of BChE, or to inhibition of a set of proteins. A search for additional targets used biotinylated-OP as a marker. *In vitro* experiments found that biotinylated-OP appeared to label as many as 55 proteins in the 100,000xg supernatant of mouse brain. Chlorpyrifos oxon bound a set of proteins (bands 12, 41, 45) that did not completely overlap with the set of proteins bound by diazoxon (bands 9, 12, 41, 47) or dichlorvos (bands 12, 23, 24, 32, 44, 45, 51) or malaoxon (band 9). These results support the idea that a variety of proteins could be interacting with a given OP to give the neurotoxic symptoms characteristic of a particular OP.

A copy of this publication is attached.

Task 3.3. Relation to statement of work. Task 3.3 searched for OP reactive proteins in human brain.

# 3.3. OP Reactive Proteins in Human Brain

Abstract
The goal was to get background information on the number and size of OP reactive proteins in human brain, in preparation for analysis by mass spectrometry in Task 4.3. Proteins in the human hypothalamus and human basal ganglia were labeled with Canadian FP-biotin, excess OP was removed by dialysis, and the OP-derivatized proteins were partially purified by binding to avidin/streptavidin beads. The bound proteins were released from the beads by boiling in buffer containing SDS and dithiothreitol. Proteins were separated on a polyacrylamide gel and visualized by staining with Coomassie blue. FP-biotinylated proteins were visualized by fluorescence of Streptavidin Alexa 680, a probe that bound specifically to biotin. Approximately 20-30 proteins in human hypothalamus and basal ganglia covalently bound FP-biotin.

Introduction
The goal of this task was to prepare for Task 4.3. We wanted to know the maximum number of proteins in human hypothalamus and human basal ganglia that can react with OP under conditions where OP is saturating. Hypothalamus was selected because tracer studies with radiolabeled DFP, soman, and sarin showed a high amount of OP accumulated in the hypothalamus after intravenous injection into mice (Little et al., 1988). The hypothalamus has only low amounts of AChE and BChE, so that binding to cholinesterases does not explain OP accumulation. The basal ganglia was selected because it is rich in AChE, thus maximizing the possibility of detecting OP-bound AChE.

Methods
Canadian FP-biotin. A biotinylated OP was purchased from TRC (Toronto Research Chemicals, Inc. 2 Brisbane Rd., North York, Ontario, Canada M3J 2J8; www.trc-canada.com). The name of the biotinylated OP is 6-N-biotinylaminohexyl isopropyl phosphorofluoride, hemihydrate. Catalog # B394900. Molecular weight 467.20. The structure of the Canadian FP-biotin is shown in Figure 3.3.1. A 174 µM solution was made up in 10% methanol and stored at -80°C.
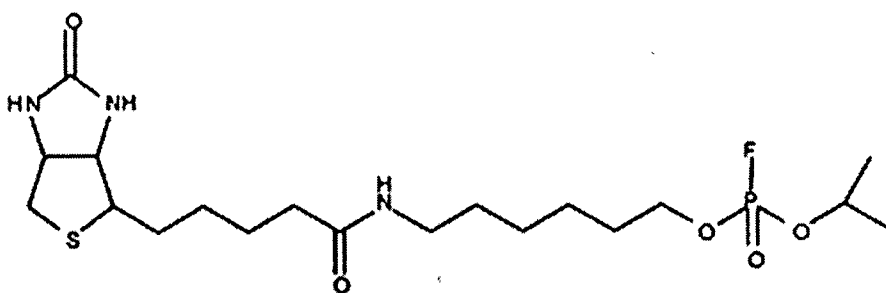
Figure 3.3.1 Canadian FP-biotin. This structure differs from that of the FP-biotin used in other experiments in this report (see Figure 3.1.4) in that the biotin is attached to the phosphate through an oxygen atom. Another important difference is the shorter linker between the phosphorus atom and biotin.

Human brain. One gram of human hypothalamus and 1 gram of human basal ganglia were purchased from the National Disease Research Interchange, Philadelphia, PA (http://www.ndri.com). The donors were an 81 year old Caucasian male who died of prostate cancer and an 82 year old Caucasian male who died after a cerebrovascular accident.

Sample preparation. 0.25 g of human brain was homogenized in 10 volumes of ice cold buffer (50 mM potassium phosphate pH 7.4, 0.5% Tween 20) in a Polytron for 2-5 seconds. The 2.5 ml of homogenate was incubated with 750 µl of 174 µM Canadian FP-biotin for 12 h at 25°C. Excess reagent was removed by dialysis against 5 x 4 L of 50 mM TrisCl, 5 mM EDTA pH 8.0, 4°C over a period of 5 days. After dialysis, the proteins were denatured in the presence of 0.5% SDS by boiling for 3 minutes. The mixture was diluted to 0.2% SDS by the addition of 50 mM TrisCl pH 8,0, 5 mM EDTA, and added to 2.5 ml of packed, washed beads. The beads were a mixture of 60% immobilized Avidin-agarose (Pierce, Rockford, IL; catalog 20225), and 40% Streptavidin-agarose (Sigma, S1638) that had been washed 3 times with 50 mM TrisCl, 5 mM EDTA pH 8.0, to give 2.5 ml of beads. Biotinylated proteins were allowed to bind to the beads by continuous, slow inversion for 16 h at room temperature. To remove nonspecifically bound proteins, the beads were washed 3 times with 10 ml of 50 mM TrisCl, 5 mM EDTA pH 8.0, 0.2% SDS. Bound proteins were released from the beads by boiling the sample in the presence of dithiothreitol and SDS for 3 min.

SDS gel. A 4-30% polyacrylamide gradient gel, 1.5 mm thick, was poured in a Hoefer apparatus. The entire 3.0 ml of beads and liquid were loaded on the 4% stacking gel. Electrophoresis was for 3800 volt hours (210 volts x 18 h) at 4°C. The gel was stained with Coomassie blue.

Visualizing FP-biotin labeled proteins. An FP-biotinylated homogenate of human hypothalamus was subjected to SDS gel electrophoresis on a 4-30% gradient gel. The proteins were transferred to PVDF membrane, and the blot was hybridized with

27

Streptavidin Alexa 680 as described (Peeples et al., 2005). The membrane was scanned with the Odyssey Intrared Imaging system (LI-COR, Lincoln, NE) to reveal fluorescent bands.

Results

Coomassie stained SDS gel. Figure 3.3.2 shows Coomassie stained SDS gels of the proteins in human hypothalamus and basal ganglia that bound to immobilized avidin/streptavidin beads. There were 20 to 30 bands in each gel. The entire gel was sliced into 10 sections in preparation for mass spectral analysis.
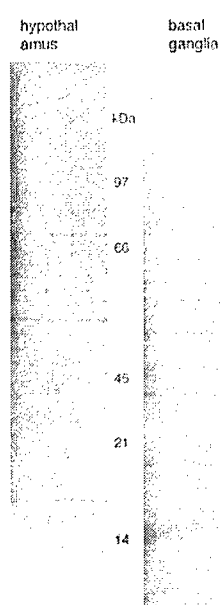
Figure 3.3.2. Coomassie stained SDS gels. The gel on the left shows the proteins from human hypothalamus and the gel on the right the proteins from human basal ganglia that bound to immobilized avidin/streptavidin beads. The numbers are molecular weight estimates.

Figure 3.3.3 shows about 20 fluorescent bands in human hypothalamus as a result of reaction with FP-biotin. The most intense band migrates with the albumin standard at 66 kDa.

MW 50 100 μg

kDa
116
97
66

45

21

14
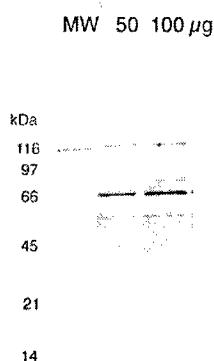
Figure 3.3.3. FP-biotinylated proteins in human hypothalamus. The blot was hybridized with Streptavidin Alexa 680 and the fluorescence was visualized on the Odyssey Infrared Imaging System (LI-COR, Lincoln, NE). The first lane contains molecular weight markers (MW), and the next two lanes contain 50 and 100 μg of human hypothalamus protein labeled with Canadian FP-biotin.

Discussion

The OP-binding proteins in human hypothalamus appear to be somewhat different than the OP-binding proteins in human basal ganglia. Comparison of Coomassie stained gels for proteins that bind to avidin/streptavidin beads shows bands on one gel that are not present on the other, though there are also bands that migrate to the same position on both gels. There appear to be 20-30 OP-binding proteins in human hypothalamus and basal ganglia.

The most intense fluorescent band in Figure 3.3.3 is a band of 66 kDa. This is likely to be human albumin. It is known that 60% of the albumin in a person is extravascular (Peters, 1996). Albumin makes a covalent bond with FP-biotin by attaching to Tyrosine 411 of human albumin (Sanger, 1963; Peters, 1996; Schopfer et al., 2005).

Task 4

The protein bands isolated in task 3 will be partially sequenced. The partial sequences will be used to search the Human and Mouse Genome Databases, for the purpose of obtaining the complete amino acid sequences and identifying the proteins.

Task 4.1. Relation to statement of work. Task 4 has been completed.

4.1. Albumin, a new biomarker of organophosphorus toxicant exposure, identified by mass spectrometry

Eric Peeples, Lawrence M. Schopfer, Ellen G. Duysen, Reggie Spaulding, Troy Voelker, Charles M. Thompson, Oksana Lockridge

Abstract
The classical laboratory tests for exposure to organophosphorus toxicants (OP) are inhibition of acetylcholinesterase (AChE) and butyrylcholinesterase (BChE) activity in blood. In a search for new biomarkers of OP exposure, we treated mice with a biotinylated organophosphorus agent, FP-biotin. The biotinylated proteins in muscle were purified by binding to avidin-Sepharose, separated by gel electrophoresis, digested with trypsin, and identified from their fragmentation patterns on a quadrupole time of flight mass spectrometer. Albumin and ES1 carboxylesterase (EC 3.1.1.1) were found to be major targets of FP-biotin. These FP-biotinylated proteins were also identified in mouse plasma by comparing band patterns on nondenaturing gels stained for albumin and carboxylesterase activity, with band patterns on blots hybridized with Streptavidin Alexa-680. Two additional FP-biotin targets, AChE (EC 3.1.1.7) and BChE (EC 3.1.1.8), were identified in mouse plasma by finding that enzyme activity was inhibited 50-80%. Mouse plasma contained eight additional FP-biotinylated bands whose identity has not yet been determined. In vitro experiments with human plasma showed that chlorpyrifos oxon, echothiophate, malaoxon, paraoxon, methyl paraoxon, diazoxon, diisopropylfluorophosphate, and dichlorvos competed with FP-biotin for binding to human albumin. Though experiments with purified albumin have previously shown that albumin covalently binds OP, this is the first report of OP binding to albumin in a living animal. Carboxylesterase is not a biomarker in man because humans have no carboxylesterase in blood. It is concluded that OP bound to albumin could serve as a new biomarker of OP exposure in man.

A copy of this publication is attached.

Task 4.2. Relation to statement of work. Mass spectroscopy of mouse brain proteins is part of Task 4.

4.2. Mass spectroscopy to identify OP-reactive proteins in mouse brain

Abstract
Procedures for purification of FP-biotin labeled proteins have been developed, and a protocol for digestion of the isolated proteins has been adopted. These procedures have allowed preliminary identification of 26 OP-labeled proteins by mass spectrometry. The 26 proteins are from the 100,000xg supernatant fraction of mouse brain.

Introduction
Samples were prepared at the University of Nebraska Medical Center and sent for mass spectral analysis to the laboratory of our collaborator, Dr. Charles Thompson, at the University of Montana. Purified tryptic peptides were fragmented on a Micromass Q-TOF mass spectrometer. The mass and sequence information for each peptide were analyzed with ProteinLynx or MASCOT software to identify the protein.

Methods
Protein digestion protocol. The proteins isolated from SDS PAGE (Task 3.1, Figure 3.1.2) were digested with trypsin to prepare them for identification by mass spectral analysis. The procedure we used was established in Dr. Thompson's laboratory at the University of Montana. Gloves were worn throughout these procedures, all solutions were made with Milli-Q purified water, and all glassware, plasticware, and tools were rinsed with Milli-Q purified water in order to minimize keratin contamination. Each band from one lane of the SDS PAGE was excised, placed into a separate 1.5 ml microfuge tube, and chopped into bits. The amount of gel excised was kept to a minimum. The gel bits were destained by washing with 200 μl of 25 mM ammonium bicarbonate (Aldrich) in 50% acetonitrile (synthesis grade, from Fisher). After three washes, the gel bits were colorless and had shrunken considerably. Residual liquid was removed and the gel bits dried by evaporation in a Speedvac (Jouan). Protein in each sample was then reduced by incubating the gel bits with 10 mM dithiothreitol (molecular biology grade, from Sigma) in 200 μl of 100 mM ammonium bicarbonate for 1 hour at 56°C. The gel pieces were then centrifuged, excess solution was removed, and the protein was alkylated with 55 mM iodoacetamide (Sigma) in 120 μl of 100 mM ammonium bicarbonate for 1 hour at room temperature in the dark. The gel bits were again centrifuged, excess solution was removed, and the bits were washed with 200 μl of 25 mM ammonium bicarbonate in 50% acetonitrile (three times). Residual liquid was again removed and the gel bits dried by evaporation in the Speedvac. The proteins were digested with trypsin, 12.5 ng/μl of sequencing grade trypsin (Promega) in 25 mM ammonium bicarbonate. Ninety μl of the trypsin solution were added to the dry gel bits

and incubated at 4°C for 20 minutes, to allow the gel to re-swell. Then 60 µl of 25 mM ammonium bicarbonate were layered over each sample and the samples were incubated at 37°C overnight (about 17 hours). Peptides were extracted by incubating each reaction mixture with 200 µl of 0.1% trifluoroacetic acid (sequencing grade from Beckman) in 60% acetonitrile for one hour at room temperature. Extraction was repeated three times and the extracts for each sample were pooled. The pooled extracts were evaporated to dryness in the Speedvac, and the dry samples were stored at -20°C until analyzed.

Mass spectral analysis. Each tryptic peptide digest was resuspended in 40 µl of 5% acetonitrile/0.05% trifluoroacetic acid/95% water. A 10 µL aliquot of the digest was injected into a CapLC (capillary liquid chromatography system from Waters Corp) using 5% acetonitrile/0.05% trifluoroacetic acid (auxiliary solvent) at a flow rate of 20 µL per minute. Peptides were concentrated on a C_{18} PepMap ^{TM} Nano-Precolumn ^{TM} (5 mm × 0.3 mm id, 5µm particle size) for 3 minutes, and then eluted onto a C_{18} PepMap ^{TM} capillary column (15 cm × 75 µm id, 3 µm particle size both from LC Packings), using a flow rate of 200-300 nL per minute. Peptides were partially resolved using gradient elution. The solvents were 2% acetonitrile/0.1% formic acid (solvent A), and 90% acetonitrile/10% iso-propanol/0.2% formic acid (solvent B). The solvent gradient increased from 5% B to 50% B over 22 minutes, then to 80% B over 1 minute, and remained at 80% B for 4 minutes. The column was then flushed with 95% B for 3 minutes and equilibrated at 5% B for 3 minutes before the next sample injection.

Peptides were delivered to the Z-spray source (nano-sprayer) of a Micromass Q-TOF (tandem quadrupole/time-of-flight mass spectrometer from Waters Corp.) through a 75-µm id capillary, which connected to the CapLC column. In order to ionize the peptides, 3300 volts were applied to the capillary, 30 volts to the sample cone, and zero volts to the extraction cone. Mass spectra for the ionized peptides were acquired throughout the chromatographic run, and collision induced dissociation spectra were acquired on the most abundant peptide ions (having a charge state of 2+, 3+, or 4+). The collision induced dissociation spectrum is unique for each peptide, and is based on the amino acid sequence of that peptide. For this reason, identification of proteins using collision induced dissociation data is superior to identification by only the peptide mass fingerprint of the protein. The collision cell was pressurized with 1.5 psi ultra-pure Argon (99.999%), and collision voltages were dependent on the mass-to-charge ratio and the charge state of the parent ion. The time of flight measurements were calibrated daily using fragment ions from collision induced dissociation of [Glu^1]-fibrinopeptide B. Each sample was post-processed using this calibration and Mass Measure (Micromass). The calibration was adjusted to the exact mass of the autolytic tryptic fragment at 421.76, found in each sample.

The mass and sequence information for each detected peptide was submitted either to ProteinLynx Global Server 1.1 (a proprietary software package, from Micromass), or to MASCOT (a public access package provided by Matrix Science at http//www.matrix-science.com/cgi/index.pl?page=../home.html). Data were compared to all mammalian entries (ProteinLynx) or just mouse entries (MASCOT) in the NCBInr database (National Center for Biotechnology Information). Search criteria for ProteinLynx were set to a mass accuracy of 0.25 Da, and one missed cleavage by

trypsin was allowed. Search criteria for MASCOT were set to a mass accuracy of ±0.1 Da, one missed cleavage, variable modification of methionine (oxidation) and cysteine (carbamidomethylation), and peptide charge +2 and +3. Both software packages calculated a score for each identified protein based on the match between the experimental peptide mass and the theoretical peptide mass, as well as between the experimental collision induced dissociation spectra and the theoretical fragment ions from each peptide. Results were essentially the same from both packages.

Results
Identification of the proteins labeled by FP-biotin.
The 22 FP-biotin labeled bands from the SDS PAGE shown in Figure 3.1.2 were excised, destained, reduced, alkylated, digested with trypsin, and the peptides extracted as described in the Methods section. The dried peptides were sent to Dr Thompson's laboratory for tandem-ms/ms mass spectral analysis. Peptide mass and sequence information from each band was compared to the NCBInr database using either MASCOT or ProteinLynx software. Out of the 22 bands, proteins could be identified in 15 (see Table 4.2.1). To be included in the list, a protein needed to be matched to at least 2 peptides, which accounted for at least 3% of the total sequence, and have a protein score greater than 34. Both programs evaluated the sequence and peptide mass information before assigning a reliability score to the protein identity. Scores greater than 34 (MASCOT) or 50 (ProteinLynx) indicated that the identity of the protein was well established.

A total of 26 proteins were identified in the 15 bands. Seven bands (17,18, 41, 44/45, 46/47, 50 &53) indicated the presence of two or more proteins. Fourteen were hydrolases: puromycin-sensitive aminopeptidase, prolylendopeptidase, RIKEN D030038o16 which is related to prolylendopeptidase, protein phosphatase 2, dihydropyrimidase-like 2, dihydropyrimidase-like 3, dihydropyrimidase-like 5 ,acyl-CoA hydrolase, esterase 10, tyrosine 3-monooxygenase/tryptophan 5-monooxygenase activation protein, platelet-activating factor acetylhydrolase alpha 2, platelet-activating factor acetylhydrolase alpha 1, lysophospholipase 1, and lysophospholipase 2. Only 5 of these hydrolases contained the serine nucleophile consensus sequence (GXSXG). Table 4.2.3 shows that the 5 hydrolases with the GXSXG consensus sequence were prolylendopeptidase, dihydropyrimidinase-like 5, esterase 10, lysophospholipase 1 and lysophospholipase 2. A sixth protein with the GXSXG sequence was heat shock protein 8.

Four of the proteins were dehydrogenases: formyltetrahydrofolate dehydrogenase, D-3-phosphoglycerate dehydrogenase, glyceraldehyde-3-phosphate dehydrogenase, and lactate dehydrogenase. Two proteins were heat shock proteins, and 3 were forms of tubulin. The remaining 3 proteins were serum albumin precursor, RIKEN 4931406N15, and peroxiredoxin.

The molecular weights of the identified proteins matched the molecular weights of the bands excised from the SDS gel. This supports the assigned identities.

Table 4.2.1 Analysis of the Mass Spectral Data for FP-biotinylated proteins in mouse brain supernatant (100,000xg) [1]

Band information		Protein Identification Information				
Band #	MW from SDS PAGE, kDa	protein score >50=good	Number Peptides found	% Total Protein	GXSXG sequence	Protein name (mouse proteins only) MW, kDa
1	200	-	no data		-	
5	110	-	no data		-	
6	100	174	4	4	no	Puromycin-sensitive aminopeptidase MW 103
7	95	426	10	15	no	Formyltetrahydrofolate dehydrogenase MW 97
8	90	352	5	10	no	Heat shock protein 90-Beta MW 84
12	85	827	16	26	yes	Prolylendopeptidase MW 81
15	80	-	no data		-	
17	75	372	10	22	no	RIKEN D030028o16 MW 73
		270	5	9	no	Serum albumin precursor MW 67
		173	4	6	no	RIKEN 4931406N15 MW 70
		154	3	6	yes	Heat shock protein 8 MW 71
18	65	70	2	3	no	Protein phosphatase 2 MW 65
		62	2	3	no	Dihydropyrimidinase-like 2 MW 61
		59	2	3	no	Dihydropyrimidinase-like 3 MW 62
		43	3	4	yes	Dihydropyrimidinase-like 5 MW 61 dihydropyrimidase is also called 5,6-dihydro-pyrimidine amido hydrolase
23	60	195	3	7	no	D-3-phosphoglycerate dehydrogenase MW 51
24	55	5320	15	50	no	Tubulin MW 50
29	50	-	no data			
32	45	-	no data		-	
35	40	296	6	21	no	Acyl-CoA hydrolase MW 38
38	35	275	5	23	no	Glyceraldehyde-3-phosphate dehydrogenase MW 36
37	35	-	no data		-	
41	30	576	11	43	no	Tubulin alpha-1 MW 50
		423	9	33	no	Tubulin beta-5 MW 50
		337	8	27	no	Lactate dehydrogenase 1 MW 36
		261	7	34	yes	Esterase 10 MW 35
44/45	25	286	5	16	no	Tubulin alpha-1 MW 50
		65	2	12	no	Platelet-activating factor acetylhydrolase alpha-2 MW 25
46/47	22	354	7	36	no	Tyrosine 3-monooxygenase/tryptophan 5-monooxygenase activation protein MW 28
		273	4	56	no	Platelet-activating factor acetylhydrolase alpha-1 MW 26
49	20	-	no data		-	
50	20	206	4	20	yes	Lysophospholipase 1 MW 25
		160	5	25	yes	Lysophospholipase 2 MW 25
53	20	245	5	31	no	Peroxiredoxin 1 MW 22
		101	3	12	no	Platelet-activating factor acylhydrolase alpha-1 MW 26

1 Data were analyzed using software from either MASCOT (all entries except bands 23 and 24) or ProteinLynx (entries 23 and 24).

Tubulin alpha-1 was found in two bands, in bands 41 and 44/45. Platelet-activating factor acetylhydrolase alpha-1 was also found in two bands, in bands 46/47 and 53. All other proteins were found in a single band. The 28 entries above represent 26 different proteins. The computer databank number of each protein listed in Table 4.2.1 is given in Table 4.2.2.

Table 4.2.2 . Databank numbers for the proteins identified in Table 4.2.1

Protein name (mouse proteins only) MW kDa	Databank #
Puromycin-sensitive aminopeptidase MW 103	gi 6679491
Formyltetrahydrofolate dehydrogenase MW 97	gi 27532959
Heat shock protein 90-Beta MW 84	gi 123681
Prolylendopeptidase MW 81	gi 6755152
RIKEN D030028o16 MW 73	gi 22122431
Serum albumin precursor MW 67	gi 5915682
RIKEN 4931406N15 MW 70	gi 28076969
Heat shock protein 8 MW 71	gi 13242237
Protein phosphatase 2 MW 65	gi 8394027
Dihydropyrimidinase-like 2 MW 61	gi 6753676
Dihydropyrimidinase-like 3 MW 62	gi 6681219
Dihydropyrimidinase-like 5 MW 61	gi 12746424
D-3-phosphoglycerate dehydrogenase MW 51	gi 3122875
Tubulin MW 50	gi 20455323
Brain acyl-CoA hydrolase MW 38	gi 19923052
Glyceraldehyde-3-phosphate dehydrogenase MW 36	gi 6679937
Tubulin alpha-1 MW 50	gi 6755901
Tubulin beta-5 MW 50	gi 7106439
Lactate dehydrogenase 1 MW 36	gi 6754524
Esterase 10 MW 35	gi 12846304
Tubulin alpha-1 MW 50	gi 6755901
Platelet-activating factor acetylhydrolase alpha-2 MW 25	gi 6679199
Tyrosine 3-monooxygenase/tryptophan 5-monooxygenase activation protein MW 28	gi 6756039
Platelet-activating factor acetylhydrolase alpha-1 MW 26	gi 6679201
Lysophospholipase 1 MW 25	gi 6678760
Lysophospholipase 2 MW 25	gi 7242156
Peroxiredoxin 1 MW 22	gi 6754976
Platelet-activating factor acylhydrolase alpha-1 MW 26	gi 6679201

Table 4.2.3. GXSXG motif in FP-biotinylated proteins in mouse brain.

GXSXG sequence	Protein name (mouse protein)	MW, kDa
yes	Prolylendopeptidase	81
yes	Heat shock protein 8	71
yes	Dihydropyrimidinase-like 5 dihydropyrimidase is also called 5,6-dihydro-pyrimidine amido hydrolase	61
yes	Esterase 10	35
yes	Lysophospholipase 1	25
yes	Lysophospholipase 2	25

Discussion

The 26 proteins identified by mass spectrometry were an unexpected mixture of peptidases, hydrolases, dehydrogenases, lipases, phosphatases, heat shock protein, tubulin, and others. Only 6 proteins had the conserved GXSXG sequence characteristic of serine esterases and serine proteases (Derewenda and Derewenda, 1991). Acetylcholinesterase was not in the set. This was not a surprise because the mouse brain supernatant did not have AChE activity.

Every protein in Table 4.2.1 is assumed to carry the FP-biotin tag. The most likely amino acid residues to form a covalent bond with an OP are serine, tyrosine, and histidine. Serine has been documented as the site of OP attachment in enzymes that have the conserved GXSXG motif. Serine is also the site of OP attachment in enzymes with a trypsin-like catalytic triad. Platelet-activating factor acetylhydrolase alpha-1 does not have the GXSXG sequence, but it does have a trypsin-like triad of Ser 47, His 195 and Asp 192 (Ho et al., 1997). The active site serine of platelet-activating factor acetylhydrolase is in the sequence GDSLV. Tyrosine has been documented as the site of attachment of sarin and soman in human albumin (Black et al., 1999). Tyrosine 410 of bovine albumin has been identified as the site of covalent attachment of DFP and FP-biotin (Sanger, 1963; Schopfer et al., 2005). Tyrosine has also been shown to be the site of attachment of DFP to papain (Chaiken and Smith, 1969). Histidine as well as serine are the sites of attachment of DFP to rabbit liver carboxylesterase (Korza and Ozols, 1988).

Task 4.3. Relation to statement of work. Mass spectroscopy of human brain proteins is part of Task 4.

4.3. Mass spectroscopy to identify OP-reactive proteins in human brain

Abstract
The goal was to identify all the proteins in human hypothalamus that bind OP irreversibly. Brain homogenates were reacted with 40 µM Canadian FP-biotin. The biotinylated proteins were purified by binding to avidin/streptavidin beads, separated by gel electrophoresis, digested with trypsin, and the tryptic peptides analyzed on a Q-Trap mass spectrometer. We identified 74 proteins. The binding of 18 proteins was explained by the presence of avidin binding sequences HPXP or XXHXHXX and the streptavidin binding sequence HPQ. These binding motifs have been reported to specifically bind avidin or streptavidin at sites distinct from the biotin-binding site. Two carboxylases were endogenously biotinylated, thus explaining their binding to avidin beads. The other 54 proteins could be biotinylated, but this has not yet been proven. Proof will require evidence of the presence of the FP-biotin tag on a peptide.

Introduction
In this task, our goal is to identify all the proteins in human brain that react with OP. The proteins in human hypothalamus and human basal ganglia were examined for reactivity with OP. Hypothalamus was selected because tracer studies with radiolabeled DFP, soman, and sarin showed a high amount of OP accumulated in the hypothalamus after intravenous injection into mice (Little et al., 1988). The hypothalamus has only low amounts of AChE and BChE, so that binding to cholinesterases does not explain OP accumulation. It has been suggested that not all the pharmacological effects of OP are mediated via inhibition of cholinesterases (Little et al., 1988). It was of interest to determine the identity of the OP-reactive proteins in the hypothalamus. The basal ganglia was selected because it is rich in AChE, thus maximizing the possibility of detecting OP-bound AChE. We used mass spectroscopy to identify OP labeled proteins.

Materials and Methods
Materials. Sequencing grade modified trypsin Cat # V5113 was from Promega.

Reaction with FP-biotin. Task 3.3 describes the preparation of brain homogenates and reaction with FP-biotin.

In gel trypsin digestion. The SDS gels in Task 3.3, Figure 3.3.2, were sliced into 10 sections, so that each gel slice contained 2 to 4 protein bands. The gel slices were chopped into bits with a spatula. Coomassie blue was washed out of the gel bits with

25 mM ammonium bicarbonate in 50% acetonitrile. The gel bits were dried in a Speedvac. The proteins in the gel bits were reduced with 10 mM dithiothreitol in 100 mM ammonium bicarbonate at 56°C for 1 h. The dithiothreitol solution was removed and the free sulfhydryl groups were alkylated with 55 mM iodoacetamide in 100 mM ammonium bicarbonate. The first iodoacetamide solution was removed, and fresh iodoacetamide solution was added. This was repeated one more time. The gel pieces were dried in a Speedvac. The reduced and alkylated proteins were digested with trypsin by adding 500 µl of trypsin solution (12.5 µg/µl) to each tube. The tubes were incubated on ice for 20 min to re-swell the gel, and then the trypsin solution was overlayed with 100 µl of 25 mM ammonium bicarbonate. Digestion was at 37°C for 8 h.

Extraction of tryptic peptides. Each tube received 500 µl of 0.1% trifluoroacetic acid in 60% acetonitrile. The tubes were vortexed and incubated at room temperature for 1 h. During this extraction period, the tubes were vortexed every 20 min. The gel pieces were spun down and the liquid was transferred to clean 1.5 ml microfuge tubes. The extraction was repeated two more times and the extracts were combined. The extracts were evaporated to dryness in the Speedvac.

Preparation of samples for analysis on the Q-Trap mass spectrometer. Peptides were dissolved in 0.1% formic acid, 5% acetonitrile. The volume added was estimated to make the peptide concentration 1 picomole/µl. The peptide solutions were transferred to 250 µl conical polypropylene vials that fit into the autoinjector and stored at -80°C.

Mass spectrometry of the tryptic digests. Samples were analyzed on the Q-Trap hybrid-quadrupole, linear ion trap mass spectrometer (Applied Biosystems) at the University of Nebraska Medical Center. A FAMOS autosampler in conjunction with a SWITCHOS and ULTIMATE capillary liquid chromatography system (LC Packings Dionex) was used to deliver peptides to the mass spectrometer. Samples were adjusted to a protein concentration of 1 pmole/µl with 5% acetonitrile/water containing 0.1% formic acid. Five µl of sample was loaded onto a micro-precolumn (LC Packings Dionex, PepMap C18 silica-based support, 5 micron particles with 100 angstrom pores, 300 micron ID x 5 mm long) and washed with 5% acetonitrile/water containing 0.1% formic acid for 10 minutes, at 20 µl/min, to remove salts. Peptides were eluted from the precolumn and partially resolved on a nanocolumn (Grace-Vydac, 218MS, C18 polymeric-silica support, with a 300 angstrom pore size, 75 micron ID x 150 mm long) using an acetonitrile gradient at 300 nl/min from 5%-40% B over 60 minutes, then to 80% B over 10 minutes, with washing and re-equilibration at 5% B (A = 5% acetonitrile 0.1% formic acid, B = 98% acetonitrile 0.1% formic acid). Peptides were delivered directly from the nanocolumn to the mass spectrometer via a fused silica emitter (360 OD, 20 µm ID, 10 µm taper from New Objective) attached to a flow NanoSpray source. 1500 volts were applied to the emitter, and mass spectra were acquired throughout the chromatographic run. Information Dependent Acquisition was utilized to collect an Enhanced MS (EMS) survey scan, followed by automatic Enhanced resolution scans (ER), and Enhanced Product Ion (EPI or MS/MS) scans of the three most intense precursor ions from each survey scan. MS/MS spectra were taken on all precursors

having a charge of 2+ to 4+, and ions were excluded after two MS/MS spectra were acquired on each precursor. The collision cell was pressurized at 40 µTorr with pure nitrogen and collision voltages of 20-35 volts for each precursor were automatically determined based on the mass and charge of the precursor ion. The spectrometer was calibrated with [Glu]-fibrinopeptide B.

Database searches. The Mascot program by Matrix Science was used offline (www.matrixscience.com). The MS/MS ion search in Mascot was used to identify proteins. The Error Tolerant search in Mascot was used to search for the FP-biotin tag.
Bioinformatics Harvester (harvester.embl.de) was used to search for biotin mimetic sequences in identified proteins.

Results
Proteins identified by mass spectroscopy. A total of 74 proteins in human hypothalamus bound to avidin/streptavidin beads (Table 4.3.1). Several proteins were found in more than one, nonadjacent gel band. For example, glial fibrillary acidic protein was found in bands 5 and 9. The presence of the same protein in several bands may be explained by post-translational modifications such as phosphorylation, glycosylation, and alternative splicing.

Table 4.3.1. Proteins in human hypothalamus identified by mass spectroscopy; these 74 proteins bound to avidin/streptavidin beads.

Band #	Protein Name	Protein ID	MW	Score	#pep tides	%co ver
1	Phosphodiesterase 5A isoform 3	gi|61744432	93570	33	1	2
1	KIAA0572 protein (MCM3-associated protein, GANP protein)	gi|3043668		37	2	0
1	PRO2044 (serum albumin precursor)	gi|6650826	29229	58	1	5
1	5-methyltetrahydrofolate-homocysteine methyltransferase	gi|4557765	140497	41	4	3
1	Unnamed protein product	gi|34532818		44	2	1
1	Similar to centromeric protein E	gi|41149911	741434	46	6	1
1	Envoplakin	gi|4097998		32	2	0
1,9,10	Microtubule associated protein 1a	gi|1790380	306045	34	7	2
2	Alpha globin	gi|28549	13574	67	1	11
2	Myelin basic protein	gi|187403	6460	61	1	16
2	Enaptin	gi|22597198		35	3	0
3	MYOM3 protein	gi|45501305		32	2	1
3	Chromosome-associated protein C	gi|47271354		30	1	2
3,7	HEJ1	gi|14719299		34	1	15
3,9	Similar to 40S ribosomal protein S6	gi|51471198	26020	62	3	5
4	G3PD	gi|31645	36031	58	1	4
4	Skeletal muscle tropomyosin	gi|339956		36	1	4
4	COL1A1 & PDGFB fusion transcript	gi|3288487	36963	32	1	6
4	SMF protein	gi|2495717	156810	32	2	2
5	Gamma-actin	gi|178045	25862	32	1	5
5	Mutant beta-actin	gi|28336	41786	91	2	6
5	Creatine kinase-B	gi|180555	42460	32	1	3

5	Ig heavy chain variable region, VH3 family	gi|33318984		32	2	23
5,9	Glial fibrillary acidic protein	gi|4503979	49850	98	3	9
6	Fibulin-6	gi|13872813		30	3	1
6	Unnamed protein product	gi|10436240	27529	141	4	16
6	Nuclear mitotic apparatus (NuMA) protein	gi|35119		32	3	1
6	Tubulin, beta polypeptide (TUBB)	gi|18088719	49640	195	4	13
6	Tubulin, 5-beta	gi|35959	49599	205	4	11
6	Tubulin alpha 6	gi|38648679	49863	343	11	28
6	Beta-tubulin	gi|1805274	48403	94	2	5
6	Similar to beta tubulin	gi|2661079	38545	175	4	14
6	TUBB2 protein	gi|20809886	49776	419	7	21
6	RP11-203S24.5	gi|55958263	48701	32	1	3
6	Amiloride-sensitive sodium channel	gi|7406623	57427	38	1	2
6	KIAA2013 protein	gi|23271560		49	2	5
6	Similar to golgin-67 isoform C	gi|51472350	102273	45	3	4
6	Cytochrome P-450 HPH	gi|23885		30	2	10
6	Ribosomal protein SA	gi|663209	48498	30	3	4
6,7	Alpha-tubulin	gi|32015	49761	313	10	28
7	Ig heavy chain variable region	gi|9968340		35	1	9
7	Propionyl-CoA carboxylase	gi|296366	77305	69	3	5
7	Unnamed protein product	gi|34532818	174461	37	1	0
7	LOC144501	gi|40807176	47212	93	2	5
7	Oxysterol-binding protein-like OSBPL1B	gi|17529999		41	2	1
7	KIAA0393 protein	gi|6683697	158552	34	2	2
7	NADH/NADPH thyroid oxidase p138-tox	gi|6636099	137474	31	2	2
8	Latent transforming growth factor-beta	gi|3327808	161051	41	3	2
8	Pyruvate carboxylase	gi|632808	129530	180	5	6
8	Procollagen, type III, alpha 1	gi|4502951	138470	41	2	2
8	Ankyrin-like protein	gi|3287188		35	1	0
8	Collagen type V alpha 3 chain	gi|7329074		32	4	3
8	Acyl-CoA synthetase 3	gi|12698001	179314	32	2	1
8	Transcriptional regulator ATRX	gi|17380440	282391	40	3	2
8	TAOK2 protein	gi|30353923		36	3	3
8	KIAA1842 protein	gi|14017901	60774	40	2	4
8	KIAA1728 protein	gi|12698001	179314	32	3	1
8,9	Helicase-MOI	gi|5019620		33	2	1
8,9	Unnamed protein product	gi|28317	59492	66	2	6
9	Ryanodine receptor 2	gi|4506757	564137	41	4	0
9	Myosin-IXa	gi|5732618	292523	38	3	1
9	CLTC protein	gi|30353925	187771	107	2	2
9	Unnamed protein product	gi|1015526	41601	31	1	3
9	Tubulin beta	gi|223429	49767	85	2	11
9	Cell surface adhesion glycoprotein	gi|7717438	84726	49	3	10
9	Low density lipoprotein	gi|62088576	261846	39	4	2
9	Inward rectifier potassium channel	gi|1765989	26107	40	1	5
9	Protein tyrosine kinase-receptor	gi|406868	110216	38	2	2
9	Receptor-associated coactivator 3	gi|2318006	154438	34	2	1
9,10	Bullous pemphigoid antigen 1	gi|55960290		65	7	1
10	Nyctalopin	gi|57210101	51967	34	2	8
10	A28-RGS14p (Regulator of G-protein signaling 16)	gi|1813544	22693	38	2	5
10	Chain B, human mitochondrial Nad(P)-dependent malic enzyme	gi|5822327		32	3	6
10	Unnamed protein product	gi|16553682	52810	45	3	11

Band# is the section of the SDS gel from which the peptides were prepared. Proteins in band #1 migrated fastest and are expected to have the lowest subunit molecular weight. Proteins in band #10 migrated slowest. Protein ID is the protein identification number assigned by the Mascot Program. MW is the molecular weight, exclusive of post-translational modifications. Score is the probability, calculated by the Mascot Program, that the protein has been correctly identified. A score higher than 42 is considered a strong score, (http://www.matrixscience.com/help/scoring_help.html). # peptides is the number of peptides from a particular protein. % coverage is the percent of the protein represented by the identified peptides.

Two proteins, propionyl-CoA carboxylase and pyruvate carboxylase, are endogenously biotinylated and therefore they bound to avidin and streptavidin through the biotin-binding site (Table 4.3.2).

Table 4.3.2. Endogenous biotinylated proteins in human hypothalamus

Band #	Protein Name	Protein ID	MW	Score	# peptides	% coverage
7	Propionyl-CoA carboxylase	gi|296366	77305	69	3	5
8	Pyruvate carboxylase	gi|632808	129530	180	5	6

The binding of 18 proteins can be explained by the presence of the avidin binding sequences HPXP or XXHXHXX in the 14 proteins listed in Table 4.3.3 and the streptavidin binding sequence HPQ in the 4 proteins listed in Table 4.3.4. These binding motifs have been reported to specifically bind avidin or streptavidin at sites distinct from the biotin-binding site (Lam et al., 1991; Ostergaard et al., 1995b).

Table 4.3.3. Avidin binding proteins containing the avidin binding sequence HPXP or XXHXHXX

Band #	Protein Name	Protein ID	MW	Score	# peptides	% cover	Binding sequence
1&9&10	Microtubule associated protein 1a	gi|1790380	306045	34	7	2	HPRP
2	Alpha globin	gi|28549	13574	67	1	11	DLHAHKL
2	Myelin basic protein	gi|187403	6460	61	1	16	RHHHHHH
2	Enaptin	gi|22597198		35	3	0	NSHEHEL
6	Fibulin-6	gi|13872813		30	3	1	HPVP
8	Transcriptional regulator ATRX	gi|17380440	282391	40	3	2	HPEP
8	TAOK2 protein	gi|30353923		36	3	3	HPLP
8	KIAA1842 protein	gi|14017901	60774	40	2	4	AAHKHSG
8	KIAA1728 protein	gi|12698001	179314	32	3	1	HPLP
8&9	Helicase-MOI	gi|5019620		33	2	1	HPIP
9	Myosin-IXa	gi|5732618	292523	38	3	1	HPTP
9	CLTC protein	gi|30353925	187771	107	2	2	VVHTHLL
9&10	Bullous pemphigoid antigen 1	gi|55960290		65	7	1	ASHKHKE
10	Nyctalopin	gi|57210101	51967	34	2	8	LTHAHLE

Table 4.3.4.   Streptavidin binding proteins containing the streptavidin binding sequence HPQ

1	Envoplakin	gi|4097998		32	2	0	HPQ
4	SMF protein	gi|2495717	156810	32	2	2	HPQ
7	NADH/NADPH thyroid oxidase p138-tox	gi|6636099	137474	31	2	2	HPQ
9	Ryanodine receptor 2	gi|4506757	564137	41	4	0	HPQ

The binding of 54 proteins to avidin/streptavidin beads is unexplained at this time.   It is not known whether these 54 proteins became labeled with FP-biotin. We searched for characteristic fragment sizes that would show FP-biotin had bound, but no such fragments were found. The characteristic fragment sizes for Canadian FP-biotin are 227, 326, and 466 m/z if the FP-biotin bound to serine. If the FP-biotin bound to tyrosine, then only the ions at 227 and 326 m/z would be present.

Table 4.3.5. Characteristic ions of Canadian FP-biotin produced by collision induced fragmentation in the mass spectrometer.

bound to serine, m/z	bound to tyrosine, m/z
227	227
326	326
466	

If all 3 ions are present the FP-biotin is bound to serine.
If only 227 and 326 are present, the FP-biotin is bound to tyrosine.

Discussion
The search for OP reactive proteins in human brain is a work in progress.   We want to see the FP-biotin tag in the mass spectrometer before we believe that a particular protein has been covalently modified by FP-biotin. To date we have not seen characteristic FP-biotin fragment ions in a human brain peptide. We interpret this to mean that the amount of FP-biotinylated peptides has been too low to be detected. The peptides go through the C18 reverse phase column and then directly into the mass spectrometer. The spectrometer has time to fragment only three peptides before the peptides exit the ion trap. As a result, low abundance peptides are not analyzed.

Our plan is to increase the signal 100-fold by infusing the sample continuously at a flow rate of 0.2 nanoliters per min for 1 hour and to obtain fragmentation data for all peptides. This procedure bypasses the C18 column, and bypasses the limitation of being able to analyze only three peptides for any given time of elution. We will be able to analyze all peptides. We will also be able to optimize the collision energy and the length of time ions are collected in the trap before they are fragmented.

Task 5

The reactivity with insecticides of the new biochemical markers will be compared to the reactivity of AChE and BChE with the same insecticides. The set of proteins identified in task 3, as well as AChE and BChE, will be ranked for reactivity with chlorpyrifos oxon, dichlorvos, diazinon-O-analog, and malathion-O-analog. This will be accomplished by measuring second order rate constants for individual proteins in brain extracts.

Relation to statement of work. Task 5 has been completed.

Platelet-activating factor acetylhydrolase alpha-2 and acylpeptide hydrolase are more sensitive targets of dichlorvos than acetylcholinesterase in mouse brain

Abstract

Subcellular fractions of mouse brain (the 100,000xg supernatant and the 17,000xg pellet) were screened for reaction with chlorpyrifos-oxon, dichlorvos, diazoxon (diazinon-O-analog), and malaoxon (malathion-O-analog), using an FP-biotin screening protocol. The screening protocol allowed proteins to react with OP and then the unreacted proteins were visualized by binding FP-biotin. Signal intensity after hybridization of blots with streptavidin-Alexafluor was reduced for OP reactive proteins. Only seven of the 55 protein bands from the 100,000xg supernatant, and seven of the 52 protein bands from the 17,000xg pellet showed significant sensitivity to these OP. Each OP reacted with a somewhat different set of proteins. IC_{50} values were determined for each of the sensitive proteins. The identity of 8 OP-reactive proteins was determined by mass spectrometry. They were prolylendopeptidase, D-3-phosphoglycerate dehydrogenase, esterase 10, platelet-activating factor acetylhydrolase alpha-2, tyrosine 3-monooxygenase/tryptophan 5-monooxygenase activation protein, platelet-activating factor acetylhydrolase alpha-1, lysophospholipase 1, and lysophospholipase 2. Comparison of IC_{50} values for AChE and IC_{50} values for these OP-reactive proteins suggested that platelet-activating factor acetylhydrolase alpha-2 and acylpeptide hydrolase reacted more readily with dichlorvos than AChE.

Introduction

The goal of these studies is to identify proteins that react with OP insecticides at doses that do not have a significant effect on AChE activity. Proteins that are more reactive toward OP than AChE do exist. Richards et al. have shown that acylpeptide hydrolase reacts with selected OP more readily than does AChE (Richards et al., 2000); while

Quistad et. al. have made similar observations with fatty acid amide hydrolase (Quistad et al., 2001; Quistad et al., 2002). Other highly reactive OP targets probably exist. In this section, methods for OP reactivity screening and identification of OP reactive proteins have been applied to subcellular fractions from mouse brain (100,000xg supernatant and 17,000xg pellet). Four OP were tested: chlorpyrifos-oxon, diazoxon, dichlorvos, and malaoxon. Fifty-five FP-biotin reactive bands were found in the 100,000xg supernatant; 22 of these were extracted with avidin-agarose and submitted to mass spectral analysis; 15 yielded information on the proteins associated with the bands. Six proteins showed significant reactivity toward the test OP. One protein, platelet-activating factor acetylhydrolase alpha-2, was more reactive toward dichlorvos than was AChE. Fifty-two FP-biotin reactive bands were found in the 17,000xg pellet; 7 of these showed significant reactivity toward the test OP.

Methods

The screening method. The IC_{50} screening method was used to determine the OP reactivity of proteins in the 100,000xg supernatant and 17,000xg pellet fractions from mouse brain. In brief, that method involved incubating aliquots of the mouse brain fraction (1.3 mg protein/ml) with various concentrations of the OP (0.05 to 300 µM) in 50 mM TrisCl buffer, pH 8.0 containing 5 mM EDTA and 2.4% methanol (94 µl total volume) for 30 minutes at 25°C. Reactions were stopped by gel filtration through Performa SR spin columns, equilibrated in the reaction buffer. Six µl of 170 µM FP-biotin were immediately added to each column eluant, to yield 10 µM FP-biotin, and incubation was continued for 300 minutes, to completely react all remaining FP-biotin reactive proteins. Reactions were stopped by adding 20 µl of 6x-SDS PAGE loading buffer (0.2 M TrisCl pH 6.8 containing 10% SDS, 30% glycerol, 0.6 M dithiothreitol and 0.012% bromophenol blue) and heating to 85°C for 5 minutes. Aliquots (30 µg protein) from each reaction mixture were separated on a 10-20% gradient SDS PAGE by electrophoresis at a constant voltage of 250 volts for 14 hours (4000 volt-hours). Biotinylated proteins were electrophoretically transferred to PVDF membrane, and reacted with 9.5 nM Streptavidin-Alexa 680 (Molecular Probes, Inc., Eugene, OR). The Streptavidin-Alexa 680 served to place a fluorescent tag on the biotinylated proteins. Fluorescent signals were collected with an Odyssey flat plate scanner (Li-COR , Lincoln, NE), and signal intensity was integrated with Kodak 1D software, where applicable. IC_{50} values (defined as the concentration of OP at which 50% of the protein had been reacted) were estimated. Due to difficulties in accurately integrating the fluorescence intensities for bands with weak signals, IC_{50} values were sometimes assigned by visual inspection of the fluorescence pattern.

Mass spectral analysis. Isolation of FP-biotin labeled proteins is described in Task 3. Preparation of tryptic peptides and analysis of these peptides by mass spectrometry are described in Task 4.

Human AChE. Recombinant human AChE was secreted from Chinese Hamster Ovary cells into serum-free culture medium. The AChE was purified by chromatography on procainamide-Sepharose affinity column. The resulting AChE was free of albumin.

Results
Screening for organophosphate reactivity in the 100,000xg mouse brain
supernatant. Four OP were used to assess reactivity of the mouse brain 100,000xg
supernatant fraction: chlorpyrifos-oxon, dichlorvos, diazoxon, and malaoxon. Only a
few of the 55 FP-biotin reactive proteins were also reactive toward these OP. Three
bands were found to disappear upon reaction with chlorpyrifos-oxon (0.05 to 304 µM).
Figure 5.1 shows that the three bands that reacted with chlorpyrifos oxon had band
numbers 12, 41, and 44/45. Their molecular weights were 85, 30 and 25 kDa.

Figure 5.2 shows four bands that reacted with dichlorvos (0.64 to 382 µM). Their
band numbers were 12, 32, 44/45 and 50. Their molecular weights were 85, 45, 25, 20
kDa. Figure 5.3 shows the four bands that reacted with diazoxon (0.11 to 510 µM) as
having band numbers 9, 12, 41, and 47. Their molecular weights were 89, 85, 30, and
22 kDa. Figure 5.4 shows that one band reacted with malaoxon (0.11 to 510 µM). The
band number was 9 and its molecular weight was 89 kDa. These results show that
each OP reacted with sets of proteins that only partially overlapped.

The OP-reactive bands were typically present at low level. For such weak
signals, determination of IC_{50} values (concentration of OP that causes 50% inhibition)
was complicated by heterogeneity in the Western blot process. In some cases, a plot of
the "integrated signal intensity" versus "OP concentration" was sufficiently well-behaved
to allow determination of the IC_{50} (see Figure 5.5a & b). However, in many cases the
IC_{50} was best determined by visual inspection of the signal pattern (see Figures 5.1 to
5.4). Estimated IC_{50} values are presented in Tables 5.1 and 5.2.

IC_{50} values are critically dependent upon the conditions of measurement.
Temperature and pH are normal variables which must be controlled in order to make
comparisons meaningful, but the time for which the inhibitor is allowed to react is also
critical. IC_{50} values for mouse AChE, taken from the literature (see Table 5.3), were
determined under a variety of conditions and therefore serve only as approximate
reference values. Most of the OP reactive bands in mouse brain supernatant appear to
be substantially less reactive than mouse AChE. Only the reaction of bands 44/45 with
dichlorvos appears to be substantially faster than that for AChE. However, the reaction
of diazoxon with band 9 is rapid, and there is no literature value for mouse AChE with
which to compare, so this band remains of interest. Band 41 is quite reactive with
chlorpyrifos-oxon, and also could be of interest. In addition, there are missing IC_{50}
values for the reaction of band 9 with chlorpyrifos-oxon and dichlorvos. Band 9 was not
always seen in the Western blot, which accounts for the missing data. Since band 9
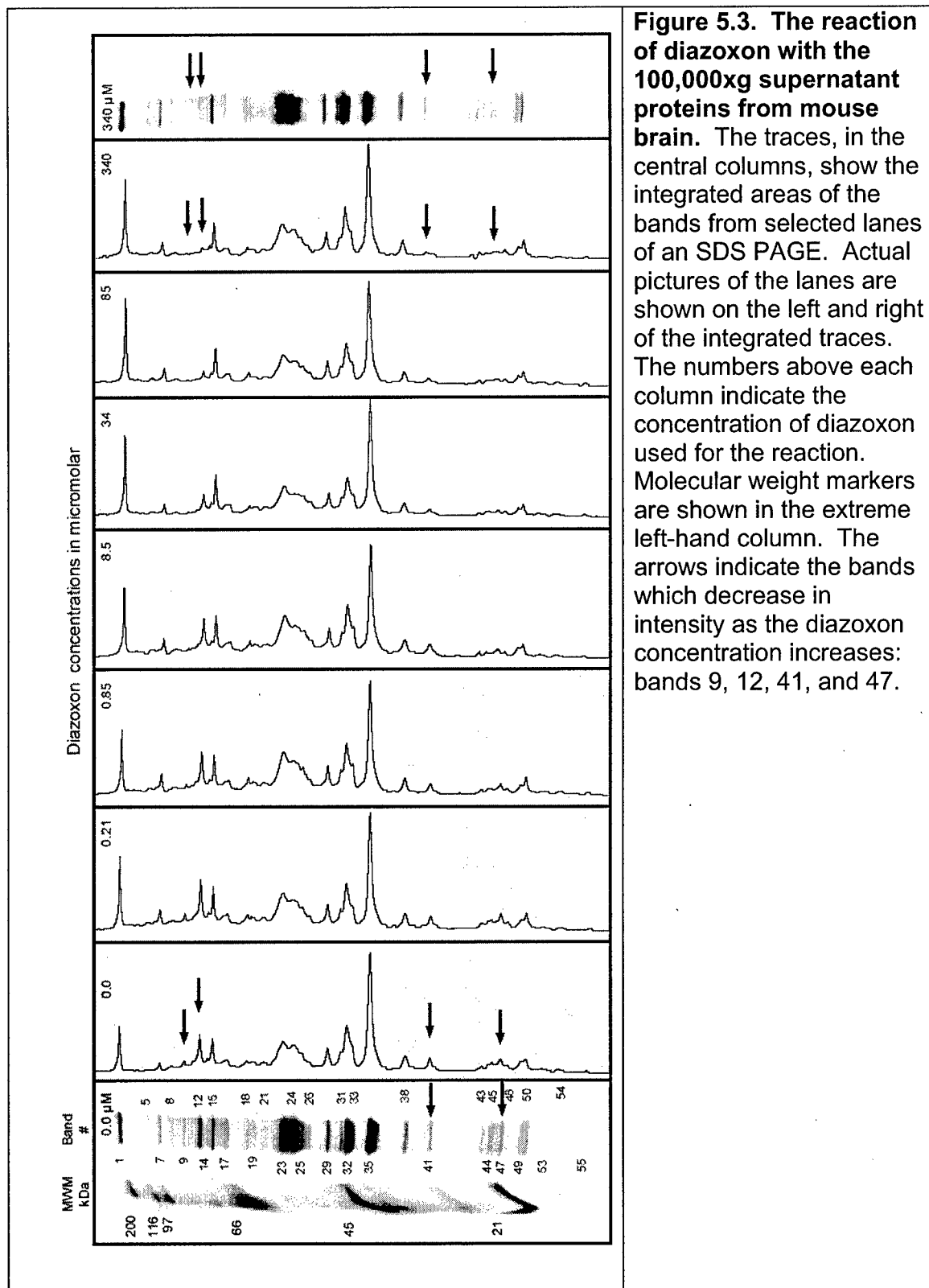was reactive toward diazoxon and malaoxon, this band is of interest.

AChE control. Sensitivity of AChE to reaction with OP varies from species to species
(see literature values in Table 5.3). Direct comparison of mouse AChE reactivity to the
reactivity of the other OP sensitive bands, in the screening assay format, would be the
best way to determine the relative sensitivity of alternate OP targets and AChE.
However, AChE is not present in the mouse brain supernatant at sufficiently high
concentration to be visible on blots. We added purified human red blood cell AChE (gift
from Dr. Terrone Rosenberry, Mayo, Jacksonville, FL) to the reaction of OP with mouse
brain supernatant, as an approximate internal control, but that AChE gave several
bands which obscured the 70-80 kDa region. Purified, recombinant wild type AChE
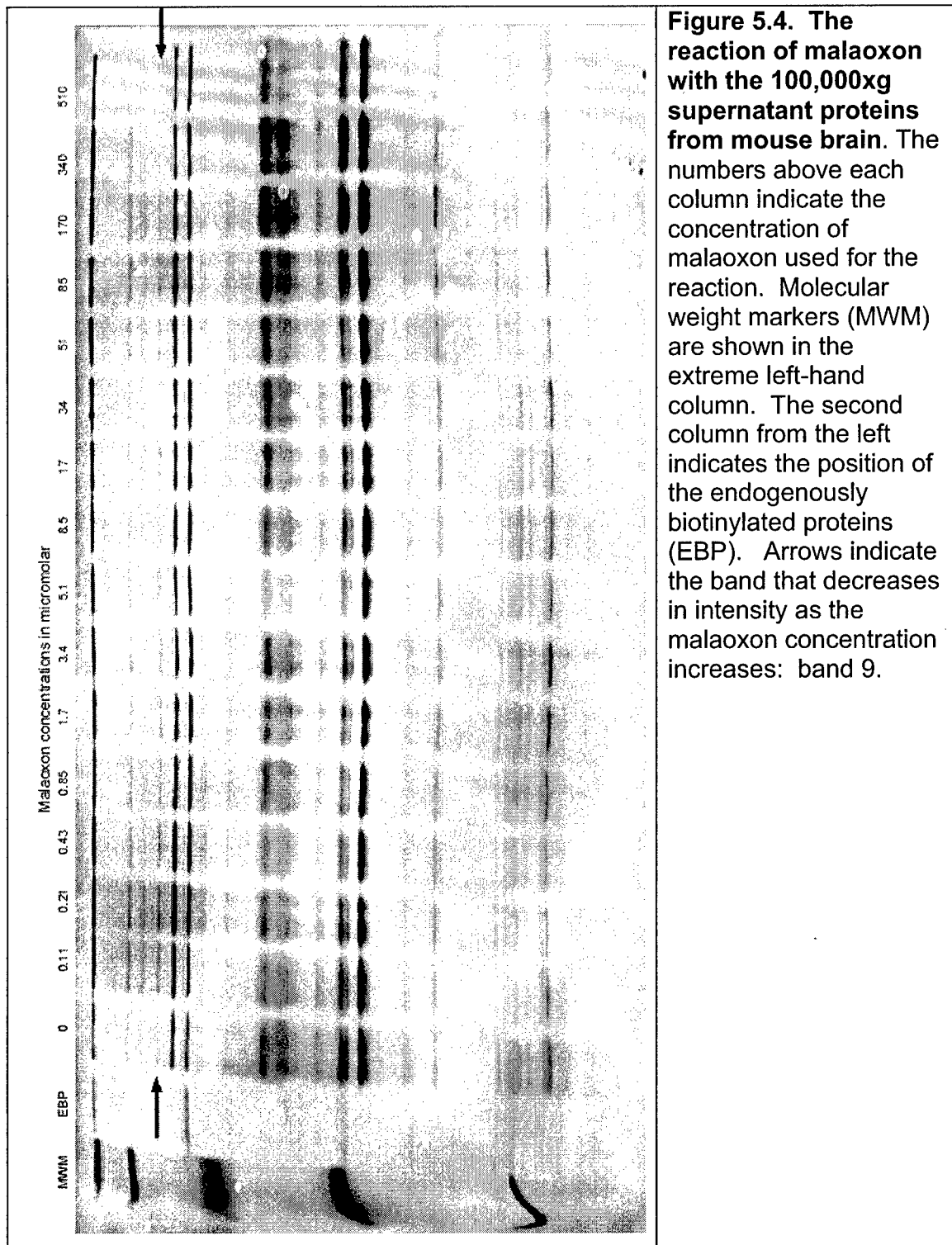
made in CHO K1 cells also gave several bands. Since OP reactive bands 9 and 12 are in the 70-80 kDa region, the human AChE control could not be used.
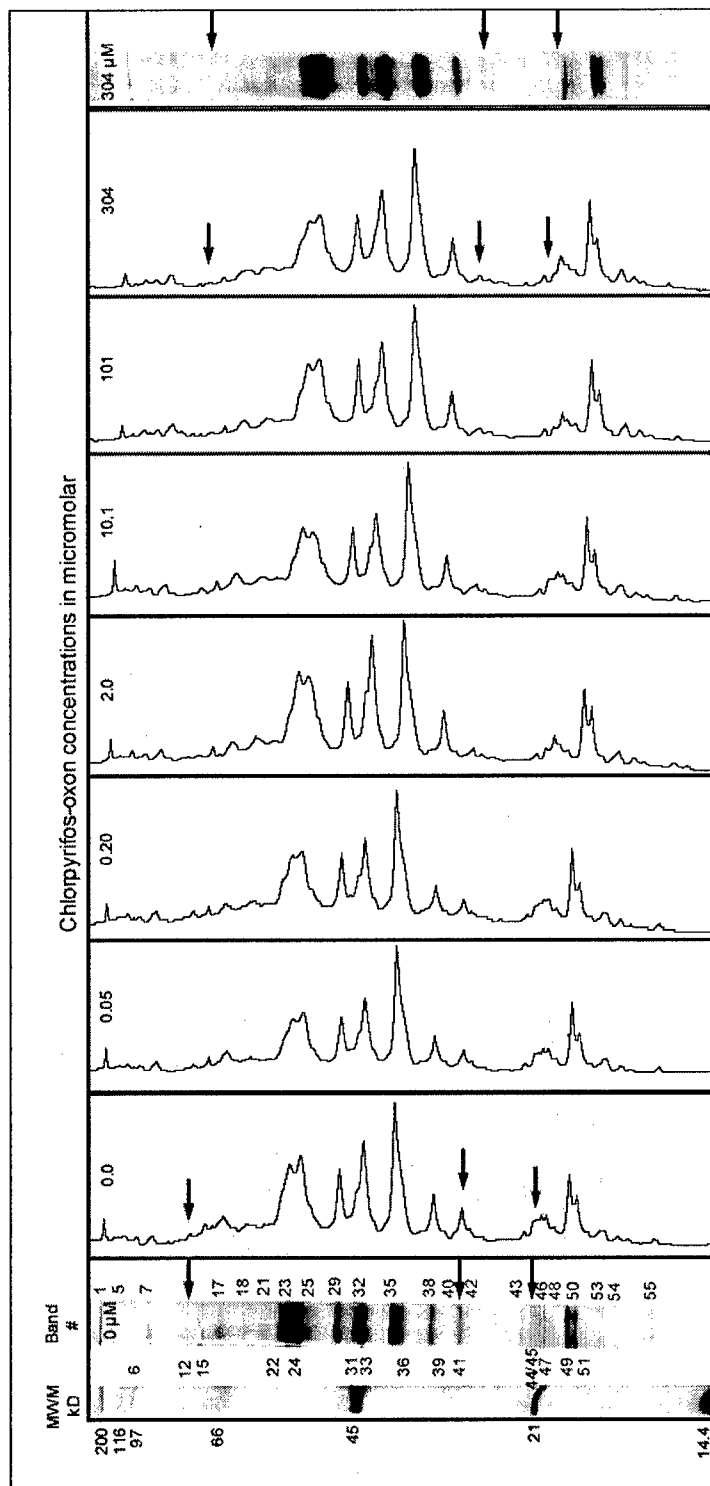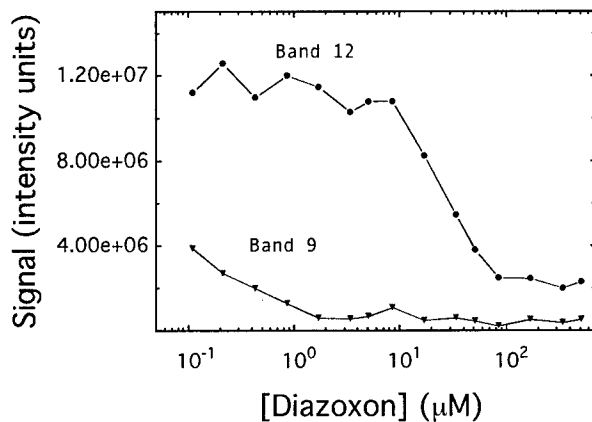

Figure 5.1. The reaction of chlorpyrifos-oxon with the 100,000xg supernatant proteins from mouse brain. The traces, in the central columns, show the integrated areas of the bands from selected lanes of an SDS PAGE. Actual pictures of the lanes are shown on the left and right of the integrated traces. The numbers above each column indicate the concentration of chlorpyrifos-oxon used for the reaction. Molecular weight markers are shown in the extreme left-hand column. The arrows indicate the bands which decrease in intensity as the chlorpyrifos-oxon concentration increases: bands 12, 41, and 44/45.

Figure 5.2. The reaction of dichlorvos with the 100,000xg supernatant proteins from mouse brain. The traces, in the central columns, show the integrated areas of the bands from selected lanes of an SDS PAGE. Actual pictures of the lanes are shown on the left and right of the integrated traces. The numbers above each column indicate the concentration of dichlorvos used for the reaction. Molecular weight markers are shown in the extreme left-hand column. The arrows indicate the bands which decrease in intensity as the dichlorvos concentration increases: bands 12, 32, 44/45, and 50.

Figure 5.3. The reaction of diazoxon with the 100,000xg supernatant proteins from mouse brain. The traces, in the central columns, show the integrated areas of the bands from selected lanes of an SDS PAGE. Actual pictures of the lanes are shown on the left and right of the integrated traces. The numbers above each column indicate the concentration of diazoxon used for the reaction. Molecular weight markers are shown in the extreme left-hand column. The arrows indicate the bands which decrease in intensity as the diazoxon concentration increases: bands 9, 12, 41, and 47.

Figure 5.4. The reaction of malaoxon with the 100,000xg supernatant proteins from mouse brain. The numbers above each column indicate the concentration of malaoxon used for the reaction. Molecular weight markers (MWM) are shown in the extreme left-hand column. The second column from the left indicates the position of the endogenously biotinylated proteins (EBP). Arrows indicate the band that decreases in intensity as the malaoxon concentration increases: band 9.

Figure 5.5a. The dependence of the integrated band intensity on diazoxon concentration for bands 9 and 12.
IC_{50} = 0.4 µM for band 9.
IC_{50} = 20 µM for band 12
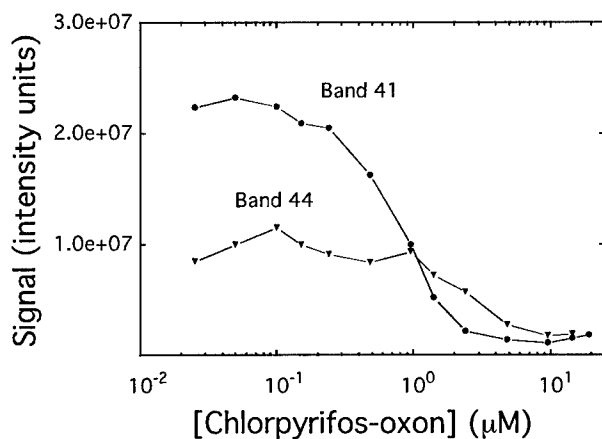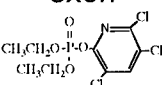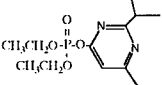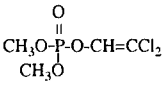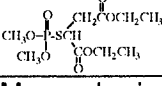
Figure 5.5b. The dependence of the integrated band intensity on chlorpyrifos-oxon concentration for bands 41 and 44.
IC_{50} = 3 µM for band 44.
IC_{50} = 0.8 µM for band 41.

Table 5.1 IC$_{50}$ values for the reaction of OP with soluble proteins in mouse brain

	IC$_{50}$ (nM) 30 min, pH 8.0, 25°C experimental values						
OP	band 9	band 12	bands 23/24	band 41	band 44/45	band 47	band 50
Chlorpyrifos oxon	??	>100,000	-	800	3000	-	-
Diazoxon	400	20,000	-	30,000	-	10,000	-
Dichlorvos	??	10,000	20,000	-	2000	-	50,000
Malaoxon	170,000	-	-	-	-	-	-

Mouse brain 100,000xg supernatant. ?? indicates that an IC$_{50}$ value is not available, but the protein in the band reacts rapidly with OP
band 9 is acylpeptide hydrolase, 80 kDa
band 12 is prolylendopeptidase, 81 kDa
band 23/24 is D-3-phosphoglycerate dehydrogenase, 51 kDa, and tubulin, 50 kDa
band 41 is esterase 10, 35 kDa (and three other proteins)
band 44/45 is platelet-activating factor acetylhydrolase alpha 2, 25 kDa
band 47/46 is platelet-activating factor acetylhydrolase alpha 1, 26 kDa and tyrosine 3-mono-
    oxygenase/tryptophan 5-monooxygenase activation protein (a protein phosphatase) 28 kDa
band 50 is lysophospholipase 1 and 2, 25 kDa.

Table 5.2 IC$_{50}$ values for the reaction of OP with proteins in mouse brain membranes.

	IC$_{50}$ (nM) 30 min, pH 8.0, 25°C						
OP	band 8	band 15	band 17	band 19	band 34	band 40	band 43
Chlorpyrifos oxon	1000	300	200	1000	2000	??	20,000
Diazoxon	-	60,000	-	-	-	10,000	1000
Dichlorvos	20,000	-	-	-	-	-	-
Malaoxon	-	10,000	-	-	-	-	-

Mouse brain 17,000Xg pellet. ?? indicates that an IC$_{50}$ value is not available, but the protein in the band reacts rapidly with OP
band 8 is heat shock protein 90-Beta, 84 kDa.
band 15 has not been identified
band 17 is a mixture of 4 proteins (RIKEN D030028o16, 73 kDa; serum albumin, 67 kDa;
    RIKEN 4931406N15, 70 kDa; heat shock protein 8, 71 kDa)
bands 19, 34, 40 and 43 have not been identified

Table 5.3 Literature IC_{50} values for the reaction of OP with AChE, fatty acid amide hydrolase (FAAH) and acylpeptide hydrolase (APH).

| | Literature References IC_{50} (nM) | | | | |
| | human 30 min, pH 7-7.6, 25-37°C | mouse 15 min, pH 8-9, 25-37°C | | pig 20 min, pH 7.4, 37°C | |
OP	AChE	AChE	FAAH	AChE	APH
Chlorpyrifos oxon	2 [5]	19 [1], 9 [5]	56 [1]	-	-
Diazoxon	60 [6]	-	9300 [1]	269 [3]	1386 [3]
Dichlorvos	200 [7]	5100 [2]	1800 [2]	788 [3]	118 [3]
Malaoxon	300 [8]	159 [4]	-	296 [3]	1,000,000 [3]

IC_{50} values for some of the literature values were calculated from reported second-order rate constants using the equation: $IC_{50} = (\ln 2)/kt.$ [9] Where k is the second-order rate constant and t is the inhibition time in minutes.

1 (Quistad et al., 2001)
2 (Quistad et al., 2002)
3 (Richards et al., 2000)
4 (Johnson and Wallace, 1987)
5 (Amitai et al., 1998)
6 Schopfer unpublished
7 (Skrinjaric-Spoljar et al., 1973)
8 (Rodriguez et al., 1997)
9 (Main, 1979)

Identity of the proteins that react with the test battery of OP. Proteins were identified by mass spectroscopy as described in task 4. Six of the 7 OP reactive bands in Table 5.1 yielded identifiable proteins, 5 of which were hydrolases. Band 12 was prolylendopeptidase 81 kDa; band 23/24 was D-3-phosphoglycerate dehydrogenase 51 kDa and tubulin 50 kDa; band 41 contained esterase 10 with a molecular weight of 35 kDa (and three other proteins); band 44/45 was platelet-activating factor acetylhydrolase alpha 2 with a molecular weight of 25 kDa; band 47/46 contained platelet-activating factor acetylhydrolase alpha 1 with a molecular weight of 26 kDa and tyrosine 3-monooxygenase/tryptophan 5-monooxygenase activation protein (a protein phosphatase) 28 kDa; band 50 gave lysophospholipase 1 and 2 with molecular weights of 25 kDa. The remaining OP-reactive band (band 9) can be tentatively assigned to acylpeptide hydrolase (APH). This assignment is based on the molecular weight of acylpeptide hydrolase (MW= 80 kDa), the position of band 9 in the blot pattern, and the fact that acylpeptide hydrolase already has been shown to be highly reactive toward the type of OP tested in these experiments (Richards et al., 2000).

Band 47/46 showed greater reactivity with dichlorvos (IC_{50}=2000 nM) than did AChE (IC_{50}=5100 nM). No literature information on the reaction of dichlorvos with either

of the enzymes in this band (platelet-activating factor acetylhydrolase alpha 1 and tyrosine 3-monooxygenase/tryptophan 5-monooxygenase activation protein) could be found.

Band 41 was relatively reactive toward chlorpyrifos-oxon (IC_{50}=800 nM). Of the 4 proteins which were identified in this sample, esterase 10 is the most likely to be a target for chlorpyrifos-oxon.
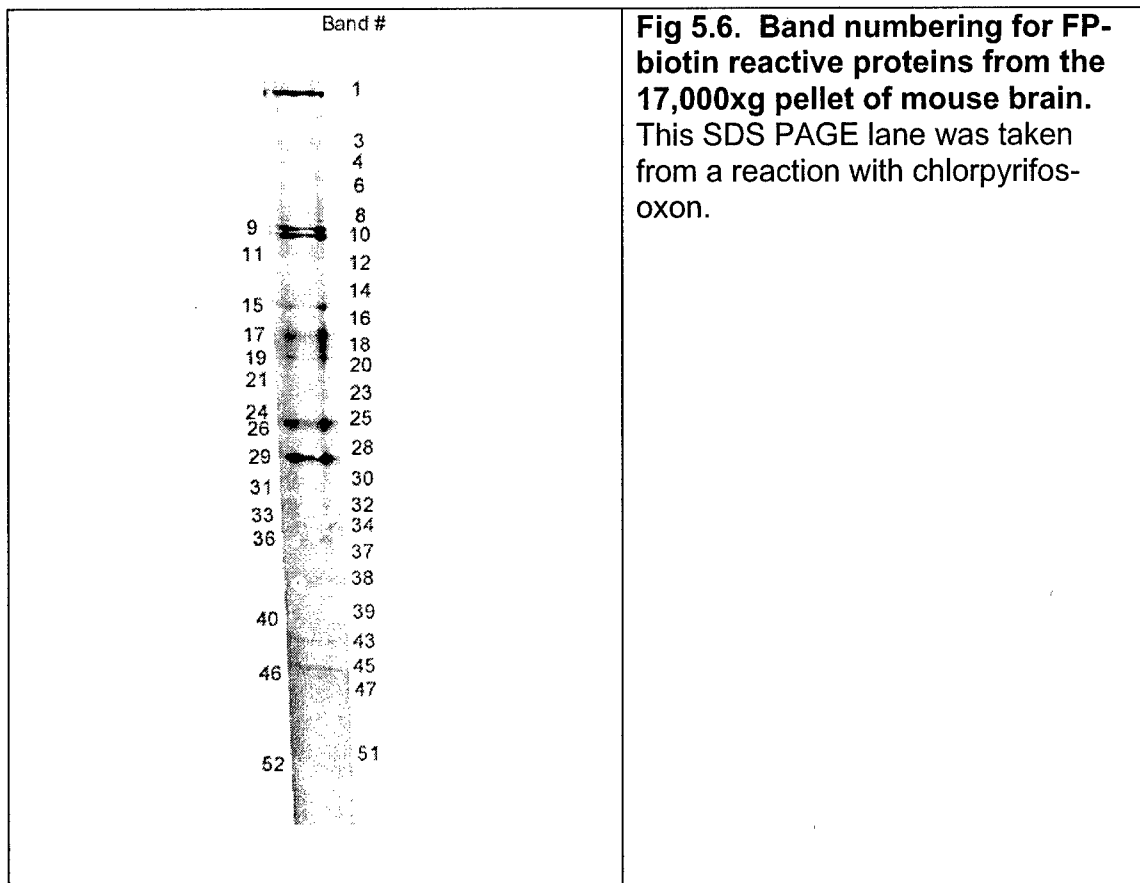
Band 9 remains of interest. It shows a relative reactivity with diazoxon and malaoxon which is similar to that of acylpeptide hydrolase (APH) (Table 5.1). This supports the suggestion that band 9 is APH. If so, then band 9 would be expected to show greater reactivity with dichlorvos than does AChE (refer to the IC_{50} values for pig APH and pig AChE in Table 5.1).

Screening for organophosphate reactivity in 17,000xg mouse brain pellet. The screening has been extended to the 17,000xg pellet from mouse brain (the synaptosomal fraction). Fifty-two FP-biotin reactive proteins were found in the synaptosomal fraction (Figure 5.6). As with the 100,000xg supernatant, minor bands and shoulders from major bands were included in the numbering. The proteins in this fraction would be expected to be mostly membrane bound, therefore representing a different selection of targets than were available in the 100,000xg supernatant.

The same four OP used on the 100,000x g supernatant were tested with the 17,000xg pellet (Table 5.1): chlorpyrifos oxon, diazoxon, dichlorvos, and malaoxon. Bands which were sensitive to these OP were all present at low levels, therefore IC_{50} values were evaluated by visual inspection of the banding patterns (see Figure 5.7 for an example). Seven bands were found to disappear with chlorpyrifos-oxon (8, 15, 17, 19, 34, 40, and 43). Band 8 is heat shock protein 90-Beta 84 kDa. Band 15 has not been identified. Band 17 is a mixture of 4 proteins (see Table 4.1 in task 4). Bands 19, 34, 40 and 43 have not been identified.

The most reactive were bands 15 and 17 (IC_{50} values of 200 to 300 nM with chlorpyrifos-oxon). These values are about 10-fold higher than those found in the literature for mouse AChE (9-19 nM), indicating that the proteins in bands 15 and 17 are less reactive than AChE with chlorpyrifos oxon.

The other three OP (diazoxon, dichlorvos, and malaoxon) reacted with a few of the bands in the chlorpyrifos-oxon set, but with no other bands. Diazoxon reacted with bands 15, 40, and 43. Dichlorvos reacted with band 8. Malaoxon reacted with band 15. Dichlorvos and malaoxon were less reactive with those bands than with AChE (Table 5.1). Diazoxon has no literature value for reaction with mouse AChE so a comparison cannot be made at this time.

Band #

Fig 5.6. Band numbering for FP-biotin reactive proteins from the 17,000xg pellet of mouse brain. This SDS PAGE lane was taken from a reaction with chlorpyrifos-oxon.

Figure 5.7. The reaction of chlorpyrifos-oxon with the 17,000xg pellet proteins from mouse brain. The numbers above each column indicate the concentration of chlorpyrifos-oxon used for the reaction. Molecular weight markers (MWM) are shown in the extreme right-hand column. The second column from the right indicates the position of the endogenously biotinylated proteins (EBP). Selected bands have been numbered. Arrows indicate the bands that decrease in intensity as the chlorpyrifos-oxon concentration increases: bands 8, 15, 17, 19, 34, 40, and 43.

Discussion

Methods for screening complex mixtures of proteins for reaction with OP have been established by us. They have been applied to the reactions of chlorpyrifos-oxon, diazoxon, dichlorvos, and malaoxon with mouse brain supernatant (100,000xg) and synaptosomal (17,000xg pellet) fractions. In addition, mass spectral methods for identification of the reactive proteins are operational, and the 100,000xg supernatant has been checked for OP reactive proteins.

Experiments suggest that only the reaction of dichlorvos with platelet-activating factor acetylhydrolase alpha-2 and with acylpeptide hydrolase (Richards et al., 2000) occurs more readily than with AChE.

Fatty acid amide hydrolase is an interesting candidate, which should appear in the synaptosomal fraction. It is a membrane bound enzyme which has been shown to react with diazinon and chlorpyrifos more readily than does AChE (Quistad et al., 2001; Quistad et al., 2002).

The acute toxicity of organophosphorus agents (OP) is explained by inhibition of acetylcholinesterase (AChE). However, toxicity from low dose exposure is not understood. Using mass spectroscopy, we have developed the hypothesis that multiple targets for each OP exist, and that target identity varies with the OP. Thus, dichlorvos covalently binds to acetylcholinesterase, butyrylcholinesterase, platelet-activating factor acetylhydrolase alpha 2, and acylpeptide hydrolase. FP-biotin binds not only to these proteins but also to albumin (Peeples et al., 2005), platelet-activating factor acetylhydrolase alpha 1, esterase 10, and fatty acid amide hydrolase (Liu et al., 1999). Covalent binding to a set of proteins is hypothesized to explain low dose toxicity. Each OP is hypothesized to bind to a slightly different set, and therefore to have a unique mechanism of toxicity.

Task 6

The toxicological relevance of the biochemical markers
identified in task 3 will be determined. Mice will be
treated with the dose of insecticide determined in Task 2,
that is, a dose that is not toxic to wild-type mice, but is
toxic to AChE deficient mice.

Task 6.1. Relation to statement of work: The following work was essential to understanding why AChE and BChE were not showing up in the mass spectral analysis of OP-treated mice. It was concluded that AChE and BChE reacted rapidly with OP, but the abundance of AChE and BChE was too low to be detected in the mass spectrometer under our conditions.

6.1. Reaction kinetics of biotinylated organophosphorus toxicant, FP-biotin, with human acetylcholinesterase and human butyrylcholinesterase

Lawrence M. Schopfer, Troy Voelker, Cynthia F. Bartels, Charles M. Thompson, Oksana Lockridge

Abstract
A biotinylated organophosphate could be useful for identifying proteins that react with organophosphorus toxicants (OP). FP-biotin, 10-(fluoroethoxyphosphinyl)-N-(biotinamidopentyl)decanamide, was synthesized and found to be stable in methanol and chloroform, but less stable in water. Since acetylcholinesterase (AChE, EC 3.1.1.7) and butyrylcholinesterase (BChE, EC 3.1.1.8) are known to be sensitive targets of OP, their reactivity with FP-biotin was tested. The rate constant for reaction with human acetylcholinesterase was $1.8 \times 10^7 \, M^{-1}min^{-1}$, and for human butyrylcholinesterase it was $1.6 \times 10^8 \, M^{-1}min^{-1}$. A phosphorus stereoisomer, constituting about 60% of the FP-biotin preparation, appeared to be the reactive species. The binding affinity was estimated to be > 85 nM for AChE and > 5.8 nM for BChE. It was concluded that FP-biotin is a potent OP, well suited for searching for new biomarkers of OP exposure.

A copy of this publication is attached.

Task 6.2. Relation to statement of work: The following method was developed to enable us to identify OP-labeled proteins in the mass spectrometer with 100% confidence. This method excludes false positives, that is, proteins that nonspecifically copurify with OP-labeled proteins.

6.2. Characteristic Mass Spectral Fragments of the Organophosphorus Agent FP-biotin and FP-biotinylated Peptides from Trypsin and Bovine Albumin (Tyr410)

Lawrence M. Schopfer, Mark M. Champion, Nate Tamblyn, Charles M. Thompson and Oksana Lockridge

Abstract
A mass spectrometry-based method was developed for selective detection of FP-biotinylated peptides in complex mixtures. Mixtures of peptides, at the low picomole level, were analyzed by liquid chromatography and positive ion, nanospray, triple-quadrupole, linear ion trap, mass spectrometry. Peptides were fragmented by collision activated dissociation in the mass spectrometer. The free FP-biotin and peptides containing FP-biotinylated serine or FP-biotinylated tyrosine yielded characteristic ions at 227, 312 and 329 m/z. FP-biotinylated serine yielded an additional characteristic ion at 591 m/z. Chromatographic peaks containing FP-biotinylated peptides were indicated by these diagnostic ions. Data illustrating the selectivity of the approach are presented for tryptic digests of FP-biotinylated trypsin and FP-biotinylated serum albumin. A 16 residue peptide from bovine trypsin was biotinylated on the active site serine. A 3-residue peptide from bovine albumin, YTR, was biotinylated on Tyr 410. This latter result confirms that the organophosphorus binding site of albumin is a tyrosine. This method can be used to search for new biomarkers of organophosphorus agent exposure.

A copy of this publication is attached.

Task 6.3. Relation to statement of work: To understand the toxicological relevance of OP modification of proteins in blood, it is important to know what esterases are present in blood. The following presentation identifies the esterases in human and mouse plasma.

6.3. Butyrylcholinesterase, paraoxonase, and albumin esterase, but not carboxylesterase, are present in human plasma

Bin Li, Meghan Sedlacek, Indumathi Manoharan, Rathnam Boopathy, Ellen G. Duysen, Patrick Masson, Oksana Lockridge

Abstract

The goal of this work was to identify the esterases in human plasma and to clarify common misconceptions. The method for identifying esterases was nondenaturing gradient gel electrophoresis stained for esterase activity. We report that human plasma contains 4 esterases: butyrylcholinesterase (EC 3.1.1.8), paraoxonase (EC 3.1.8.1), acetylcholinesterase (EC 3.1.1.7), and albumin. Butyrylcholinesterase (BChE), paraoxonase (PON1), and albumin are in high enough concentrations to contribute significantly to ester hydrolysis. However, only trace amounts of acetylcholinesterase (AChE) are present. Monomeric AChE is seen in wild-type as well as in silent BChE plasma. Albumin has esterase activity with alpha- and beta-naphthylacetate as well as with p-nitrophenyl acetate. Misconception #1 is that human plasma contains carboxylesterase. We demonstrate that human plasma contains no carboxylesterase (EC 3.1.1.1), in contrast to mouse, rat, rabbit, horse, cat, and tiger that have high amounts of plasma carboxylesterase. Misconception #2 is that lab animals have BChE but no AChE in their plasma. We demonstrate that mice, unlike humans, have substantial amounts of soluble AChE as well as BChE in their plasma. Plasma from AChE and BChE knockout mice allowed identification of AChE and BChE bands without the use of inhibitors. Human BChE is irreversibly inhibited by diisopropylfluorophosphate, echothiophate and paraoxon, but mouse BChE spontaneously reactivates. Since human plasma contains no carboxylesterase, only BChE, PON1, and albumin esterases need to be considered when evaluating hydrolysis of an ester drug in human plasma.

Introduction

Esterases in human plasma have an important role in the disposition of drugs. They participate in activation of ester prodrugs, for example, the prodrug bambuterol is converted to the antiasthma drug terbutaline, and isosorbide-based prodrugs release aspirin. A second role is to inactivate drugs. For example, esterases in plasma inactivate the local anesthetics procaine and tetracaine, the muscle relaxants,

succinylcholine and mivacurium, and the analgesics, aspirin and cocaine. A third role for esterases in plasma is to detoxify natural and synthetic ester-containing poisons, for example eserine (physostigmine) from the Calabar bean and organophosphorus pesticides are detoxified by hydrolysis or by binding. Table 6.3.1 lists drugs modified by the action of esterases in human plasma. Note that aspirin is hydrolyzed by BChE and albumin, and that paraoxon is hydrolyzed by PON1 and albumin. Paraoxon also interacts with BChE, but is not listed in the BChE column because the binding is stoichiometric rather than catalytic. To understand individual variation in response to drugs it is important to know the identity of the esterase responsible for drug hydrolysis. A classic example is the case of the muscle relaxant succinylcholine. The era of pharmacogenetics was born when it was discovered that people who responded abnormally to succinylcholine had an inherited deficiency of butyrylcholinesterase (Kalow and Staron, 1957; Kalow and Grant, 1995). Today more than 56 mutations in the BChE gene have been identified (Souza *et al.*, 2005). People who have two deficient BChE alleles cannot metabolize succinylcholine and therefore are unable to breathe for two hours from a dose intended to paralyze for 3-5 min.

Table 6.3.1 Clinically relevant compounds hydrolyzed by human plasma esterases.

Drug action	BChE	PON1	albumin	reference
analgesic	aspirin		aspirin	(Morikawa *et al.*, 1979; Rainsford *et al.*, 1980; Masson *et al.*, 1998)
analgesic	isosorbide diaspirinate			(Gilmer *et al.*, 2002)
anti-asthma	bambuterol			(Tunek and Svensson, 1988)
analgesic, vasoconstrictor	(-)-cocaine			(Stewart *et al.*, 1977; Lynch *et al.*, 1997)
anti-cancer	irinotecan (CPT-11)			(Morton *et al.*, 1999)
reduce heart rate	flestolol		flestolol	(Quon and Stampfli, 1993)
alpha-blocker, erectile dysfunction	moxisylyte			(Chapuis *et al.*, 2001)
stimulates eating	n-octanoyl ghrelin			(De Vriese *et al.*, 2004)
analgesic	heroin			(Lockridge *et al.*, 1980)
local anesthetic	procaine			(Foldes *et al.*, 1953)
muscle relaxant	succinylcholine			(Lockridge, 1990; Kalow and Grant, 1995)
muscle relaxant	mivacurium			(Savarese et al., 1988; Ostergaard et al., 1995a)
anti-inflammatory	methyl prednisolone acetate			(Meyers *et al.*, 1982)

local anesthetic	chloroprocaine			(O'Brien et al., 1979)
local anesthetic	tetracaine			(Becker, 1973)
diuretic		spironolactone		(Billecke et al., 2000)
lower cholesterol		lovastatin, mevastatin, simvastatin		(Billecke et al., 2000)
pesticide		paraoxon	paraoxon	(Ortigoza-Ferado et al., 1984; Smolen et al., 1991)
pesticide		diazoxon		(Davies et al., 1996)
nerve agent		sarin		(Davies et al., 1996)
antibacterial		prulifloxacin		(Tougou et al., 1998)
anti-asthma		glucocorticoid-lactones		(Biggadike et al., 2000)
antabuse			disulfiram	(Agarwal et al., 1986)
anti-cancer			cyclophosphamide	(Kwon et al., 1987)
anti-inflammatory			ketoprofen glucuronide	(Dubois-Presle et al., 1995)
topical analgesic			nicotinate esters	(Salvi et al., 1997)
pesticide			carbaryl	(Sogorb et al., 2004)
insecticide			O-hexyl O-2,5-dichlorphenyl phosphoramidate	(Sogorb et al., 1998)

Knowledge of the identity of the esterases involved in drug hydrolysis can help explain drug response in individuals with disease. For example, diabetics have higher than average BChE levels in their plasma (Abbott et al., 1993; Alcantara et al., 2002; Cucuianu et al., 2002) and might therefore require higher doses of aspirin.

A drug that requires the action of an esterase could be ineffective if that esterase were inhibited by another drug. For example, echothiophate eyedrops administered for treatment of glaucoma, inhibit plasma BChE (Gesztes, 1966). Bambuterol might be ineffective as an asthma drug in a patient receiving echothiophate. Natural toxins present in food may also affect the metabolism of esters, and thus cause side effects. For instance, potato glyco-alkaloids (solanine and chaconine) that reversibly inhibit BChE have been reported to slow the degradation of the myorelaxant mivacurium (McGehee et al., 2000).

While BChE, AChE, and PON1 are well known esterases, albumin is not usually included in the family of esterases. Albumin does not have an enzyme commission number, which signifies that this protein is considered to be inert without catalytic activity. However, albumin has been conclusively proven to be an esterase (Erdos and Boggs, 1961; Tove, 1962; Means and Wu, 1979; Hagag et al., 1983; Yoshida et al., 1985; Awad-Elkarim and Means, 1988; Salvi et al., 1997; Sogorb et al., 1998; Watanabe et al., 2000; Kragh-Hansen et al., 2002; Sakurai et al., 2004; Ahmed et al., 2005). The active site of human albumin is Tyr 411 and of bovine albumin is Tyr 410

(Sanger, 1963; Schopfer et al., 2005). The active site of bovine albumin was identified by mass spectroscopy after labeling albumin with a biotinylated organophosphorus agent (Schopfer et al., 2005). Although the enzymatic activity of a single molecule of human albumin is low, the concentration of albumin is very high, so that albumin makes a significant contribution to drug metabolism.

Our goal is to identify the esterases in human plasma, and to demonstrate the absence of carboxylesterase (EC 3.1.1.1) in human plasma.

Materials and Methods

Materials. Silent BChE plasma samples were from the United States, India, and France. Silent plasma was stored at -20°C. Silent BChE samples had no detectable activity with butyrylthiocholine or benzoylcholine. Human serum from people with wild-type BChE contained no anticoagulant and was stored at -80°C. Serum containing wild-type BChE had an activity of 3 to 4 µmoles per min per ml (1 mM butyrylthiocholine, pH 7, 0.1 M potassium phosphate ? buffer, 25°C).

All mice were strain 129Sv. Mouse serum was freshly drawn from the hind leg vein. Gene-targeted BChE knockout mice (BChE-/-) and AChE knockout mice (AChE-/-) were from colonies created and maintained at the University of Nebraska Medical Center (Li et al., ; Duysen et al., 2002).

Eserine, diisopropylfluorophosphate (DFP), butyrylthiocholine, acetylthiocholine, alpha-naphthylacetate, beta-naphthylacetate, Fast Blue RR, and human albumin fatty acid free were from Sigma. Echothiophate was from Wyeth-Ayerst. Paraoxon was from ChemService, West Chester, PA. Purified human BChE was prepared from outdated human plasma (Lockridge *et al.*, 2005).

Nondenaturing gradient gel electrophoresis. 4-30% polyacrylamide gels, 0.75 mm thick, were poured in a Hoefer gel apparatus. Electrophoresis was for 5000 volt hours (250 volts for 20 h) at 4°C. Plasma samples were mixed with an equal volume of 50% glycerol, 0.1 M TrisCl, 0.1% bromophenol blue before loading on the gel. The equivalent of 5 µl of plasma or serum was loaded per lane.

Staining for AChE activity. The histochemical method of Karnovsky and Roots was adapted to polyacrylamide gels (Karnovsky and Roots, 1964). The staining solution contained 180 ml of 0.2 M maleic acid pH 6.0, 15 ml of 0.10 M sodium citrate, 30 ml of 0.030 M $CuSO_4$, 30 ml water, 30 ml of 5 mM potassium ferricyanide and 150 mg of acetylthiocholine iodide. Gels were incubated for 2 to 5 hours, or overnight, with gentle shaking. Brown-red bands of activity developed.

Identification of AChE bands on gels. Gels stained with acetylthiocholine revealed both AChE and BChE because both enzymes have high activity with acetylthiocholine. Comparison to a gel stained with butyrylthiocholine, which stains only BChE, identified AChE. Silent BChE plasma had no BChE bands, but did have a band for AChE, thus confirming the identity of the AChE band in human plasma. AChE activity is inhibited by DFP, echothiophate, and paraoxon. The organophosphorus agents (OP) distinguish serine esterases from PON1 because PON1 is not inhibited by OP. Serum from

knockout mice that had zero BChE activity allowed identification of AChE bands without the use of inhibitors.

Staining for BChE activity. The same Karnovsky and Roots staining solution was used to stain for BChE activity except that in place of acetylthiocholine, the substrate was 2 mM butyrylthiocholine iodide (180 mg in 300 ml).

Identification of BChE bands on gels. Bands of BChE activity were revealed on a gel in the presence of the BChE-specific substrate, butyrylthiocholine. AChE has only weak activity with butyrylthiocholine and does not stain, unless the amount of AChE is very high. Purified human BChE confirmed the identity of the tetramer BChE band in serum. Another confirmation was the absence of bands in plasma from people with silent BChE. Organophosphorus inhibitors, DFP, echothiophate, and paraoxon, distinguished between serine esterases and PON because serine esterases are inhibited but PON is not inhibited by OP. Serum from knockout mice that had zero AChE activity allowed identification of BChE bands without the use of inhibitors.

Staining for PON1 activity. The method was adapted from (Furlong *et al.*, 1991). The staining solution contained 100 ml of 50 mM TrisCl pH 8, 10 mM calcium chloride and 50 mg of beta-naphthylacetate dissolved in 1 ml ethanol. Some of the beta-naphthylacetate fell out of solution after addition to aqueous buffer, but this was not a problem. Solid Fast Blue RR, 50 mg, was added. Though Fast Blue RR did not dissolve, the reaction worked. Pink bands of activity formed within minutes. After 20-60 min the gel was washed with water. Spots of dye were washed off with 50% methanol, 10% acetic acid.

Identification of PON1 on gels. Paraoxonase is a calcium-dependent enzyme associated with the high-density lipoprotein complex. PON stains with beta-naphthylacetate. PON is positively identified by its sensitivity to inhibition by 5 mM EDTA. Chelation of calcium inactivates PON. None of the other esterases in human and mouse plasma are inactivated by EDTA. The broad smear of PON activity on a gel is due to its association with high-density lipoprotein.

Staining for carboxylesterase activity. Staining with beta-naphthylacetate revealed PON1 as well as carboxylesterase activity. When it was desired to visualize carboxylesterase activity without PON1 activity, the substrate was alpha-naphthylacetate. 50 mg of alpha-naphthylacetate in 1 ml ethanol and 50 mg of solid Fast Blue RR in 100 ml of 50 mM TrisCl pH 8 buffer gave dark green bands (Hashinotsume *et al.*, 1978).

Identification of carboxylesterase on gels. Carboxylesterase stains well with alpha-naphthylacetate and with beta-naphthylacetate. Carboxylesterase is a serine esterase and is therefore inhibited by organophosphorus agents. However, carboxylesterase is distinguished from AChE and BChE by its lack of reactivity with positively charged substrates and positively charged OP (Maxwell *et al.*, 1994). Thus, carboxylesterase does not stain with the positively charged acetylthiocholine and butyrylthiocholine, and it

is not inhibited by the positively charged echothiophate. Carboxylesterase is not inhibited by EDTA.

Staining for albumin esterase activity. Nondenaturing gels revealed albumin esterase activity when they were incubated in 100 ml buffer containing either alpha or beta-naphthylacetate (50 mg dissolved in 1 ml ethanol) and 50 mg of solid Fast Blue RR, for 10 to 60 min.

Identification of albumin on gels. Albumin esterase activity was identified by staining with alpha or beta-naphthylacetate. However, albumin showed no esterase activity with butyrylthiocholine or acetylthiocholine. Albumin esterase activity was resistant to inhibition by DFP, echothiophate, paraoxon, and EDTA. Albumin reacts covalently with OP at high pH and high concentrations of OP (Means and Wu, 1979; Peeples et al., 2005), but not under our experimental conditions. Gel electrophoresis of purified fatty acid free human albumin confirmed the location of the albumin band on gels. During electrophoresis, the location of albumin is clearly seen as the slow migrating blue band in samples that contain bromophenol blue tracking dye. Bromophenol blue binds to human albumin. The bromophenol blue washes out of the gel during overnight incubation in staining solution.

Inhibitor treatment to identify esterases. To identify serine esterases, human and mouse plasma samples were incubated with 0.1 mM DFP, echothiophate, or paraoxon for 2 h at 25°C, assayed for enzyme activity, and subjected to gel electrophoresis. In some cases, at the end of electrophoresis and before staining, the gels were pre-incubated in 0.1 mM OP in staining solution for 30 min before addition of substrate. To identify calcium requiring esterase, plasma samples were preincubated with 10 mM EDTA.

Enzyme activity assays. BChE activity was measured with 1 mM butyrylthiocholine in 0.1 M potassium phosphate buffer pH 7.0 at 25°C (Ellman et al., 1961). Combined AChE and BChE activity was measured with 1 mM acetylcholine.

Results
Human plasma contains 4 esterases.
The esterases in human plasma are BChE, PON1, albumin, and AChE. The migration of each of these esterases relative to each other on nondenaturing gels is shown in Figures 6.3.1-6.3.4. Figure 6.3.1 shows the monomer, dimer, trimer, and tetramer bands of BChE in human serum. Figure 6.3.1 also shows that plasma from 6 individuals with silent BChE have no BChE activity as the lanes are blank. In Figure 6.3.2 human plasma samples were run on a gel stained with acetylthiocholine, revealing a band of monomeric human AChE in silent BChE as well as in wild-type BChE samples. Figure 6.3.3 shows PON activity in human serum and the absence of PON activity in EDTA-treated plasma. Figures 6.3.3 and 6.3.4 show albumin esterase activity in gels developed with beta-naphthylacetate.

wild-type BChE   silent BChE plasma

tetramer
trimer

dimer
BChE alb

monomer

albumin

1   2   3   4   5   6   7   8   9   10   11   12
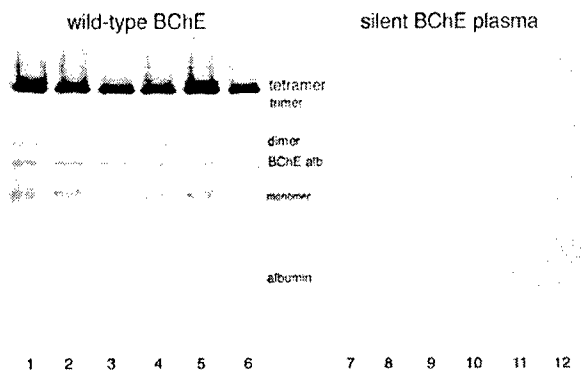
Figure 6.3.1. Nondenaturing gel stained for BChE activity with butyrylthiocholine.
Six wild-type BChE serum or plasma samples, and 6 silent BChE plasma samples from
12 different people were loaded at 5 μl per lane. Wild-type BChE samples show a
predominance of BChE tetramers, and weak bands of BChE trimers, dimers, and
monomers.   Silent BChE samples are blank in corresponding regions. Albumin is
identified by its transient binding of bromophenol blue. The band labeled BChE-alb is a
disulfide-bonded dimer between one subunit of BChE and one molecule of albumin
(Masson, 1989).

wild-type BChE   silent BChE plasma

AChE

1   2   3   4   5   6
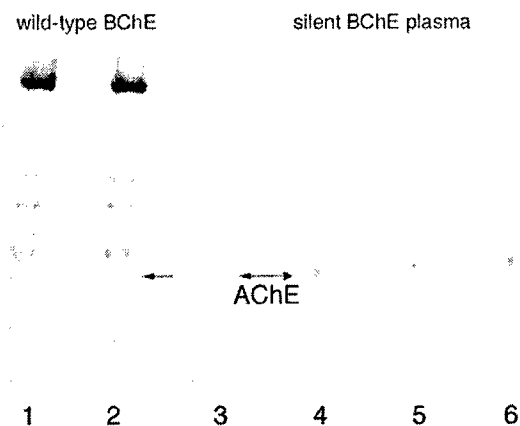
Figure 6.3.2. Nondenaturing gel stained for activity with acetylthiocholine. A new
band, not present in Figure 6.3.1, appears below the BChE monomer band. This new
band is AChE monomer. The AChE monomer is present in wild-type as well as in silent
BChE human plasma.   Human BChE tetramer, trimer, dimer and monomer bands are
also present. There is no albumin band on this gel because the bromophenol blue
washed off. Two wild-type BChE sera were loaded at 5 μl per lane. One silent plasma
was loaded at 5, 10, 15, and 20 μl per lane.

65
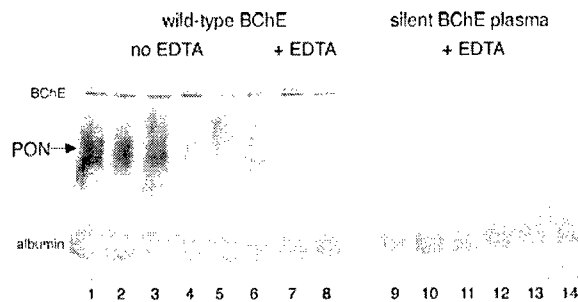
Figure 6.3.3. Gel stained for PON activity with beta-naphthylacetate. Samples from 14 individuals were loaded on the gel: 6 serum samples contained wild-type BChE and no EDTA, 2 wild-type BChE samples with EDTA, and 6 silent BChE plasma samples with EDTA. The broad PON band is missing from all samples that contain EDTA. Albumin stains well with beta-naphthylacetate. The BChE tetramer shows up as a distinct band near the top of the gel. One wild-type sample contains a BChE doublet, representing the C5 BChE phenotype (Simpson, 1972). EDTA had no effect on BChE and albumin esterase activity.
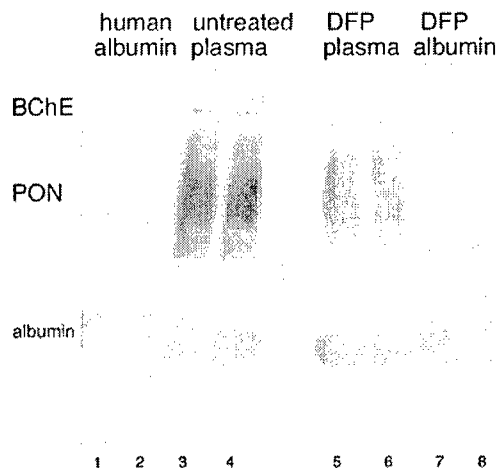
Figure 6.3.4. Albumin esterase activity. The gel was stained with beta-naphthylacetate. Pure fatty acid free human albumin has the same band of activity as the albumin in untreated human plasma. The intensity of the albumin band is unaffected by treatment with DFP under our experimental conditions. PON activity is also unaffected by treatment with DFP, but the BChE band disappears.

Albumin esterase activity stains equally well with beta- and alpha-naphthylacetate. Others have reported albumin esterase activity with naphthylacetate esters ((Casida and Augustinsson, 1959; Ecobichon and Kalow, 1962; Tove, 1962; Hess *et al.*, 1963).

Sensitivity of detection. It has been estimated by immunochemical methods that human plasma contains 8 ng/ml of AChE (Sorensen *et al.*, 1986; Brimijoin and

66

Hammond, 1988). A nondenaturing gel stained for AChE activity visualized a band of AChE activity in as little as 5 µl of human plasma, representing 0.04 ng of AChE.

Only monomeric AChE was detected, though tetrameric AChE has also been reported to be present in fresh human serum (Sorensen *et al.*, 1986). Silent BChE samples should have shown tetrameric AChE because silent BChE plasma has no interference from BChE. The absence of tetrameric AChE in silent BChE plasma is probably explained by the fact that plasma samples had been stored at -20°C and freeze-thawed more than once, resulting in degradation of tetrameric AChE (Saez-Valero *et al.*, 1993).

No carboxylesterase in human serum

Carboxylesterase migrates very close to albumin on nondenaturing gels. An intense band of activity with alpha-naphthylacetate is seen in the plasma of animals that have carboxylesterase, that is mouse, rat, rabbit, cat, tiger, and horse (Figure 6.3.5). In contrast, man, monkey, chicken, cow, goat, sheep, and pig have no carboxylesterase enzyme in their plasma. A similar intense band of carboxylesterase activity is seen when the gel is stained with beta-naphthylacetate (data not shown).

The band was identified as carboxylesterase by its resistance to inhibition by EDTA, resistance to inhibition by the positively charged organophosphorus agent, echothiophate, and its sensitivity to inhibition by DFP and paraoxon. Resistance to inhibition by eserine, a specific cholinesterase inhibitor, was seen when the gel was preincubated with eserine before addition of alpha-naphthylacetate. None of the other esterases have all of these characteristics. In addition, we used mass spectroscopy to identify FP-biotin labeled carboxylesterase in mouse serum, and found that the FP-biotinylated carboxylesterase migrated on a nondenaturing gel just above albumin (Peeples *et al.*, 2005).

human monkey mouse   rat   rabbit chicken   cat   tiger

— BChE

← CE
←albumin

1   2   3   4   5   6   7   8

human   horse   cow   fetal calf   goat   sheep   pig

— BChE

AChE

CE

albumin

9   10   11   12   13   14   15
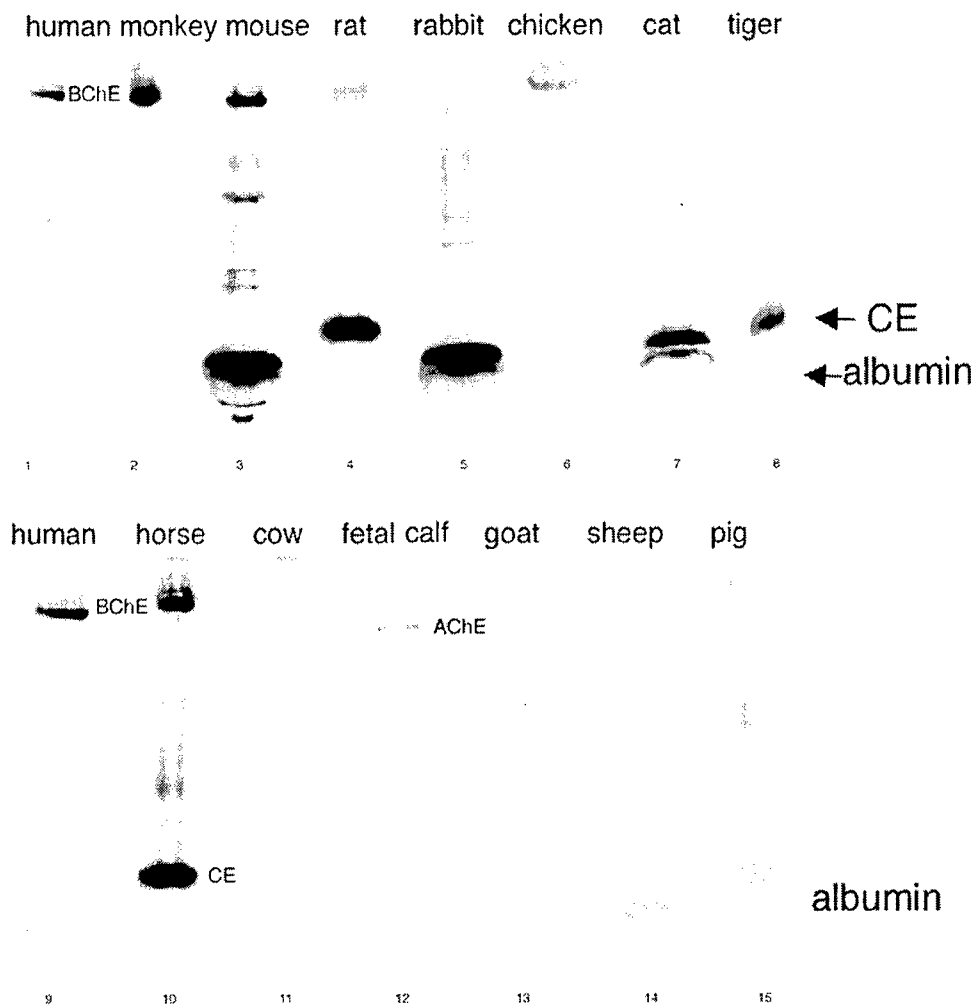
Figure 6.3.5. No carboxylesterase in human serum. The nondenaturing gel was stained for activity with alpha-naphthylacetate. Five µl of serum or plasma from each animal was loaded per lane. The intense band above albumin in mouse, rat, rabbit, cat, tiger, and horse is carboxylesterase (CE). Fetal calf but not adult cow serum has AChE.

Visualizing AChE and BChE bands in knockout mouse plasma. Plasma from knockout mice completely deficient in either AChE or BChE allowed clear identification of AChE and BChE bands without the use of inhibitors. Figure 6.3.6 compares the pattern of staining with acetylthiocholine for wild-type, BChE-/-, and AChE-/- mouse plasma. All the bands in lane 5 are AChE, while all the bands in lane 6 are BChE. The bands in lane 6 are darker than the bands in lane 5, consistent with activity assays which show 1.6 u/ml for BChE activity with acetylthiocholine in AChE-/- plasma and 0.2-0.5 u/ml for AChE activity in BChE-/- plasma. In lane 5 the heaviest band is an AChE tetramer. A weak band below the AChE tetramer band is at about the same level as the

trimer band of BChE. AChE monomers and dimers are diffusely spread. The mouse BChE bands in lane 6 line up with some of the human BChE bands in lane 2. Mouse BChE tetramers , dimers, and monomers have corresponding BChE bands in human serum. However, the presumed BChE trimer in mouse serum migrates somewhat faster than the BChE trimer in human serum.
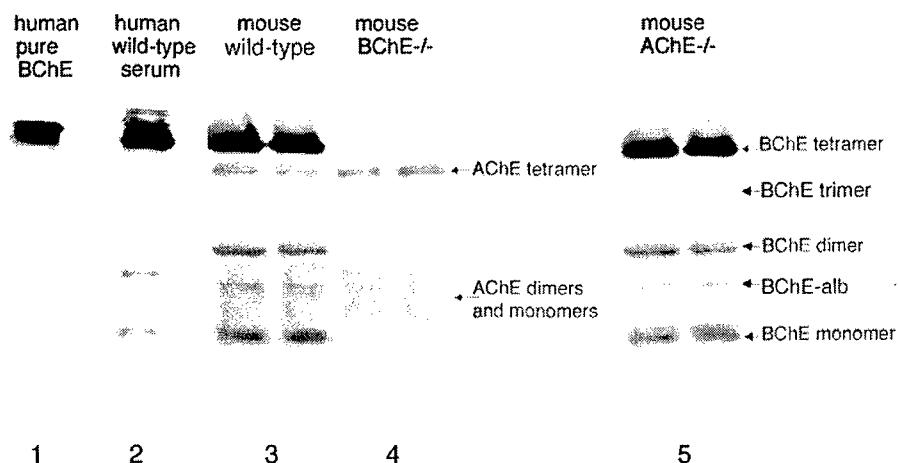
Figure 6.3.6. BChE-/- and AChE-/- mouse plasma. The nondenaturing gel was stained with acetylthiocholine. Lane 5 containing BChE-/- mouse plasma, shows bands of AChE activity. Lane 6 containing AChE-/- mouse plasma, shows bands of BChE activity. For comparison, purified human BChE (lane 1), wild-type human BChE serum (lane 2) and silent BChE human plasma (lane 3) are shown.

Storage bands

Serum or plasma stored at -20°C has bands of BChE not seen in freshly drawn blood or in blood stored at -80°C. These bands have been referred to as storage bands (Simpson, 1972). Figure 6.3.7 illustrates storage bands in mouse serum. The storage bands are seen as 3 new bands migrating more slowly than tetrameric BChE, as well as new bands and more intense bands in the dimer region. Broad fuzzy bands appear in the region between dimers and tetramers. Storage bands are probably caused by desialylation and proteolysis (Saxena et al., 2003).

Note the slow-migrating thin doublet in lane 2 of Figure 6.3.6 for wild-type human serum. These inconstant minor bands of MW approx. 900 KDa are different from storage bands; they correspond to monomeric BChE bound to α2-macroglobulin doublet (Masson, unpublished result). Not all individuals show these bands.

Fresh serum   Stored at -20°C

BChE
tetramers
trimer
dimers
BChE-alb
monomers

1   2   3   4
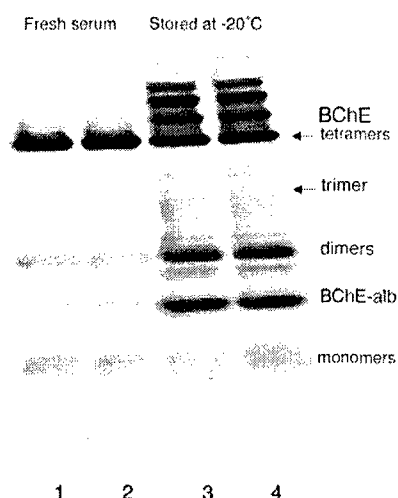
Figure 6.3.7. Storage bands in mouse serum. The nondenaturing gel was stained for activity with butyrylthiocholine to show BChE bands.

Unidentified bands of esterase activity in mouse plasma

On nondenaturing gels stained with alpha-naphthylacetate, mouse plasma had 4 novel bands. These bands were neither BChE nor AChE because they were present in AChE-/- as well as in BChE-/- plasma. See Figure 6.3.8. These bands completely disappeared when the gel was preincubated in 0.1 mM DFP for 30 min before staining. The carboxylesterase and cholinesterase bands also disappeared, suggesting that the unknown esterases could be serine esterases.

human
wt BChE serum   BChE+/+   BChE+/-   BChE-/-   AChE+/+   AChE+/-   AChE-/-

mouse   mouse

BChE

CE

1   2   3   4   5   6   7   8
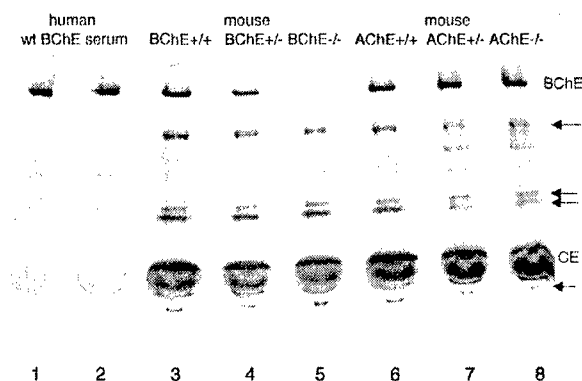
Figure 6.3.8. Four unidentified esterase bands. The gel was stained with alpha-naphthylacetate. Five µl of serum from two humans, and from six mice were loaded per lane. The mice were wild-type, heterozygous for the BChE knockout, homozygous for the BChE knockout (BChE-/-), wild-type, heterozygous for the AChE knockout, and homozygous for the AChE knockout (AChE-/-). The four unidentified esterase bands are indicated with an arrow. The heaviest staining is for mouse carboxylesterase (CE).

Spontaneous reactivation of OP-inhibited mouse BChE. Mouse BChE spontaneously reactivated after inhibition by OP, but human BChE did not. The mouse and human plasma samples in Figure 6.3.9 were treated with 0.1 mM DFP,

70

echothiophate, or paraoxon for 2 hours, assayed for activity with acetylthiocholine, and then loaded on a nondenaturing gel. After 20 hours of electrophoresis at 4°C the gel was stained for activity with acetylthiocholine. The surprising result in Figure 6.3.9 was the presence of BChE activity in samples treated with OP. These samples had shown no cholinesterase activity before they were loaded on the gel. We conclude that some of the OP spontaneously detached from BChE during the 20 hours of electrophoresis. Excess OP separated from enzyme on the gel, allowing the reactivated BChE to stay active. Reactivation after DFP phosphorylation was weaker than for enzyme inhibited by echothiophate and paraoxon, because aging of the diisopropylphosphate-adduct competed with reactivation.
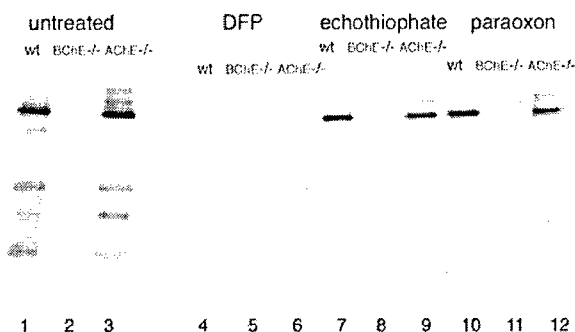
Figure 6.3.9. Spontaneous reactivation of OP-inhibited mouse BChE. The gel was stained for activity with acetylthiocholine. Samples were incubated with 0.1 mM DFP, echothiophate, or paraoxon before being loaded on the gel.

In another experiment (data not shown) the gel was preincubated in 0.1 mM DFP, 0.1 mM echothiophate, or 0.1 mM paraoxon for 30 min before being stained for activity. Under these conditions BChE enzyme activity was completely inhibited.

Human BChE did not spontaneously reactivate after treatment with 0.1 mM DFP, echothiophate, or paraoxon. Spontaneous reactivation of OP-inhibited mouse BChE has also been reported by others (Matsubara and Horikoshi, 1984; Kaliste-Korhonen *et al.*, 1996; Quistad *et al.*, 2005).

Discussion
Three esterases in human plasma. The convention of naming an esterase for the drug being studied gives the impression that human plasma contains dozens of different esterases. However, we find only 4 esterases in human plasma, and one of these, AChE, is present in negligible amounts. This leaves only BChE, PON1, and albumin to carry out ester hydrolysis.

Our analysis assumes that any esterase present in significant quantity would have been stained with alpha or beta-naphthylacetate. This assumption is verified by searching the proteomics databases.

Proteomics. New mass spectroscopy tools have allowed investigators to undertake the project of identifying all the proteins in human plasma. The Plasma Proteome Institute suggests that human plasma may contain most, if not all, human

proteins, though many will be present at very low concentrations. In the year 2004 the number of nonredundant distinct gene products in human plasma was 1175 (Anderson *et al.*, 2004). In the year 2005 this number had grown to 3778 (Muthusamy *et al.*, 2005). The lists include butyrylcholinesterase, paraoxonase, and albumin, but not acetylcholinesterase or carboxylesterase. The absence of acetylcholinesterase from the list suggests that a low abundance protein, present at a concentration no higher than 0.005 mg/L, is not easily detected by mass spectroscopy.

No carboxylesterase in human plasma. The idea that human plasma contains carboxylesterase (Shirai *et al.*, 1985; Shirai *et al.*, 1988; Kaliste-Korhonen *et al.*, 1996; Satoh and Hosokawa, 1998; Guemei *et al.*, 2001) comes from the fact that carboxylesterase activity is assayed with p-nitrophenyl acetate, and this same substrate is also hydrolyzed by BChE and albumin. PON1, called arylesterase and A esterase in the earlier literature, also has activity with p-nitrophenyl acetate (Aldridge, 1953; Albers *et al.*, 1969; Smolen *et al.*, 1991). After BChE activity is inhibited with eserine or iso-OMPA, the residual p-nitrophenyl acetate activity has been erroneously attributed to carboxylesterase, whereas it is our contention that the residual activity comes from albumin and PON1. Albumin esterase activity is routinely assayed with p-nitrophenyl acetate (Means and Wu, 1979; Awad-Elkarim and Means, 1988; Sakurai *et al.*, 2004).

Our finding that human plasma contains no carboxylesterase is confirmed by the reports of others who also find no carboxylesterase in human plasma (Leng *et al.*, 1999; Morton *et al.*, 2005). Aliesterase, an early name for carboxylesterase, was reported to be absent in human, monkey, pig, ruminant, and chicken plasma, consistent with our finding (Augustinsson, 1961). We cannot rule out the presence of a negligible amount of carboxylesterase, too low to detect by our methods, and too low to detect by mass spectrometry techniques. We did not find carboxylesterase listed in any human proteomics databank. Since acetylcholinesterase is also absent from these lists, yet we know AChE is present, we can conclude that if carboxylesterase is present, its concentration is in the same low range as AChE.

We cannot rule out the possibility that under specific pathological conditions significant amounts of carboxylesterase may be released into the blood circulation.

Mouse plasma. The esterases in mouse plasma are BChE, PON, albumin, AChE, and carboxylesterase. In addition there are 4 OP-sensitive bands whose identity is not yet known. The amount of AChE in mouse plasma is 25-fold higher than in human plasma. See Table 6.3.2.

Table 6.3.2. Esterases in human and mouse plasma

Esterase	human plasma, mg/Liter	mouse plasma, mg/Liter
BChE (EC 3.1.1.8)	5	2.6
AChE (EC 3.1.1.7)	0.008	0.2
PON1 (EC 3.1.8.1)	50	25
albumin	50,000-60,000	50,000-60,000
carboxylesterase (EC 3.1.1.1)	0	80

BChE activity in units/ml was converted to mg/L by using a specific activity of 720 units/mg for butyrylthiocholine. The value for AChE in human plasma is from (Brimijoin and Hammond, 1988). AChE

activity in mouse plasma was converted to mg/L by using a specific activity of 2600 units/mg for acetylthiocholine. The value for PON1 in human plasma is from (Gan *et al.*, 1991; Blatter Garin *et al.*, 1994). The value for PON in mouse plasma was calculated from (Oda *et al.*, 2002). Albumin concentration is from (Peters, 1996). The value for carboxylesterase in mouse plasma was calculated from a specific activity of 228 u/mg with p-nitrophenyl acetate (Lexow *et al.*, 1980) and an activity of 18.6 u/ml (Peeples *et al.*, 2005).

Carboxylesterase is 30-fold more abundant than BChE. The high amount of carboxylesterase in rodent and rabbit plasma makes these animals inappropriate models for drug and OP effects in humans. Only after carboxylesterase was inactivated by treatment with cresylbenzodioxaphosphorin oxide did interspecies differences disappear with regard to soman toxicity (Maxwell *et al.*, 1987). The pharmacokinetic profile for irinotecan in carboxylesterase deficient mice more closely reflected that seen in humans (Morton *et al.*, 2005).

Whole blood. Whole blood contains additional esterases not described in this report. The short duration of action of esmolol, a very short-acting beta1-adrenoceptor antagonist, is attributed to rapid enzymatic hydrolysis by esterases in the cytosol of red blood cells (Quon and Stampfli, 1985). This esterase could be Esterase D (also called S-formylglutathione hydrolase) since Esterase D is known to be present in the red blood cell cytosol. Another esterase in red blood cells is acetylcholinesterase. AChE is attached to the outer surface of the red cell membrane via a glycolipid anchor. Though AChE is inhibited by anti-Alzheimer disease drugs, AChE is not known to participate in hydrolysis of drug esters.

Platelets and lymphocytes contain neuropathy target esterase, while T-lymphocytes contain ubiquitin carboxyl terminal esterase L1 (Muthusamy *et al.*, 2005). These esterases are present in low abundance and have not been reported to have a role in ester hydrolysis.

Key Research Accomplishments

- A new biomarker of OP exposure has been identified. This new biomarker is albumin.

- The reaction of human acetylcholinesterase and human butyrylcholinesterase with biotinylated OP was very fast, similar to the rate with sarin. This makes FP-biotin a suitable marker for OP reactive proteins. FP-biotin was used to identify albumin as a new biomarker of OP exposure.

- Dichlorvos reacts faster with platelet-activating factor acetylhydrolase alpha-2 and with acylpeptide hydrolase than with acetylcholinesterase. Each of the OP tested reacts with a set of proteins and not just with acetylcholinesterase.

- A mass spectrometry method for identifying OP-labeled proteins by use of characteristic ion fragments was developed. Using this method we identified tyrosine 410 of bovine albumin (Tyr 411 in human albumin) as the site of covalent attachment of OP.

- The esterases in human plasma are paraoxonase, butyrylcholinesterase, and albumin esterase. A very small amount of acetylcholinesterase is also present. There is no carboxylesterase in human plasma. In contrast, rodent plasma contains a high level of carboxylesterase. Though albumin esterase activity is low per albumin molecule, the concentration of albumin in plasma is very high, so that albumin esterase activity contributes significantly to drug hydrolysis.

Reportable Outcomes

- Manuscript published in Toxicological Sciences (2005) 83: 303-312.
  Eric Peeples, Lawrence M. Schopfer, Ellen G. Duysen, Reggie Spaulding, Troy Voelker, Charles M. Thompson, Oksana Lockridge. Albumin, a new biomarker of organophosphorus toxicant exposure, identified by mass spectrometry.

- Manuscript published in Chem Res Toxicol (2005) 18: 747-754.
  Lawrence M. Schopfer, Troy Voelker, Cynthia F. Bartels, Charles M. Thompson, Oksana Lockridge. Reaction kinetics of biotinylated organophosphorus toxicant, FP-biotin, with human acetylcholinesterase and human butyrylcholinesterase.

- Manuscript published in Environ Toxicol Pharmacol (2005) 19: 463-469.
  Oksana Lockridge, Ellen G. Duysen, Troy Voelker, Charles M. Thompson, Lawrence M. Schopfer. Life without acetylcholinesterase: the implications of cholinesterase inhibitor toxicity in AChE-knockout mice.

- Manuscript published in Anal Biochem (2005) In press.
  Lawrence M. Schopfer, Matthew M. Champion, Nate Tamblyn, Charles M. Thompson, Oksana Lockridge. Characteristic mass spectral fragments of the organophosphorus agent FP-biotin and FP-biotinylated peptides from trypsin and bovine albumin (Tyr 410).

74

- Manuscript submitted August 2005.
  Bin Li, Meghan Sedlacek, Indumathi Manoharan, Rathnam Boopathy, Ellen G. Duysen, Patrick Masson, Oksana Lockridge. Butyrylcholinesterase, paraoxonase, and albumin esterase, but not carboxylesterase, are present in human plasma.

- Funding received based on the work supported by this grant.
  DOD grant W911SR-04-C-0019 supplied funds for the purchase of our own mass spectrometers. We purchased a MALDI-TOF mass spectrometer and a Q-Trap mass spectrometer from Applied Biosystems. This equipment has been operational for about 11 months, since August 2004. Before we had our own mass spectrometers, we sent samples to the University of Montana for mass spec analysis.

Conclusions
- A new biomarker of exposure to organophosphorus poisons has been identified. The new biomarker is albumin. This is a novel result that should be useful for diagnosing exposure.
- The hypothesis has been developed that each organophosphorus agent reacts with a set of proteins in addition to acetylcholinesterase and butyrylcholinesterase. The proteins in the set depend on the identity of the organophosphorus agent. For example, dichlorvos reacts not only with acetylcholinesterase and butyrylcholinesterase, but also with platelet-activating factor acetylhydrolase alpha-2 and with acylpeptide hydrolase. Each organophosphorus agent has a distinct mechanism of toxicity, when the dose is low. This hypothesis is useful for understanding symptoms of low dose exposure.
- Rodents are not a good model for toxicity studies with organophosphorus agents because rodent plasma contains a high concentration of carboxylesterase. In contrast, human plasma contains no carboxylesterase.
- People who are partially deficient in acetylcholinesterase are expected to be healthy and fertile, but to be unusually sensitive to the toxicity of organophosphorus agents. This prediction is based on our study of AChE+/- mice, who show no abnormalities until they are exposed to organophosphorus toxicants.

Personnel who received pay from this research effort
Oksana Lockridge, Ph.D.
Lawrence M. Schopfer, Ph.D.
Ellen G. Duysen
Stacy Wieseler
Andreea Ticu

References

Abbott CA, Mackness MI, Kumar S, Olukoga AO, Gordon C, Arrol S, Bhatnagar D, Boulton AJ and Durrington PN (1993) Relationship between serum butyrylcholinesterase activity, hypertriglyceridaemia and insulin sensitivity in diabetes mellitus. *Clin Sci (Lond)* **85**:77-81.

Agarwal RP, Phillips M, McPherson RA and Hensley P (1986) Serum albumin and the metabolism of disulfiram. *Biochem Pharmacol* **35**:3341-3347.

Ahmed N, Dobler D, Dean M and Thornalley PJ (2005) Peptide mapping identifies hotspot site of modification in human serum albumin by methylglyoxal involved in ligand binding and esterase activity. *J Biol Chem* **280**:5724-5732.

Albers LV, Dray S and Knight KL (1969) Allotypes and isozymes of rabbit alpha-1-aryl esterase. Allelic products with different enzymatic acitivities for the same substrates. *Biochemistry* **8**:4416-4424.

Alcantara VM, Chautard-Freire-Maia EA, Scartezini M, Cerci MS, Braun-Prado K and Picheth G (2002) Butyrylcholinesterase activity and risk factors for coronary artery disease. *Scand J Clin Lab Invest* **62**:399-404.

Aldridge WN (1953) Serum esterases. I. Two types of esterase (A and B) hydrolysing p-nitrophenyl acetate, propionate and butyrate, and a method for their determination. *Biochem J* **53**:110-117.

Amitai G, Moorad D, Adani R and Doctor BP (1998) Inhibition of acetylcholinesterase and butyrylcholinesterase by chlorpyrifos-oxon. *Biochem Pharmacol* **56**:293-299.

Anderson NL, Polanski M, Pieper R, Gatlin T, Tirumalai RS, Conrads TP, Veenstra TD, Adkins JN, Pounds JG, Fagan R and Lobley A (2004) The human plasma proteome: a nonredundant list developed by combination of four separate sources. *Mol Cell Proteomics* **3**:311-326.

Augustinsson KB (1961) Multiple forms of esterase in vertebrate blood plasma. *Ann NY Acad Sci* **94**:844-860.

Awad-Elkarim A and Means GE (1988) The reactivity of p-nitrophenyl acetate with serum albumins. *Comp Biochem Physiol B* **91**:267-272.

Becker CE (1973) Cholinesterase genotype and hydrolysis of choline esters, procaine and tetracaine. *Hum Hered* **23**:394-399.

Biggadike K, Angell RM, Burgess CM, Farrell RM, Hancock AP, Harker AJ, Irving WR, Ioannou C, Procopiou PA, Shaw RE, Solanke YE, Singh OM, Snowden MA, Stubbs RJ, Walton S and Weston HE (2000) Selective plasma hydrolysis of glucocorticoid gamma-lactones and cyclic carbonates by the enzyme paraoxonase: an ideal plasma inactivation mechanism. *J Med Chem* **43**:19-21.

Billecke S, Draganov D, Counsell R, Stetson P, Watson C, Hsu C and La Du BN (2000) Human serum paraoxonase (PON1) isozymes Q and R hydrolyze lactones and cyclic carbonate esters. *Drug Metab Dispos* **28**:1335-1342.

Black RM, Harrison JM and Read RW (1999) The interaction of sarin and soman with plasma proteins: the identification of a novel phosphonylation site. *Arch Toxicol* **73**:123-126.

Blatter Garin MC, Abbott C, Messmer S, Mackness M, Durrington P, Pometta D and James RW (1994) Quantification of human serum paraoxonase by enzyme-linked immunoassay: population differences in protein concentrations. *Biochem J* **304** (Pt 2):549-554.

Brimijoin S and Hammond P (1988) Butyrylcholinesterase in human brain and acetylcholinesterase in human plasma: trace enzymes measured by two-site immunoassay. *J Neurochem* **51**:1227-1231.

Carrington CD and Abou-Donia MB (1985) Characterization of [3H]di-isopropyl phosphorofluoridate-binding proteins in hen brain. Rates of phosphorylation and sensitivity to neurotoxic and non-neurotoxic organophosphorus compounds. *Biochem J* **228**:537-544.

Casida JE and Augustinsson KB (1959) Reaction of plasma albumin with I-naphthyl N-methylcarbamate and certain other esters. *Biochim Biophys Acta* **36**:411-426.

Chaiken IM and Smith EL (1969) Reaction of a specific tyrosine residue of papain with diisopropylfluorophosphate. *J Biol Chem* **244**:4247-4250.

Chapuis N, Bruhlmann C, Reist M, Carrupt PA, Mayer JM and Testa B (2001) The esterase-like activity of serum albumin may be due to cholinesterase contamination. *Pharm Res* **18**:1435-1439.

Cucuianu M, Nistor T, Hancu N, Orbai P, Muscurel C and Stoian I (2002) Serum cholinesterase activity correlates with serum insulin, C-peptide and free fatty acids levels in patients with type 2 diabetes. *Rom J Intern Med* **40**:43-51.

Davies HG, Richter RJ, Keifer M, Broomfield CA, Sowalla J and Furlong CE (1996) The effect of the human serum paraoxonase polymorphism is reversed with diazoxon, soman and sarin. *Nat Genet* **14**:334-336.

De Vriese C, Gregoire F, Lema-Kisoka R, Waelbroeck M, Robberecht P and Delporte C (2004) Ghrelin degradation by serum and tissue homogenates: identification of the cleavage sites. *Endocrinology* **145**:4997-5005.

Derewenda ZS and Derewenda U (1991) Relationships among serine hydrolases: evidence for a common structural motif in triacylglyceride lipases and esterases. *Biochem Cell Biol* **69**:842-851.

Dubois-Presle N, Lapicque F, Maurice MH, Fournel-Gigleux S, Magdalou J, Abiteboul M, Siest G and Netter P (1995) Stereoselective esterase activity of human serum albumin toward ketoprofen glucuronide. *Mol Pharmacol* **47**:647-653.

Duysen EG, Stribley JA, Fry DL, Hinrichs SH and Lockridge O (2002) Rescue of the acetylcholinesterase knockout mouse by feeding a liquid diet; phenotype of the adult acetylcholinesterase deficient mouse. *Brain Res Dev Brain Res* **137**:43-54.

Ecobichon DJ and Kalow W (1962) Properties and classification of the soluble esterases of human liver. *Biochem Pharmacol* **11**:573-583.

Ellman GL, Courtney KD, Andres V, Jr. and Feather-Stone RM (1961) A new and rapid colorimetric determination of acetylcholinesterase activity. *Biochem Pharmacol* **7**:88-95.

Erdos EG and Boggs LE (1961) Hydrolysis of paraoxon in mammalian blood. *Nature* **190**:716-717.

Foldes FF, McNall PG, Ellis CH, Davis DL and Wnuck AL (1953) Substrate competition procaine and succinylcholine diiodide for plasma cholinesterase. *Science* **117**:383-386.

Furlong CE, Richter RJ, Chapline C and Crabb JW (1991) Purification of rabbit and human serum paraoxonase. *Biochemistry* **30**:10133-10140.

Gan KN, Smolen A, Eckerson HW and La Du BN (1991) Purification of human serum paraoxonase/arylesterase. Evidence for one esterase catalyzing both activities. *Drug Metab Dispos* **19**:100-106.

Gesztes T (1966) Prolonged apnoea after suxamethonium injection associated with eye drops containing an anticholinesterase agent. *Br J Anaesth* **38**:408-409.

Gilmer JF, Moriarty LM, Lally MN and Clancy JM (2002) Isosorbide-based aspirin prodrugs. II. Hydrolysis kinetics of isosorbide diaspirinate. *Eur J Pharm Sci* **16**:297-304.

Gray EG and Whittaker VP (1962) The isolation of nerve endings from brain: an electron-microscopic study of cell fragments derived by homogenization and centrifugation. *J Anat* **96**:79-88.

Green NM (1965) A Spectrophotometric Assay for Avidin and Biotin Based on Binding of Dyes by Avidin. *Biochem J* **94**:23C-24C.

Guemei AA, Cottrell J, Band R, Hehman H, Prudhomme M, Pavlov MV, Grem JL, Ismail AS, Bowen D, Taylor RE and Takimoto CH (2001) Human plasma carboxylesterase and butyrylcholinesterase enzyme activity: correlations with SN-38 pharmacokinetics during a prolonged infusion of irinotecan. *Cancer Chemother Pharmacol* **47**:283-290.

Hagag N, Birnbaum ER and Darnall DW (1983) Resonance energy transfer between cysteine-34, tryptophan-214, and tyrosine-411 of human serum albumin. *Biochemistry* **22**:2420-2427.

Hashinotsume M, Higashino K, Hada T and Yamamura Y (1978) Purification and enzymatic properties of rat serum carboxylesterase. *J Biochem (Tokyo)* **84**:1325-1333.

Hess AR, Angel RW, Barron KD and Bernsohn J (1963) Proteins and Isozymes of Esterases and Cholinesterases from Sera of Different Species. *Clin Chim Acta* **19**:656-667.

Ho YS, Swenson L, Derewenda U, Serre L, Wei Y, Dauter Z, Hattori M, Adachi T, Aoki J, Arai H, Inoue K and Derewenda ZS (1997) Brain acetylhydrolase that inactivates platelet-activating factor is a G-protein-like trimer. *Nature* **385**:89-93.

Johnson JA and Wallace KB (1987) Species-related differences in the inhibition of brain acetylcholinesterase by paraoxon and malaoxon. *Toxicol Appl Pharmacol* **88**:234-241.

Kaliste-Korhonen E, Tuovinen K and Hanninen O (1996) Interspecies differences in enzymes reacting with organophosphates and their inhibition by paraoxon in vitro. *Hum Exp Toxicol* **15**:972-978.

Kalow W and Grant DM (1995) *Pharmacogenetics*. McGraw-Hill, NY.

Kalow W and Staron N (1957) On distribution and inheritance of atypical forms of human serum cholinesterase, as indicated by dibucaine numbers. *Can J Med Sci* **35**:1305-1320.

Karnovsky MJ and Roots L (1964) A "direct-coloring" thiocholine method for cholinesterases. *J Histochem Cytochem* **12**:219-221.

Keshavarz-Shokri A, Suntornwat O and Kitos PA (1999) Identification of serine esterases in tissue homogenates. *Anal Biochem* **267**:406-411.

Kidd D, Liu Y and Cravatt BF (2001) Profiling serine hydrolase activities in complex proteomes. *Biochemistry* **40**:4005-4015.

Korza G and Ozols J (1988) Complete covalent structure of 60-kDa esterase isolated from 2,3,7,8-tetrachlorodibenzo-p-dioxin-induced rabbit liver microsomes. *J Biol Chem* **263**:3486-3495.

Kragh-Hansen U, Chuang VT and Otagiri M (2002) Practical aspects of the ligand-binding and enzymatic properties of human serum albumin. *Biol Pharm Bull* **25**:695-704.

Kwon CH, Maddison K, LoCastro L and Borch RF (1987) Accelerated decomposition of 4-hydroxycyclophosphamide by human serum albumin. *Cancer Res* **47**:1505-1508.

Lam KS, Salmon SE, Hersh EM, Hruby VJ, Kazmierski WM and Knapp RJ (1991) A new type of synthetic peptide library for identifying ligand-binding activity. *Nature* **354**:82-84.

Leng G, Lewalter J, Rohrig B and Idel H (1999) The influence of individual susceptibility in pyrethroid exposure. *Toxicol Lett* **107**:123-130.

Lexow U, Ronai A and von Deimling O (1980) Purification and characterization of esterase 2B of the house mouse, Mus musculus. *Eur J Biochem* **107**:123-130.

Li B, Duysen EG, Saunders TL and Lockridge O Production of the butyrylcholinesterase knockout mouse. *Adv Exp Med Biol.*

Little PJ, Scimeca JA and Martin BR (1988) Distribution of [3H]diisopropylfluorophosphate, [3H]soman, [3H]sarin, and their metabolites in mouse brain. *Drug Metab Dispos* **16**:515-520.

Liu P, Jenkins NA and Copeland NG (2003) A highly efficient recombineering-based method for generating conditional knockout mutations. *Genome Res* **13**:476-484.

Liu Y, Patricelli MP and Cravatt BF (1999) Activity-based protein profiling: the serine hydrolases. *Proc Natl Acad Sci U S A* **96**:14694-14699.

Lockridge O (1990) Genetic variants of human serum cholinesterase influence metabolism of the muscle relaxant succinylcholine. *Pharmacol Ther* **47**:35-60.

Lockridge O, Mottershaw-Jackson N, Eckerson HW and La Du BN (1980) Hydrolysis of diacetylmorphine (heroin) by human serum cholinesterase. *J Pharmacol Exp Ther* **215**:1-8.

Lockridge O, Schopfer LM, Winger G and Woods JH (2005) Large scale purification of butyrylcholinesterase from human plasma suitable for injection into monkeys; a potential new therapeutic for protection against cocaine and nerve agent toxicity. *J Medical Chemical Biological & Radiological Defense* **3**:online publication.

Lynch TJ, Mattes CE, Singh A, Bradley RM, Brady RO and Dretchen KL (1997) Cocaine detoxification by human plasma butyrylcholinesterase. *Toxicol Appl Pharmacol* **145**:363-371.

Main AR (1979) Mode of action of anticholinesterases. *Pharmac Ther* **6**:579-628.

Masson P (1989) A naturally occurring molecular form of human plasma cholinesterase is an albumin conjugate. *Biochim Biophys Acta* **998**:258-266.

Masson P, Froment MT, Fortier PL, Visicchio JE, Bartels CF and Lockridge O (1998) Butyrylcholinesterase-catalysed hydrolysis of aspirin, a negatively charged ester, and aspirin-related neutral esters. *Biochim Biophys Acta* **1387**:41-52.

Matsubara T and Horikoshi I (1984) Spontaneous reactivation of mouse plasma cholinesterase after inhibition by various organophosphorus compounds. *J Pharmacobiodyn* **7**:322-328.

Maxwell DM, Brecht KM and O'Neill BL (1987) The effect of carboxylesterase inhibition on interspecies differences in soman toxicity. *Toxicol Lett* **39**:35-42.

Maxwell DM, Lieske CN and Brecht KM (1994) Oxime-induced reactivation of carboxylesterase inhibited by organophosphorus compounds. *Chem Res Toxicol* **7**:428-433.

McDaniel KL and Moser VC (1993) Utility of a neurobehavioral screening battery for differentiating the effects of two pyrethroids, permethrin and cypermethrin. *Neurotoxicol Teratol* **15**:71-83.

McGehee DS, Krasowski MD, Fung DL, Wilson B, Gronert GA and Moss J (2000) Cholinesterase inhibition by potato glycoalkaloids slows mivacurium metabolism. *Anesthesiology* **93**:510-519.

Means GE and Wu HL (1979) The reactive tyrosine residue of human serum albumin: characterization of its reaction with diisopropylfluorophosphate. *Arch Biochem Biophys* **194**:526-530.

Meyers C, Lockridge O and La Du BN (1982) Hydrolysis of methylprednisolone acetate by human serum cholinesterase. *Drug Metab Dispos* **10**:279-280.

Morikawa M, Inoue M, Tsuboi M and Sugiura M (1979) Studies on aspirin esterase of human serum. *Jpn J Pharmacol* **29**:581-586.

Morton CL, Iacono L, Hyatt JL, Taylor KR, Cheshire PJ, Houghton PJ, Danks MK, Stewart CF and Potter PM (2005) Activation and antitumor activity of CPT-11 in plasma esterase-deficient mice. *Cancer Chemother Pharmacol*.

Morton CL, Wadkins RM, Danks MK and Potter PM (1999) The anticancer prodrug CPT-11 is a potent inhibitor of acetylcholinesterase but is rapidly catalyzed to SN-38 by butyrylcholinesterase. *Cancer Res* **59**:1458-1463.

Moser VC (1995) Comparisons of the acute effects of cholinesterase inhibitors using a neurobehavioral screening battery in rats. *Neurotoxicol Teratol* **17**:617-625.

Muthusamy B, Hanumanthu G, Suresh S, Rekha B, Srinivas D, Karthick L, Vrushabendra BM, Sharma S, Mishra G, Chatterjee P, Mangala KS, Shivashankar HN, Chandrika KN, Deshpande N, Suresh M, Kannabiran N, Niranjan V, Nalli A, Keshava Prasad TS, Arun KS, Reddy R, Chandran S, Jadhav T, Julie D, Mahesh M, John SL, Palvankar K, Sudhir D, Bala P, Rashmi NS, Vishnupriya G, Dhar K, Reshma S, Chaerkady R, Gandhi TK, Harsha HC, Sujatha Mohan S, Deshpande KS, Sarker M and Pandey A (2005) Plasma Proteome Database as a resource for proteomics research. *Proteomics*.

O'Brien JE, Abbey V, Hinsvark O, Perel J and Finster M (1979) Metabolism and measurement of chloroprocaine, an ester-type local anesthetic. *J Pharm Sci* **68**:75-78.

Oda MN, Bielicki JK, Ho TT, Berger T, Rubin EM and Forte TM (2002) Paraoxonase 1 overexpression in mice and its effect on high-density lipoproteins. *Biochem Biophys Res Commun* **290**:921-927.

Ortigoza-Ferado J, Richter RJ, Hornung SK, Motulsky AG and Furlong CE (1984) Paraoxon hydrolysis in human serum mediated by a genetically variable arylesterase and albumin. *Am J Hum Genet* **36**:295-305.

Ostergaard D, Jensen FS, Skovgaard LT and Viby-Mogensen J (1995a) Dose-response relationship for mivacurium in patients with phenotypically abnormal plasma cholinesterase activity. *Acta Anaesthesiol Scand* **39**:1016-1018.

Ostergaard S, Hansen PH, Olsen M and Holm A (1995b) Novel avidin and streptavidin binding sequences found in synthetic peptide libraries. *FEBS Lett* **362**:306-308.

Peeples ES, Schopfer LM, Duysen EG, Spaulding R, Voelker T, Thompson CM and Lockridge O (2005) Albumin, a new biomarker of organophosphorus toxicant exposure, identified by mass spectrometry. *Toxicol Sci* **83**:303-312.

Peters T, Jr. (1996) *All about albumin. Biochemistry, genetics, and medical applications.* Academic Press Ltd., London.

Pope CN (1999) Organophosphorus pesticides: do they all have the same mechanism of toxicity? *J Toxicol Environ Health B Crit Rev* **2**:161-181.

Quistad GB, Klintenberg R and Casida JE (2005) Blood acylpeptide hydrolase activity is a sensitive marker for exposure to some organophosphate toxicants. *Toxicol Sci* **86**:291-299.

Quistad GB, Sparks SE and Casida JE (2001) Fatty acid amide hydrolase inhibition by neurotoxic organophosphorus pesticides. *Toxicol Appl Pharmacol* **173**:48-55.

Quistad GB, Sparks SE, Segall Y, Nomura DK and Casida JE (2002) Selective inhibitors of fatty acid amide hydrolase relative to neuropathy target esterase and acetylcholinesterase: toxicological implications. *Toxicol Appl Pharmacol* **179**:57-63.

Quon CY and Stampfli HF (1985) Biochemical properties of blood esmolol esterase. *Drug Metab Dispos* **13**:420-424.

Quon CY and Stampfli HF (1993) Biochemical characterization of flestolol esterase. *Res Commun Chem Pathol Pharmacol* **81**:309-322.

Rainsford KD, Ford NL, Brooks PM and Watson HM (1980) Plasma aspirin esterases in normal individuals, patients with alcoholic liver disease and rheumatoid arthritis: characterization and the importance of the enzymic components. *Eur J Clin Invest* **10**:413-420.

Richards P and Lees J (2002) Functional proteomics using microchannel plate detectors. *Proteomics* **2**:256-261.

Richards PG, Johnson MK and Ray DE (2000) Identification of acylpeptide hydrolase as a sensitive site for reaction with organophosphorus compounds and a potential target for cognitive enhancing drugs. *Mol Pharmacol* **58**:577-583.

Rodriguez OP, Muth GW, Berkman CE, Kim K and Thompson CM (1997) Inhibition of various cholinesterases with the enantiomers of malaoxon. *Bull Environ Contam Toxicol* **58**:171-176.

Saez-Valero J, Tornel PL, Munoz-Delgado E and Vidal CJ (1993) Amphiphilic and hydrophilic forms of acetyl- and butyrylcholinesterase in human brain. *J Neurosci Res* **35**:678-689.

Sakurai Y, Ma SF, Watanabe H, Yamaotsu N, Hirono S, Kurono Y, Kragh-Hansen U and Otagiri M (2004) Esterase-like activity of serum albumin: characterization of its structural chemistry using p-nitrophenyl esters as substrates. *Pharm Res* **21**:285-292.

Salvi A, Carrupt PA, Mayer JM and Testa B (1997) Esterase-like activity of human serum albumin toward prodrug esters of nicotinic acid. *Drug Metab Dispos* **25**:395-398.

Sanger F (1963) Amino-acid sequences in the active centers of certain enzymes. *Proc Chem Soc* **5**:76-83.

Satoh T and Hosokawa M (1998) The mammalian carboxylesterases: from molecules to functions. *Annu Rev Pharmacol Toxicol* **38**:257-288.

Savarese JJ, Ali HH, Basta SJ, Embree PB, Scott RP, Sunder N, Weakly JN, Wastila WB and el-Sayad HA (1988) The clinical neuromuscular pharmacology of mivacurium chloride (BW B1090U). A short-acting nondepolarizing ester neuromuscular blocking drug. *Anesthesiology* **68**:723-732.

Saxena A, Hur RS, Luo C and Doctor BP (2003) Natural monomeric form of fetal bovine serum acetylcholinesterase lacks the C-terminal tetramerization domain. *Biochemistry* **42**:15292-15299.

Schopfer LM, Champion MM, Tamblyn N, Thompson CM and Lockridge O (2005) Characteristic mass spectral fragments of the organophosphorus agent FP-biotin and FP-biotinylated peptides from trypsin and bovine albumin (Tyr 410). *Anal Biochem.* In press.

Shirai K, Ohsawa I, Ishikawa Y, Saito Y and Yoshida S (1985) Human plasma carboxyl esterase-catalyzed triolein hydrolysis. Existence of promoting factor in serum. *J Biol Chem* **260**:5225-5227.

Shirai K, Ohsawa I, Saito Y and Yoshida S (1988) Effects of phospholipids on hydrolysis of trioleoylglycerol by human serum carboxylesterase. *Biochim Biophys Acta* **962**:377-383.

Simpson NE (1972) Polyacrylamide electrophoresis used for the detection of C5+ cholinesterase in Canadian caucasians, Indians, and Eskimos. *Am J Hum Genet* **24**:317-320.

Skrinjaric-Spoljar M, Simeon V and Reiner E (1973) Spontaneous reactivation and aging of dimethylphosphorylated acetylcholinesterase and cholinesterase. *Biochim Biophys Acta* **315**:363-369.

Smolen A, Eckerson HW, Gan KN, Hailat N and La Du BN (1991) Characteristics of the genetically determined allozymic forms of human serum paraoxonase/arylesterase. *Drug Metab Dispos* **19**:107-112.

Sogorb MA, Carrera V and Vilanova E (2004) Hydrolysis of carbaryl by human serum albumin. *Arch Toxicol* **78**:629-634.

Sogorb MA, Diaz-Alejo N, Escudero MA and Vilanova E (1998) Phosphotriesterase activity identified in purified serum albumins. *Arch Toxicol* **72**:219-226.

Song X, Seidler FJ, Saleh JL, Zhang J, Padilla S and Slotkin TA (1997) Cellular mechanisms for developmental toxicity of chlorpyrifos: targeting the adenylyl cyclase signaling cascade. *Toxicol Appl Pharmacol* **145**:158-174.

Sorensen K, Brodbeck U, Rasmussen AG and Norgaard-Pedersen B (1986) Normal human serum contains two forms of acetylcholinesterase. *Clin Chim Acta* **158**:1-6.

Souza RL, Mikami LR, Maegawa RO and Chautard-Freire-Maia EA (2005) Four new mutations in the BCHE gene of human butyrylcholinesterase in a Brazilian blood donor sample. *Mol Genet Metab* **84**:349-353.

Stewart DJ, Inaba T, Tang BK and Kalow W (1977) Hydrolysis of cocaine in human plasma by cholinesterase. *Life Sci* **20**:1557-1563.

Tougou K, Nakamura A, Watanabe S, Okuyama Y and Morino A (1998) Paraoxonase has a major role in the hydrolysis of prulifloxacin (NM441), a prodrug of a new antibacterial agent. *Drug Metab Dispos* **26**:355-359.

Tove SB (1962) The esterolytic activity of serum albumin. *Biochim Biophys Acta* **57**:230-235.

Tunek A and Svensson LA (1988) Bambuterol, a carbamate ester prodrug of terbutaline, as inhibitor of cholinesterases in human blood. *Drug Metab Dispos* **16**:759-764.

Watanabe H, Tanase S, Nakajou K, Maruyama T, Kragh-Hansen U and Otagiri M (2000) Role of arg-410 and tyr-411 in human serum albumin for ligand binding and esterase-like activity. *Biochem J* **349 Pt 3**:813-819.

Xie W, Stribley JA, Chatonnet A, Wilder PJ, Rizzino A, McComb RD, Taylor P, Hinrichs SH and Lockridge O (2000) Postnatal developmental delay and supersensitivity to organophosphate in gene-targeted mice lacking acetylcholinesterase. *J Pharmacol Exp Ther* **293**:896-902.

Yoshida K, Kurono Y, Mori Y and Ikeda K (1985) Esterase-like activity of human serum albumin. V. Reaction with 2,4-dinitrophenyl diethyl phosphate. *Chem Pharm Bull (Tokyo)* **33**:4995-5001.

Life without acetylcholinesterase: the implications of cholinesterase inhibitor toxicity in AChE-knockout mice

Oksana Lockridge[a],*, Ellen G. Duysen[a], Troy Voelker[b], Charles M. Thompson[b], Lawrence M. Schopfer[a]

[a] *University of Nebraska Medical Center, Eppley Institute, 986805 Omaha, NE 68198-6805, USA*
[b] *University of Montana, Department of Pharmaceutical Sciences, Missoula, MT 59812-1552, USA*

Available online 26 January 2005

Abstract

The acetylcholinesterase (AChE)-knockout mouse is a new tool for identifying physiologically relevant targets of organophosphorus toxicants (OP). If AChE were the only important target for OP toxicity, then mice with zero AChE would have been expected to be resistant to OP. The opposite was found. AChE−/− mice were more sensitive to the lethality of DFP, chlorpyrifos oxon, iso-OMPA, and the nerve agent VX. A lethal dose of OP caused the same cholinergic signs of toxicity in mice with zero AChE as in mice with normal amounts of AChE. This implied that the mechanism of toxicity of a lethal dose of OP in AChE−/− mice was the same as in mice that had AChE, namely accumulation of excess acetylcholine followed by overstimulation of receptors. OP lethality in AChE−/− mice could be due to inhibition of BChE, or to inhibition of a set of proteins. A search for additional targets used biotinylated-OP as a marker. In vitro experiments found that biotinylated-OP appeared to label as many as 55 proteins in the $100,000 \times g$ supernatant of mouse brain. Chlorpyrifos oxon bound a set of proteins (bands 12, 41, 45) that did not completely overlap with the set of proteins bound by diazoxon (bands 9, 12, 41, 47) or dichlorvos (bands 12, 23, 24, 32, 44, 45, 51) or malaoxon (band 9). These results support the idea that a variety of proteins could be interacting with a given OP to give the neurotoxic symptoms characteristic of a particular OP.
© 2004 Elsevier B.V. All rights reserved.

Keywords: Organophosphorus agent; Acetylcholinesterase; Knockout mouse; Butyrylcholinesterase; FP-biotin; Chlorpyrifos oxon

1. Introduction

The biochemical event that triggers convulsions and death after exposure to organophosphorus agents is inhibition of acetylcholinesterase. When AChE is inhibited, excess acetylcholine overstimulates acetylcholine receptors. This starts a cascade of neuronal excitation involving the glutamate receptors and excessive influx of calcium ions, that is responsible for the onset and maintenance of seizure activity (McDonough and Shih, 1997). Inhibition of AChE has been documented in thousands of papers, and is the gold standard for measuring exposure to OP. This understanding of the mechanism of OP toxicity has led to effective therapies against OP poisoning. Administration of atropine to

block muscarinic receptors, of 2-PAM to reactivate AChE, and of anticonvulsant drugs, is standard clinical practice for treatment of OP toxicity. In view of the overwhelming evidence for a critical role for AChE in OP toxicity, it was of interest to determine the response of a mouse that had no AChE. If AChE were the only important target of OP, then mice with no AChE were expected to be resistant to OP toxicity.

2. Methods

2.1. Mice

AChE-knockout mice were made by gene-targeting (Xie et al., 2000). The ACHE gene (5 kb) including the signal peptide, the catalytic triad, and 93% of the coding se-

---

* Corresponding author. Tel.: +1 402 559 6032; fax: +1 402 559 4651.
 E-mail address: olockrid@unmc.edu (O. Lockridge).

quence were deleted. No AChE protein is made, and no AChE activity is present in any tissue. Animal work was carried out in accordance with the Guide for the Care and Use of Laboratory Animals as adopted by the National Institutes of Health. Formal approval to conduct the experiments was obtained from the animal subjects review board.

2.2. Organophosphorus agents and dose

The nerve agent O-ethyl S-(2-(diisopropylamino)ethyl) methylphosphonothioate (VX) was from the Edgewood Chemical Biological Center (Aberdeen Proving Ground, MD). Animals were shipped to the U.S. Army Institute of Chemical Defense, Aberdeen Proving Ground, for experiments with VX. Tetraisopropyl pyrophosphoramide (iso-OMPA) and diisopropylfluorophosphate (DFP) were from Sigma (St. Louis, MO). Chlorpyrifos oxon (CPO), diazoxon, dichlorvos, and malaoxon were from Chem Service Inc. (West Chester, PA). FP-biotin (10-(fluoroethoxyphos phinyl)-N-(biotinamidopentyl) decanamide) was synthesized by Troy Voelker in the laboratory of Charles Thompson (Univ Montana, Missoula). FP-biotin has a reactive phosphonofluoridate group tethered to biotin via a spacer arm (Liu et al., 1999).

VX was dissolved in sterile saline and injected subcutaneously in the back of the neck at a dose of 8.0–25.0 μg/kg. Male and female animals were 34–55 days old. The number of animals for LD_{50} experiments was $n = 21$ AChE+/+, $n = 18$ AChE+/−, $n = 16$ AChE−/−. Control animals, $n = 7$ AChE+/+, $n = 6$ AChE+/−, $n = 5$ AChE−/− received saline alone. The data for male and female mice were combined because no differences were found based on gender.

DFP was dissolved in sterile phosphate buffered saline and injected intraperitoneally at a dose of 2.5 mg/kg. Male and female animals were 12 days old. The number of animals was $n = 8$ AChE+/+, $n = 15$ AChE+/−, $n = 3$ AChE−/−.

Chlorpyrifos oxon was dissolved in dimethylsulfoxide and injected intraperitoneally at a dose of 0.1–4.0 mg/kg. Male animals were 49–200 days old. The number of animals was $n = 13$ AChE+/+, $n = 3$ AChE+/−, $n = 9$ AChE−/−. Control animals, $n = 3$ AChE+/+ and 3 AChE−/−, received only DMSO.

Iso-OMPA was dissolved in sterile water and injected intraperitoneally at a dose of 1–550 mg/kg. Female mice were 90–210 days old. The number of animals was $n = 21$ AChE+/+, $n = 42$ AChE+/−, $n = 11$ AChE−/−. Control animals, $n = 5$ AChE+/+, $n = 5$ AChE+/− and $n = 3$ AChE−/−, received water alone.

2.3. Enzyme activity assays in tissue extracts

Tissues were collected at time of death or 6 h after treatment, and frozen. Age and sex matched untreated control tissues were collected and stored in the same manner as the treated samples. Tissues were homogenized in 10 volumes of 50 mM potassium phosphate, pH 7.4, containing 0.5% Tween 20, in a Tissumizer (Tekmar, Cincinnati, OH) for 10 s. The suspension was centrifuged in a microfuge for 10 min, and the supernatant was saved for enzyme activity assays. The extraction buffer contained Tween 20 rather than Triton X-100 because mouse BChE activity was inhibited up to 95% by 0.5% Triton X-100, but was not inhibited by 0.5% Tween 20 (Li et al., 2000).

AChE and BChE activity was measured by the method of Ellman et al. (1961) at 25 °C, in a Gilford spectrophotometer interfaced to MacLab 200 (ADInstruments Pty Ltd., Castle Hill, Australia) and a Macintosh computer. Samples were preincubated with 5,5-dithio-bis(2-nitrobenzoic acid) in 0.1 M potassium phosphate buffer, pH 7.0, to react free sulfhydryl groups before addition of substrate. AChE activity in tissues from VX treated animals was measured with 1 mM acetylthiocholine after inhibiting BChE activity with 0.1 mM iso-OMPA (1 mM was required for complete BChE inhibition in liver). AChE activity in tissues from iso-OMPA treated mice was measured with 1 mM acetylthiocholine after inhibiting BChE with 0.01 mM ethopropazine. BChE activity was measured with 1 mM butyrylthiocholine. Units of activity are defined as μmole substrate hydrolyzed per minute. Units of activity were calculated per gram wet weight of tissue.

2.4. Observations of OP treated animals

Mice treated with organophosphorus toxicant (OP) were monitored up to 24 h. Observations included salivation, lacrimation, increased urination, abnormal defecation, hyperactivity or lethargy, tremor, convulsions, muscle weakness, vasodilation. Body temperature was measured with a digital thermometer using a surface microprobe.

2.5. Preparation of sub-cellular fractions from mouse brain, and protein quantitation

Mouse brain was separated into its sub-cellular fractions by centrifugation, essentially as described by Gray and Whittaker (1962). Brain tissue was homogenized by two 1-min disruptions with a Potter–Elvehjem homogenizer (Teflon pestle with glass vessel) rotating at 840 rpm (in 10-volumes of ice cold 50 mM Tris/Cl buffer, pH 8.0, containing 0.32 M sucrose, to prevent disruption of organelles). The suspension was centrifuged at $1000 \times g$ for 10 min at 4 °C to pellet nuclei, mitochondria, plasma membranes and unbroken cells. The supernatant was re-centrifuged at $17,000 \times g$ for 55 min at 4 °C to pellet myelin, synaptosomes and mitochondria. That supernatant was re-centrifuged at $100,000 \times g$ for 60 min at 4 °C to separate microsomes (pellet) from soluble proteins (supernatant).

Protein in the supernatant fraction was estimated by absorbance at 280 nm, using $A_{280} = 1.0$ for 1 mg protein/ml. The $100,000 \times g$ supernatant was divided into 0.4 ml aliquots

and stored at −70 °C, along with the other sub-cellular fractions.

2.6. Labeling with FP-biotin

Mouse brain supernatant (1.25 mg protein/ml was reacted with 2–40 μM FP-biotin in 50 mM Tris/Cl buffer, pH 8.0, containing 5 mM EDTA and 2.4% methanol at 25 °C for up to 450 min). The reaction was stopped by addition of one-fifth volume of 10% SDS, 30% glycerol, 0.6 M dithiothreitol, and 0.012% bromophenol blue in 0.2 M Tris/Cl buffer, pH 6.8; followed by heating at 80 °C for 5 min.

A 10–20% gradient polyacrylamide gel with 4% stacking gel was used (overall dimensions, 16 cm × 18 cm × 0.075 cm; with 20 lanes). Thirty micrograms of total protein were loaded per lane, and run for 3600 V h in the cold room (4 °C), with stirring. The bottom tank contained 60 mM Tris/Cl buffer, pH 8.1, plus 0.1% SDS. The top tank buffer contained 25 mM Tris, 192 mM glycine buffer, pH 8.2, plus 0.1% SDS. Protein was transferred from gel to PVDF membrane (ImmunBlot from BioRad) electrophoretically in a tank using plate electrodes (TransBlot from BioRad), at 0.5 A, for 1 h, in 25 mM Tris, 192 mM glycine buffer, pH 8.2, in the cold room (4 °C), with stirring. The membrane was blocked with 3% gelatin (BioRad) in 20 mM Tris/Cl buffer, pH 7.5, containing 0.5 M NaCl for 1 h at room temperature. Then it was washed twice with 20 mM Tris/Cl buffer, pH 7.5, containing 0.5 M NaCl and 0.05% Tween-20, for 5 min. Biotinylated proteins were labeled with 9.5 nM Streptavidin-Alexa 680 conjugate (Molecular Probes) in 20 mM Tris/Cl buffer, pH 7.5, containing 0.5 M NaCl, 0.05% Tween, 0.2% SDS, and 1% gelatin, for 1 h, at room temperature, while protected from light. Shorter reaction times resulted in less labeling. Then the membrane was washed twice with 20 mM Tris/Cl buffer, pH 7.5, containing 0.5 M NaCl and 0.05% Tween-20, and twice with 20 mM Tris/Cl buffer, pH 7.5, containing 0.5 M NaCl, for 20 min each. This is essentially the BioRad protocol (BioRad Lit 171 Rev D). Membranes were scanned with the Odyssey Flat Bed Fluorescence Scanner (LI-COR) at 42 microns per pixel. The intensity of the signal from each labeled protein was determined using a Gaussian deconvolution routine from the Kodak 1D Image Analysis program, v 3.5.3 (Kodak).

2.7. Binding of OP to brain proteins

Chlorpyrifos oxon, diazoxon, dichlorvos, or malaoxon were incubated with mouse brain extract at 25 °C with concentrations of OP ranging from 0.1 to 500 μM. At the end of the 30 min incubation period, excess OP was separated from protein on a spin column. The protein was incubated with 10 μM FP-biotin for 5 h at 25 °C. The intensity of FP-biotin labeling was determined as described above. Proteins that had reacted with OP were identified by disappearance of a biotinylated band.

3. Results

3.1. Phenotype of the adult AChE−/− mouse

Adult AChE−/− mice are not normal in appearance. When they walk, the tail and abdomen drag on the ground. Their feet splay out and their gait is abnormal. They have no grip strength. By one year of age, AChE−/− mice never stand on their hind legs and they do not climb. They have a hump in their back, suggesting a deformed skeleton. They do not eat solid food, and cannot lift the head to drink from a suspended bottle. Body tremor is noticeable when they are moving about, but not when they are asleep. They have pin-point pupils.

They are lethargic, spending most of the time hiding in a small dark box inside their cage. Another behavioral abnormality is their lack of housekeeping behavior; they defecate and urinate in their nest. They do not engage in mating behavior. AChE−/− mice have never become pregnant despite being housed all their life with male AChE−/− mice (n = 600).

About 25% of adult AChE−/− mice make a bird-like chattering sound when they are disturbed. This vocalization is a response to stress.

Adult female AChE−/− mice are small, averaging 18 g. In contrast, wild-type female littermates weigh 27–32 g. A few male AChE−/− mice reach a weight of 30–35 g, though the average male knockout mouse weighs 18 g. The surface body temperature of adult AChE−/− mice is 36.5 °C, while that of AChE+/+ mice is 37.1 °C.

The average lifespan of AChE−/− mice is 120 days, though several have lived a normal lifespan of 2 years. In contrast, AChE+/+ mice live for 2 years. AChE−/− mice die of seizures. A disproportionate number of AChE−/− mice die on postnatal days 25–35. More details on the phenotype of adult AChE−/− mice are in Duysen et al. (2002).

3.2. Phenotype of AChE+/− mice

Heterozygous mice, carrying one deficient ACHE allele, and expressing 50% of the normal AChE activity in tissues (Xie et al., 2000; Li et al., 2000), are indistinguishable from wild-type mice in appearance. They have a normal lifespan, are sexually active, and fertile. Their litter sizes are the normal six to eight pups for strain 129Sv. A female AChE+/− mouse has an average of six to eight litters in her lifetime, similar to the number of litters produced by an AChE+/+ mouse of strain 129Sv. No health problems have been noticed in AChE+/− mice. They do not have seizures. AChE+/− mice have a reduced number of functional muscarinic receptors (Li et al., 2003), and are more sensitive to OP than wild-type mice.

3.3. LD₅₀ of OP

Strain 129Sv mice, differing only at the ACHE gene locus, were tested with four organophosphorus toxicants (Table 1).

Table 1
LD$_{50}$ of organophosphorus toxicants (OP) in wild-type and AChE deficient mice, strain 129Sv

AChE genotype	AChE activity (%)	DFP LD$_{50}$	Chlorpyrifos oxon LD$_{50}$	VX LD$_{50}$	Iso-OMPA LD$_{50}$
AChE+/+	100	>2.5	3.5	0.024	350
AChE+/−	50	2.5	2.5	0.017	350
AChE−/−	0	<2.5	0.5	0.011	1

Doses are in mg/kg.

Mice with no AChE were more sensitive to the lethal effects of DFP, chlorpyrifos oxon, VX, and iso-OMPA. Iso-OMPA discriminated between AChE−/− and +/+ mice more effectively than the other OP. A dose of 1 mg/kg was lethal to half of the AChE−/− mice but produced no toxic symptoms in AChE+/+ and +/− mice. The dose had to be increased 350-fold before iso-OMPA was lethal to AChE+/+ and +/− animals. The nerve agent VX is the most potent OP known. Microgram quantities are lethal. The finding that AChE−/− mice succumbed to VX shows that VX reacts with targets other than AChE and that reaction results in death.

3.4. Symptoms of toxicity after OP treatment

Untreated AChE−/− mice have cholinergic symptoms of OP toxicity even though they have never received any OP. Whole body tremor, pinpoint pupils, mucus on the eyes, and reduced body temperature are characteristic of untreated AChE−/− mice and are also cholinergic signs of toxicity attributed to excess acetylcholine.

Treatment with a nonlethal dose of VX caused a hypothermic response reminiscent of the response to oxotremorine (Li et al., 2003). AChE−/− mice were resistant to the hypothermic effects of VX, whereas AChE+/+ mice lost 8 °C of surface body temperature and did not regain normal temperature for 24 h (Duysen et al., 2001). The resistance of AChE−/− mice to the hypothermic effects of VX can be explained by a reduced number of functional M2 muscarinic receptors (Li et al., 2003). The receptors involved in thermal regulation are M2 (Gomeza et al., 1999).

Since the signs of OP toxicity are attributed to inhibition of AChE, it was of interest to determine whether mice with no AChE activity had different symptoms. Table 2 summarizes the symptoms observed in response to lethal injections of four different OP. AChE−/− mice exhibited the same symptoms as wild-type and heterozygous mice. Exceptions to this pattern are the salivation and defecation in iso-OMPA treated AChE−/− mice and the absence of hyperactivity in DFP treated AChE−/− mice. The lack of hyperactivity in DFP treated AChE−/− mice is explained by the fact that they died instantly, before movement could be observed.

The pattern of symptoms was different for each OP. This observation has been taken as evidence that OP react with several targets, and that the toxicity is not explained by inhibition of AChE alone (Pope, 1999; Moser, 1995).

3.5. Enzyme activity in tissues

Tissues from VX (Duysen et al., 2001) and iso-OMPA treated animals have been tested. The results in Table 3 show that a lethal dose of VX inhibited AChE in brain 50%. BChE in brain was also inhibited about 50%. The extent of BChE inhibition in AChE−/− brain was no greater than in AChE+/+ and +/− brains. Similarly, AChE in muscle and serum was also inhibited about 50%, whereas AChE in intestine showed almost no inhibition. BChE activity was inhibited in all tissues tested.

A dose of 5 mg/kg iso-OMPA had no toxic effects on AChE+/+ and +/− mice, but was lethal to AChE−/− mice. Iso-OMPA is regarded as a specific inhibitor of BChE, however, AChE activity in serum was inhibited 50% and AChE

Table 2
Toxic signs in OP treated AChE+/+, +/−, and −/− mice, following a lethal dose of OP

OP	AChE genotype	Salivation	Mucus in eyes	Urination	Defecation	Reduced body temp	Hyperactivity	Tremor (clonic or tonic)	Convulsions	Vasodilation
CPO	+/+	No	Yes	No	No	Yes	No	Yes	Yes	Yes
CPO	+/−	No	Yes	No	No	Yes	No	Yes	Yes	Yes
CPO	−/−	No	Yes	No	No	Yes	No	Yes	Yes	Yes
VX	+/+	Yes	Yes	No	No	Yes	No	Yes	Yes	Yes
VX	+/−	Yes	Yes	No	No	Yes	No	Yes	Yes	Yes
VX	−/−	Yes	Yes	No	No	Yes	No	Yes	Yes	Yes
Iso-OMPA	+/+	No	Yes	No	Yes	Yes	Yes	Yes	No	No
Iso-OMPA	+/−	No	Yes	No	Yes	Yes	Yes	Yes	No	No
Iso-OMPA	−/−	Yes	Yes	No	No	Yes	Yes	Yes	No	No
DFP	+/+	Yes	−	Yes	No	Yes	Yes	Yes	−	−
DFP	+/−	Yes	−	Yes	No	Yes	Yes	Yes	−	−
DFP	−/−	Yes	−	Yes	No	Yes	No	Yes	−	−

CPO is chlorpyrifos oxon. The dash indicates no data.

Table 3
AChE and BChE activity in tissues of mice treated with a lethal dose of VX

AChE genotype	Tissue	AChE activity		BChE activity	
		Control	VX	Control	VX
+/+	Brain	1.71	0.86[a]	0.13	0.05[a]
+/−	Brain	0.91	0.53[a]	0.11	0.05[a]
−/−	Brain	0	0	0.10	0.05[a]
+/+	Muscle	0.28	0.15[a]	0.26	0.14
+/−	Muscle	0.22	0.11[a]	0.25	0.11[a]
−/−	Muscle	0	0	0.27	0.11[a]
+/+	Intestine	0.21	0.20	5.97	5.08
+/−	Intestine	0.15	0.14	4.37	3.77
−/−	Intestine	0	0	7.95	6.28
+/+	Serum	0.54	0.31[a]	2.79	1.64
+/−	Serum	0.28	0.21	1.75	1.14[a]
−/−	Serum	0	0	1.88	1.48

ND: not determined. Units of enzyme activity are μmole substrate hydrolyzed per min per gram wet weight of tissue. The standard deviations were 3–30% of the average values shown. The VX dose for AChE+/+ mice was 25 μg/kg, for AChE+/− mice was 18–22 μg/kg, and for AChE−/− mice was 10–12 μg/kg.

[a] Significantly different from control $p \leq 0.025$ by ANOVA using Bonferroni correction to adjust for multiple comparisons.

activity in liver was inhibited 95% in both AChE+/+ and +/− mice, demonstrating that iso-OMPA inhibits AChE as well as BChE. AChE activity in brain was not inhibited by 5 mg/kg iso-OMPA. However, BChE activity in brain was inhibited 25% in AChE+/+, 25% in AChE+/−, and 65% in AChE−/− mouse. Serum and liver BChE activity were almost completely inhibited in all three genotypes. These results show that BChE is a significant target for inhibition by OP.

3.6. Noncholinesterase targets of OP

An assay to identify proteins inhibited by OP was developed. FP-biotin labeled at least 55 proteins in mouse brain 100,000 × g supernatant (Fig. 1). When brain extract was preincubated with chlorpyrifos oxon, three of the FP-biotinylated protein bands disappeared: bands 12, 41, and 44/45 in Fig. 2. Preincubation with diazoxon caused four bands to disappear (bands 9, 12, 41, 47); with dichlorvos, seven bands disappeared (bands 12, 23, 24, 32, 44, 45, 51); and with malaoxon, one band disappeared (band 9). The set of bands that disappeared was unique for each OP, though there was overlap.
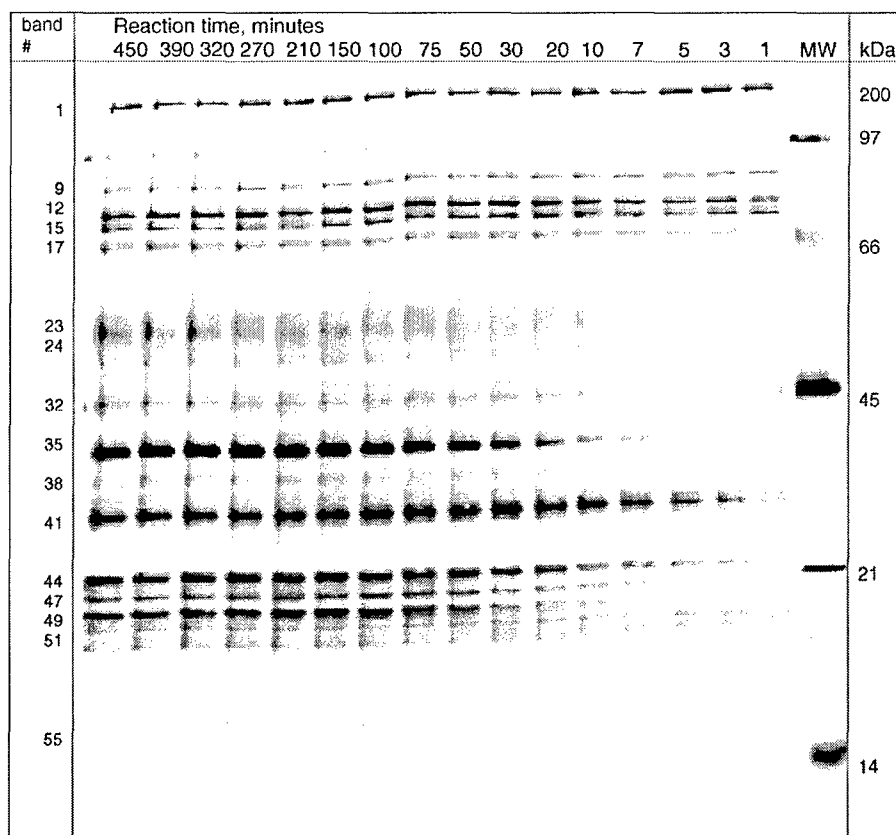
Fig. 1. Time course for the reaction of FP-biotin with proteins extracted from mouse brain. The 10 μM FP-biotin was reacted with 1.25 mg protein/ml of mouse brain supernatant in 50 mM Tris/Cl buffer, pH 8.0, containing 5 mM EDTA and 2.4% methanol, at 25 °C, for selected times. The numbers above each lane indicate the reaction times in minutes. Each lane of an SDS gel received 30 μg protein. FP-biotin labeled proteins were visualized by reaction with Streptavidin Alexa 680. Biotinylated molecular weight markers were from BioRad. Endogenous biotinylated proteins are in bands 1, 14, and 15.
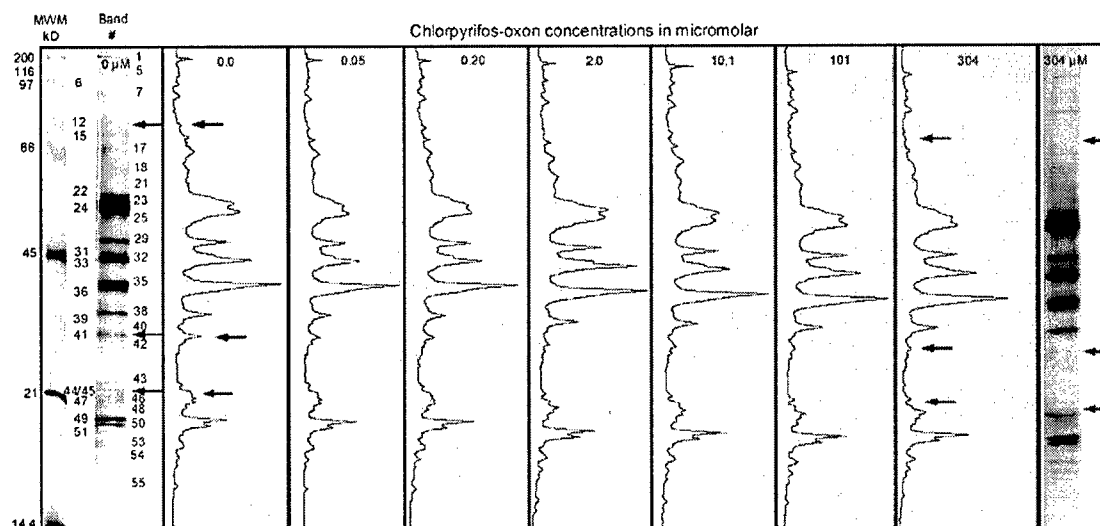
Fig. 2. Detection of proteins in mouse brain that reacted with chlorpyrifos oxon. Proteins that reacted with chlorpyrifos oxon disappeared from this blot because they were not available to react with FP-biotin. Mouse brain proteins were treated with 0–304 μM chlorpyrifos oxon for 30 min at 25 °C. Unreacted chlorpyrifos oxon was removed by gel filtration. Proteins that had not reacted with chlorpyrifos oxon were labeled with 10 μM FP-biotin for 300 min. Proteins were separated on a 10–20% gradient SDS PAGE gel, transferred to PVDF and visualized by reaction with 9.5 nM Streptavidin Alexa 680. Fluorescent signals were collected with an Odyssey flat plate scanner (Licor, Lincoln, NE). The traces show the integrated areas of the biotinylated bands. Actual pictures of the lanes are shown on the left and right. Molecular weight markers are in the extreme left-hand column. The arrows indicate the three bands which decreased in intensity as the chlorpyrifos oxon concentration increased: bands 12, 41, and 44/45.

4. Discussion

4.1. Why is the acetylcholinesterase knockout mouse supersensitive to organophosphorus agent (OP) toxicity?

Since this mouse has zero AChE activity, it must be concluded that OP inhibited enzymes other than AChE and that the consequence of this inhibition was lethal to the AChE−/− mouse.

Our results suggest that inhibition of BChE is part of the explanation for the lethality of OP in AChE-knockout mice. Evidence to support the idea that BChE inhibition is lethal to AChE−/− mice includes the following. (1) BChE was inhibited in OP treated AChE−/− mice. (2) AChE−/− mice had the same cholinergic signs of toxicity following treatment with OP, as AChE+/+ mice. This means the mechanism of toxicity was the same, even though AChE−/− mice have no AChE. The common mechanism would be accumulation of excess acetylcholine, followed by overstimulation of acetylcholine receptors. Inhibition of BChE could lead to accumulation of excess acetylcholine, because BChE is capable of hydrolyzing acetylcholine. The implication in this conclusion is that BChE has a function in AChE−/− mice to hydrolyze the neurotransmitter acetylcholine at cholinergic synapses. Mesulam et al. (2002) proposed such a function for BChE in brain.

Binding of OP to noncholinesterase proteins may explain why each OP is associated with a distinct set of symptoms. Preliminary identification of a few of the FP-biotin labeled proteins can be made by comparing our results to the literature. Eight FP-biotin reactive proteins from rat testis supernatant have been identified by Kidd et al. (2001). Three, with molecular weights around 80 kDa, would be expected to travel in the vicinity of bands 9–17. They are acyl peptide hydrolase (82 kDa), prolyloligopeptidase (80 kDa) and carboxylesterase 1 (80 kDa). One or more of these enzymes probably reacts with dichlorvos, chlorpyrifos oxon, malaoxon, and diazoxon. Long chain acyl CoA hydrolase (48 kDa) and LDL-associated PLA2 (45 kDa) would appear in the region of bands 29–35, a region where reactivity was observed with dichlorvos.

4.2. Implications for man

Our finding that heterozygous mice who carry one deficient ACHE allele are healthy, suggests that humans who carry one deficient ACHE allele are healthy. To date, an ACHE deficient allele has not been found in humans. It is expected that partial AChE deficiency exists in healthy humans. These humans are expected to be more sensitive to OP toxicity than the average person. Noncholinesterase targets of OP binding may provide new biomarkers of OP exposure.

Acknowledgements

References

Duysen, E.G., Li, B., Xie, W., Schopfer, L.M., Anderson, R.S., Broomfield, C.A., Lockridge, O., 2001. Evidence for non-acetylcholinesterase targets of organophosphorus nerve agent; supersensitivity of the acetylcholinesterase knockout mouse to VX lethality. J. Pharmacol. Exp. Ther. 299, 542–550.

Duysen, E.G., Stribley, J.A., Fry, D.L., Hinrichs, S., Lockridge, O., 2002. Rescue of the acetylcholinesterase knockout mouse by feeding a liquid diet; phenotype of the adult acetylcholinesterase deficient mouse. Brain Res. Dev. Brain Res. 137, 43–54.

Ellman, G.L., Courtney, K.D., Andres Jr., V., Featherstone, R.M., 1961. A new and rapid colorimetric determination of acetylcholinesterase activity. Biochem. Pharmacol. 7, 88–95.

Gomeza, J., Shannon, H., Kostenis, E., Felder, C., Zhang, L., Brodkin, J., Grinberg, A., Sheng, H., Wess, J., 1999. Pronounced pharmacologic deficits in M2 muscarinic acetylcholine receptor knockout mice. Proc. Natl. Acad. Sci. U.S.A. 96, 1692–1697.

Gray, E.G., Whittaker, V.P., 1962. The isolation of nerve endings from brain: an electron-microscopic study of cell fragments derived by homogenization and centrifugation. J. Anat. 96, 79–88.

Kidd, D., Liu, Y., Cravatt, B.F., 2001. Profiling serine hydrolase activities in complex proteomes. Biochemistry 40, 4005–4015.

Li, B., Stribley, J.A., Ticu, A., Xie, W., Schopfer, L.M., Hammond, P., Brimijoin, S., Hinrichs, S.H., Lockridge, O., 2000. Abundant tissue butyrylcholinesterase and its possible function in the acetylcholinesterase knockout mouse. J. Neurochem. 75, 1320–1331.

Li, B., Duysen, E.G., Volpicelli-Daley, L.A., Levey, A.I., Lockridge, O., 2003. Regulation of muscarinic acetylcholine receptor function in acetylcholinesterase knockout mice. Pharmacol. Biochem. Behav. 74, 977–986.

Liu, Y., Patricelli, M.P., Cravatt, B.F., 1999. Activity-based protein profiling: the serine hydrolases. Proc. Natl. Acad. Sci. U.S.A. 96, 14694–14699.

McDonough, J.H., Shih, T.M., 1997. Neuropharmacological mechanisms of nerve agent-induced seizure and neuropathology. Neurosci. Biobehav. Rev. 21, 559–579.

Mesulam, M.M., Guillozet, A., Shaw, P., Levey, A., Duysen, E.G., Lockridge, O., 2002. Acetylcholinesterase knockouts establish central cholinergic pathways and can use butyrylcholinesterase to hydrolyze acetylcholine. Neuroscience 110, 627–639.

Moser, V.C., 1995. Comparisons of the acute effects of cholinesterase inhibitors using a neurobehavioral screening battery in rats. Neurotoxicol. Teratol. 17, 617–625.

Pope, C.N., 1999. Organophosphorus pesticides: do they all have the same mechanism of toxicity? J. Toxicol. Environ. Health B: Crit. Rev. 2, 161–181.

Xie, W., Stribley, J.A., Chatonnet, A., Wilder, P.J., Rizzino, A., McComb, R.D., Taylor, P., Hinrichs, S.H., Lockridge, O., 2000. Postnatal developmental delay and supersensitivity to organophosphate in gene-targeted mice lacking acetylcholinesterase. J. Pharmacol. Exp. Ther. 293, 896–902.

Albumin, a New Biomarker of Organophosphorus Toxicant Exposure, Identified by Mass Spectrometry

Eric S. Peeples,* Lawrence M. Schopfer,* Ellen G. Duysen,* Reggie Spaulding,† Troy Voelker,†
Charles M. Thompson,† and Oksana Lockridge*·1

*University of Nebraska Medical Center, Eppley Institute, Omaha, Nebraska 68198–6805; and †University of Montana, Department of Biomedical
and Pharmaceutical Sciences, Missoula, Montana 59812

The classical laboratory tests for exposure to organophosphorus toxicants (OP) are inhibition of acetylcholinesterase (AChE) and butyrylcholinesterase (BChE) activity in blood. In a search for new biomarkers of OP exposure, we treated mice with a biotinylated organophosphorus agent, FP-biotin. The biotinylated proteins in muscle were purified by binding to avidin-Sepharose, separated by gel electrophoresis, digested with trypsin, and identified from their fragmentation patterns on a quadrupole time-of-flight mass spectrometer. Albumin and ES1 carboxylesterase (EC 3.1.1.1) were found to be major targets of FP-biotin. These FP-biotinylated proteins were also identified in mouse plasma by comparing band patterns on nondenaturing gels stained for albumin and carboxylesterase activity, with band patterns on blots hybridized with Streptavidin Alexa-680. Two additional FP-biotin targets, AChE (EC 3.1.1.7) and BChE (EC 3.1.1.8), were identified in mouse plasma by finding that enzyme activity was inhibited 50–80%. Mouse plasma contained eight additional FP-biotinylated bands whose identity has not yet been determined. *In vitro* experiments with human plasma showed that chlorpyrifos oxon, echothiophate, malaoxon, paraoxon, methyl paraoxon, diazoxon, diisopropylfluorophosphate, and dichlorvos competed with FP-biotin for binding to human albumin. Though experiments with purified albumin have previously shown that albumin covalently binds OP, this is the first report of OP binding to albumin in a living animal. Carboxylesterase is not a biomarker in man because humans have no carboxylesterase in blood. It is concluded that OP bound to albumin could serve as a new biomarker of OP exposure in man.

Key Words: acetylcholinesterase; butyrylcholinesterase; organophosphate; FP-biotin; albumin.

Organophosphorus toxicants (OP) are used in agriculture as pesticides, in medical practice as antihelminthics, in the airline industry as additives to hydraulic fluid and jet engine oil, and as chemical warfare agents. These compounds are known to exert their acute effects by inhibiting acetylcholinesterase

(EC 3.1.1.7, AChE). The excess acetylcholine that accumulates causes an imbalance in the nervous system that can result in death (McDonough and Shih, 1997).

Though AChE is the clinically important target of OP exposure, other proteins also form a covalent bond with OP, depending on the identity of the OP (Casida and Quistad, 2004). These secondary targets include butyrylcholinesterase, acylpeptide hydrolase, neurotoxic esterase, fatty acid amide hydrolase, arylformamidase, cannabinoid CB1 receptor, muscarinic acetylcholine receptor, and carboxylesterase. With the exception of neurotoxic esterase, whose inhibition is responsible for delayed neuropathy, the toxicological relevance of inhibition of these secondary targets is not yet understood (Casida and Quistad, 2004; Ray and Richards, 2001). Albumin has not previously been shown to bind OP in a living animal, though *in vitro* experiments with purified albumin have demonstrated covalent binding to diisopropylfluorophosphate, sarin, and soman (Black *et al.*, 1999; Means and Wu, 1979; Murachi, 1963; Sanger, 1963; Schwartz, 1982). Albumin hydrolyzes chlorpyrifos oxon and paraoxon (Ortigoza-Ferado *et al.*, 1984; Sultatos *et al.*, 1984).

The toxic effects of a particular OP cannot be attributed entirely to inhibition of AChE. Toxic signs are different for each OP when that OP is administered at low doses (Moser, 1995). For example, a low dose of fenthion decreased motor activity in rats by 86% but did not alter the tail-pinch response, whereas a low dose of parathion did not affect motor activity but did decrease the tail-pinch response (Moser, 1995). These toxicological observations suggest that OP have other biological actions in addition to their cholinesterase-inhibitory properties.

Another confounding observation is the finding that toxic signs do not correlate with degree of AChE inhibition. Rats given doses of OP that inhibited AChE to similar levels had more severe toxicity from parathion than chlorpyrifos (Pope, 1999). There are also examples of toxic signs unaccompanied by AChE inhibition. Workers who manufacture the OP pesticide quinalphos have significantly low scores for memory, learning ability, vigilance, and motor response, though their blood AChE activity levels are the same as in control subjects (Srivastava *et al.*, 2000). Chronic low-level exposure to OP

1 To whom correspondence should be addressed at University of Nebraska Medical Center, Eppley Institute, 986805 Nebraska Medical Center, Omaha, NE 68198–6805. Fax: (402) 559-4651. E-mail: olockrid@unmc.edu.

induces neuropsychiatric disorders without inhibition of esterase activity (Ray and Richards, 2001; Salvi et al., 2003). These observations have led to the suggestion that some OP have toxicologically relevant sites of action in addition to AChE (Moser, 1995; Pope, 1999; Ray and Richards, 2001). The hypothesis arose that a given OP reacts not only with AChE, but with a set of proteins unique for each OP.

Our goal is to identify the proteins in a living animal that covalently bind the biotin-tagged OP called FP-biotin (Kidd et al., 2001; Liu et al., 1999). In this report we used tandem mass spectrometry, enzyme activity assays, gel electrophoresis, and blots to identify four FP-biotin-labeled proteins in the muscle and plasma of mice that had been injected with FP-biotin ip. We found FP-biotin-labeled albumin, carboxylesterase, BChE, and AChE. This is the first report to demonstrate that albumin is a significant target of OP binding in a living animal. Eight other proteins in mouse blood became labeled but have not yet been identified.

MATERIALS AND METHODS

Materials. FP-biotin (MW 592.3) was custom synthesized by Troy Voelker in the laboratory of Charles M. Thompson at the University of Montana (Liu et al., 1999). Purity was checked by NMR and mass spectrometry, and no evidence of contamination was detected. FP-biotin was stored as a dry powder at −70°C. Just before use, the dry powder was dissolved in 100% ethanol to a concentration of 13.3 mg/ml and diluted with saline to 15% ethanol containing 2 mg/ml FP-biotin.

Immun-Blot PVDF membrane for protein blotting, 0.2 μm (catalog #162-0177) and biotinylated molecular weight markers (catalog #161–0319) were from Bio-Rad Laboratories, Hercules, CA. Streptavidin Alexa-680 fluorophore (catalog #S-21378) was from Molecular Probes, Eugene, OR. Avidin-agarose beads (catalog # A-9207), iso-OMPA, and bovine albumin, essentially fatty acid-free (Sigma A 7511) were from Sigma-Aldrich, St. Louis, MO. Echothiophate iodide was from Wyeth-Ayerst, Rouses Point, NY. All other OP were from Chem Service Inc, West Chester, PA.

Mice. The Institutional Animal Care and Use Committee of the University of Nebraska Medical Center approved all procedures involving mice. Animal care was provided in accordance with the principles and procedures outlined in the National Institutes of Health Guide for the Care and Use of Laboratory Animals. Mice completely lacking AChE protein were made by gene targeting (Xie et al., 2000) at the University of Nebraska Medical Center. Exons 2, 3, 4, and 5 of the ACHE gene were deleted to make AChE−/− mice. The AChE−/− animals are in strain 129Sv genetic background. The colony is maintained by breeding heterozygotes because AChE−/− mice do not breed (Duysen et al., 2002). Wild-type mice are littermates of AChE−/− mice. The strain 129Sv mice were used for experiments with FP-biotin.

Injection of FP-biotin into mice. Mice were injected intraperitoneally with FP-biotin dissolved in 15% ethanol to give a dose of 56 or 5 mg/kg, or with vehicle alone. The dose of FP-biotin was calculated from dry weight. No correction was made for the fact that FP-biotin is a mixture of phosphorus stereoisomers. Mice were euthanized 120 min after FP-biotin injection, by inhalation of carbon dioxide. Blood was washed out of tissues by intracardial perfusion with saline solution. Tissues from six mice were analyzed by mass spectrometry: two AChE−/− FP-biotin treated (5 and 56 mg/kg), two AChE−/− untreated, one wild-type FP-biotin treated (56 mg/kg), and one wild-type untreated. In addition wild-type mice were treated with 0, 0.5, 1.0, 5.0, or 18.8 mg/kg FP-biotin ($n = 2$ for each dose). Blood was analyzed by gel electrophoresis, blotting, and enzyme activity assays.

Enzyme activity. AChE activity was measured with 1 mM acetylthiocholine in the presence of 0.5 mM dithiobisnitrobenzoic acid (Ellman et al., 1961) after inhibiting BChE activity for 30 min with 0.1 mM iso-OMPA, in 0.1 M potassium phosphate pH 7.0, at 25°C. BChE activity was measured with 1 mM butyrylthiocholine. $\Delta E_{412nm} = 13,600\ M^{-1}\ cm^{-1}$ at pH 7.0. Carboxylesterase activity was measured with 5 mM p-nitrophenyl acetate after inhibiting AChE and BChE with 0.01 mM eserine, and after inhibiting paraoxonase with 12.5 mM EDTA. $\Delta E_{400nm} = 9000\ M^{-1}\ cm^{-1}$ at pH 7.0. AChE, BChE, and carboxylesterase units of activity are micromoles hydrolyzed per minute at pH 7.0, 25°C.

Isolation of FP-biotin-labeled protein. To prepare OP-labeled proteins for mass spectrometry, FP-biotin-labeled proteins in muscle were purified on avidin-agarose beads and separated by SDS–polyacrylamide gel electrophoresis. Proteins from mice that had received no FP-biotin were purified by the same procedure.

Tissues were homogenized in 10 volumes of 50 mM TrisCl pH 8.0 containing 5 mM EDTA, and centrifuged for 10 min in a microfuge at 12,000 rpm to partially clarify the suspension. A detailed example of the protocol follows. The 0.96 ml of muscle homogenate (7.4 mg protein/ml) was diluted with 3.75 ml of 50 mM TrisCl pH 8.0, 5 mM EDTA to make 1.5 mg/ml protein solution. SDS was added to make the solution 0.5% SDS. The protein solution was heated for 3 min in a boiling water bath and then diluted with buffer to make the final SDS concentration 0.2%. The protein solution was incubated with 100 μl of washed avidin-agarose beads (1.9 mg avidin/ml of beads) overnight at room temperature, with continuous inversion, to bind the FP-biotin-labeled proteins to the beads. Beads were washed three times with the TrisCl/EDTA buffer, containing 0.2% SDS, to remove nonspecifically bound protein. Twenty-five μl of 6× SDS–PAGE loading buffer (0.2 M TrisCl, pH 6.8, 10% SDS, 30% glycerol, 0.6 M dithiothreitol and 0.012% bromophenol blue) were added to the 100 μl of beads, and the mixture was heated at 85°C for 3 min. This step released the biotinylated proteins from the avidin beads. Equal amounts of the bead mixture were loaded directly into two wells of a 10–20% gradient SDS–PAGE (10-well format, 1.5-mm thick) and run for 4000 volt-hours in the cold room. The gel was stained with Coomassie blue G250 (Bio-Safe from BioRad), and destained with water. Coomassie G250 is reportedly 2–8 fold more sensitive than Coomassie R250 (BioRad specifications). To minimize contamination from keratin, the staining dish had been cleaned with sulfuric acid, and the water was Milli-Q purified. For the same reason, gloves were worn for all operations involving the gel.

Protein digestion protocol. The proteins separated on SDS–PAGE were digested with trypsin to prepare them for identification by mass spectral analysis. Gloves were worn throughout these procedures, all solutions were made with Milli-Q purified water, and all glassware, plasticware, and tools were rinsed with Milli-Q purified water to minimize keratin contamination. Each Coomassie-stained band from one lane of the SDS–PAGE was excised, placed into a separate 1.5-ml microfuge tube, and chopped into bits. The amount of gel excised was kept to a minimum. The gel bits were destained by washing with 200 μl of 25 mM ammonium bicarbonate (Aldrich) in 50% acetonitrile (synthesis grade, from Fisher). After three washes, the gel bits were colorless and had shrunken considerably. Residual liquid was removed, and the gel bits dried by evaporation in a Speedvac (Jouan). Disulfide bonds in the protein were reduced by incubating the gel bits with 10 mM dithiothreitol (molecular biology grade, from Sigma) in 200 μl of 100 mM ammonium bicarbonate for 1 h at 56°C. The gel pieces were then centrifuged, excess solution was removed, and the protein was alkylated with 55 mM iodoacetamide (Sigma) in 120 μl of 100 mM ammonium bicarbonate for 1 h at room temperature in the dark. The gel bits were again centrifuged, excess solution was removed, and the bits were washed with 200 μl of 25 mM ammonium bicarbonate in 50% acetonitrile (three times). Residual liquid was again removed and the gel bits dried by evaporation in the Speedvac. The proteins were digested in the gel with trypsin, using 12.5 ng/μl of sequencing grade trypsin (Promega) in 25 mM ammonium bicarbonate. Ninety μl of the trypsin solution were added to the dry gel bits and incubated at 4°C for 20 min, to allow the gel to re-swell. Then 60 μl of 25 mM ammonium bicarbonate were layered over each sample, and the samples were incubated at 37°C overnight (about 17 h). Peptides were extracted by incubating each reaction mixture with 200 μl of 0.1% trifluoroacetic acid (sequencing grade from Beckman) in 60% acetonitrile for one h at

room temperature. Extraction was repeated three times, and the extracts for each sample were pooled. The pooled extracts were evaporated to dryness in the Speedvac, and the dry samples were stored at −20°C until analyzed.

Mass spectral analysis. Each tryptic peptide digest was resuspended in 40 µl of 5% aqueous acetonitrile/0.05% trifluoroacetic acid. A 10-µl aliquot of the digest was injected into a CapLC (capillary liquid chromatography system from Waters Corp) using 5% aqueous acetonitrile/0.05% trifluoroacetic acid (auxiliary solvent) at a flow rate of 20 µl per min. Peptides were concentrated on a C_{18} PepMap™ Nano-Precolumn™ (5 mm × 0.3 mm id, 5µm particle size) for 3 min, and then eluted onto a C_{18} PepMap™ capillary column (15 cm × 75 µm id, 3 µm particle size both from LC Packings), using a flow rate of 200–300 nl per min. Peptides were partially resolved using gradient elution. The solvents were 2% aqueous acetonitrile/0.1% formic acid (solvent A), and 90% acetonitrile/10% isopropanol/0.2% formic acid (solvent B). The solvent gradient increased from 5% B to 50% B over 22 min, then to 80% B over 1 min, and remained at 80% B for 4 min. The column was then flushed with 95% B for 3 min and equilibrated at 5% B for 3 min before the next sample injection.

Peptides were delivered to the Z-spray source (nano-sprayer) of a Micromass Q-TOF (tandem quadrupole/time-of-flight mass spectrometer from Waters Corp.) through a 75-µm id capillary, which connected to the CapLC column. In order to ionize the peptides, 3300 volts were applied to the capillary, 30 volts to the sample cone, and zero volts to the extraction cone. Mass spectra for the ionized peptides were acquired throughout the chromatographic run, and collision-induced dissociation spectra were acquired on the most abundant peptide ions (having a charge state of 2+, 3+, or 4+). The collision-induced dissociation spectrum is unique for each peptide and is based on the amino acid sequence of that peptide. For this reason, identification of proteins using collision-induced dissociation data is superior to identification by only the peptide mass fingerprint of the protein. The collision cell was pressurized with 1.5 psi ultrapure argon (99.999%), and collision voltages were dependent on the mass-to-charge ratio and the charge state of the parent ion. The time-of-flight measurements were calibrated daily using fragment ions from collision-induced dissociation of [Glu¹]-fibrinopeptide B. Each sample was post-processed using this calibration and Mass Measure (Micromass). The calibration was adjusted to the exact mass of the autolytic tryptic fragment at 421.76, found in each sample.

The mass and sequence information for each detected peptide was submitted either to ProteinLynx Global Server 1.1 (a proprietary software package, from Micromass), or to MASCOT (a public access package provided by Matrix Science at http://www.matrix-science.com). Data were compared to all mammalian entries (ProteinLynx) or just mouse entries (MASCOT) in the NCBInr database (National Center for Biotechnology Information). Search criteria for ProteinLynx were set to a mass accuracy of 0.25 Da, fixed modification of methionine (oxidation), and variable modification of cysteine (carbamidomethylation). One missed cleavage by trypsin was allowed. Search criteria for MASCOT were set to a mass accuracy of ±0.1 Da, one missed cleavage, variable modification of methionine (oxidation) and cysteine (carbamidomethylation), and peptide charge +2 and +3. Both software packages calculated a score for each identified protein based on the match between the experimental peptide mass and the theoretical peptide mass, as well as between the experimental collision-induced dissociation spectra and the theoretical fragment ions from each peptide. Results were essentially the same from both packages.

Polyacrylamide gel electrophoresis. Gradient polyacrylamide gels (4–30%) were cast in a Hoefer gel apparatus. Electrophoresis was for 5000 volt-hours (200 volts for 25 h) at 4°C for nondenaturing gels and 2500 volt-hours (100 volts for 25 h) at 4°C for gels containing 0.1% SDS.

Staining gels for BChE activity. Nondenaturing gels were stained for BChE activity by the method of Karnovsky and Roots (1964). The staining solution contained 180 ml of 0.2 M sodium maleate pH 6.0, 15 ml of 0.1 M sodium citrate, 30 ml of 0.03 M cupric sulfate, 30 ml of 5 mM potassium ferricyanide, and 0.18 g butyrylthiocholine iodide in a total volume of 300 ml. Gels were incubated, with shaking, at room temperature for 3 to 5 h. The reaction was stopped by washing the gels with water. To determine the location of albumin, activity-stained gels were stained with Coomassie blue.

Staining gels for carboxylesterase activity and albumin. Nondenaturing gels were incubated in 100 ml of 50 mM TrisCl pH 7.4 in the presence of 50 mg beta-naphthylacetate dissolved in 1 ml ethanol, and 50 mg of solid Fast Blue RR. The naphthylacetate precipitates when it is added to the buffer, but enough remains in solution that the reaction works. Though the Fast Blue RR does not dissolve, pink to purple bands develop on the gel within minutes (Nachlas and Seligman, 1949). A maximum of 30 min incubation at room temperature was needed. The gels were washed with water and photographed. This stain is primarily for carboxylesterase. Albumin gives a faint band with this method because albumin slowly hydrolyzes beta-naphthylacetate (Tove, 1962). Activity-stained gels were counterstained with Coomassie blue to verify the location of albumin.

To align bands on gels stained for enzyme activity with biotinylated bands on a PVDF membrane, the transparent activity-stained gels were placed on top of a printed image of the fluorescent bands in the PVDF membrane.

Visualizing FP-biotin-labeled proteins. For determination of the number and size of proteins labeled by FP-biotin, proteins were subjected to gel electrophoresis, transfer to a PVDF membrane, and hybridization with a fluorescent probe. The details of the procedure follow.

Proteins were transferred from the polyacrylamide gel to PVDF membrane electrophoretically in a tank using plate electrodes (Immun-Blot from BioRad) electrophoretically in a tank using plate electrodes (TransBlot from BioRad), at 0.5 amps, for 1 h, in 3 l of 25 mM Tris/192 mM glycine buffer, pH 8.2, in the cold room (4°C), with stirring. The membrane was blocked with 3% gelatin (BioRad) in 20 mM TrisCl buffer, pH 7.5, containing 0.5 M NaCl for 1 h at room temperature. The 3% gelatin solution had been prepared by heating the gelatin in buffer in a microwave oven for several seconds. The blocked membrane was washed three times with 20 mM TrisCl buffer, pH 7.5, containing 0.5 M NaCl and 0.05% Tween-20, for 5 min.

Biotinylated proteins were labeled with 9.5 nM Streptavidin Alexa-680 fluorophore in 20 mM TrisCl buffer, pH 7.5, containing 0.5 M NaCl, 0.05% Tween-20, 0.2% SDS, and 1% gelatin, for 2 h, at room temperature, protected from light. Shorter reaction times resulted in less labeling. The SDS was found to increase the intensity of labeling. The membrane was washed twice with 20 mM TrisCl buffer, pH 7.5, containing 0.5 M NaCl and 0.05% Tween-20, and twice with 20 mM TrisCl buffer, pH 7.5, containing 0.5 M NaCl, for 20 min each, while protected from light.

Membranes were scanned with the Odyssey Infrared Imaging System (LI-COR, Lincoln, NE) at 42 microns per pixel. The Odyssey employs an infrared laser to excite a fluorescent probe, which is attached to the target protein, and then collects the emitted light. The emitted light intensity is directly proportional to the amount of probe. Both the laser and the detector are mounted on a moving carriage positioned directly below the membrane. The membrane can be scanned in step sizes as small as 21 microns, providing resolution comparable to X-ray film. Data are collected using a 16-bit dynamic range. The fluorophore is stable in the laser, making it possible to scan the membrane repeatedly, while using different intensity settings to optimize data collection for both strong and weak signals. The membrane was kept wet during scanning.

Biotinylated protein standards. The biotinylated bovine serum albumin (BSA) standard was prepared by incubating 10 µM BSA (0.5 mg/ml) with 20 µM FP-biotin in 20 mM TrisCl pH 7.4 at room temperature for 16 h. The biotinylated BChE standard was prepared by incubating 50 nM human BChE (3 units/ml; 4.2 µg/ml) with 10 µM FP-biotin, in 20 mM TrisCl pH 7.4 at room temperature for 16 h.

Amount of biotinylated albumin in mouse plasma. The percentage of FP-biotinylated albumin in mouse plasma was estimated from the relative intensities of the biotinylated albumin band and the biotinylated BChE band on a blot stained with Streptavidin Alexa-680. The concentration of BChE in mouse plasma is 0.003 mg/ml. The concentration of biotinylated BChE was calculated from the reduction in enzyme activity. The concentration of albumin in mouse plasma is 50 mg/ml. These values allowed estimation of percent biotinylated albumin in plasma. For example, when BChE activity was inhibited 35%, the biotinylated BChE band represented about 0.001 mg/ml biotinylated BChE. A biotinylated albumin band of similar intensity would contain 0.001 mg/ml biotinylated albumin. When mouse plasma had to be diluted

1000-fold to reduce the intensity of biotinylated albumin to a similar intensity as the biotinylated BChE in undiluted plasma, it was calculated that the concentration of biotinylated albumin in undiluted plasma was 1 mg/ml.

Binding various OP to human albumin. Human plasma was diluted 1:100 to reduce the albumin concentration to 10 µM. The diluted plasma was reacted *in vitro* with 10 mM malaoxon. paraoxon, chlorpyrifos oxon, methyl paraoxon. dichlorvos, diisopropylfluorophosphate diazoxon. echothiophate. or iso-OMPA for 1 h in 20 mM TrisCl pH 7.5 at 25°C. Then FP-biotin was added to 10 µM and allowed to react for 1 h, and 10 µl containing the equivalent of 0.1 µl plasma was loaded per lane on a nondenaturing gel. Biotinylated proteins were visualized with Streptavidin Alexa-680 after transfer to PVDF membrane.

Statistical analysis. Samples were analyzed by independent samples *t*-test assuming equal variances. Probability values less than 0.05 were considered significant.

RESULTS

Toxicity of FP-Biotin

The structure of FP-biotin is given in Figure 1. A dose of 56 mg/kg FP-biotin ip was lethal to AChE–/– mice and reduced plasma BChE activity from 1.9 ± 0.4 units/ml in untreated animals to 0.006 ± 0.003 units/ml post treatment, a 99.7% inhibition. A dose of 18.8 mg/kg ip was not lethal, but did cause severe cholinergic signs of toxicity. This dose reduced plasma BChE activity to 0.34 ± 0.09 units/ml, an 82% inhibition. A dose of 5 mg/kg caused only mild signs of toxicity and inhibited plasma BChE of AChE–/– mice 37%, to 1.2 ± 0.4 units/ml. In contrast, wild-type mice showed no signs of toxicity after treatment with 18.8 or 5 mg/kg FP-biotin ip, even though their plasma BChE activity was inhibited to the same extent as in the AChE–/– mice.

Plasma AChE activity in wild-type mice treated with 18.8 mg/kg FP-biotin was inhibited from a predose level of 0.30 ± 0.01 units/ml to 0.13 units/ml, a 56% inhibition. There was no inhibition at lower doses. AChE activity was

not measured in AChE–/– mice, because these knockout animals have no AChE activity (Xie *et al.*, 2000). AChE has a 10-fold lower affinity for FP-biotin compared to BChE (Schopfer, unpublished). This explains why a given dose of FP-biotin caused less inhibition of AChE than of BChE.

Plasma carboxylesterase activity was inhibited to the same extent in AChE–/– and +/+ mice. A dose of 18.8 mg/kg FP-biotin caused a reduction from the untreated values of 18.6 ± 0.6 units/ml to 3.5 units/ml, an 81% inhibition, while a dose of 5 mg/kg reduced the carboxylesterase levels to 9.2 ± 1.6 units/ml, a 50% reduction.

Fp-Biotin Does Not Cross the Blood–Brain Barrier

FP-biotin treated AChE–/– mice showed no inhibition of BChE in brain, supporting the conclusion that FP-biotin does not cross the blood–brain barrier.

Identification of FP-Biotinylated Proteins by Mass Spectrometry

Muscle proteins from mice that had been treated with FP-biotin, as well as from untreated control mice, were isolated by binding to avidin beads. The proteins were released from avidin by boiling in SDS and separated by SDS gel electrophoresis. Protein bands visible with Coomassie blue staining were excised and digested with trypsin. Fragmentation of tryptic peptides yielded amino acid sequence information characteristic of the protein. The proteins listed in Table 1 were consistently identified in three separate experiments. The probability score for correct identification (MOWSE score) was extremely high at 1157 for albumin and 655 for ES1 carboxylesterase. A MOWSE score of 69 is significant ($p < 0.05$), so scores of 1157 and 655 show complete confidence. Though albumin and ES1 carboxylesterase were found in samples prepared from muscle, these proteins are typically expressed at high levels in
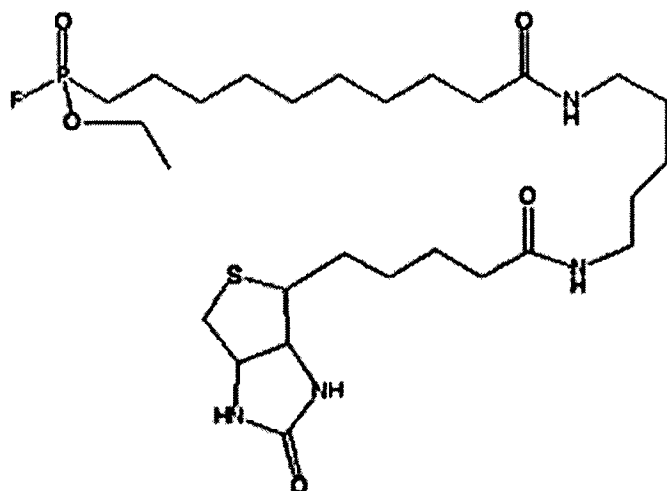

FIG. 1. Structure of FP-biotin. The OP has a reactive phosphonofluoridate group tethered to biotin via a spacer arm.

TABLE 1
Mass Spectral Identification of Proteins in Muscle That Became Biotinylated After Treatment of Mice with FP-Biotin

Protein	MW, kDa	Genbank #	MOWSE score	% Cover	# Peptides identified
Albumin	67	Gi5915682	1157	51	17
Es1 carboxylesterase	61	Gi22135640	655	40	11

Note. MW is the protein molecular weight in kilodaltons. Genbank # is the protein accession number in the computerized databank accessible through PubMed. MOWSE score: Molecular Weight Search, a measure of the probability of a match between the experimental data and the peptide mass in the database. MOWSE scores greater than 69 are significant ($p < 0.05$). % Cover is the percent of the protein represented by the sequenced peptides. # Peptides identified is the number of peptides whose sequence matched albumin or ES1 carboxylesterase. The enzyme commission number for carboxylesterase is EC 3.1.1.1.
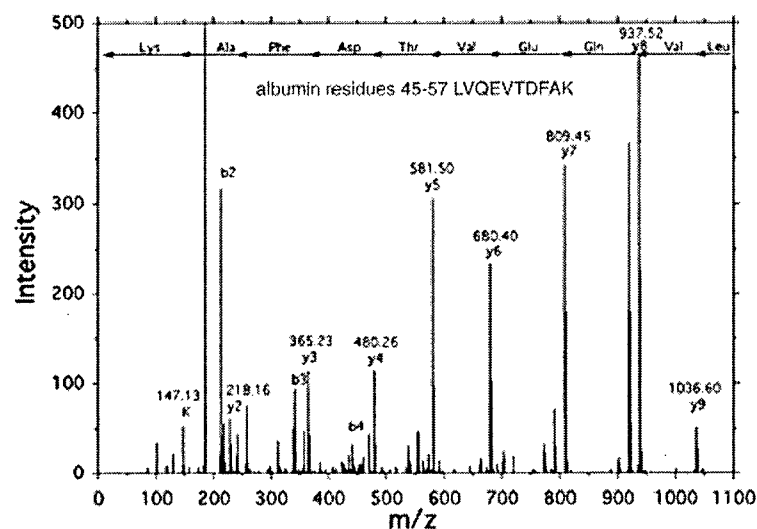
FIG. 2. Identification of albumin by mass spectrometry. The collision-induced dissociation mass spectrum of peptide Leu Val Gln Glu Val Thr Asp Phe Ala Lys of mouse albumin is shown. The parent ion has a mass-to-charge ratio (m/z) of 1149.64. The FP-biotinylated albumin was recovered from three mice treated with FP-biotin.

TABLE 2

Mass Spectral Identification of Biotinylated Proteins Extracted from Muscle of Untreated As Well As FP-Biotin Treated Mice

Protein	MW, kDa	Genbank #	EC #	MOWSE score	% Cover	# Peptides identified
Propionyl CoA carboxylase alpha	80	Gi29612536	6.4.1.3	1309	53	20
Pyruvate carboxylase	130	Gi464506	6.4.1.1	92	7	2
Methylcrotonyl CoA carboxylase alpha	79	Gi31980706	6.4.1.4	830	46	15

Note. EC# is the number assigned by the enzyme commission to identify the enzyme. Other abbreviations are defined in Table 1.

blood (Kadner *et al.*, 1992; Peters, 1996). It is likely that they were transported from the blood into the extravascular fluid where they were not washed out by perfusion. Albumin was identified by 17 peptides. A representative mass spectrum of an albumin peptide is shown in Figure 2. These 17 peptides represented 51% of the mouse albumin sequence, leaving no doubt that albumin was labeled by FP-biotin. The untreated control tissues did not show albumin, thus demonstrating that only biotinylated albumin had bound to avidin beads. This control experiment eliminated the possibility that the albumin might have bound nonspecifically to the avidin beads or that albumin was endogenously biotinylated.

FP-biotinylated AChE and BChE were not found because these proteins are not abundant enough to give a Coomassie blue stained band on SDS gels. In this work only proteins that gave a Coomassie stained band were analyzed by mass spectrometry.

Identification of Endogenous Biotinylated Proteins

Endogenous biotinylated proteins were identified by mass spectrometry. The proteins in Table 2 were found in muscle of untreated as well as in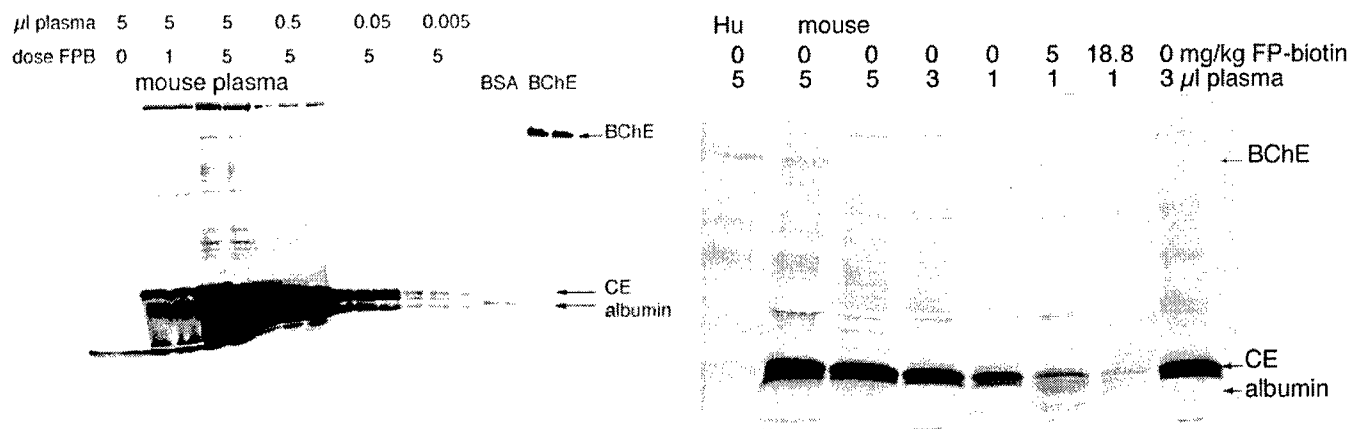 FP-biotin treated mice. They are propionyl CoA carboxylase alpha, pyruvate carboxylase, and methylcrotonyl CoA carboxylase alpha. These endogenous biotinylated proteins bound to avidin beads and were abundant enough to be visualized as Coomassie blue bands on an SDS gel.

Blot Showing FP-Biotinylated Proteins in Mouse Plasma

A blot showing the proteins in plasma that became labeled with FP-biotin after treatment of mice with FP-biotin, is shown in Figure 3. Doses of 1 and 5 mg/kg FP-biotin were not toxic to the animals. The intense broad band in the middle of the gel resolved into three bands upon serial dilution of mouse plasma. The top band in the triplet is carboxylesterase (CE), the middle band is albumin, and the bottom band has not been identified.

A band for biotinylated BChE was visible in plasma from mice treated with 5 mg/kg but not 1 mg/kg FP-biotin. This is consistent with our finding that BChE activity was inhibited about 35% after treatment with 5 mg/kg but was not inhibited after treatment with 1 mg/kg FP-biotin.

In addition to albumin, carboxylesterase, and butyrylcholinesterase, mouse plasma contains about eight other biotinylated bands whose protein identity is unknown. The intensity of the

| µl plasma | 5 | 5 | 5 | 0.5 | 0.05 | 0.005 | | |
| dose FPB | 0 | 1 | 5 | 5 | 5 | 5 | | |

mouse plasma   BSA BChE

Hu   mouse

| 0 | 0 | 0 | 0 | 0 | 5 | 18.8 | 0 mg/kg FP-biotin |
| 5 | 5 | 5 | 3 | 1 | 1 | 1 | 3 µl plasma |

FIG. 3. FP-biotinylated proteins in mouse plasma visualized with Streptavidin Alexa-680. Mice were treated with 0, 1, or 5 mg/kg FP-biotin ip. Two h later blood was collected. Plasma proteins were separated on a nondenaturing 4–30% gradient polyacrylamide gel. Proteins were transferred to PVDF membrane. and biotinylated proteins were visualized by hybridizing the blot with Streptavidin Alexa-680. The volume of mouse plasma loaded per lane ranged from 5 to 0.005 µl. Two lanes marked BSA received 0.25 µg biotinylated BSA per lane. Two lanes marked BChE received 0.020 µg biotinylated BChE per lane.

FIG. 4. Nondenaturing gel stained for carboxylesterase activity. Mice were treated with 0, 5, or 18.8 mg/kg FP-biotin ip. Blood was collected 2 h later; 1–5 µl of plasma was loaded per lane. The nondenaturing gel was stained for carboxylesterase activity. The intense band is carboxylesterase (CE). Albumin migrates immediately below carboxylesterase. The lane marked Hu received 5 µl of untreated human plasma. Note that human plasma contains no carboxylesterase.

band at the top of the gel is higher than that of mouse BChE, suggesting that this protein is more abundant than BChE and that it is highly reactive. The intensity of the other bands is equal to that of BChE or lower. Thus, mouse plasma contains at least 11 proteins that bind OP at physiological conditions, at doses of OP that produce no toxic signs.

About 1–2% of the albumin in mouse plasma is estimated to have bound FP-biotin in a mouse treated with 5 mg/kg FP-biotin ip. However, there is so much more albumin (50 mg/ml) than BChE (0.003 mg/ml) in mouse plasma that albumin consumes a significant amount of FP-biotin. Similar biotinylated band intensities were obtained in Figure 3 for BChE in undiluted plasma and for albumin diluted 1000-fold, suggesting that albumin bound 1000-fold more FP-biotin than was bound by BChE.

Activity-Stained Gels

The gels for Figures 3–5 were nondenaturing polyacrylamide gels. Nondenaturing gels were used because under these conditions the BChE tetramer of 340 kDa separated well from the 67 kDa albumin. This separation is not possible on SDS gels because albumin (67,000 MW) is 10,000 times more abundant in plasma than BChE (85,000 MW), and spreads into a broad band that overlaps with the BChE band, making it impossible to visualize BChE. A second reason for using nondenaturing gels is that nondenaturing gels allow identification of BChE and carboxylesterase based on activity. Figure 4 shows activity

Hu   mouse   FP-biotin
0   0   5   18 mg/kg
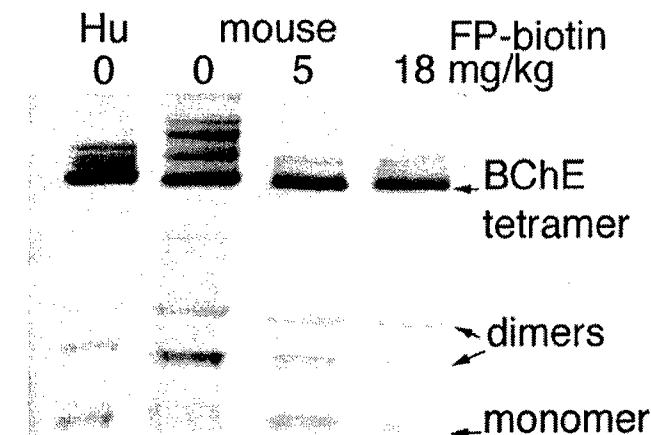
FIG. 5. Nondenaturing gel stained for BChE activity. Mice were treated with 0, 5, or 18.8 mg/kg FP-biotin ip. Blood was collected 2 h later. 5 µl of mouse plasma was loaded per lane. The lane marked Hu received 5 µl of untreated human plasma. Despite 35 to 80% inhibition of mouse BChE, enough BChE activity remained to give the characteristic pattern of BChE bands. The tetramer band contains about 95% of the total activity. Monomer and dimer bands are minor components. Note that the human and mouse BChE tetramer bands migrate to similar positions.
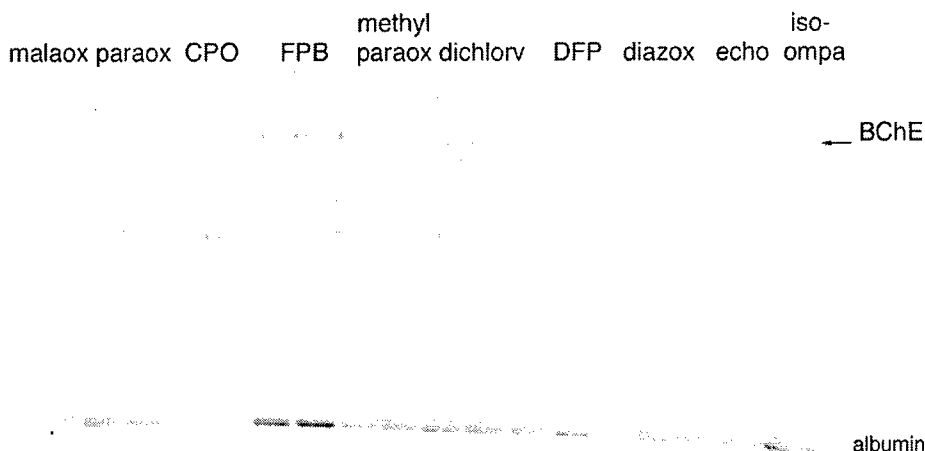
FIG. 6. Binding of FP-biotin to human albumin is inhibited by chlorpyrifos oxon and other OP. This experiment tests the ability of OP to block binding of FP-biotin to albumin. Human plasma, diluted 1:100, was incubated *in vitro* with malaoxon, paraoxon, chlorpyrifos oxon (CPO), methyl paraoxon, dichlorvos, diisopropylfluorophosphate (DFP), diazoxon, echothiophate (echo), or iso-OMPA for 1 h. before addition of FP-biotin (FPB). The lane marked FPB was treated only with FP-biotin. 10 μl containing the equivalent of 0.1 μl plasma was loaded per lane, in duplicate, on a nondenaturing gel. Biotinylated proteins were visualized with Streptavidin Alexa-680 after transfer to PVDF membrane. The intensity of the biotinylated albumin band was reduced by all OP except iso-OMPA indicating that all OP except iso-OMPA competed with FP-biotin for binding to human albumin.

with beta-naphthylacetate. The intense band is carboxylesterase (EC 3.1.1.1, CE) in mouse plasma. The bubble below carboxylesterase is albumin. BChE as well as several unidentified proteins also react with beta-naphthylacetate. Figure 5 shows activity of blood proteins with butyrylthiocholine. The BChE tetramer is the intense band near the top of the gel. By aligning bands in Figures 3, 4, and 5 we confirmed the identities of biotinylated albumin, carboxylesterase, and BChE in Figure 3.

Other OP Compete with FP-Biotin for Binding to Albumin

The goal of this experiment was to determine whether other OP bind to albumin. We wanted to know whether binding to albumin was a special property of FP-biotin or whether other OP also bound to albumin. If the OP binding site is a specific tyrosine (Black *et al.*, 1999; Sanger, 1963) then pretreatment with other OP was expected to block binding of FP-biotin. Human plasma was used in this experiment because it does not contain carboxylesterase. The absence of carboxylesterase facilitated interpretation of the results, as there was no confusion between carboxylesterase and albumin. Figure 6 shows that other OP competed with FP-biotin for binding to albumin to varying extents. Pretreatment with chlorpyrifos oxon, echothiophate, malaoxon, paraoxon, methyl paraoxon, diazoxon, dichlorvos,

and diisopropylfluorophosphate (DFP) reduced the binding of FP-biotin to human albumin *in vitro*. The only OP tested that gave no evidence of binding to albumin was tetraisopropylpyrophosphoramide (iso-OMPA).

These results suggest that OP binding to albumin is a general property of OP. It is to be noted that in this report FP-biotin has been demonstrated to bind to albumin from three species: mouse, bovine, and human. The albumins were in mouse plasma, purified bovine serum albumin, and human plasma.

DISCUSSION

OP Labels Proteins That Have No Active Site Serine

Organophosphorus toxicants are well known as inhibitors of serine proteases and serine esterases. Enzymes such as trypsin, chymotrypsin, thrombin, AChE, BChE, acylpeptide hydrolase, and carboxylesterase have a conserved active site serine with the consensus sequence GXSXG. When the active site serine is covalently modified by OP, the enzyme loses activity. Loss of enzyme activity allows one to conveniently measure reactivity with OP.

Proteins with no catalytic activity are a novel class of OP target proteins. They have no active site serine and have been

shown to bind OP *in vitro*, but not in living animals. The advent of quadrupole time-of-flight mass spectrometry has made it possible to positively identify albumin as a protein that binds the OP FP-biotin in living mice.

Experiments with purified proteins have documented covalent attachment of OP not only to serine, but also to tyrosine and histidine. For example, human albumin covalently binds sarin, soman, and DFP at tyrosine (Black *et al.*, 1999; Means and Wu, 1979). Bovine serum albumin is readily phosphorylated by DFP with a stoichiometry of one DFP molecule bound per molecule of albumin (Murachi, 1963). The sequence of the albumin peptide that covalently binds DFP was reported by Sanger as Arg-TyrThrLys for human and rabbit albumin, and ArgTyrThrArg for bovine albumin (Sanger, 1963). After the complete amino acid sequences of the albumins was known, these reactive tyrosines were identified as Tyr 411 in human and Tyr 410 in bovine albumin (Meloun *et al.*, 1975; Peters, 1996). Papain binds DFP on tyrosine (Chaiken and Smith, 1969), while rabbit liver carboxylesterase binds DFP on histidine as well as on the active site serine (Korza and Ozols, 1988). Bromelain is not inhibited by DFP, but it does react with DFP, leading to the formation of a fully active, phosphorus-containing enzyme (Murachi, 1963; Murachi *et al.*, 1965). The rat M2 muscarinic acetylcholine receptor covalently binds chlorpyrifos oxon, though the binding site has not yet been identified (Bomser and Casida, 2001; Huff *et al.*, 1994).

Living animals have previously been demonstrated to bind OP to noncholinesterase sites. The tissue distribution of radiolabeled DFP in rabbits (Jandorf and McNamara, 1950), and radiolabeled soman in rats and mouse brain (Little *et al.*, 1988; Traub, 1985) had no correlation with cholinesterase localization. These results have been interpreted to mean that tissue proteins other than cholinesterase are capable of binding OP poisons (Jandorf and McNamara, 1950; Kadar *et al.*, 1985).

Existing Mass Spectrometric Methods for Diagnosis of OP Exposure

Gas chromatography combined with mass spectrometry was used to detect sarin in archived blood samples from victims of the 1995 Tokyo subway attack (Polhuijs *et al.*, 1997). The covalently bound sarin in 0.12 to 0.5 ml of serum was released by incubation with 2 M potassium fluoride at pH 4.0. This method confirmed that the people had been exposed to OP and, in addition, identified the OP as sarin. The mass-to-charge ratios of the released OP fragments were 81, 99, and 125, values characteristic of sarin.

The GC-MS method is a significant advance over simple inhibition assays, but it has limitations. (1) The method relies on being able to release the OP from its covalent attachment site on BChE with potassium fluoride. The release step requires the catalytic machinery of BChE to be intact. Samples that have been stored in ways that denature the BChE cannot undergo

fluoride-induced release of OP (Polhuijs *et al.*, 1997). (2) Proteins other than BChE, AChE, and carboxylesterase may not be able to release OP upon treatment with potassium fluoride. Human albumin after phosphylation with sarin is not amenable to reactivation with fluoride ions (Van Der Schans *et al.*, 2004). (3) OP-derivatized protein samples that have lost an alkyl group from the phosphonate in the process called 'aging' would not be capable of releasing their OP upon treatment with potassium fluoride.

GC-MS of OP metabolites is the method recommended by the Centers for Disease Control for monitoring potential exposure to nerve agents. Measurement of OP metabolites is limited by the fact that these compounds are rapidly cleared from the body. Sarin metabolites were found in urine on post-exposure days 1 and 3, and in trace amounts on day 7 in a man who had inhaled a dose that made him unconscious (Nakajima *et al.*, 1998). Urine samples from four patients hospitalized for sarin exposure showed that most of the sarin metabolites had cleared within 24 h (Hui and Minami, 2000).

Many of these limitations were overcome in an approach where plasma BChE was purified by affinity chromatography and digested with pepsin. The peptides were separated by liquid chromatography, and the OP-derivatized peptide as well as the OP it carried were identified by electrospray tandem mass spectrometry (Fidder *et al.*, 2002). This method is well suited to detect OP exposure and will become even more valuable if OP-derivatized proteins other than BChE are included in the analysis. A major advantage of using protein-bound OP to diagnose exposure is that the OP-derivatized proteins remain in the circulation for weeks (Cohen and Warringa, 1954; Grob *et al.*, 1947; Munkner *et al.*, 1961; Van Der Schans *et al.*, 2004).

Albumin Properties

Albumin is a nonglycosylated single chain of 585 amino acids folded into three domains by 17 intrachain disulfide bonds. Albumin is the most abundant soluble protein in the body of all vertebrates and is the most prominent protein in plasma. It is synthesized in the liver and discharged into the bloodstream. Of the 360 g total albumin in a human, 40% resides in the blood and 60% in extravascular fluids of tissues (Peters, 1996). The rate of transfer to the extravascular space is about 4.5% per hour. About 40% of the extravascular albumin is in muscle. Albumin is responsible for the colloid osmotic pressure of plasma and for maintenance of blood volume and supplies most of the acid/base buffering action of plasma proteins in extravascular fluids. Albumin binds and transports metabolites and drugs. Analbuminenia, a rare deficiency of albumin, is compatible with nearly normal health in humans. The study of analbuminemia shows that albumin is helpful in coping with stress and in containing environmental and physiological toxins.

Albumin and BChE are Attractive Biomarkers for OP Poisoning

Both albumin and BChE are found in human plasma, a tissue that can be readily sampled for biomarkers of OP exposure. Both proteins bind OP, though the binding to albumin of OP other than FP-biotin has not been demonstrated *in vivo*. Both proteins have a long half-life in the circulation of humans, 20 days for albumin (Chaudhury *et al.*, 2003; Peters, 1996) and 10–16 days for BChE (Cohen and Warringa, 1954; Jenkins *et al.*, 1967; Munkner *et al.*, 1961; Ostergaard *et al.*, 1988). The long half-life of OP-labeled proteins contrasts with the short half-life of OP and OP metabolites in urine. This provides a significant advantage to a method that uses OP-labeled proteins for diagnosis of OP exposure.

Role of Albumin in OP Toxicity

Binding of OP to albumin could serve to scavenge OP molecules and therefore reduce the amount of OP available for reaction with AChE. The affinity of various OP for albumin is likely to vary, so the effectiveness of albumin as an OP scavenger is likely to depend on the identity of the OP.

Another consideration in evaluating the role of albumin in OP toxicity is competition with drugs for binding to the same site in albumin. Several drugs, including diazepam (Fehske *et al.*, 1979; Peters, 1996) and ibuprofen, bind to the same region of albumin that binds OP (see Tables 3–5 in Peters, 1996). Since the free form of a drug is active, the extent of binding to albumin controls both the effect and duration of the drug. Decreased binding of a drug to albumin can cause toxicity owing to an increase in the concentration of its free form. Thus, a person being treated for intestinal worms with metrifonate (an OP that is converted nonenzymatically to dichlorvos) might be unable to tolerate a standard dose of diazepam or ibuprofen. Or conversely, a person taking ibuprofen, could be intolerant of a standard dose of metrifonate.

ACKNOWLEDGMENTS

REFERENCES

Black, R. M., Harrison, J. M., and Read, R. W. (1999). The interaction of sarin and soman with plasma proteins: The identification of a novel phosphonylation site. *Arch. Toxicol.* **73**, 123–126.

Bomser, J. A., and Casida, J. E. (2001). Diethylphosphorylation of rat cardiac M2 muscarinic receptor by chlorpyrifos oxon *in vitro*. *Toxicol. Lett.* **119**, 21–26.

Casida, J. E., and Quistad, G. B. (2004). Organophosphate toxicology: Safety aspects of nonacetylcholinesterase secondary targets. *Chem. Res. Toxicol.* **17**, 983–998.

Chaiken, I. M., and Smith, E. L. (1969). Reaction of a specific tyrosine residue of papain with diisopropylfluorophosphate. *J. Biol. Chem.* **244**, 4247–4250.

Chaudhury, C., Mehnaz, S., Robinson, J. M., Hayton, W. L., Pearl, D. K., Roopenian, D. C., and Anderson, C. L. (2003). The major histocompatibility complex-related Fc receptor for IgG (FcRn) binds albumin and prolongs its lifespan. *J. Exp. Med.* **197**, 315–322.

Cohen, J. A., and Warringa, M. G. (1954). The fate of P32 labelled diisopropyl-fluorophosphonate in the human body and its use as a labelling agent in the study of the turnover of blood plasma and red cells. *J. Clin. Invest.* **33**, 459–467.

Duysen, E. G., Stribley, J. A., Fry, D. L., Hinrichs, S. H., and Lockridge, O. (2002). Rescue of the acetylcholinesterase knockout mouse by feeding a liquid diet; phenotype of the adult acetylcholinesterase deficient mouse. *Brain Res. Dev. Brain Res.* **137**, 43–54.

Ellman, G. L., Courtney, K. D., Andres, V., Jr., and Feather-Stone, R. M. (1961). A new and rapid colorimetric determination of acetylcholinesterase activity. *Biochem. Pharmacol.* **7**, 88–95.

Fehske, K. J., Muller, W. E., and Wollert, U. (1979). A highly reactive tyrosine residue as part of the indole and benzodiazepine binding site of human serum albumin. *Biochim. Biophys. Acta* **577**, 346–359.

Fidder, A., Hulst, A. G., Noort, D., de Ruiter, R., van der Schans, M. J., Benschop, H. P., and Langenberg, J. P. (2002). Retrospective detection of exposure to organophosphorus anti-cholinesterases: Mass spectrometric analysis of phosphylated human butyrylcholinesterase. *Chem. Res. Toxicol.* **15**, 582–590.

Grob, D., Lilienthal, J. L., Harvey, A. M., and Jones, B. F. (1947). The administration of di-isopropylfluorophosphate (DFP) to man. I. Effect on plasma and erythrocyte cholinesterase; general systemic effects; use in study of hepatic function and erythropoiesis; and some properties of plasma cholinesterase. *Bull. Johns Hopkins Hosp.* **81**, 217–244.

Huff, R. A., Corcoran, J. J., Anderson, J. K., and Abou-Donia, M. B. (1994). Chlorpyrifos oxon binds directly to muscarinic receptors and inhibits cAMP accumulation in rat striatum. *J. Pharmacol. Exp. Ther.* **269**, 329–335.

Hui, D. M., and Minami, M. (2000). Monitoring of fluorine in urine samples of patients involved in the Tokyo sarin disaster, in connection with the detection of other decomposition products of sarin and the by-products generated during sarin synthesis. *Clin. Chim. Acta* **302**, 171–188.

Jandorf, B. J., and McNamara, P. D. (1950). Distribution of radiophosphorus in rabbit tissues after injection of phosphorus-labeled diisopropyl fluoro-phosphate. *J. Pharmacol. Exp. Ther.* **98**, 77–84.

Jenkins, T., Balinsky, D., and Patient, D. W. (1967). Cholinesterase in plasma: First reported absence in the Bantu; half-life determination. *Science* **156**, 1748–1750.

Kadar, T., Raveh, L., Cohen, G., Oz, N., Baranes, I., Balan, A., Ashani, Y., and Shapira, S. (1985). Distribution of 3H-soman in mice. *Arch. Toxicol.* **58**, 45–49.

Kadner, S. S., Katz, J., and Finlay, T. H. (1992). Esterase-1: Developmental expression in the mouse and distribution of related proteins in other species. *Arch. Biochem. Biophys.* **296**, 435–441.

Karnovsky, M. J., and Roots, L. (1964). A 'direct-coloring' thiocholine method for cholinesterases. *J. Histochem. Cytochem.* **12**, 219–221.

Kidd, D., Liu, Y., and Cravatt, B. F. (2001). Profiling serine hydrolase activities in complex proteomes. *Biochemistry* **40**, 4005–4015.

Korza, G., and Ozols, J. (1988). Complete covalent structure of 60-kDa este-rase isolated from 2,3,7,8-tetrachlorodibenzo-p-dioxin-induced rabbit liver microsomes. *J. Biol. Chem.* **263**, 3486–3495.

Little, P. J., Scimeca, J. A., and Martin, B. R. (1988). Distribution of [3H]diisopropylfluorophosphate, [3H]soman, [3H]sarin, and their metabolites in mouse brain. *Drug Metab. Dispos.* **16,** 515–520.

Liu, Y., Patricelli, M. P., and Cravatt, B. F. (1999). Activity-based protein profiling: The serine hydrolases. *Proc. Natl. Acad. Sci. U.S.A.* **96,** 14694–14699.

McDonough, J. H., Jr., and Shih, T. M. (1997). Neuropharmacological mechanisms of nerve agent-induced seizure and neuropathology. *Neurosci. Biobehav. Rev.* **21,** 559–579.

Means, G. E., and Wu, H. L. (1979). The reactive tyrosine residue of human serum albumin: Characterization of its reaction with diisopropylfluorophosphate. *Arch. Biochem. Biophys.* **194,** 526–530.

Meloun, B., Moravek, L., and Kostka, V. (1975). Complete amino acid sequence of human serum albumin. *FEBS Lett.* **58,** 134–137.

Moser, V. C. (1995). Comparisons of the acute effects of cholinesterase inhibitors using a neurobehavioral screening battery in rats. *Neurotoxicol. Teratol.* **17,** 617–625.

Munkner, T., Matzke, J., and Videbaek, A. (1961). Cholinesterase activity of human plasma after intramuscular diisopropyl fluorophosphonate (DFP). *Acta Pharmacol. Toxicol. (Copenh.)* **18,** 170–174.

Murachi, T. (1963). A general reaction of diisopropylphosphorofluoridate with proteins without direct effect on enzymic activities. *Biochim. Biophys. Acta* **71,** 239–241.

Murachi, T., Inagami, T., and Yasui, M. (1965). Evidence for alkylphosphorylation of tyrosyl residues of stem bromelain by diisopropylphosphorofluoridate. *Biochemistry* **4,** 2815–2825.

Nachlas, M. M., and Seligman, A. M. (1949). The histochemical demonstration of esterase. *J. Natl. Cancer Inst.* **9,** 415–425.

Nakajima, T., Sasaki, K., Ozawa, H., Sekjima, Y., Morita, H., Fukushima, Y., and Yanagisawa, N. (1998). Urinary metabolites of sarin in a patient of the Matsumoto sarin incident. *Arch. Toxicol.* **72,** 601–603.

Ortigoza-Ferado, J., Richter, R. J., Hornung, S. K., Motulsky, A. G., and Furlong, C. E. (1984). Paraoxon hydrolysis in human serum mediated by a genetically variable arylesterase and albumin. *Am. J. Hum. Genet.* **36,** 295–305.

Ostergaard, D., Viby-Mogensen, J., Hanel, H. K., and Skovgaard, L. T. (1988). Half-life of plasma cholinesterase. *Acta Anaesthesiol. Scand.* **32,** 266–269.

Peters, T., Jr. (1996). *All about Albumin. Biochemistry, Genetics, and Medical Applications.* Academic Press Ltd., London.

Polhuijs, M., Langenberg, J. P., and Benschop, H. P. (1997). New method for retrospective detection of exposure to organophosphorus anticholinesterases: Application to alleged sarin victims of Japanese terrorists. *Toxicol. Appl. Pharmacol.* **146,** 156–161.

Pope, C. N. (1999). Organophosphorus pesticides: Do they all have the same mechanism of toxicity? *J. Toxicol. Environ. Health B Crit. Rev.* **2,** 161–181.

Ray, D. E., and Richards, P. G. (2001). The potential for toxic effects of chronic, low-dose exposure to organophosphates. *Toxicol. Lett.* **120,** 343–351.

Salvi, R. M., Lara, D. R., Ghisolfi, E. S., Portela, L. V., Dias, R. D., and Souza, D. O. (2003). Neuropsychiatric evaluation in subjects chronically exposed to organophosphate pesticides. *Toxicol. Sci.* **72,** 267–271.

Sanger, F. (1963). Amino-acid sequences in the active centres of certain enzymes. *Proc. Chem. Soc.* **5,** 76–83.

Schwartz, M. (1982). A serine protease activity of human serum albumin towards 4-methylumbelliferyl-guanidinobenzoate (MUGB) and diisopropyl fluorophosphate (DEP): Implications for the use of MUGB reactivity in amniotic fluid in prenatal diagnosis of cystic fibrosis. *Clin. Chim. Acta* **124,** 213–223.

Srivastava, A. K., Gupta, B. N., Bihari, V., Mathur, N., Srivastava, L. P., Pangtey, B. S., Bharti, R. S., and Kumar, P. (2000). Clinical, biochemical and neuro-behavioural studies of workers engaged in the manufacture of quinalphos. *Food Chem. Toxicol.* **38,** 65–69.

Sultatos, L. G., Basker, K. M., Shao, M., and Murphy, S. D. (1984). The interaction of the phosphorothioate insecticides chlorpyrifos and parathion and their oxygen analogues with bovine serum albumin. *Mol. Pharmacol.* **26,** 99–104.

Tove, S. B. (1962). The esterolytic activity of serum albumin. *Biochim. Biophys. Acta* **57,** 230–235.

Traub, K. (1985). *In vivo* distribution of 14C radiolabeled soman [3,3-dimethyl-2-butoxy)-methylphosphorylfluoride) in the central nervous system of the rat. *Neurosci. Lett.* **60,** 219–225.

Van Der Schans, M. J., Polhuijs, M., Van Dijk, C., Degenhardt, C. E., Pleijsier, K., Langenberg, J. P., and Benschop, H. P. (2004). Retrospective detection of exposure to nerve agents: Analysis of phosphofluoridates originating from fluoride-induced reactivation of phosphylated BuChE. *Arch. Toxicol.* **78,** 508–524.

Xie, W., Stribley, J. A., Chatonnet, A., Wilder, P. J., Rizzino, A., McComb, R. D., Taylor, P., Hinrichs, S. H., and Lockridge, O. (2000). Postnatal developmental delay and supersensitivity to organophosphate in gene-targeted mice lacking acetylcholinesterase. *J. Pharmacol. Exp. Ther.* **293,** 896–902.

Characteristic mass spectral fragments of the organophosphorus agent FP-biotin and FP-biotinylated peptides from trypsin and bovine albumin (Tyr410)

Lawrence M. Schopfer [a,*], Matthew M. Champion [b], Nate Tamblyn [c],
Charles M. Thompson [c], Oksana Lockridge [a]

[a] *University of Nebraska Medical Center, Eppley Institute, Omaha, NE 68198, USA*
[b] *Applied Biosystems, Foster City, CA 94404, USA*
[c] *Department of Biomedical and Pharmaceutical Sciences, University of Montana, Missoula, MT 59812, USA*

Received 3 May 2005

Abstract

A mass spectrometry-based method was developed for selective detection of FP-biotinylated peptides in complex mixtures. Mixtures of peptides, at the low-picomole level, were analyzed by liquid chromatography and positive ion, nanospray, triple quadrupole, linear ion trap mass spectrometry. Peptides were fragmented by collision-activated dissociation in the mass spectrometer. The free FP-biotin and peptides containing FP-biotinylated serine or FP-biotinylated tyrosine yielded characteristic fragment ions at 227, 312, and 329 m/z. FP-biotinylated serine yielded an additional characteristic fragment ion at 591 m/z. Chromatographic peaks containing FP-biotinylated peptides were indicated by these diagnostic ions. Data illustrating the selectivity of the approach are presented for tryptic digests of FP-biotinylated trypsin and FP-biotinylated serum albumin. A 16-residue peptide from bovine trypsin was biotinylated on the active site serine. A 3-residue peptide from bovine albumin, YTR, was biotinylated on Tyr410. This latter result confirms that the organophosphorus binding site of albumin is a tyrosine. This method can be used to search for new biomarkers of organophosphorus agent exposure.
© 2005 Elsevier Inc. All rights reserved.

Keywords: FP-biotin; Quadrupole mass spectrometry; Characteristic ions; Albumin; Trypsin

FP-biotin (10-fluoroethoxyphosphinyl-*N*-biotinamidopentyldecanamide)[1] is a fluorophosphinate linked to biotin via a 17-atom spacer (Fig. 1, [593]). It is an important

---

* Corresponding author. Fax: +1 402 559 4651.
  E-mail address: lmschopf@unmc.edu (L.M. Schopfer).

[1] *Abbreviations used:* FP-biotin, 10-fluoroethoxyphosphinyl-*N*-biotinamidopentyldecanamide; SDS–PAGE, sodium dodecyl sulfate–polyacrylamide gel electrophoresis; MALDI, matrix-assisted laser desorption ionization; LC–MS/MS, liquid chromatography–tandem mass spectrometry; CAD, collision-activated dissociation; TPCK, *N*-tosyl-L-Phe-chloromethyl ketone; HABA, 4-hydroxy azobenzene-2-carboxylic acid; TAME, *N*α-*p*-toluene-sulfonyl-L-arginine methyl ester HCl; +EMS, positive ion enhanced mass spectrum; +ER, positive ion enhanced resolution; EPI, positive ion enhanced product ion; TIC, total ion chromatogram; XIC, extracted ion chromatogram.
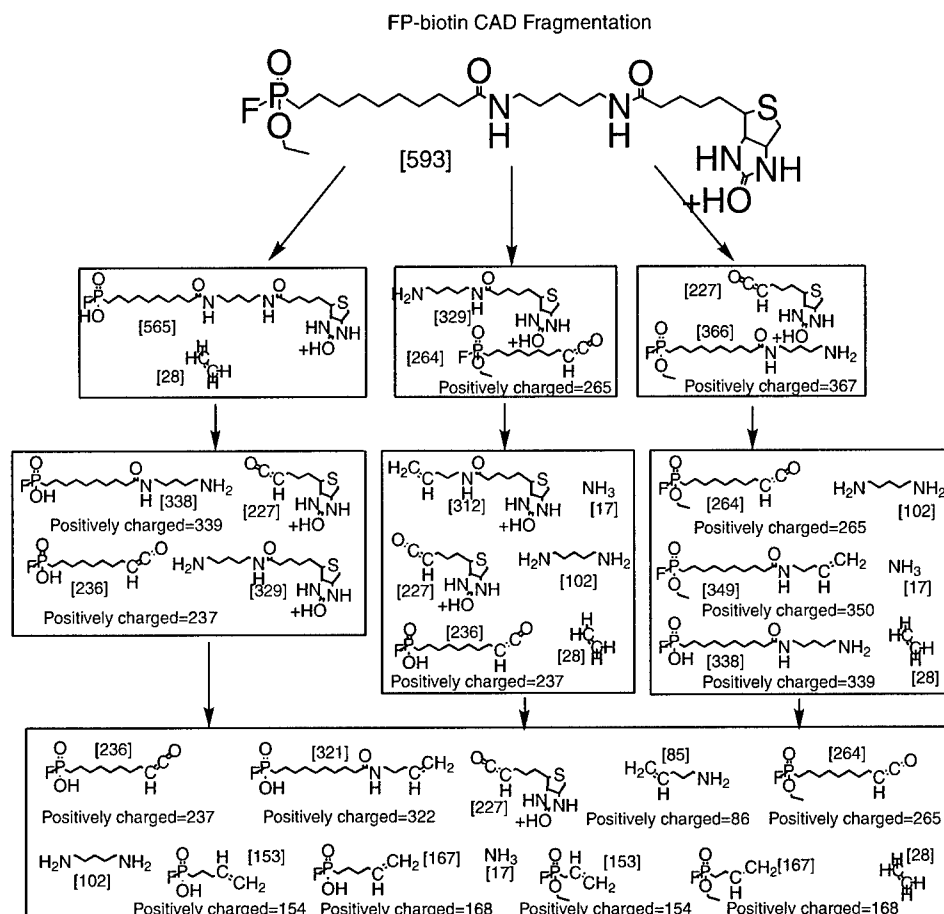
new probe that was designed for directed, activity-based protein profiling of the serine hydrolase superfamily [1,2]. The fluoroethoxyphosphinate moiety forms a covalent adduct with the catalytic serine (e.g., Ser198 of human butyrylcholinesterase). The biotin moiety provides a convenient handle that can be used for (i) identifying the labeled protein via fluorescently labeled avidin and for (ii) purifying and enriching the labeled proteins via avidin-agarose. The linker is sufficiently long that the biotin is accessible even when the phosphinate is bound to active sites buried deep in the target protein (e.g., butyrylcholinesterase, acetylcholinesterase) [3].

To date, identification of FP-biotinylated proteins has been made by mass spectrometry using the following

YABIO 7464

ARTICLE IN PRESS

No. of Pages 11; DTD=5.0.1

1 August 2005   Disk Used

Shankar (CE) / Selvi (TE)

2   *Mass spectrometry of FP-biotin and FP-biotinylated peptides / L.M. Schopfer et al. / Anal. Biochem. xxx (2005) xxx–xxx*

FP-biotin CAD Fragmentation

Fig. 1. Fragments of FP-biotin produced by collision-activated dissociation (CAD). The singly charged FP-biotin ion has an *m/z* of 593 amu. The fragments were produced by CAD. A total of 18 positively charged fragments were observed and are listed in Table 1. The structures presented are not intended to imply fragmentation mechanisms; rather, they are simply consistent with the masses of the observed fragments and serve to indicate the types of fragmentation that occurred and the sites of fragmentation. The number in square brackets next to each structure indicates the molecular weight of the piece.

41 protocol. A complex proteome was labeled. The labeled
42 proteins were partially purified and enriched by avidin–
43 agarose chromatography. Then the purified proteins
44 were separated by sodium dodecyl sulfate–polyacryl-
45 amide gel electrophoresis (SDS–PAGE). Proteins visible
46 on Coomassie blue staining were digested with trypsin.
47 The tryptic peptides were matched to proteins by mass
48 spectrometry using either matrix-assisted laser desorp-
49 tion ionization (MALDI) [1,2] or liquid chromatogra-
50 phy–tandem   mass   spectrometry   (LC–MS/MS)
51 quadrupole time-of-flight [4]. In no case was the FP-bio-
52 tinylated peptide specifically identified. Although identi-
53 fication of a protein by matching it to peptides derived
54 from a tryptic digest is the state of the art, the identifica-
55 tion would be more compelling if it included the labeled
56 peptide. This is especially important when the identified
57 protein does not fall into the serine hydrolase superfam-
58 ily. Peeples et al. [4] identified such a protein when they
59 found serum albumin to be labeled after FP-biotin was
60 injected into mice.

61 To address this issue, we have developed a mass spec-
62 trometry-based strategy specifically for identification of
63 FP-biotin-labeled peptides that uses characteristic frag-
64 ments of FP-biotin that are generated by collision-acti-
65 vated dissociation (CAD). This approach was modeled
66 after work on phosphoproteins [5–7].
67 Although simple MALDI spectra can be used to
68 identify FP-biotinylated peptides, CAD was chosen
69 because it provides extensive sequence information for
70 the selected peptide from which the labeled amino acid
71 can be specifically identified. Direct identification of
72 the labeled residue is particularly important when the
73 FP-biotin reacts with proteins that are not part of the
74 serine hydrolase superfamily such as serum albumin. In
75 addition, MALDI is best suited for relatively simple
76 samples such as the digest of a single protein. When
77 CAD is used in conjunction with electrospray ioniza-
78 tion and liquid chromatography on a quadrupole mass
79 spectrometer, a convenient system suitable for more
80 complex samples is created. The ultimate purpose of

YABIO 7464

ARTICLE IN PRESS

No. of Pages 11; DTD=5.0.1

August 2005   Disk Used

Shankar (CE) / Selvi (TE)

Mass spectrometry of FP-biotin and FP-biotinylated peptides / L.M. Schopfer et al. / Anal. Biochem. xxx (2005) xxx–xxx   3

81 developing this process is to apply the analysis to com-
82 plex proteomes.
83   We found that FP-biotin was easily fragmented under
84 CAD conditions both as a free compound and as a
85 peptide adduct. Cleavage occurred at both amide bonds
86 to create intense $[M + H]^{+1}$ fragments of 227 and 329
87 *m/z* (Figs. 1 and 2). Another intense fragment was
88 detected at 312 *m/z*, corresponding to loss of amine from
89 the 329 *m/z* fragment. An additional prominent 591-*m/z*
90 fragment was released from a peptide containing FP-
91 biotinylated serine. This fragment corresponded to the
92 β-elimination product of the serine adduct, that is, a
93 fragment in which OH has replaced F from the original
94 FP-biotin structure. These four fragments are suitable
95 candidates for identifying FP-biotinylated peptides. In
96 addition, a multitude of minor fragments could be iden-
97 tified in the CAD product ion spectrum of free FP-bio-
98 tin, including several that reflected fragmentation at the
99 phosphoester bond (Figs. 1 and 2 and Table 1). To illus-
100 trate the utility of using characteristic fragments of FP-
101 biotin for identifying FP-biotinylated peptides, two
102 model proteins were studied: bovine serum albumin and
103 bovine trypsin. Trypsin is a well-established member of
104 the serine hydrolase superfamily. FP-biotin labeled it on
105 the catalytic serine. This is consistent with the type of
106 target for which FP-biotin was designed. With serum

Table 1
CAD fragmentation of FP-biotin

Ion (amu)	Identification	Precursor for dehydration/ deamination (amu)
593.2	Parent FP-biotin	
575.2	Dehydration	593.2
565.2	Deethyl FP-biotin	
547.2	Dehydration	565.2
367.3	Fluoroethoxyphosphinate + double linker arm	
350.3	Deamination	367.3
339.4	Fluorophosphinate + double linker arm	
329.3	Biotinamide + 1 linker arm	
322.3	Deamination	339.4
312.2	Deamination	329.3
311.3	Dehydration	329.3
294.2	Dehydration	312.2
265.3	Fluoroethoxyphosphinate + 1 linker arm	
237.2	Fluorophosphinate + 1 linker arm	
227.2	Dehydro-biotin	
209.2	Dehydration	227.2
167.2	Fluorophosphinate + 6 carbon arm or Fluoroethoxyphosphinate + 4 carbon arm	
153.0	Fluorophosphinate + 5 carbon arm or Fluoroethoxyphosphinate + 3 carbon arm	
86.0	N-amino-1-pentene	

albumin, FP-biotin labeled a tyrosine. This tyrosine 107
(Tyr410) is part of a three-amino acid tryptic peptide 108
that was shown by Sanger to be the target for covalent 109
binding of diisopropylfluorophosphate, a commonly 110
used organophosphate [8]. 111

Materials and methods 112

   FP-biotin was synthesized as described previously [3]. 113
Sequencing-grade, modified, porcine trypsin was 114
obtained from Promega (reductively methylated and 115
treated with N-tosyl-L-Phe-chloromethyl ketone 116
[TPCK]). Bovine pancreatic trypsin (type XIII, TPCK 117
treated), bovine serum albumin (essentially fatty acid 118
free), TAME (Nα-p-toluene-sulfonyl-L-arginine methyl 119
ester HCl), [Glu[1]]-fibrinopeptide B, avidin, 4-hydroxy 120
azobenzene-2-carboxylic acid (HABA), and iodoaceta- 121
mide were obtained from Sigma–Aldrich. Dithiothreitol 122
(molecular biology grade) was obtained from Fisher Sci- 123
entific. Urea (ultra pure) was obtained from Invitrogen. 124
Acetonitrile (for HPLC, gas chromatography, pesticide 125
residue analysis, and spectrophotometry) was obtained 126
from Burdick & Jackson. Formic acid (puriss. pa for 127
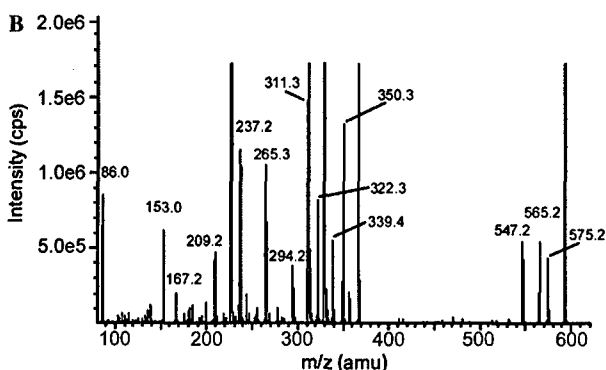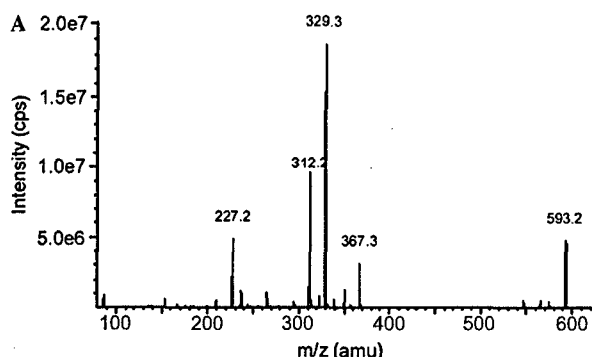mass spectrometry) was obtained from Fluka. 128

Fig. 2. Enhanced product ion spectrum for the CAD of free FP-biotin. FP-biotin, at 1 pmol/μl, was infused into the QTrap 2000 mass spectrometer at 1 μl/min using a Harvard syringe pump. A total of 20 scans on the products from the dissociation of the 593 ± 1 *m/z* parent ion were averaged. (A) Has a 10-fold larger *y* axis than (B).

Preparation of tryptic peptides from FP-biotinylated bovine trypsin

Approximately 3 mg bovine trypsin was dissolved in 10 ml of 50 mM ammonium bicarbonate buffer (pH 8.6). The concentration of the trypsin stock was determined to be 0.26 mg/ml (11 μM) by measuring the absorbance at 280 nm after diluting 200 μl into 1800 μl of 0.001 N HCl, where $A_{280} \times 0.70 =$ milligrams/milliliter trypsin [9]. Trypsin activity was measured in 50 mM Tris–Cl (pH 8.1) containing 11.5 mM calcium chloride and 0.33 mM TAME ($N\alpha$-p-toluene-sulfonyl-L-arginine methyl ester HCl) at 25 °C, and progress of the reaction was monitored spectrophotometrically at 247 nm [9,10]. Trypsin was labeled by mixing 130 μl of 170 μM FP-biotin (in water) with 1 ml of the stock trypsin to give 25 μM FP-biotin and 11 μM trypsin. FP-biotinylation caused the trypsin activity to decrease to 4% of its original level in 90 min.

Excess FP-biotin was removed by gel filtration over Sephadex G25 (5 × 1.5-cm column) in 50 mM ammonium bicarbonate (pH 8.6). FP-biotinylated trypsin appeared at the void volume, and fractions were identified by protein absorbance at 280 nm. Solid urea was added to the fractions containing the FP-biotinylated trypsin to give a final concentration of 8.2 M. Solid dithiothreitol was added to the urea-denatured protein to give a final concentration of 10 mM, and then the solution was incubated at 37 °C for 1 h. Solid iodoacetamide was added to the dithiothreitol-reduced protein to give a final concentration of 50 mM, and then the solution was incubated at 37 °C for 1 h in the dark. The reduced and alkylated protein solution was diluted with 50 mM ammonium bicarbonate (pH 8.6) to give a final urea concentration of 2 M. Sequencing-grade trypsin (5.2 μg) was added to the diluted FP-biotinylated trypsin (260 μg) to give a final ratio of sequencing-grade trypsin to FP-biotinylated trypsin of 1:50 (w/w). The mixture was incubated at 37 °C for 24 h. Aliquots of the digest, containing 1 nm bovine tryptic peptides, were dried in a Speedvac and stored at −20 °C. All glassware was rinsed with Milli-Q water (produced by a Milli-Q Plus system, Millipore), and Milli-Q water was used for all reagents.

Preparation of tryptic peptides from FP-biotinylated bovine serum albumin

Bovine serum albumin (218 μg) was dissolved in 436 μl of 50 mM ammonium bicarbonate buffer (pH 8.6) to give 50 mg/ml albumin. The albumin stock (39 μl) was mixed with 200 μl of 137 μM FP-biotin (freshly prepared in 50 mM ammonium bicarbonate buffer, pH 8.6) to give a solution containing 126 μM of each. This was incubated at 37 °C for 24 h. Then calcium chloride and bovine trypsin were added to give final concentrations of 6 mM calcium, 60 μM trypsin, 60 μM albumin, and 60 μM FP-biotin, all in 50 mM ammonium bicarbonate buffer (pH 8.6). The concentration of trypsin was chosen so that there would be enough trypsin to scavenge any excess FP-biotin that might be remaining after the labeling as well as to digest the albumin. The mixture was incubated at 37 °C overnight and then frozen at −70 °C. All glassware was muffle-oven cleaned, and the water for all reagents was freshly double distilled, to minimize keratin contamination.

This preparation is substantially different from that used to prepare the tryptic peptides, yet identifiable labeled peptides were produced by both methods. This demonstrates the robust nature of the characteristic fragment ion process for finding labeled peptides in a complex mixture.

Mass spectrometry of the tryptic digests

A FAMOS autosampler in conjunction with a SWITCHOS and ULTIMATE capillary liquid chromatography system (LC Packings Dionex) was used to deliver peptides to a QTrap hybrid quadrupole, linear ion trap mass spectrometer (Applied Biosystems). Samples were adjusted to a protein concentration of 1 μM, assuming no losses during handling (initial protein concentration 1 pmol/μl) with 5% acetonitrile/water containing 0.1% formic acid. Approximately 250 fmol of the digested bovine trypsin or 1200 fmol of the bovine serum albumin digest was loaded onto a micro-precolumn (PepMap C18 silica-based support, 5-μm particles with 100-Å pores, 300 μm i.d. × 5 mm long, LC Packings Dionex) and washed with 5% acetonitrile/water containing 0.1% formic acid for 5 min, at 20 μl/min, to remove salts. Peptides were eluted from the precolumn and partially resolved on a nanocolumn (218MS, C18 polymeric-silica support, with 300 Å pore size, 75 μm i.d. × 150 mm long, Grace-Vydac) using an acetonitrile gradient at 200 nl/min from 5 to 60% B over 30 min, and then to 80% B over 10 min, with washing and reequilibration at 5% B (A = 5% acetonitrile and 0.1% formic acid, B = 98% acetonitrile and 0.1% formic acid). Peptides were delivered directly from the nanocolumn to the mass spectrometer via a fused silica emitter (360 μm o.d., 20 μm i.d., 10 μm taper, New Objective) attached to a flow nanospray source. A total of 1500 V was applied to the emitter, and mass spectra were acquired throughout the chromatographic run. Information-dependent acquisition was used to collect an enhanced MS (+EMS) survey scan, followed by automatic enhanced resolution scans (+ER) and enhanced product ion (EPI or MS/MS) scans of the three most intense precursor ions, having a charge of 2+ to 4+, from each survey scan. Ions were excluded after two MS/MS spectra were acquired on each precursor. The collision cell was pressurized at 40 μTorr with pure nitrogen, and collision voltages of 20–35 V for each precursor were automatically determined, based on the

YABIO 7464

1 August 2005   Disk Used

ARTICLE IN PRESS

No. of Pages 11; DTD=5.0.1

Shankar (CE) / Selvi (TE)

Mass spectrometry of FP-biotin and FP-biotinylated peptides / L.M. Schopfer et al. / Anal. Biochem. xxx (2005) xxx–xxx   5

mass and charge of the precursor ion, by the Analyst software (Applied Biosystems) that drives the QTrap spectrometer. The spectrometer was calibrated biweekly on selected fragments from the CAD spectrum of [Glu]-fibrinopeptide B.

FP-biotin-labeled peptides were identified either online (from precursor ion scans) or offline (by extracted ion chromatographic analysis of the enhanced product ion scan data).

Mass spectrometry of free FP-biotin

FP-biotin was dissolved in methanol (HPLC grade, Sigma–Aldrich) and stored at $-70\,^\circ$C until used. The concentration of the FP-biotin stock was determined to be 170 µM by titration against an avidin–HABA complex, as described by Green [11].

The FP-biotin stock was diluted to 0.85 µM (0.85 pmol/µl), with 50% acetonitrile/water containing 0.1% formic acid, and was infused into the QTrap at 1 µl/min through a nanospray source (75 µm i.d. silicon emitter with 17 µm taper, New Objective) using a Harvard syringe pump. FP-biotin was fragmented by CAD using a collision voltage of 47 V, and enhanced product ion spectra were taken.

Results

The objective of this study was to identify characteristic fragments of FP-biotin that could serve as markers for the identification of FP-biotinylated peptides in proteolytic digests of labeled proteins. Chromatographic peaks identified as containing FP-biotinylated peptides could then be further analyzed by positive ion MS/MS to corroborate the presence of the FP-biotin label, to determine the sequence of the labeled peptide, to identify the labeling site, and to identify the protein that was labeled. To test this concept, we examined free FP-biotin and two FP-biotinylated protein models (bovine serum albumin and bovine trypsin). Only positive ion mass spectra were recorded. We chose the positive ion mode for two reasons. First, we expected the fused ring structure of biotin to be protonated in the mass spectrometer because it has a pK_a value of 4.66 [12,13] and the buffers for positive mode have a pH below 4 because they include 0.1% formic acid. Second, the positive mode provided the greatest sensitivity and the greatest ease of operation for peptide fragmentation and amino acid sequence determination.

Fragmentation of free FP-biotin

FP-biotin was infused into the mass spectrometer and subjected to CAD in the ion trap at a collision energy of 47 V. A signal was detected for the parent ion at 593.2 m/z.

Three prominent product ion signals were detected at 329.3, 312.2, and 227.2 m/z (Fig. 2A). Fig. 1 illustrates the fragments that correspond to these masses. In addition, a multitude of minor fragments were found (Figs. 1 and 2B). All fragments and the parent ion were singly charged $[M + H]^{+1}$. See Table 1 for a listing of fragment masses.

Fragmentation occurred at each of the amide linkages and at the phosphoester bond. Dehydration was detected for all fragments in which the 5–5 biotin ring system existed (593.2, 565.2, 329.3, 312.2, and 227.2 amu) but not for any other fragments. This suggests that the water is lost from that ring system. Although dehydration is commonly found with peptides [14,15], it is unlikely that the same mechanism is responsible for the dehydration that is occurring here. Deamination was detected for all fragments carrying a terminal amine (329.4, 339.4, and 367.3 amu) but not for other fragments. CAD-induced deamination at the N terminus has been described for peptides [14]. Finally, minor fragments detected at 167.2 and 153.0 amu were consistent with C–C cleavage in the linker arm nearest the phosphinate.

Tentative structural representations for the fragments and the relationship between fragments are outlined in Fig. 1. These structures are primarily intended to highlight the sites of cleavage. The cleavage products presented are isobaric with the observed masses but are not intended to be precise representations of the true products or to reflect the mechanism of cleavage. Some possible cleavage mechanisms are presented in the Discussion.

The three major fragments (227.2, 312.2, and 329.3 amu) are suitable for use as characteristic fragments of FP-biotin. In addition, there is a fourth fragment (591 amu) that is also suitable for use as a characteristic fragment. This fragment is derived from FP-biotinylated serine by β-elimination and is described in the next section.

FP-biotinylated trypsin

Bovine trypsin was FP-biotinylated, reduced with dithiothreitol, alkylated with iodoacetamide, and digested with porcine trypsin. Approximately 250 fmol of the resultant peptide mixture were subjected to LC–MS/MS. Ions separated in the first stage of the mass spectrometer were fragmented by CAD in the collision cell. These fragments were scanned in the second stage of the mass spectrometer for the presence of 591 m/z ions. A 591-amu target was selected because it is the expected mass for the singly charged β-elimination product from an FP-biotin-labeled serine, and serine was the residue expected to be labeled in trypsin. The mechanism of β-elimination is expanded on in the Discussion. A single peak from the total ion chromatogram (TIC) yielded a 591-m/z fragment (Fig. 3, precursor ion, 591 amu). This

YABIO 7464

ARTICLE IN PRESS

No. of Pages 11; DTD=5.0.1

1 August 2005   Disk Used

Shankar (CE) / Selvi (TE)

6   *Mass spectrometry of FP-biotin and FP-biotinylated peptides / L.M. Schopfer et al. / Anal. Biochem. xxx (2005) xxx–xxx*
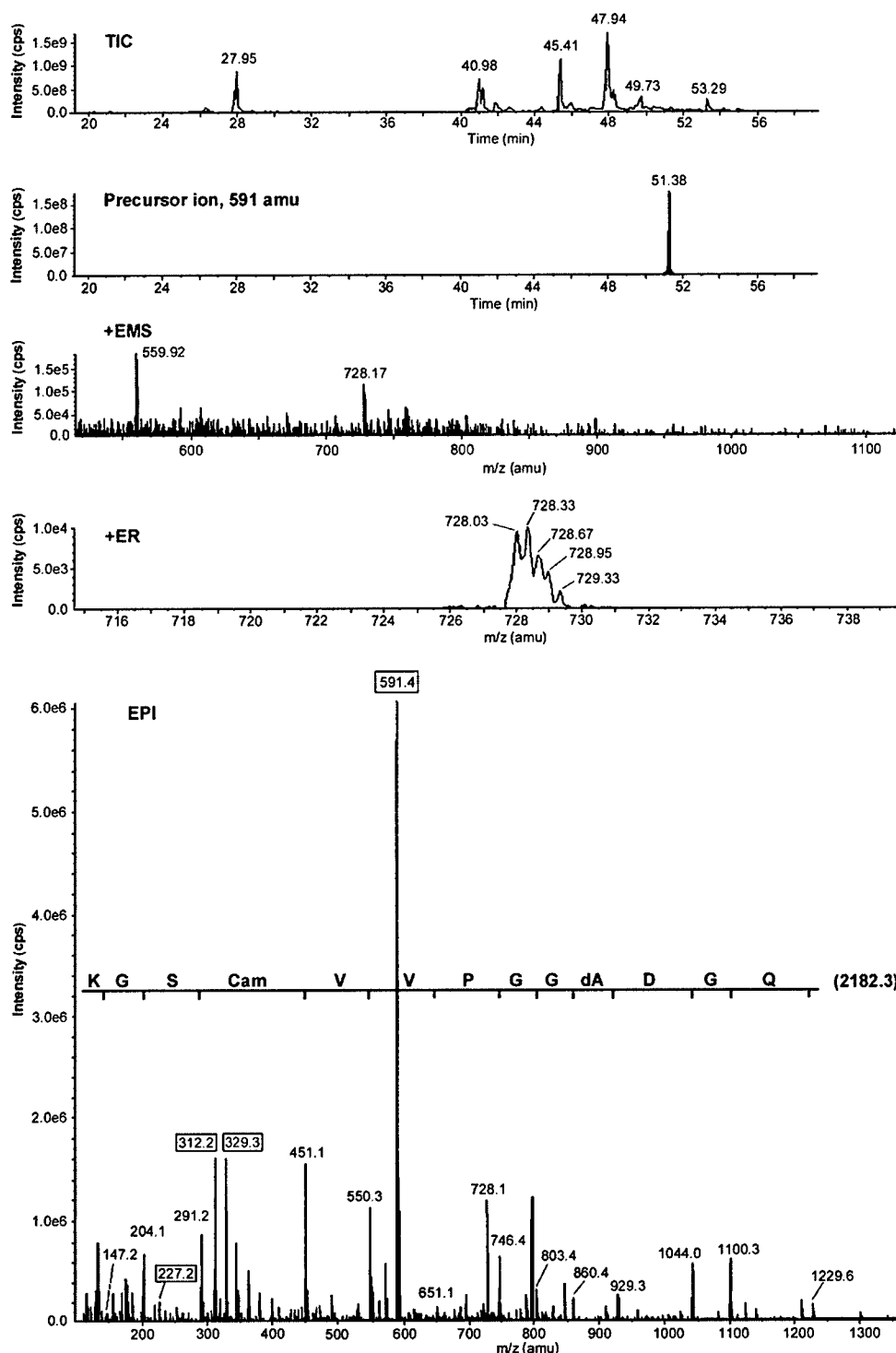

Fig. 3. An LC–MS/MS study of FP-biotinylated bovine trypsin. Approximately 250 fmol of a reduced and alkylated tryptic digest of FP-biotinylated bovine trypsin was separated by HPLC and injected into an Applied Biosystems quadrupole, linear ion trap mass spectrometer (QTrap 2000) in positive ion mode. The total ion chromatogram of the eluted peptides is shown in the panel labeled "TIC." A precursor ion survey scan was used to look for 591-amu fragments (panel labeled "precursor ion, 591 amu"). An enhanced mass spectral scan of the chromatographic peak that yielded the 591-amu ions (the 51.38-min peak) is shown in the panel labeled "+EMS." The triply charged state of the FP-biotinylated ion (728 *m/z*) was determined from an enhanced resolution scan (panel labeled "+ER"). An enhanced product ion scan of the CAD-induced fragmentation of the 728-*m/z* ion is shown in the panel labeled "EPI." The amino acid sequence of the biotinylated peptide, deduced from the marked peaks, is QGDdAGGPV VCamSGK, where dA stands for dehydroalanine and Cam stands for carbamidomethyl-cysteine. The numbers enclosed in boxes are the *m/z* values for the FP-biotin characteristic fragments.

YABIO 7464

ARTICLE IN PRESS

No. of Pages 11; DTD=5.0.1

1 August 2005   Disk Used

Shankar (CE) / Selvi (TE)

Mass spectrometry of FP-biotin and FP-biotinylated peptides / L.M. Schopfer et al. / Anal. Biochem. xxx (2005) xxx–xxx   7

339 peak eluted at 51.38 min. Two major parent ions, 559.9
340 and 728.2 *m/z*, appeared in the 51.38-min LC peak
341 (Fig. 3, +EMS). The 728.2-*m/z* ion was identified as the
342 FP-biotinylated peptide (Fig. 3, EPI). It was triply
343 charged (Fig. 3, +ER).

344 The EPI spectrum of the 728.2-*m/z* ion (Fig. 3, EPI)
345 yielded a 13-amino acid y-series sequence that corre-
346 sponded to residues 174 to 186 from a tryptic peptide of
347 bovine trypsin. This peptide included the catalytic serine
348 [16]. Reading from the N terminus, the sequence deter-
349 mined from the mass spectrum was QGDdAGGPV
350 VCamSGK, where dA stands for dehydroalanine and
351 Cam stands for carbamidomethyl-cysteine. The dehy-
352 droalanine is in the position expected for the catalytic
353 serine. β-Elimination of the FP-biotin label would be
354 expected to convert FP-biotinylated serine into dehydro-
355 alanine.

356 The EPI scan of the 728.2-*m/z* ion also showed four
357 characteristic ions for FP-biotin: 227.2, 312.2, 329.3, and
358 591.4 *m/z* (boxed values in Fig. 3, EPI).

359 Three residues (CSD) from the N terminus of the
360 tryptic peptide are not seen in the EPI scan. However,
361 they can be accounted for in the measured mass of the
362 triply charged parent ion at 728.1 *m/z*. This can be shown
363 by converting the measured mass of the triply charged
364 parent ion, $[M + 3H]^{+3} = 728.1$ *m/z*, to that of the singly
365 charged parent ion, $[M + H]^{+1} = 2182.3$ *m/z*, and sum-
366 ming all the mass contributions. The 2182.3 mass comes
367 from the 16 amino acids in the peptide, including the
368 missing CSD (1495.6) plus the 2 carbamidomethyl modi-
369 fications for the two cysteines (114) plus FP-biotinyla-
370 tion of serine (572.3). Fig. 4 illustrates the source of the
371 572.3-amu added mass on FP-biotinylation.

372 *FP-biotinylated serum albumin*

373 FP-biotinylated bovine serum albumin was digested
374 with trypsin without prior reduction or alkylation.
375 Approximately 1.2 pmol of the peptide mixture was sub-
376 jected to LC–MS/MS. Ions separated in the first stage of
377 the mass spectrometer were fragmented by CAD in the
378 linear ion trap. The masses of these product ion frag-
379 ments were determined in the second stage of the mass
380 spectrometer. An extracted ion chromatogram (XIC)

381 analysis of the product ions was made after the data
382 were collected. The 329-amu characteristic ion of FP-
383 biotin was used as the search criteria in the XIC because
384 this ion was expected to appear for both FP-biotinylated
385 serine (or threonine) and FP-biotinylated tyrosine. A
386 single peak from the TIC yielded intense 329-*m/z* frag-
387 ments (Fig. 5, XIC, 329 amu). This peak eluted at
388 23.54 min. Two major parent ions eluted in the 23.54-min
389 LC peak: 506.4 and 853.8 *m/z* (Fig. 5, +EMS). The 506.4-
390 *m/z* ion was identified as the FP-biotinylated peptide
391 (Fig. 5, EPI). It was doubly charged (Fig. 5, +ER).

392 The EPI spectrum of the 506.4-*m/z* ion (Fig. 5, EPI)
393 yielded a three-amino acid y-series sequence that corre-
394 sponded to residues 410 to 412 from the mature
395 sequence of bovine serum albumin [17]. This peptide
396 included a tyrosine but no serine. Reading from the N
397 terminus, the sequence was Y(FP-biotin)TR where the
398 tyrosine was FP-biotinylated. Peaks for Arg and ArgThr
399 are visible in the EPI spectrum at 175.1 and 276.2 amu.
400 The mass of the singly charged ArgThrTyr-FP-biotin is
401 1011.6 *m/z*, but this ion was not seen. A peak for the dou-
402 bly charged ArgThrTyr-FP-biotin was seen at 506.3 *m/z*.
403 The difference between 1011.6 of the parent ion and
404 276.2 of the ArgThr fragment is equal to the mass of a
405 singly charged, y-series N-terminal tyrosine covalently
406 bound to FP-biotin (163 + 572 = 735.4 amu), confirming
407 the sequence.

408 Because the albumin tryptic digest was prepared with-
409 out denaturation, it is possible to speculate that the FP-
410 biotinylated peptide arose from a noncovalent interac-
411 tion of FP-biotin with the YTR peptide. To address this
412 issue, it is necessary only to add the masses of the com-
413 ponents of the peptide—the dehydro mass of YTR
414 (420 amu) plus the mass of a water (18 amu) and a pro-
415 ton (1 amu)—to yield the mass of the positively charged
416 peptide plus the mass added on covalent reaction of FP-
417 biotin (unprotonated) with tyrosine (572 amu) (Fig. 4).
418 The total is equal to the measured mass of the singly
419 charged parent ion (1011 amu). If FP-biotin were nonco-
420 valently attached to the peptide, it would have contrib-
421 uted 592 amu to the complex and the singly charged
422 parent ion would have had a mass of 1031 amu instead
423 of 1011 amu.

424 The EPI spectrum of the 506.4-*m/z* ion also showed
425 three characteristic ions for FP-biotin: 227.0, 312.4, and
426 329.4 *m/z* (boxed values in Fig. 5, EPI). There was no evi-
427 dence at all of the 591-*m/z* ion characteristic of FP-bio-
428 tinylated serine. The absence of this 591 *m/z* is consistent
429 with a labeled tyrosine. This point is expanded on in the
430 Discussion.

431 Other major peaks in the EPI spectrum could be
432 assigned to the parent ion minus various fragments of
433 FP-biotin. These fragments were either singly or doubly
434 charged. There was a doublet of equal-amplitude peaks
435 at 682.3/683.3 *m/z* (labeled 682.3), which corresponded to
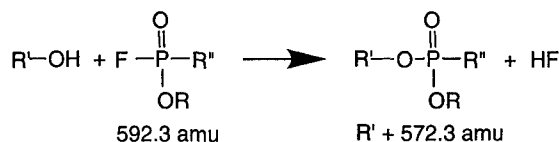436 the singly charged parent ion minus the 329-amu

Fig. 4. Scheme for FP-biotinylation of the active site serine of bovine trypsin. R represents ethyl, and R″ represents unprotonated biotin with a 17-atom spacer arm. Formation of the adduct results in the addition of the 592.3-amu mass of FP-biotin (unprotonated) and in the elimination of 20 amu in the form of HF, for a net increase in mass of the serine of 572.3 amu.
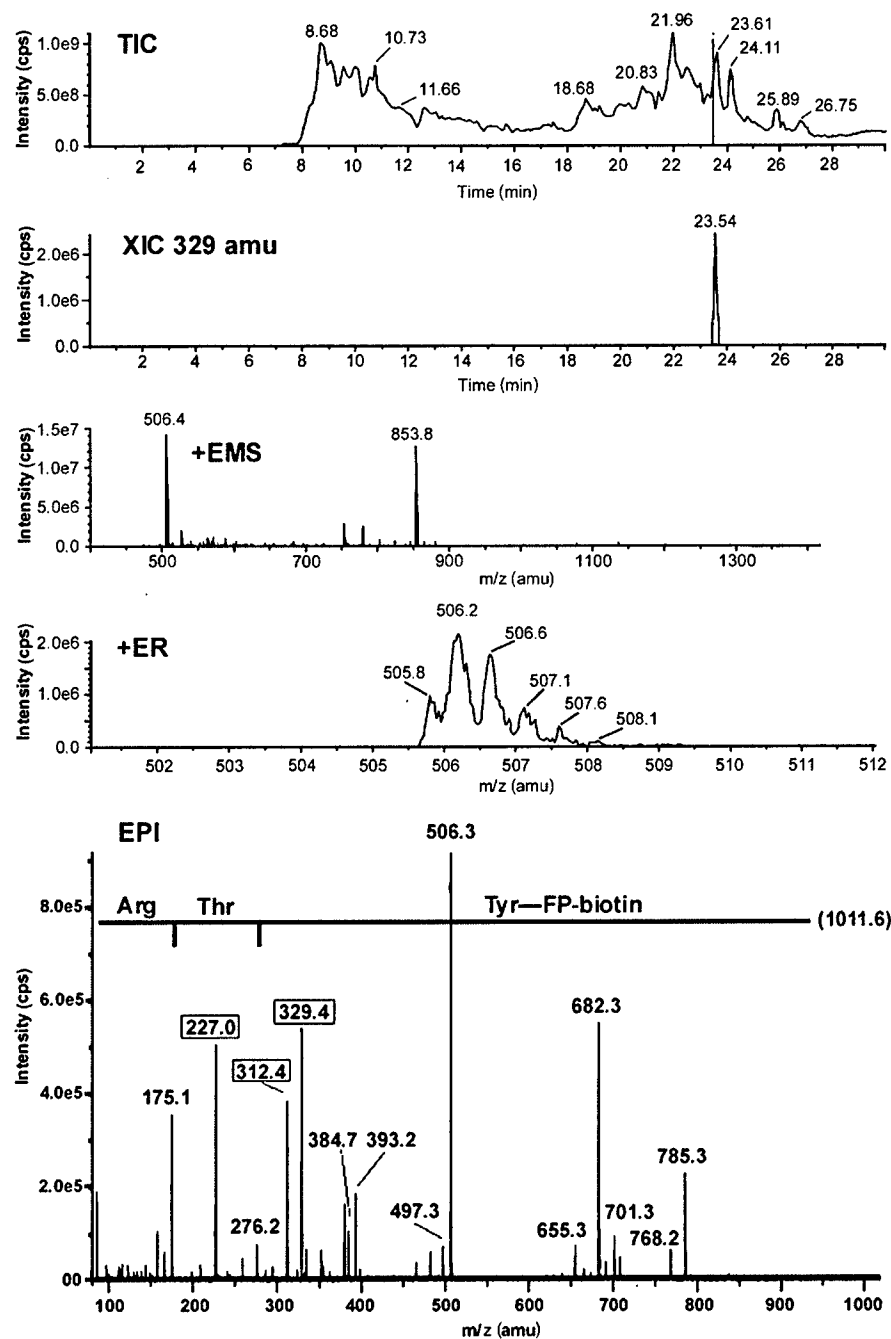
YABIO 7464

ARTICLE IN PRESS

No. of Pages 11; DTD=5.0.1

, 1 August 2005   Disk Used

Shankar (CE) / Selvi (TE)

8   *Mass spectrometry of FP-biotin and FP-biotinylated peptides / L.M. Schopfer et al. / Anal. Biochem. xxx (2005) xxx–xxx*

Fig. 5. An LC–MS/MS study of FP-biotinylated bovine serum albumin. Approximately 1200 fmol of a tryptic digest of FP-biotinylated serum albumin was separated by HPLC and injected into an Applied Biosystems quadrupole, linear ion trap mass spectrometer (QTrap 2000) in positive ion mode. The total ion chromatogram of the eluted peptides is shown in the panel labeled "TIC." After the data were collected, an extracted ion chromatography scheme was used to search the product ion data for 329-*m/z* fragments (panel labeled "XIC, 329 amu"). The panel labeled "+EMS" shows the ions in the chromatographic peak that yielded the 329-*m/z* fragments, eluting at 23.54 min. The peptide of interest had a mass of 506.2 *m/z*, and it was determined to be doubly charged from an enhanced resolution scan (panel labeled "+ER"). The enhanced product ion scan from the CAD fragments of the 506-*m/z* ion is shown in the panel labeled "EPI." The sequence of the FP-biotinylated peptide was TyrThrArg, where the Tyr was covalently attached to FP-biotin. The FP-biotinylated Tyr is Tyr410 of bovine albumin.

437 fragment of FP-biotin $[M + H - 329]^{+1}$ and to the singly
438 charged parent ion minus the 329-amu fragment of FP-
439 biotin plus a hydrogen $[M + 2H - 329]^{+1}$. The source of
440 the extra proton in the 683.3-*m/z* peak is unclear, but it

does not appear to be an artifact. A related doublet at 441
654.1/655.3 *m/z* (labeled 655.3) corresponded to the 682.3/ 442
683.3 pair of ions minus an additional 28 amu (a CO frag- 443
ment) $[M + H - 329 - 28]^{+1}$ and $[M + 2H - 329 - 28]^{+1}$. 444

YABIO 7464

ARTICLE IN PRESS

No. of Pages 11; DTD=5.0.1

1 August 2005   Disk Used

Shankar (CE) / Selvi (TE)

Mass spectrometry of FP-biotin and FP-biotinylated peptides / L. M. Schopfer et al. / Anal. Biochem. xxx (2005) xxx–xxx   9

445 The peak at 785.3 *m/z* corresponded to the singly
446 charged parent ion minus the 227-amu fragment of FP-
447 biotin plus a hydrogen $[M + 2H - 227]^{+1}$. The peak at
448 768.2 *m/z* corresponded to the 785.3-amu peak minus an
449 ammonia (17 amu) $[M + 2H - 227 - 17]^{+1}$. The peak at
450 701.3 *m/z* corresponded to the singly charged parent ion
451 minus the 312-amu fragment from FP-biotin plus a
452 hydrogen $[M + 2H - 312]^{+1}$. The 497.3-*m/z* fragment was
453 consistent with a loss of water from the doubly charged
454 parent ion at 506.3 *m/z* $[M + 2H - 18]^{+2}$. The 393.2-*m/z*
455 peak was consistent with loss of 227 amu from the dou-
456 bly charged parent ion plus a hydrogen
457 $[M + 3H - 227]^{+2}$. The 384.7-*m/z* peak was consistent
458 with a subsequent loss of water from this fragment
459 $[M + 3H - 227 - 18]^{+2}$. Many of the fragments include
460 the mass of an extra hydrogen, the source of which is
461 unclear.

462 **Discussion**

463 *Characteristic fragments from FP-biotin*

464   FP-biotin is an important new tool in the emerging
465 field of proteomics. It was designed as an activity-based,
466 protein-profiling probe for the serine hydrolase super-
467 family [1,2]. However, it has been found to react with
468 proteins that are not characteristic of that family, both
469 in vivo (serum albumin [4]) and in vitro (α-tubulin and
470 β-tubulin [L.M. Schopfer, unpublished results]). To bet-
471 ter understand the nature of the reactions of FP-biotin
472 with all of its target proteins, we have devised a method
473 for selecting the labeled peptide from a proteolytic mix-
474 ture of peptides. With this approach, we can identify the
475 labeled protein more definitively, determine the site of
476 labeling, and better ascertain the nature of the reaction
477 that has occurred.
478   This method is based on the identification of charac-
479 teristic fragments from FP-biotinylated peptides after
480 CAD in the mass spectrometer. In Fig. 2A, we demon-
481 strated that the free FP-biotin yields three prominent
482 characteristic fragments: 227, 312, and 329 amu. In addi-
483 tion, cleavage of the FP-biotin–serine adduct yielded a
484 characteristic fragment at 591.4 amu (Fig. 3, EPI).
485   The 591-amu fragment is attributable to a phospho-
486 nyl elimination product from FP-biotinylated serine.
487 This elimination is assumed to be analogous to phos-
488 phate elimination from phosphorylated serine, which
489 has been shown to be readily induced by CAD, in the
490 mass spectrometer [5–7]. Tholey et al. [18] showed that
491 phosphonylated serine does in fact undergo the same
492 facile elimination that phosphoserine exhibits. During
493 the phosphate elimination from phosphoserine, the P–
494 O–C bond is cleaved between the oxygen and the car-
495 bon. The elimination may proceed through a six-cen-
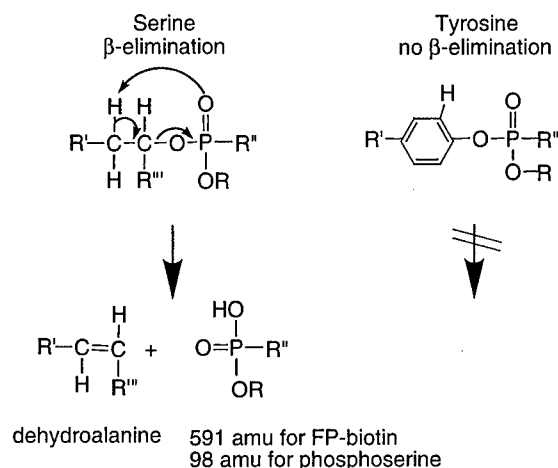496 tered cyclic intermediate and involve transfer of a proton

Fig. 6. Serine β-elimination. Phosphoserine or FP-biotinylated serine undergoes β-elimination in the collision cell of the mass spectrometer to yield dehydroalanine and characteristic ions (98 amu for phosphoserine, neutral; 591 amu for FP-biotinylated serine, positive). Neither phosphotyrosine nor FP-biotinylated tyrosine fragments in this way.

497 from the β-carbon of the alkyl to the oxygen of the phos-
498 phate with concomitant double bond formation between
499 the α- and β-carbons of the alkyl [18]. This process is
500 referred to as β-elimination and is illustrated in Fig. 6
501 under serine β-elimination, where R″ = OH and R = H.
502 For phosphoserine, this results in the release of a 98-amu
503 neutral phosphate and in the formation of dehydroala-
504 nine. For FP-biotinylated serine, β-elimination would
505 result in the release of a 591-amu oxidized form of FP-
506 biotin (protonated) and in the formation of dehydroala-
507 nine (Fig. 6, under serine β-elimination, where R″ = the
508 positively charged biotin plus the spacer arm and
509 R = CH₂CH₃). The 591-amu fragment is characteristic
510 of CAD fragmentation of FP-biotinylated serine (or
511 threonine). It is interesting to note that β-elimination of
512 the O-ethyl moiety from free FP-biotin also occurs,
513 resulting in the formation of ethylene (28 amu) (Figs. 1
514 and 2).
515   β-Elimination does not occur for phosphotyrosine
516 because the β-proton is attached to a phenyl ring and,
517 therefore, is energetically unavailable for transfer to the
518 oxygen (Fig. 6, under tyrosine). However, CAD of phos-
519 photyrosine can still cause cleavage of the P–O–C bond.
520 In this case, the cleavage happens between the oxygen
521 and the phosphorus [18]. This likely occurs along with
522 transfer of a proton from one of the hydroxyl ligands of
523 the phosphorus to the alkoxy-oxygen of the amino acid.
524 Cleavage of phosphotyrosine in this way results in the
525 release of an 80-amu neutral phosphorus fragment and
526 in the reformation of the tyrosine. Comparable reactions
527 occur for phosphoserine and phosphothreonine [7,19].
528 The equivalent reaction does not seem to occur for FP-
529 biotinylated tyrosine. With FP-biotin, there is an ethyl
530 group in the position equivalent to that proposed for the

YABIO 7464

1 August 2005   Disk Used

ARTICLE IN PRESS

No. of Pages 11; DTD=5.0.1

Shankar (CE) / Selvi (TE)

10   *Mass spectrometry of FP-biotin and FP-biotinylated peptides / L.M. Schopfer et al. / Anal. Biochem. xxx (2005) xxx–xxx*

531 mobile proton (Fig. 6, tyrosine, $R = CH_2CH_3$). Transfer
532 of the ethyl group to the leaving oxygen would generate
533 a 545-amu biotinylated-phosphorus fragment (proton-
534 ated) or a 467-amu peptide fragment (protonated). No
535 evidence of these fragments was detected in the EPI
536 spectrum of the FP-biotinylated peptide from serum
537 albumin, where tyrosine was labeled. Transfer of a pro-
538 ton from anywhere on the phosphinate to the leaving
539 oxygen would generate a 573-amu biotinylated-phos-
540 phorus fragment (protonated) or a 439-amu peptide
541 fragment (protonated). No evidence of these fragments
542 was detected either.
543   However, fragmentation of FP-biotin itself can still
544 occur while it is attached to the tyrosine peptide. Charac-
545 teristic fragments at 227, 312, and 329 amu were seen in
546 the EPI spectrum of the FP-biotinylated peptide from
547 serum albumin (Fig. 5, EPI). The 329-amu ion provided
548 a suitable means of identifying the FP-biotinylated pep-
549 tide (Fig. 5, XIC, 329 amu). XIC of the 227- and 312-amu
550 ions can also be used.
551   In summary, there are four useful marker ions for the
552 presence of FP-biotinylated peptides: 227, 312, 329, and
553 591 amu. All four may be expected to appear if the pep-
554 tide is FP-biotinylated on serine (and probably threo-
555 nine). However, the 591-amu marker will not appear if
556 the peptide is FP-biotinylated on tyrosine. These marker
557 ions make LC–MS/MS a useful method for locating FP-
558 biotinylated peptides during HPLC separation of com-
559 plex peptide mixtures.

560 *CAD fragmentation at the amide bonds*

561   CAD fragmentation at amide bonds is commonly
562 seen in peptides. The bond between the carbonyl carbon
563 and the amide nitrogen is frequently cleaved, resulting in
564 y- and b-series fragments. Several mechanisms to accom-
565 modate this cleavage have been proposed. The most
566 popular model proposes that the carbonyl oxygen (from
567 the amide on the N-terminal side of the bond to be
568 cleaved) attacks the carbonyl carbon of the target amide,
569 forming the five-membered cyclic intermediate oxazo-
570 lone. If the oxazolone is protonated, a b-ion results. If
571 the C-terminal product becomes protonated, a y-ion is
572 generated [20]. Alternatively, it has been proposed that
573 bond cleavage is initiated by attack from the amide
574 nitrogen, of the second amino acid to the N-terminal
575 side of the bond to be cleaved, on the carbonyl carbon of
576 the target amide to form a diketopiperazine ring struc-
577 ture [21]. A third proposal is that bond cleavage is initi-
578 ated by attack of the N-terminal nitrogen on the
579 carbonyl carbon to form a macrocycle [21,22].
580   Because FP-biotin carries two amide bonds, cleavage
581 could be initiated by attack of either the amide nitrogen
582 or the carbonyl oxygen from one amide on the carbonyl
583 carbon of the other amide. Attack by the amide nitrogen
584 would generate an 8-membered ring, whereas attack by

585 the carbonyl oxygen would generate a 10-membered
586 ring. It is not clear which of these possibilities is opera-
587 tive or whether an entirely different mechanism is
588 involved.

589 *Organophosphate-reactive residue in serum albumin*

590   In the course of this work, we determined that Tyr410
591 from bovine serum albumin is labeled by FP-biotin. San-
592 ger was the first to address the issue of which peptide in
593 serum albumin was labeled by organophosphates [8].
594 They used high-voltage paper ionophoresis to demon-
595 strate that a tyrosine in human, bovine, and rabbit serum
596 albumins was labeled by [^{32}P]diisopropylfluorophos-
597 phate. They further showed that the sequence of the
598 labeled peptide in humans and rabbits was Arg-Tyr-Thr-
599 Lys, whereas that in bovine was Arg-Tyr-Thr-Arg [8].
600 Sanger reported his findings in the Pedler Lecture before
601 the Chemical Society in London in 1962. At that time, he
602 referred to a publication by Shaw that was "in press."
603 That publication does not seem to have ever appeared.
604 During the succeeding 40 years, considerable interest
605 was given to this organophosphate reactive tyrosine on
606 serum albumin, but the identity of the reactive residue
607 was never reexamined. All discussion about its identity
608 referred to the Sanger lecture. We have confirmed the
609 accuracy of Sanger's original report. Using modern mass
610 spectral techniques, we showed that the labeled residue
611 in bovine serum albumin is Tyr410 from a Tyr-Thr-Arg
612 peptide. The homologous residue in human serum albu-
613 min would be Tyr411.

614 *XIC analysis*

615   To identify the FP-biotinylated peptide from serum
616 albumin, it was necessary to mine the EPI data from the
617 LC–MS/MS using the XIC technique. Using a precursor
618 ion scan as the survey scan for the IDA method did not
619 directly reveal the labeled peptide in LC–MS/MS data.
620 Better results were obtained from XIC because the EPI
621 data were taken with the linear ion trap feature of the
622 QTrap 2000, whereas the precursor ion scans used only
623 the quadrupole elements. We found approximately a 10-
624 fold increase in sensitivity for EPI data over those
625 obtained from precursor ions. The only disadvantage of
626 the XIC analysis is that it must be made offline after the
627 data have been fully collected.

628 *Potential application*

629   Organophosphorus esters are used as pesticides and
630 chemical nerve agents. The acute toxicity of these agents
631 is due to inhibition of acetylcholinesterase [23,24]. How-
632 ever, symptoms that result in chronic disability after
633 low-dose exposure cannot be explained by inhibition of
634 acetylcholinesterase alone. Other proteins have also been

YABIO 7464

ARTICLE IN PRESS

No. of Pages 11; DTD=5.0.1

9 August 2005   Disk Used

Shankar (CE) / Selvi (TE)

Mass spectrometry of FP-biotin and FP-biotinylated peptides | L.M. Schopfer et al. | Anal. Biochem. xxx (2005) xxx–xxx   11

635 demonstrated to bind organophosphorus agents in liv-
636 ing animals or humans: butyrylcholinesterase, carboxy-
637 lesterase, acyl peptide hydrolase, albumin, fatty acid
638 amide hydrolase, neuropathy target esterase, cannabi-
639 noid CB1 receptor, arylformamidase, and M2 musca-
640 rinic receptor [4,25–28]. Use of a biotinylated
641 organophosphorus agent, such as FP-biotin, combined
642 with mass spectrometry is expected to facilitate identifi-
643 cation of other modified proteins in living animals. This
644 information is expected to provide new biomarkers of
645 exposure and perhaps lead to an understanding of why
646 some people become chronically ill after an exposure
647 that has no effect on the majority of people.
648 From the previous paragraph, it seems clear that
649 organophosphates can label proteins other than those of
650 the serine hydrolase superfamily. As such, the general
651 use of FP-biotin as an activity-based protein profiling
652 technique for the serine hydrolase superfamily may
653 require further studies.

654 **Acknowledgments**

667 **References**

668 [1] Y. Liu, M.P. Patricelli, B.F. Cravatt, Activity-based protein profil-
669   ing: the serine hydrolases, Proc. Natl. Acad. Sci. USA 96 (1999)
670   14694–14699.
671 [2] D. Kidd, Y. Liu, B.F. Cravatt, Profiling serine hydrolase activities
672   in complex proteomes, Biochemistry 40 (2001) 4005–4015.
673 [3] L.M. Schopfer, T. Voelker, C.F. Bartels, C.M. Thompson, O.
674   Lockridge, Reaction kinetics of biotinylated organophosphorus
675   toxicant, FP-biotin, with human acetylcholinesterase and human
676   butyrylcholinesterase, Chem. Res. Toxicol. 18 (2005) 747–754.
677 [4] E.S. Peeples, L.M. Schopfer, E.G. Duysen, R. Spaulding, T. Voel-
678   ker, C.M. Thompson, O. Lockridge, Albumin, a new biomarker of
679   organophosphorus toxicant exposure, identified by mass spec-
680   trometry, Toxicol. Sci. 83 (2005) 303–312.
681 [5] F. Zappacosta, M.J. Huddleston, R.L. Karcher, V.I. Gelfand, S.A.
682   Carr, R.S. Annan, Improved sensitivity for phosphopeptide map-
683   ping using capillary column HPLC and microionspray mass spec-
684   trometry: comparative phosphorylation site mapping from gel-
685   derived proteins, Anal. Chem. 74 (2002) 3221–3231.
686 [6] G. Neubauer, M. Mann, Mapping of phosphorylation sites of gel-
687   isolated proteins by nanoelectrospray tandem mass spectrometry:
688   Potentials and limitations, Anal. Chem. 71 (1999) 235–242.

689 [7] M.J. Huddleston, R.S. Annan, M.F. Bean, S.A. Carr, Selective
690   detection of phosphopeptides in complex mixtures by electrospray
691   liquid chromatography/mass spectrometry, J. Am. Soc. Mass
692   Spectrom. 4 (1993) 710–717.
693 [8] F. Sanger, Amino-acid sequences in the active centres of certain
694   enzymes, Proc. Chem. Soc. 5 (1963) 76–83.
695 [9] C.C. Worthington, Worthington Enzyme Manual: Enzymes and
696   Related Biochemicals, Worthington Biochemical Corporation,
697   Freehold, NJ, 1988.
698 [10] B.C.W. Hummel, A modified spectrophotometric determination
699   of chymotrypsin, trypsin, and thrombin, Can. J. Biochem. Physiol.
700   37 (1959) 1393–1399.
701 [11] N.M. Green, A spectrophotometric assay for avidin and biotin
702   based on binding of dyes by avidin, Biochem. J. 94 (1965) c23–c24.
703 [12] R. Barbucci, A. Magnani, C. Roncolini, S. Silvestri, Antigen–anti-
704   body recognition by Fourier transform IR spectroscopy/attenu-
705   ated total reflection studies: biotin–avidin complex as an example,
706   Biopolymers 31 (2004) 827–834.
707 [13] D.C. Fry, T. Fox, M.D. Lane, A.S. Mildvan, NMR studies of the
708   exchange of the amide protons of d-biotin and its derivatives,
709   Ann. NY Acad. Sci. 447 (1985) 140–151.
710 [14] R.A.J. O'Hair, The role of nucleophile–electrophile interactions in
711   the unimolecular and bimolecular gas-phase ion chemistry of pep-
712   tides and related systems, J. Mass Spectrom. 35 (2000) 1377–1381.
713 [15] K.D. Ballard, S.J. Gaskell, Dehydration of peptide [M + H]⁺ ions
714   in the gas phase, J. Am. Soc. Mass Spectrom. 4 (1993) 477–481.
715 [16] O. Mikes, V. Holeysovsky, V. Tomasek, F. Sorm, Covalent struc-
716   ture of bovine trypsinogen: the position of the remaining amides,
717   Biochem. Biophys. Res. Commun. 24 (1966) 346–352.
718 [17] K. Hirayama, S. Akashi, M. Furuya, K. Fukuhara, Rapid confir-
719   mation and revision of the primary structure of bovine serum
720   albumin by ESIMS and FRIT-FAB LC/MS, Biochem. Biophys.
721   Res. Commun. 173 (1990) 639–646.
722 [18] A. Tholey, J. Reed, W.D. Lehmann, Electrospray tandem mass
723   spectrometric studies of phosphopeptides and phosphopeptide
724   analogues, J. Mass Spectrom. 34 (1999) 117–123.
725 [19] M. Quadroni, P. James, Phosphopeptide analysis, EXS 88 (2000)
726   199–213.
727 [20] A. Schlosser, W.D. Lehmann, Five-membered ring formation in
728   unimolecular reactions of peptides: a key structural element con-
729   trolling low-energy collision-induced dissociation of peptides, J.
730   Mass Spectrom. 35 (2000) 1382–1390.
731 [21] M.J. Polce, D. Ren, C. Wesdemiotis, Dissociation of the peptide
732   bond in protonated peptides, J. Mass Spectrom. 35 (2000) 1391–
733   1398.
734 [22] X-J. Tang, P. Thibault, R.K. Boyd, Fragmentation reactions of
735   multiply-protonated peptides and implications for sequencing by
736   tandem mass spectrometry with low-energy collision-induced dis-
737   sociation, Anal. Chem. 65 (1993) 2824–2834.
738 [23] J.H. McDonough Jr., T.M. Shih, Neuropharmacological mecha-
739   nisms of nerve agent-induced seizure and neuropathology, Neuro-
740   sci. Biobehav. Rev. 21 (1997) 559–579.
741 [24] C.N. Pope, Organophosphorus pesticides: Do they all have the
742   same mechanism of toxicity? J. Toxicol. Environ. Health B Crit.
743   Rev. 2 (1999) 161–181.
744 [25] D.E. Ray, P.G. Richards, The potential for toxic effects of chronic,
745   low-dose exposure to organophosphates, Toxicol. Lett. 120 (2001)
746   343–351.
747 [26] P. Glynn, NTE: One target protein for different toxic syndromes
748   with distinct mechanisms? Bioessays 25 (2003) 742–745.
749 [27] P.J. Lein, A.D. Fryer, Organophosphorus insecticides induce air-
750   way hyperreactivity by decreasing neuronal M2 muscarinic recep-
751   tor function independent of acetylcholinesterase inhibition,
752   Toxicol. Sci. 83 (2005) 166–176.
753 [28] J.E. Casida, G.B. Quistad, Organophosphate toxicology: Safety
754   aspects of nonacetylcholinesterase secondary targets, Chem. Res.
755   Toxicol. 17 (2004) 983–998.

Reaction Kinetics of Biotinylated Organophosphorus Toxicant, FP-biotin, with Human Acetylcholinesterase and Human Butyrylcholinesterase

Lawrence M. Schopfer,*,† Troy Voelker,‡ Cynthia F. Bartels,†
Charles M. Thompson,‡ and Oksana Lockridge†

*Eppley Institute, University of Nebraska Medical Center, Omaha, Nebraska 68198-6805, and
Department of Biomedical and Pharmaceutical Sciences, University of Montana,
Missoula, Montana 59812*

A biotinylated organophosphate could be useful for identifying proteins that react with organophosphorus toxicants (OP). FP-biotin, 10-(fluoroethoxyphosphinyl)-N-(biotinamidopentyl)decanamide, was synthesized and found to be stable in methanol and chloroform but less stable in water. Because acetylcholinesterase (AChE, EC 3.1.1.7) and butyrylcholinesterase (BChE, EC 3.1.1.8) are known to be sensitive targets of OP, their reactivity with FP-biotin was tested. The rate constant for reaction with human AChE was 1.8×10^7 M^{-1} min^{-1}, and for human BChE, it was 1.6×10^8 M^{-1} min^{-1}. A phosphorus stereoisomer, constituting about 50% of the FP-biotin preparation, appeared to be the reactive species. The binding affinity was estimated to be >85 nM for AChE and >5.8 nM for BChE. It was concluded that FP-biotin is a potent OP, well-suited for searching for new biomarkers of OP exposure.

Introduction

It is generally accepted that the toxicity of organophosphorus toxicants (OP)[1] is due to a cascade of reactions that begins with inhibition of acetylcholinesterase (AChE) (*1*). Following inhibition of AChE, excess acetylcholine accumulates in nerve synapses. The excess acetylcholine overstimulates receptors. This causes an imbalance in the nervous system that leads to seizures and respiratory arrest (*2*).

AChE is not the only enzyme that is covalently modified by OP. In humans, a second enzyme that is highly reactive with OP is butyrylcholinesterase (BChE). Inhibition of BChE has no known adverse consequences. Pesticide applicators whose plasma BChE activity is inhibited up to 50% have no clinical signs of poisoning (*3*).

A third enzyme that is known to react with OP in vivo is neuropathy target esterase (*4*). Neuropathy target esterase reacts only with certain OP and does not react with nerve agents or with licensed pesticides. Inhibition of neuropathy target esterase leads to peripheral neuropathy affecting mainly the legs. More than 30 000 people became paralyzed in two separate incidents, one in 1930 and one in 1959, after drinking beverages or using cooking oil contaminated with tri-o-tolyl phosphate (*5*).

No other enzymes or proteins have been demonstrated to covalently bind OP in people exposed to OP (*6*). In vivo

studies in rodents have identified three additional proteins that bind OP: carboxylesterase (*7, 8*), acylpeptide hydrolase (*9*), and albumin (*10*). Experiments with isolated tissues and purified enzymes have identified many additional OP-binding proteins (*1, 6, 11–13*), but it is not known whether these proteins react with OP in living humans or animals.

Toxicological observations suggest that OP have other biological actions in addition to their cholinesterase inhibitory properties (*6, 14–17*). For example, they react with the acetylcholine receptor, they reduce nerve growth factor levels, and they induce developmental neurotoxicity and airway hyperreactivity (*6, 15*). Certain OP induce delayed peripheral neuropathy (*6*). OP function as teratogens in birds by inhibiting kynurenine formamidase (*6*). Each OP reacts preferentially with a set of proteins, and the set of OP reactive proteins is not completely identical for each OP (*6, 18*). These noncholinesterase OP reactive proteins could provide new biomarkers of OP exposure. To search for noncholinesterase biomarkers, we plan to inject a biotin-tagged OP called 10-(fluoroethoxyphosphinyl)-N-(biotinamidopentyl)decanamide (FP-biotin) into mice. The biotin tag will facilitate isolation and visualization of OP reactive proteins (*19, 20*).

To date, rat tissues treated in vitro with FP-biotin have allowed identification of seven FP-biotinylated proteins by mass spectroscopy, but none of these was AChE or BChE (*19, 20*). Because FP-biotin has a larger structure than most organophosphorus pesticides and nerve agents and because the affinity of a particular OP for a protein depends on the chemical, stereochemical, and physical complimentarity between the target protein and the OP, it is conceivable that failure to detect AChE and BChE was due to lack of reaction with FP-biotin. In view of the central role played by AChE in OP toxicity and the

---

* To whom correspondence should be addressed. Tel: 402-559-6014. Fax: 402-559-4651. E-mail: lmschopf@unmc.edu.
† University of Nebraska Medical Center.
‡ University of Montana.
[1] Abbreviations: BChE, butyrylcholinesterase; AChE, acetylcholinesterase; DTNB, 5,5′-dithiobis(2-nitrobenzoic acid); HABA, 4-hydroxy azobenzene-2-carboxylic acid; OP, organophosphorus toxicants; FP-biotin, 10-(fluoroethoxyphosphinyl)-N-(biotinamidopentyl)decanamide; TAME, Na-*p*-toluene-sulfonyl-L-arginine methyl ester HCl.
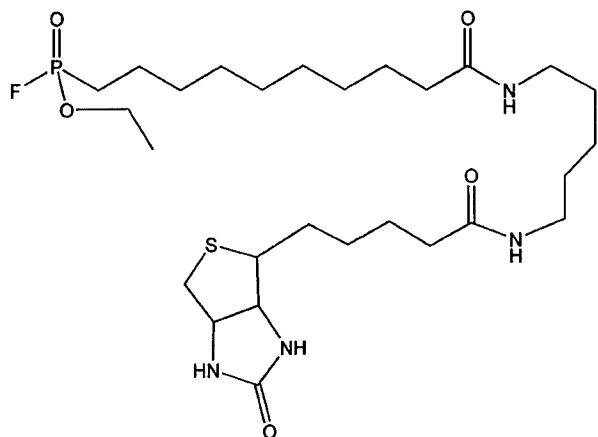
Figure 1. FP-biotin structure. The OP has a reactive phosphonofluoridate group tethered to biotin via a spacer arm. The phosphorus is astereoisomeric center.

complimentary role of BChE, it is important to determine the reactivity of FP-biotin with these enzymes. From the large size of FP-biotin, one might predict that it would be slow to react. Unexpectedly, we found that FP-biotin reacted with AChE and BChE very rapidly, at rates that were comparable to the rates of reaction with nerve agents. Failure to identify FP-biotinylated AChE and BChE in rat tissues (*19, 20*) must therefore be attributed to low levels of these proteins in those tissues.

Materials and Methods

Synthesis of FP-biotin. Troy Voelker, in Dr. Thompson's laboratory, synthesized and purified 15.5 mg of FP-biotin. See Figure 1 for the structure of FP-biotin. The steps in the synthesis of FP-biotin followed the procedure of Liu et al. (*19*). The overall yield for the multistep synthesis was 6%. FP-biotin was purified by washing the crystals sequentially with diethyl ether and ethyl acetate. The identity of the biotinylated OP and of the intermediates was confirmed by ^{1}H, ^{13}C, and ^{31}P NMR, absorbance spectra in the UV–vis wavelength range, and combustion analysis. Phosphorus NMR in chloroform showed a doublet (36.0 and 29.3 ppm from H_3PO_4), a result consistent with P–F coupling. The doublet is the result of fluorine splitting with $J = 1069$ Hz. Mass spectrometry (TOF MS ES+) showed that FP-biotin had a mass-to-charge ratio of 593.5 (*m/z*). The expected *m/z* for FP-biotin, $C_{27}FH_{50}N_4O_5PS + H^+$, is 593.3. There was a peak at 297.3 (*m/z*), i.e., 1/2 of the major peak, and at 615.6 (*m/z*), i.e., the major peak plus one sodium. No evidence for contamination was detected by NMR and mass spectrometry.

Storage of FP-biotin. Lyophilized FP-biotin was stored dry, in quantities of 3–8 mg, at −20 °C, in sealed glass ampules. Prior to use, a portion was dissolved in a small volume of solvent, (chloroform from Fisher, HPLC grade; or methanol from either EM Science, HPLC grade; or Sequemat, sequencing grade), divided into aliquots, and dried under vacuum in a Speedvac. The aliquots were in Pyrex tubes that had been cleaned in a muffle oven. The dried aliquots were returned to storage at −20 °C. Although high quality solvents were used to make the aliquots, those prepared in methanol became partly degraded. Fluorine was lost from the phosphorus, as indicated by the appearance of a new singlet in the phosphorus NMR. Aliquots redissolved in methanol (and not dried) remained stable for months at −20 °C, suggesting that degradation occurred during vacuum drying and not during storage in methanol. When aliquots were made in chloroform, no degradation was found.

AChE and BChE. Wild-type human AChE was secreted by CHO K1 cells into serum free culture medium and purified by affinity chromatography on procainamide-Sepharose. Wild-type

human BChE was purified from human plasma by ion exchange chromatography at pH 4.0, followed by affinity chromatography on procainamide-Sepharose and ion exchange chromatography at pH 7.5 (*21*).

Rate Constant for Inhibition of Human AChE by FP-biotin. The kinetics for inhibition of purified human AChE by FP-biotin were studied in 0.1 M potassium phosphate buffer, pH 7.0, at 25 °C. Bovine serum albumin (BSA), normally included to stabilize AChE, was omitted because it reduced the apparent first-order inhibition constant measured with FP-biotin. This reduction in apparent rate constant results from noncovalent binding of FP-biotin to BSA and consequent reduction in the concentration of FP-biotin free in solution. Although FP-biotin reacts covalently with BSA (*10*), preliminary experiments indicate that the rate constant is orders of magnitude slower than those measured here for BChE and AChE (data not shown). Inhibition of AChE was initiated by mixing 0.17 nM of highly purified human AChE with various amounts of FP-biotin, in 2 mL of potassium phosphate buffer. The FP-biotin stock solution was in 10% methanol and 90% water. At defined times, a 10 μL aliquot was assayed for residual AChE activity with 1.0 mM acetylthiocholine and 0.5 mM dithiobis-2-nitrobenzoic acid (DTNB) in 0.1 M potassium phosphate buffer, pH 7.0, at 25 °C (*22*). Dilution and the introduction of excess substrate were used to stop the covalent inhibition process and reverse noncovalent inhibition. This simple procedure was sufficient as judged by the fact that plots of activity vs time of inhibition when extrapolated to time zero gave the uninhibited rate (*23*).

The apparent first-order rate constant for inhibition (at each FP-biotin concentration) was measured from a semilog plot of residual enzyme activity (measured as change in absorbance at 412 nm per minute, i.e., $\Delta A412$/min) vs time of incubation with the inhibitor (see the inset to Figure 7). Plots were linear for at least 90% of the reaction. Data from the linear portion of the plots were fit to a first-order expression using SigmaPlot (version 4.16 Jandel) in order to obtain apparent first-order rate constants (k_{app}).

The apparent second-order rate constant for inhibition was measured from the slope of the plot of k_{app} vs concentration of FP-biotin (see Figure 7). This second-order value should be considered apparent since it is most likely a ratio of the true, first-order, covalent reaction, rate constant divided by the K_i for the noncovalent binding of FP-biotin to the enzyme (*24*). Concentrations of FP-biotin ranging from 4.3 to 85 nM were used in these studies.

Rate Constant for Inhibition of Human BChE by FP-biotin. Kinetics for the inhibition of human BChE by FP-biotin were studied in 0.1 M potassium phosphate buffer, pH 7.0, at 25 °C. Wild-type human BChE (0.35 nM) was incubated with various amounts of FP-biotin for defined times, in 2 mL of potassium phosphate buffer. Inhibition was stopped by diluting a 10 μL aliquot 300-fold into a mixture containing 1 mM butyrylthiocholine and 0.5 mM DTNB for determination of residual BChE activity (*22*). Concentrations of FP-biotin ranged from 0.73 to 5.8 nM.

Rate Constants for Inhibition of Human BChE and AChE by Diazoxon. The second-order rate constants for inhibition of human AChE and BChE by diazoxon were determined as described for FP-biotin. Diazoxon was from Chem Service, Inc. (West Chester, PA). Diazoxon was dissolved in methanol and stored at −70 °C. Working solutions were in pH 7 buffer. Diazoxon was unstable in water but stable in buffer. Overnight incubation in water at room temperature resulted in complete hydrolysis of diazoxon. In contrast, when diazoxon was incubated in buffer at pH 7.1, the diazoxon was still 30% intact after 5 days at room temperature.

Western Blot. FP-biotin-inhibited BChE and AChE were applied to an SDS polyacrylamide gel, within 1 h of inhibition. After electrophoreses, the proteins were transferred to PVDF membrane. To detect the biotin, the membrane was treated with an avidin-horseradish peroxidase conjugate (BioRad) and then with a chemiluminescent reagent (LumiGLO from Kirkeg-

aard & Perry) to visualize horseradish peroxidase activity. Emitted light was detected using X-ray film.

Substoichiometric Reaction of BChE with FP-biotin. FP-biotin (0.11–0.78 μM) dissolved in water was mixed with BChE (0.61 μM), in a total volume of 100 μL of 0.1 M potassium phosphate buffer, pH 7.0, at 25 °C. Inhibition reached completion during the mixing time, and the remaining activity was stable for at least an hour. The amount of active BChE remaining after inhibition was determined by adding a 10 μL portion of the reaction mixture to 3 mL of 0.1 M potassium phosphate buffer, pH 7.0, containing 0.5 mM DTNB and 1 mM butyrylthiocholine, at 25 °C. Hydrolysis of the butyrylthiocholine was followed by the absorbance increase at 412 nm (22). The concentration of BChE in the reaction mixture was calculated from the activity of an uninhibited sample, where 720 units/mL is 1 mg/mL of BChE or 11.7 nmol per mL. A unit of activity is defined as μmol of butyrylthiocholine hydrolyzed per min. The concentration of FP-biotin was determined by a combination of biotin titration and ^{31}P NMR.

Concentration of FP-biotin. The total concentration of biotin in the FP-biotin preparation was determined by titration against an avidin/4-hydroxy azobenzene-2-carboxylic acid (HABA) complex as described by Green (25). The biotin concentration measured both the intact FP-biotin and its hydrolysis product. Both HABA and avidin were from Sigma. The fraction of the preparation containing intact FP-biotin was determined by ^{31}P NMR. The total concentration of biotin and the nonhydrolyzed fraction of FP-biotin were used to calculate the concentration of intact FP-biotin.

^{31}P NMR. ^{31}P NMR data, for samples containing 120–130 μM FP-biotin (total concentration of hydrolyzed and nonhydrolyzed), were collected on a 500 MHz spectrometer (Varian INOVA), over 16 h, at 25 °C in either deuterated chloroform (CDCl$_3$, 99.% atom D from Acros Organics) or water plus 10% deuterium oxide (D$_2$O, 99.5% atom D from Acros Organics). Signals were proton decoupled. The repetition rate was 5 s. Peak positions were measured relative to 85% phosphoric acid at 0.0 ppm. Linear prediction was used in all experiments to flatten the baseline and improve signal quality. Data were collected by Paul Keifer at the NMR Core Facility at the University of Nebraska Medical Center.

Trypsin Activity Assay. Steady state turnover of trypsin was measured in 3 mL of 50 mM Tris/Cl, pH 8.1, containing 11.5 mM CaCl$_2$ and 0.33 mM TAME (Na-p-toluene-sulfonyl-L-arginine methyl ester HCl from Sigma) at 25 °C. Hydrolysis of TAME was monitored at 247 nm using an extinction coefficient of 540 M^{-1} cm^{-1}.

Inhibition Potency of the Other Isomer of FP-biotin. The assumption in this experiment was that FP-biotin was a mixture of stereoisomers and that one isomer preferentially reacted with BChE. We wanted to know whether the other isomer could react with trypsin or with other proteins. Trypsin was chosen specifically because its catalytic triad is the mirror image of that in AChE and BChE (26). An FP-biotin solution was depleted of the BChE reactive isomer. Then, trypsin was added and trypsin activity was tested at timed intervals.

In a second approach, 5.1 nmol of FP-biotin were depleted of BChE reactive isomer by reaction with 5.1 nmol of BChE. After 1 h, the mixture was spun through a 30 000 MW cutoff filter to separate residual FP-biotin from FP-biotin bound to BChE. The residual FP-biotin was reacted with mouse brain homogenate for 5 h. The positive control was the reaction of FP-biotin with mouse brain homogenate. Samples were boiled in SDS gel loading buffer and loaded on a 10–20% polyacrylamide SDS gel, at 30 μg of mouse brain protein per lane. After electrophoresis and transfer of proteins to PVDF membrane, the biotin was visualized by reaction with StreptAvidin Alexa 680 (Molecular Probes, Eugene, OR). Fluorescence emission at 700 nm was recorded on an Odyssey flat bed scanner (Li-COR, Lincoln, NE). The amount of FP-biotin in the 30 000 MW cutoff filtrate was quantified with avidin/HABA to be sure that the expected amount was actually present.
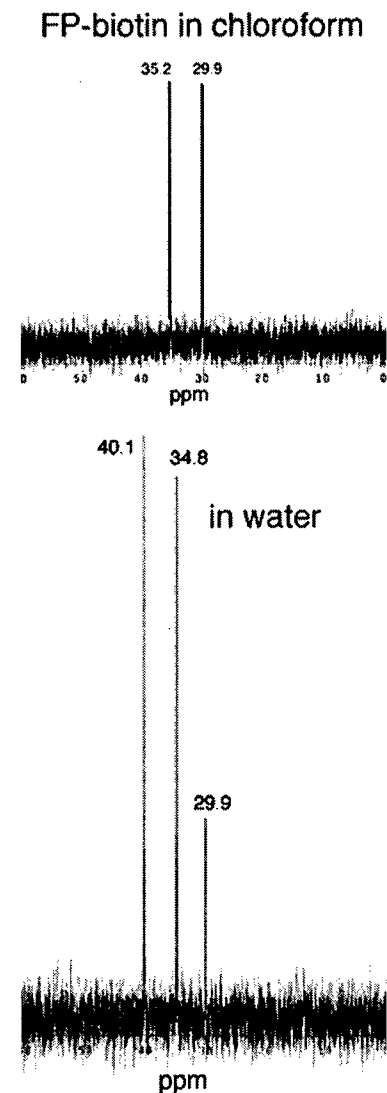

Figure 2. ^{31}P NMR of FP-biotin dissolved in chloroform and in water. Data collection was for 16 h at 25 °C. The FP-biotin in chloroform remained intact, but the FP-biotin in water degraded about 13%.

Results

Concentration of FP-biotin. The concentration of FP-biotin as determined by titration with avidin and HABA (25) was the same as the concentration calculated by weight for the lyophilized compound. This meant that the dry compound did not contain salts. The titration with avidin and HABA detected total biotin and did not distinguish between intact FP-biotin and FP-biotin that had lost its fluorine. ^{31}P NMR was used to measure the amount of defluorinated FP-biotin.

FP-biotin dissolved in chloroform was completely intact as indicated by phosphorus peaks at 35.2 and 29.9 ppm with a fluorine splitting of 1070 Hz (Figure 2). No third peak appeared during the 16 h data acquisition period to indicate defluorination of FP-biotin. In contrast, FP-biotin dissolved in water showed a doublet at 40.1 and 34.8 ppm (with a fluorine splitting of 1070 Hz) and a singlet at 29.9 ppm (Figure 2). The singlet was taken to be the defluoro hydrolysis product of FP-biotin. The amount of singlet was consistent with the amount of hydrolysis expected to occur in the 16 h, data collection
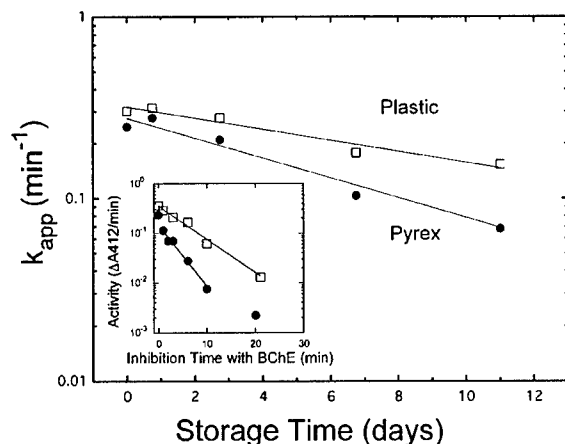
Figure 3. Decay of FP-biotin in water. Storage time is the time FP-biotin was left at room temperature; k_{app} is the apparent first-order rate constant for the inhibition of BChE by FP-biotin. Squares show the results for FP-biotin stored in a plastic microfuge tube ($t_{1/2}$ = 9.9 ± 1.5 days, k = 0.07 days^{-1}), and circles show the results for storage in a Pyrex tube ($t_{1/2}$ = 5.5 ± 0.4 days, k = 0.13 days^{-1}). Lines are from fits to a first-order process. Inset: The inhibition of BChE by FP-biotin on day 0 (circles) and day 11 (squares), by FP-biotin dissolved in water and stored in a plastic microfuge tube. The x-axis is the time in minutes that BChE was incubated with FP-biotin before BChE activity was measured. The y-axis is the log of activity measured as change in absorbance at 412 nm per minute. Lines are from fits to a first-order process.

Figure 4. Substoichiometric titration of BChE with FP-biotin. Points are the data; the line was fit to a linear equation. This titration shows that 1.1 μM FP-biotin was required to completely inhibit 0.61 μM BChE. An arrow at 0.61 μM FP-biotin demonstrates that an intercept at 0.61 μM FP-biotin would not fit the data.

period, suggesting that all of the FP-biotin had been intact when first dissolved in water.

Stability of FP-biotin in Water and Phosphate Buffer. The stability of FP-biotin in water was assessed by its ability to inhibit BChE activity. Aliquots of stock FP-biotin (0.26 mM in methanol) were diluted 1000-fold into water to yield 0.26 μM test solutions of FP-biotin at zero time. Test solutions were stored at room temperature in capped vials, either in Pyrex tubes or in colorless, plastic microfuge tubes. The apparent first-order rate constant for FP-biotin inhibition of BChE was determined by incubating 20 μL aliquots of an FP-biotin test solution with BChE (in 1.87 mL of 0.1 M potassium phosphate buffer, pH 7.0, at 25 °C) for defined times (Figure 3 inset). Active BChE remaining at the end of each incubation was determined according to the method of Ellman et al. (22). Fresh aliquots of substrate and DTNB were made daily. The stability of these reagents was routinely checked by measuring the 412 nm absorbance of the reaction mixture before adding the enzyme; no spontaneous degradation was detected. Semilog plots of inhibition time vs residual activity (measured as change in absorbance at 412 nm, i.e., ΔA412/min) were linear for at least 90% of the reaction. Apparent first-order rate constants for FP-biotin inhibition (Figure 3 inset) were determined by fitting the linear portion of these plots to a first-order expression using SigmaPlot.

The inhibition potency of the FP-biotin test solution in water decreased with time of storage at room temperature in a first-order fashion. A plot of the apparent first-order rate constant for FP-biotin inhibition of BChE turnover vs the storage time for the FP-biotin test solution gave a half-life for loss of FP-biotin of 5.5 ± 0.4 days in glass, which equals a k_{app} of 0.13 days^{-1}, or of 9.9 ± 1.5 days in plastic, which equals a k_{app} of 0.07 days^{-1} (Figure 3). Aqueous stock solutions of FP-biotin are stored routinely in colorless, plastic microfuge tubes from Midwest Scientific.
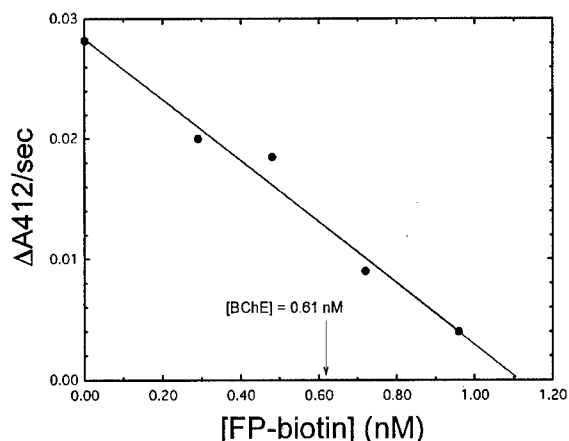
Stability of FP-biotin in phosphate buffer was assessed in a similar manner. FP-biotin was diluted into 0.1 M potassium phosphate buffer, pH 7.0, to give a final concentration of 1.4 μM and incubated at 25 °C. Colorless, plastic microfuge tubes were used for the incubation. At intervals, aliquots of the FP-biotin incubation mixture were mixed with BChE in order to determine the apparent rate constant for FP-biotin inhibition of BChE. These inhibition reactions were first-oder for at least 90% of their time courses. The apparent inhibition rate constants were then plotted vs the time of FP-biotin incubation in the phosphate buffer, yielding a half-life for hydrolysis of FP-biotin of 90 ± 3.3 min (k = 7.7 × 10^{-3} min^{-1}).

FP-biotin Is Unstable in Buffer. A 170 μM FP-biotin solution was completely degraded by 20 h of incubation in 0.1 M potassium phosphate, pH 7.0, at 25 °C. The fluoride ion was released from FP-biotin, and a new peak representing defluorinated FP-biotin appeared in the ^{31}P NMR spectrum. Complete loss of inhibition potency was confirmed by the failure of this FP-biotin solution to inhibit BChE.

Stoichiometry of the FP-biotin Reaction. The fraction of FP-biotin capable of inhibiting BChE was determined by substoichiometric reaction with BChE, as described in the Materials and Methods. The BChE activity remaining after substoichiometric reaction with FP-biotin was linearly dependent on FP-biotin concentration (Figure 4). However, the apparent concentration of FP-biotin required to fully inhibit the BChE was greater than the BChE concentration, indicating that only a fraction of the total, intact FP-biotin was capable of inhibiting BChE. In two separate experiments, 55 and 65% of the intact FP-biotin were capable of inhibiting BChE.

FP-biotin carries a chiral center at the phosphate. From the synthetic scheme, a 50−50 mixture of stereoisomers would be expected. The average of the stoichiometric measurements, 60%, is close to this theoretical expectation, if only one of the stereoisomers reacts with BChE to an appreciable extent. The possibility that the unreactive FP-biotin represented degraded material was ruled out by NMR.

To test whether a contaminant rather than intact FP-biotin was responsible for the inhibition of BChE, the
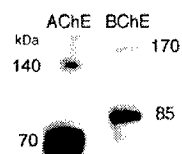
Figure 5. Western blot of FP-biotin-inhibited AChE and BChE. Two to five picomoles of protein from an SDS gel were transferred to PVDF membrane. The blot was developed with horseradish peroxidase conjugated to avidin. This confirms the identity of the inhibitor as FP-biotin (rather than a contaminant) because the inhibitor was covalently attached and carried a biotin tag.

inhibited BChE was checked for the presence of co-valently attached biotin. It was reasoned that an inhibitory contaminant in the FP-biotin preparation either would be missing the biotin moiety or would be incapable of forming a covalent adduct with BChE. SDS gel electrophoresis was used to test covalent association of biotin to protein. FP-biotin-inhibited human BChE and FP-biotin-inhibited human AChE were subjected to electrophoresis on an SDS polyacrylamide gel. The proteins labeled with biotin were detected with avidin conjugated to horseradish peroxidase (Figure 5). Because the gel was run in SDS, the biotin found migrating with BChE and AChE must have been covalently attached. Therefore, inhibition did not appear to be due to a contaminant.

Unreactive FP-biotin. The question in this experiment was whether the fraction of FP-biotin that did not react with BChE was nevertheless capable of reacting with other proteins. FP-biotin was depleted of the BChE reactive fraction by incubation with BChE for 1 h. The residual FP-biotin was separated from BChE and incubated with mouse brain homogenate. Figure 6 shows that residual FP-biotin did not label the proteins in mouse brain to a significant extent. The two intense bands at 75 and 140 kDa are endogenous biotinylated proteins. In contrast, FP-biotin that had not been precleared with BChE labeled about 50 proteins in mouse brain. It was concluded that only one stereoisomer of FP-biotin reacted with proteins in mouse brain and that this same stereoisomer reacted with human BChE.

The trypsin catalytic triad is a mirror image of that in AChE and BChE (26). The question that we asked was whether a stereoisomer of FP-biotin that did not react with BChE could react with trypsin. When trypsin was treated with an equimolar amount of FP-biotin, about 50% of the trypsin was inhibited. In contrast, when FP-biotin was depleted of the BChE reactive fraction, the residual FP-biotin did not inhibit trypsin. The trypsin experiments are consistent with the conclusion that FP-biotin is a 50—50 mixture of stereoisomers. Only one of these stereoisomers was capable of inhibiting trypsin, and this was the same stereoisomer that inhibited BChE.

In the course of these experiments, the activity of 1.5 μM trypsin was measured in the presence of 1.1 μM BChE. Under the assay conditions, 1.1 μM BChE hydrolyzed TAME at only 2% of the rate at which TAME was hydrolyzed by 1.5 μM trypsin. However, the mixture hydrolyzed TAME at 150% the rate shown by trypsin alone. This observation confirmed a previous report by Darvesh et al. (27) that BChE enhanced the activity of trypsin. The mechanism responsible for this effect is unclear.
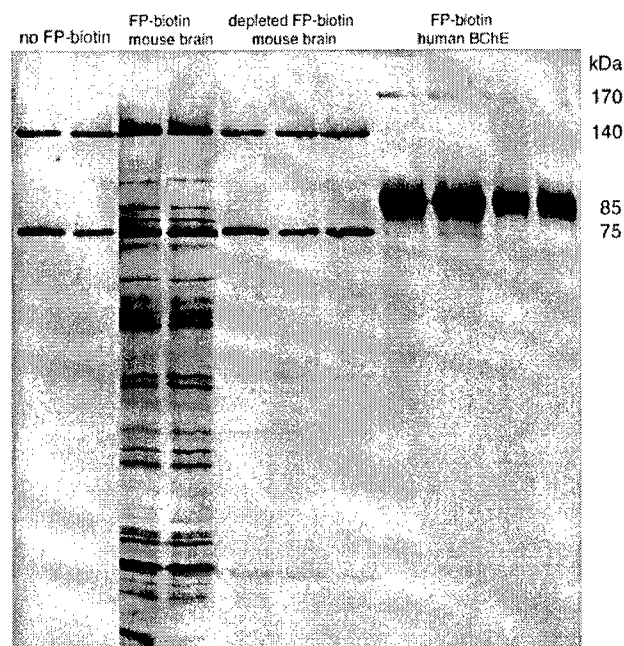

Figure 6. Only one stereoisomer of FP-biotin labels proteins in mouse brain. Lanes 1 and 2, untreated mouse brain homogenate showing endogenous biotinylated proteins at 140 and 75 kDa. Lanes 3 and 4, mouse brain homogenate incubated with a mixture of FP-biotin stereoisomers, 30 μg of protein per lane. Lane 5–7, mouse brain homogenate incubated with residual FP-biotin, after the FP-biotin had been depleted of the BChE reactive stereoisomer. Lanes 8–11, FP-biotin labeled human BChE, 1 and 0.3 pmol per lane; 1 pmol of BChE = 85 ng.
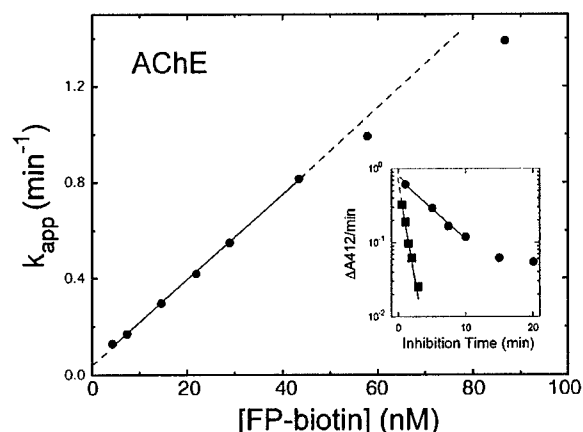
Figure 7. Rate constant for inhibition of human AChE by FP-biotin. k_{app} is the apparent first-order rate constant for the inhibition of AChE by FP-biotin. Points are the data; the solid line is from a linear fit, and the dashed line is an extrapolation of the fitted line. The slope yields an apparent second-order rate constant, $k = 1.8 \pm 0.02 \times 10^7$ M^{-1} min^{-1}. Inset: Inhibition of AChE by 4.3 nM FP-biotin (circles) and 51 nM FP-biotin (squares). Solid lines are from fits to a first-order process. The AChE concentration was 0.17 nM.

Reaction Kinetics of Purified Human AChE with FP-biotin. Inhibition of human AChE (0.17 nM) by FP-biotin was first-order for at least 90% of the reaction at all concentrations of FP-biotin tested (see Figure 7, inset for selected examples). A plot of the apparent first-order rate constant for inhibition vs the concentration of FP-biotin was linear from 4.3 to 43 nM FP-biotin (Figure 7). The concentration of FP-biotin was corrected for losses due to handling (as described in the Storage of FP-biotin section above) and for 50% inhibition potency. In the
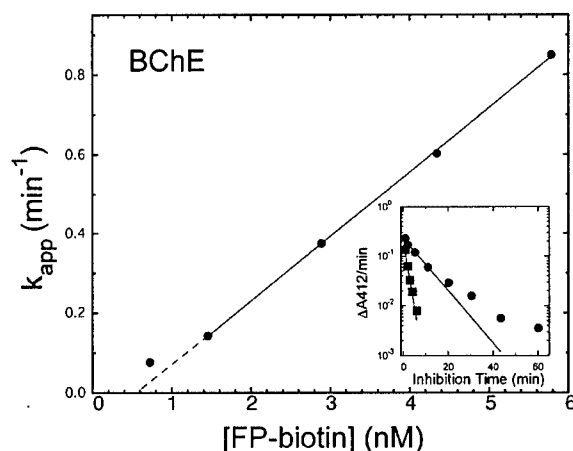
Figure 8. Inhibition of BChE by FP-biotin. k_{app} is the apparent first-order rate constant for the inhibition of human BChE by FP-biotin. Points are the data; the solid line is from a linear fit; the dashed line is an extrapolation of the fitted line. The slope yields an apparent second-order rate constant, $k = 1.6 \pm 0.03 \times 10^8$ M^{-1} min^{-1}. Inset: The inhibition of BChE by 0.73 nM FP-biotin (circles) and 5.8 nM FP-biotin (squares). Solid lines are from fits to a first-order process. The BChE concentration was 0.35 nM.

context of this work, inhibition potency refers to the stereoisomeric form of FP-biotin, which is capable of inhibiting AChE. Because the stereochemistry of the active sites of both AChE and BChE is the same (*26, 28*), it was assumed that the stereoisomer of FP-biotin, which was capable of inhibiting BChE, would also inhibit AChE. This assumption was supported by the finding that all proteins in the mouse brain were inhibited by the same stereoisomer that inhibited BChE. The apparent second-order rate constant for the reaction of human AChE with FP-biotin was determined from this linear portion of the graph to be $1.8 \pm 0.02 \times 10^7$ M^{-1} min^{-1}.

Extrapolation of the second-order line to zero FP-biotin revealed a small nonzero *y*-axis intercept, which is consistent with a minor, spontaneous loss of AChE activity due to the absence of BSA. It is well-accepted that AChE will stick to surfaces in the absence of a carrier protein such as BSA. This spontaneous loss of AChE activity was not subtracted from the OD/min measurements in the presence of FP-biotin.

The dissociation constant of FP-biotin for human AChE was estimated to be greater than 85 nM. Figure 7 shows that the data points for FP-biotin concentrations 56 nM and higher fell below the extrapolated second-order line, suggesting the onset of saturation and the existence of a noncovalent complex between FP-biotin and AChE. The reaction of FP-biotin with AChE was too fast to allow the use of FP-biotin concentrations greater than 85 nM. This meant that the dissociation constant could not be measured more precisely than the approximate value of 85 nM.

Reaction Kinetics of Purified Human BChE with FP-biotin. Loss of BChE activity (0.35 nM BChE) was first-order for at least 90% of the reaction, at all concentrations of FP-biotin except for the very lowest (0.73 nM); see Figure 8 inset. A plot of the apparent first-order rate constant for the loss of BChE activity vs FP-biotin concentration was linear from 1.4 to 5.8 nM FP-biotin (Figure 8). Concentrations of FP-biotin were corrected for losses due to handling and to 50% inhibition potency. The slope of this plot indicated an apparent second-order rate

constant for the reaction of human BChE with FP-biotin of $1.6 \pm 0.03 \times 10^8$ M^{-1} min^{-1}.

The lower limit for the dissociation constant for FP-biotin and BChE was estimated to be greater than 5.8 nM. A more precise value could not be measured because the reaction was too fast to allow use of higher concentrations of FP-biotin.

Reaction Kinetics of BChE and AChE with Diazoxon. Studies with diazoxon were included because there were no values for diazoxon in the literature against which the values for FP-biotin could be compared. Loss of both BChE and AChE activity was first-order for all concentrations of diazoxon used. With BChE, the diazoxon concentrations ranged from 2 to 30 nM, while with AChE the concentrations were 0.37−7.4 μM. Secondary plots of k_{app} vs diazoxon concentration were linear for the full diazoxon concentration range yielding apparent second-order rate constants of 7.7×10^7 M^{-1} min^{-1} for human BChE and 4.2×10^5 M^{-1} min^{-1} for human AChE, with a standard deviation of 10%.

Discussion

The products of the reaction of AChE and BChE with FP-biotin are biotinylated AChE and biotinylated BChE. It is reasonable to propose that the biotin is covalently attached to the active site serine through the phosphate group. This conclusion is supported by the fact that pretreatment of BChE with a variety of OP (malaoxon, paraoxon, chlorpyrifos oxon, methyl paraoxon, dichlorvos, diazoxon, and echothiophate) blocks formation of the FP-biotin adduct (see Figure 6 in ref *10*).

FP-biotin has good reactivity with human AChE and BChE despite its large biotin group. The spacer arm and biotin group are too large to fit inside the active site gorge. This proposition is supported by the fact that the biotin is available for reaction with avidin, a protein with a molecular weight of 68 000. We assume that the biotin either extends out the mouth of the gorge, or alternatively, extends through the putative backdoor (*29*).

FP-biotin is suitable for the proposed task of identifying OP reactive proteins. Most studies, including early studies with FP-biotin, have been conducted in vitro. Very few OP reactive proteins have been identified in vivo. Ongoing work in this laboratory is focused on expanding the list of proteins that react with OP in vivo.

Stereoselective Inhibition. The phosphate of FP-biotin is stereoisomeric (Figure 1). Our finding that approximately 50% of the FP-biotin had inhibitory potency toward BChE and trypsin is consistent with the interpretation that FP-biotin is a mixture of stereoisomers. The fraction of FP-biotin that failed to react with BChE also failed to label proteins in mouse brain, strongly suggesting that only one stereoisomer of FP-biotin is reactive.

Stereoselective inhibition by organophosphorus stereoisomers has been reported for BChE and AChE (*30−35*). The stereoselective organophosphorus agents are soman, sarin, VX, isomalathion, malaoxon, and cycloheptyl methyl S-ethylphosphonyl thioate. The difference in reactivity between stereoisomers can be as high as 75 000-fold (*35*).

Reactivity of FP-biotin. Comparison of the second-order rate constants of FP-biotin and other OP shows that FP-biotin is very potent (Table 1). The rate constant for FP-biotin reacting with BChE is similar to those for the

Table 1. Comparison of OP Reaction Rates with Human AChE and BChE

| | k (M^{-1} min^{-1}) | | |
OP	human AChE	human BChE	ref
chlorpyrifos oxon	1.0×10^7	1.7×10^9	38
MEPQ	5.2×10^8	6.3×10^8	39
cyclosarin	7.4×10^8	3.8×10^8	40
FP-biotin	1.8×10^7	1.6×10^8	present work
diazoxon	4.2×10^5	7.7×10^7	present work
soman	9.1×10^7	5.1×10^7	39
soman PsCs	1.5×10^8	4.0×10^7	35
DFP	5×10^4	1.7×10^7	36
sarin	1.8×10^7	1.2×10^7	39
VX	4.0×10^7	8.2×10^6	39
tabun	4.0×10^6	4.7×10^6	39
paraoxon	7.0×10^5	1.9×10^6	38
paraoxon	9.7×10^5	3×10^6	41, 42
dichlorvos	1.2×10^5	8.7×10^5	43
methyl paraoxon	1.6×10^6	4.2×10^4	43
malaoxon	1.3×10^5	1.5×10^4	32
malaoxon		1.1×10^4	44
oxydemeton methyl	2.2×10^4	2.2×10^3	45

nerve agents (cyclosarin and soman), for the pesticide metabolite diazoxon, and for DFP. Only chlorpyrifos oxon and MEPQ are significantly faster. Chlorpyrifos oxon is the active metabolite of the pesticide chlorpyrifos. MEPQ is related to VX in structure. Most of the active pesticide derivatives react more slowly. For AChE, only the nerve agents (cyclosarin, soman, and VX) and MEPQ react faster than FP-biotin. The reaction rates for sarin, chlorpyrifos oxon, and FP-biotin with AChE are comparable, while the rates for the remaining representatives in Table 1 are slower.

Most of the OP in Table 1, including FP-biotin, react more slowly with AChE than with BChE. This can be explained by the finding of Millard et al. (*36*) that bulky OP molecules do not easily fit into the active site of AChE. The crystal structure of DFP-inhibited AChE showed that phosphorylation with DFP distorted the structure. The main chain loop that includes residues of the acyl-binding pocket moved almost 5 Å. In contrast, BChE has more space near the active site and can accommodate large structures without bending out of shape (*28*).

Is FP-biotin Expected to React with AChE in a Living Mouse? The second-order rate constant for the reaction of AChE with FP-biotin can be used to estimate how long it will take the AChE in a mouse to react with FP-biotin. We have been injecting mice intraperitoneally with FP-biotin at a dose of 20 mg/kg. A mouse weighs 0.02 kg. If the FP-biotin is uniformly distributed in the mouse, this calculates to an FP-biotin concentration of 34 μM. Multiplying 34 μM by the second-order rate constant (1.8×10^7 M^{-1} min^{-1}) yields a first-order rate constant of 612 min^{-1}. This means that half of the AChE should react with FP-biotin in 0.07 s. The second-order rate constant for BChE is faster than for AChE. Therefore, it is expected that BChE in a mouse will also react with FP-biotin. We conclude that the rate constants are fast enough to expect AChE and BChE in a mouse to react with FP-biotin. This conclusion is supported by the finding that AChE and BChE are inhibited in mice treated in vivo with FP-biotin (*37*).

References

(1) Mileson, B. E., Chambers, J. E., Chen, W. L., Dettbarn, W., Ehrich, M., Eldefrawi, A. T., Gaylor, D. W., Hamernik, K., Hodgson, E., Karczmar, A. G., Padilla, S., Pope, C. N., Richardson, R. J., Saunders, D. R., Sheets, L. P., Sultatos, L. G., and Wallace, K. B. (1998) Common mechanism of toxicity: a case study of organophosphorus pesticides. *Toxicol. Sci. 41*, 8–20.

(2) McDonough, J. H., Jr., and Shih, T. M. (1997) Neuropharmacological mechanisms of nerve agent-induced seizure and neuropathology. *Neurosci. Biobehav. Rev. 21*, 559–579.

(3) Fillmore, C. M., and Lessenger, J. E. (1993) A cholinesterase testing program for pesticide applicators. *J. Occup. Med. 35*, 61–70.

(4) Glynn, P. (2003) NTE: One target protein for different toxic syndromes with distinct mechanisms? *Bioessays 25*, 742–745.

(5) Quistad, G. B., Barlow, C., Winrow, C. J., Sparks, S. E., and Casida, J. E. (2003) Evidence that mouse brain neuropathy target esterase is a lysophospholipase. *Proc. Natl. Acad. Sci. U.S.A. 100*, 7983–7987.

(6) Casida, J. E., and Quistad, G. B. (2004) Organophosphate toxicology: Safety aspects of nonacetylcholinesterase secondary targets. *Chem. Res. Toxicol. 17*, 983–998.

(7) Maxwell, D. M., Brecht, K. M., and O'Neill, B. L. (1987) The effect of carboxylesterase inhibition on interspecies differences in soman toxicity. *Toxicol. Lett. 39*, 35–42.

(8) Yang, Z. P., and Dettbarn, W. D. (1998) Prevention of tolerance to the organophosphorus anticholinesterase paraoxon with carboxylesterase inhibitors. *Biochem. Pharmacol. 55*, 1419–1426.

(9) Richards, P. G., Johnson, M. K., and Ray, D. E. (2000) Identification of acylpeptide hydrolase as a sensitive site for reaction with organophosphorus compounds and a potential target for cognitive enhancing drugs. *Mol. Pharmacol. 58*, 577–583.

(10) Peeples, E. S., Schopfer, L. M., Duysen, E. G., Spaulding, R., Voelker, T., Thompson, C. M., and Lockridge, O. (2005) Albumin, a new biomarker of organophosphorus toxicant exposure, identified by mass spectrometry. *Toxicol. Sci. 83*, 303–312.

(11) Ward, T. R., Ferris, D. J., Tilson, H. A., and Mundy, W. R. (1993) Correlation of the anticholinesterase activity of a series of organophosphates with their ability to compete with agonist binding to muscarinic receptors. *Toxicol. Appl. Pharmacol. 122*, 300–307.

(12) Tjoelker, L. W., Eberhardt, C., Unger, J., Trong, H. L., Zimmerman, G. A., McIntyre, T. M., Stafforini, D. M., Prescott, S. M., and Gray, P. W. (1995) Plasma platelet-activating factor acetylhydrolase is a secreted phospholipase A2 with a catalytic triad. *J. Biol. Chem. 270*, 25481–25487.

(13) Santos, M. D., Pereira, E. F., Aracava, Y., Castro, N. G., Fawcett, W. P., Randall, W. R., and Albuquerque, E. X. (2003) Low concentrations of pyridostigmine prevent soman-induced inhibition of GABAergic transmission in the central nervous system: Involvement of muscarinic receptors. *J. Pharmacol. Exp. Ther. 304*, 254–265.

(14) Moser, V. C. (1995) Comparisons of the acute effects of cholinesterase inhibitors using a neurobehavioral screening battery in rats. *Neurotoxicol. Teratol. 17*, 617–625.

(15) Pope, C. N. (1999) Organophosphorus pesticides: Do they all have the same mechanism of toxicity? *J. Toxicol. Environ. Health B Crit. Rev. 2*, 161–181.

(16) Ray, D. E., and Richards, P. G. (2001) The potential for toxic effects of chronic, low-dose exposure to organophosphates. *Toxicol. Lett. 120*, 343–351.

(17) Behra, M., Etard, C., Cousin, X., and Strahle, U. (2004) The use of zebrafish mutants to identify secondary target effects of acetylcholine esterase inhibitors. *Toxicol. Sci. 77*, 325–333.

(18) Lockridge, O., Duysen, E. G., Voelker, T., Thompson, C. M., and Schopfer, L. M. (2005) Life without acetylcholinesterase: The implications of cholinesterase inhibitor toxicity in AChE-knockout mice. *Environ. Toxicol. Pharmacol.* Published online January 26, 2005.

754 *Chem. Res. Toxicol., Vol. 18, No. 4, 2005*

Schopfer et al.

(19) Liu, Y., Patricelli, M. P., and Cravatt, B. F. (1999) Activity-based protein profiling: The serine hydrolases. *Proc. Natl. Acad. Sci. U.S.A. 96*, 14694–14699.

(20) Kidd, D., Liu, Y., and Cravatt, B. F. (2001) Profiling serine hydrolase activities in complex proteomes. *Biochemistry 40*, 4005–4015.

(21) Lockridge, O. (1990) Genetic variants of human serum cholinesterase influence metabolism of the muscle relaxant succinylcholine. *Pharmacol. Ther. 47*, 35–60.

(22) Ellman, G. L., Courtney, K. D., Andres, V., Jr., and Feather-Stone, R. M. (1961) A new and rapid colorimetric determination of acetylcholinesterase activity. *Biochem. Pharmacol. 7*, 88–95.

(23) Aldridge, W. N., and Reiner, E. (1969) Acetylcholinesterase. Two types of inhibition by an organophosphorus compound: One the formation of phosphorylated enzyme and the other analogous to inhibition by substrate. *Biochem. J. 115*, 147–162.

(24) Main, A. R. (1964) Affinity and phosphorylation constants for the inhibition of esterases by organophosphates. *Science 144*, 992–993.

(25) Green, N. M. (1965) A spectrophotometric assay for avidin and biotin based on binding of dyes by avidin. *Biochem. J. 94*, 23C–24C.

(26) Sussman, J. L., Harel, M., Frolow, F., Oefner, C., Goldman, A., Toker, L., and Silman, I. (1991) Atomic structure of acetylcholinesterase from *Torpedo californica*: A prototypic acetylcholine-binding protein. *Science 253*, 872–879.

(27) Darvesh, S., Kumar, R., Roberts, S., Walsh, R., and Martin, E. (2001) Butyrylcholinesterase-mediated enhancement of the enzymatic activity of trypsin. *Cell Mol. Neurobiol. 21*, 285–296.

(28) Nicolet, Y., Lockridge, O., Masson, P., Fontecilla-Camps, J. C., and Nachon, F. (2003) Crystal structure of human butyrylcholinesterase and of its complexes with substrate and products. *J. Biol. Chem. 278*, 41141–41147.

(29) Gilson, M. K., Straatsma, T. P., McCammon, J. A., Ripoll, D. R., Faerman, C. H., Axelsen, P. H., Silman, I., and Sussman, J. L. (1994) Open "back door" in a molecular dynamics simulation of acetylcholinesterase. *Science 263*, 1276–1278.

(30) Millard, C. B., Lockridge, O., and Broomfield, C. A. (1998) Organophosphorus acid anhydride hydrolase activity in human butyrylcholinesterase: Synergy results in a somanase. *Biochemistry 37*, 237–247.

(31) Doorn, J. A., Schall, M., Gage, D. A., Talley, T. T., Thompson, C. M., and Richardson, R. J. (2001) Identification of butyrylcholinesterase adducts after inhibition with isomalathion using mass spectrometry: Difference in mechanism between (1R)- and (1S)-stereoisomers. *Toxicol. Appl. Pharmacol. 176*, 73–80.

(32) Rodriguez, O. P., Muth, G. W., Berkman, C. E., Kim, K., and Thompson, C. M. (1997) Inhibition of various cholinesterases with the enantiomers of malaoxon. *Bull. Environ. Contam. Toxicol. 58*, 171–176.

(33) Hosea, N. A., Berman, H. A., and Taylor, P. (1995) Specificity and orientation of trigonal carboxyl esters and tetrahedral alkylphosphonyl esters in cholinesterases. *Biochemistry 34*, 11528–11536.

(34) Benschop, H. P., Konings, C. A., Van Genderen, J., and De Jong, L. P. (1984) Isolation, anticholinesterase properties, and acute toxicity in mice of the four stereoisomers of the nerve agent soman. *Toxicol. Appl. Pharmacol. 72*, 61–74.

(35) Ordentlich, A., Barak, D., Kronman, C., Benschop, H. P., De Jong, L. P., Ariel, N., Barak, R., Segall, Y., Velan, B., and Shafferman, A. (1999) Exploring the active center of human acetylcholinesterase with stereomers of an organophosphorus inhibitor with two chiral centers. *Biochemistry 38*, 3055–3066.

(36) Millard, C. B., Kryger, G., Ordentlich, A., Greenblatt, H. M., Harel, M., Raves, M. L., Segall, Y., Barak, D., Shafferman, A., Silman, I., and Sussman, J. L. (1999) Crystal structures of aged phosphonylated acetylcholinesterase: Nerve agent reaction products at the atomic level. *Biochemistry 38*, 7032–7039.

(37) Peeples, E. S., Schopfer, L. M., Duysen, E. G., Spaulding, R., Voelker, T., Thompson, C. M., and Lockridge, O. (2005) Albumin, a new biomarker of organophosphorus toxicant exposure, identified by mass spectrometry. *Toxicol. Sci. 83*, 303–312.

(38) Amitai, G., Moorad, D., Adani, R., and Doctor, B. P. (1998) Inhibition of acetylcholinesterase and butyrylcholinesterase by chlorpyrifos-oxon. *Biochem. Pharmacol. 56*, 293–299.

(39) Raveh, L., Grunwald, J., Marcus, D., Papier, Y., Cohen, E., and Ashani, Y. (1993) Human butyrylcholinesterase as a general prophylactic antidote for nerve agent toxicity. In vitro and in vivo quantitative characterization. *Biochem. Pharmacol. 45*, 2465–2474.

(40) Worek, F., Eyer, P., and Szinicz, L. (1998) Inhibition, reactivation and aging kinetics of cyclohexylmethylphosphonofluoridate-inhibited human cholinesterases. *Arch. Toxicol. 72*, 580–587.

(41) Skrinjaric-Spoljar, M., and Simeon, V. (1993) Reactions of usual and atypical human serum cholinesterase phenotypes with progressive and reversible inhibitors. *J. Enzymol. Inhib. 7*, 169–174.

(42) Ordentlich, A., Barak, D., Kronman, C., Ariel, N., Segall, Y., Velan, B., and Shafferman, A. (1996) The architecture of human acetylcholinesterase active center probed by interactions with selected organophosphate inhibitors. *J. Biol. Chem. 271*, 11953–11962.

(43) Skrinjaric-Spoljar, M., Simeon, V., and Reiner, E. (1973) Spontaneous reactivation and aging of dimethylphosphorylated acetylcholinesterase and cholinesterase. *Biochim. Biophys. Acta 315*, 363–369.

(44) Main, A. R., and Hastings, F. L. (1966) A comparison of acylation, phosphorylation and binding in related substrates and inhibitors of serum cholinesterase. *Biochem. J. 101*, 584–590.

(45) Worek, F., Diepold, C., and Eyer, P. (1999) Dimethylphosphoryl-inhibited human cholinesterases: Inhibition, reactivation, and aging kinetics. *Arch. Toxicol. 73*, 7–14.